UNIVERSITY OF
MODENA AND REGGIO EMILIA

Degree in Doctor of Philosophy in Molecular and Regenerative Medicine

ROLE OF WILD-TYPE CALRETICULIN IN PHYSIOLOGICAL HEMATOPOIESIS AND EFFECT OF CALRETICULIN MUTATIONS IN THE DEVELOPMENT OF MYELOPROLIFERATIVE NEOPLASMS

Supervisor:
Prof. ROSSELLA MANFREDINI

Candidate:
ELENA GENOVESE

Ph.D. School Director:
Prof. MICHELE DE LUCA

XXXII Cycle

ai miei nonni

INDEX

SINTESI

Calreticulina (CALR) è uno chaperone da 46 kDa residente nel reticolo endoplasmatico responsabile della regolazione del calcio intracellulare e del folding proteico. CALR è anche in grado di regolare diverse funzioni al di fuori dal reticolo, tra cui la risposta allo stress cellulare.

Nel 2013 sono state scoperte diverse mutazioni nell'esone 9 del gene CALR nelle Neoplasie Mieloproliferative (MPNs); in particolare sono state individuate circa 40 tipi diversi di mutazioni nel 60-70% dei pazienti con Trombocitemia Essenziale (ET) e Mielofibrosi Primaria (PMF) non mutati per JAK2 e MPL. Tali mutazioni consistono in inserzioni o delezioni che portano a frameshift con conseguente perdita del dominio C-terminale e della sequenza KDEL.

In quest'ottica, l'alterazione strutturale di CALR comprometterebbe la sua funzionalità e la sua localizzazione cellulare. Infatti, è stato dimostrato che i mutanti di CALR interagiscono con il recettore della trombopoietina (MPL), inducendo l'attivazione costitutiva della via JAK-STAT. Tuttavia, il preciso meccanismo d'azione dei mutanti di CALR è stato solo parzialmente chiarito e non ci sono informazioni sulla funzione di CALR Wild-Type (WT) durante l'emopoiesi fisiologica.

Per chiarire il ruolo biologico di CALR WT nella proliferazione e nel differenziamento dei progenitori emopoietici (HPSCs), abbiamo eseguito esperimenti di silenziamento e overespressione in cellule CD34+ umane. I nostri dati mostrano che l'overespressione di CALR WT è in grado di promuovere il differenziamento eritroide e megacariocitario (MK). Parallelamente, il silenziamento di CALR WT induce una marcata repressione del lineages eritroide e MK. In accordo con questi risultati, l'analisi del profilo d'espressione genica (GEP) ha confermato che CALR WT è in grado di influenzare l'espressione dei geni del differenziamento eritroide e MK. Inoltre, l'analisi trascrizionale ha mostrato la modulazione di diversi geni coinvolti nella risposta allo stress ossidativo, allo stress del reticolo, al danno al DNA e in pathways biologici alla base dello sviluppo delle MPNs.

Successivamente, per studiare l'effetto delle mutazioni di CALR sulla sua funzionalità in risposta allo stress ossidativo e del reticolo, abbiamo infettato le cellule K562 con vettori retrovirali esprimenti una delle due varianti mutate più comuni, CALRdel52 o CALRins5. Abbiamo deciso di utilizzare la linea cellulare K562, priva dell'espressione di MPL, per individuare ulteriori vie di segnalazione alla base della trasformazione MPL-mediata. In primo luogo, i nostri dati mostrano che i mutanti di CALR

compromettono la capacità di rispondere allo stress del reticolo e riducono drasticamente l'attivazione dell'apoptosi mediata dalla UPR (Unfolded Protein Response). Inoltre, abbiamo dimostrato che le mutazioni di CALR causano una maggiore sensibilità allo stress ossidativo con accumulo di danni ossidativi al DNA. Infine, abbiamo studiato la funzione del gene antiossidante OXR1, deregolato nell'analisi di GEP. La downregolazione di OXR1 altera la capacità delle cellule mutate di controbilanciare l'accumulo di specie reattive dell'ossigeno (ROS), suggerendo il possibile coinvolgimento di OXR1 nell'alterata risposta allo stress ossidativo che si osserva nei mutanti di CALR.

Nel complesso, i nostri risultati rivelano un nuovo ruolo di CALR WT nella regolazione del differenziamento eritroide e MK, due lineages coinvolti nelle MPNs. Inoltre, i mutanti di CALR incidono negativamente sulla risposta allo stress del reticolo, causando resistenza all'apoptosi. Infine, l'alterata risposta allo stress ossidativo che si osserva nei mutanti di CALR può causare instabilità genomica, promuovendo così la trasformazione tumorale.

***Parole chiave*:** Calreticulina; Neoplasie Mieloproliferative; Differenziamento Ematopoietico; Stress Ossidativo; Stress del Reticolo Endoplasmatico

ABSTRACT

Calreticulin (CALR) is a 46 kDa Endoplasmic Reticulum (ER) chaperone responsible for intracellular calcium regulation and protein folding. CALR is also able to perform different functions outside the ER, such as responses to cellular stress.

In 2013, several mutations were discovered in exon 9 of CALR gene in Myeloproliferative Neoplasms (MPNs); notably about 40 different types of mutations have been reported in 60-80% of JAK2 and MPL unmutated Essential Thrombocythemia (ET) and Primary Myelofibrosis (PMF) patients. These mutations consist of insertions or deletions that induce a frameshift, resulting in a loss of the C-terminal portion domain and the KDEL sequence.

In this view, structural alterations of CALR protein might impair its functionality and its cellular localization. Indeed, recent data demonstrated that CALR mutants interact with the thrombopoietin receptor (MPL), inducing the constitutive activation of JAK-STAT pathway. However, the precise mechanism of action through which CALR mutants contribute to the development of MPNs has only been partially clarified and there is no available information on the function of Wild-Type (WT) CALR during physiological hematopoiesis.

In order to elucidate the biological role of WT CALR in the proliferation and differentiation of hematopoietic stem/progenitor cells (HPSCs), we performed gene silencing and overexpression experiments in human CD34+ cells. Our data demonstrated that WT CALR overexpression is able to enhance erythroid and megakaryocyte (MK) differentiation. Consistently, WT CALR silencing induces a marked repression of MK and erythroid lineages. In agreement with these results, gene expression profile (GEP) analysis confirmed that WT CALR is able to affect the expression of genes of erythroid and MK differentiation. Moreover, transcriptome analysis showed the modulation of several genes implicated in oxidative stress, ER stress response, DNA damage and in several pathways already described as able to play a role in MPN development.

Next, to investigate the impact of CALR mutations in oxidative and ER stress response, we transduced K562 cells with vectors expressing one of the two commonest CALR mutated variants, either CALRdel52 or CALRins5. We chose to perform experiments in the K562 cell line, devoid of MPL expression, in order to identify additional pathways whose alterations might cooperate with cellular transformation mediated by MPL activation. Firstly, we demonstrated that CALR mutants reduce the capability

to respond to ER stress and significantly decrease the activation of the pro-apoptotic unfolded protein response (UPR) pathway. Then, we showed that CALR mutations induce increased sensitivity to oxidative stress, also driving the accumulation of oxidative DNA damage. Finally, we studied the function of the antioxidant gene OXR1, found deregulated in GEP analysis. The downregulation of OXR1 affects the capability of mutant cells to counterbalance Reactive Oxygen Species (ROS) accumulation, suggesting that lack of OXR1 expression might be one of the molecular mechanisms responsible for the impaired oxidative stress response mediated by mutant CALR.

Altogether, our results suggest a new role of WT CALR in the regulation of erythroid and MK differentiation, whose deregulation is crucial in MPNs. Moreover, CALR mutants negatively impact on the ability to respond to ER stress, conferring apoptosis resistance to the cells. Finally, the impairment in oxidative stress response due to CALR mutations can lead to genomic instability, thus promoting cell transformation.

***Key words*:** Calreticulin; Myeloproliferative Neoplasms; Hematopoietic Differentiation; Oxidative Stress; Endoplasmic Reticulum Stress

INTRODUCTION

1. PHILADELPHIA-NEGATIVE MYELOPROLIFERATIVE NEOPLASMS

1.1 Classification

The Myeloproliferative Disorders (MPDs), conceptualized for the first time in 1951 by William Dameshek[1], represent a heterogeneous group of diseases defined by altered proliferation of hematopoietic precursors in the Bone Marrow (BM) and excessive production of mature blood cells[2]. Initially Chronic Myeloid Leukemia (CML), Polycytemia Vera (PV), Essential Thrombocythemia (ET), Primary Myelofibrosis (PMF) and Di Guglielmo Syndrome was reclassified in these pathologies[1]. Subsequently, Di Guglielmo Syndrome were reclassified as erythroid leukemia and CML, PV, ET and PMF were defined classic MPDs[3].

In 1960, Nowell and Hungerford discovered a frequently acquired somatic mutation in CML patients consisting of a reciprocal translocation between chromosome 9 and 22, t(9;22)(q34;q11), called Philadelphia (Ph) chromosome or BCR-ABL fusion gene[4,5]. This cytogenetic marker allowed the distinction between CML and other classic Myeloproliferative Disorders[6].

Philadelphia-negative Myeloproliferative Neoplasms (MPNs) are subtypes of MPDs including PV, ET and PMF. These disorders are traditionally grouped together due to their overlapping features: they all derive from hematopoietic stem cells[7,8] carrying recurrent gene mutations (such as Janus Kinase 2, Calreticulin, MPL) and significant overproduction of terminally differentiated myeloid cells (erythrocytes, granulocytes, platelets)[9]. Despite being initially associated with PV, ET and PMF, the term MPN includes also other related pathologies. For reasons of simplification in this thesis we will talk about PV, ET and PMF generically as MPNs.

The World Health Organization (WHO) defined the classification of this group of diseases based on morphological, cytogenetic and molecular features. According to the WHO system, Myeloid Neoplasms include Myeloproliferative Neoplasms (MPNs), Myelodysplastic Syndrome (MDS), Acute Myeloid Leukemia (AML), Myelodysplastic/Myeloproliferative Neoplasms (MDS/MPNs) and Myeloid Neoplasms characterized by eosinophilia and rearrangement of PDGFRA, PDGFRB or FGFR1, or PCM1-JAK2. The update of *WHO Classification of Tumours of Hematopoietic and Lymphoid Tissues*, the 5th edition, was recently reviewed in 2016[10]. This new version attempts to incorporate new clinical, morphologic and genetic data that have emerged since the publication of the last edition. Unlike the old version, PMF cases have been

sub-classified into “prefibrotic” (pre-PMF) and “overtly fibrotic” stage (PMF)(**Table 1**). The specific diagnostic criteria that allow the discrimination of the two phases are of primary importance to distinguish the "true" ET from pre-PMF since they have different clinical outcomes[11].

2016 WHO classification of myeloid neoplasms

Myeloproliferative Neoplasms (MPNs)
Chronic myeloid leukaemia (CML), BCR/ABL-positive
Chronic Neutrophilic Leukaemia (CNL)
Polycythemia Vera (PV)
Primary Myelofibrosis (PMF)
PMF, prefibrotic/early stage
PMF, overt fibrotic stage
Essential Thrombocythemia (ET)
Chronic Eosinophilic Leukaemia, not otherwise specified (CEL-NOS)
MPN, unclassifiable (MPN-U)
Mastocytosis
Myeloid neoplasms with eosinophilia and rearrangement of PDGFRA, PDGFRB, or FGFR1, or with PCM1-JAK2
Myelodysplastic/myeloproliferative neoplasms (MDS/MPNs)
Myelodysplastic syndromes (MDS)
Acute myeloid leukaemia (AML) and related neoplasms

Table 1: *2016 World Health Organization (WHO) classification of myeloid malignancies.*

In this thesis I will focus my attention on Ph-negative MPNs and particularly on PMF and the recently discovered molecular diagnostic mutation, Calreticulin (CALR), which is the second most common altered gene after Janus Kinase (JAK2) in PMF.

1.2 Epidemiology

MPNs are classified as rare cancers because their incidence is lower than 6 per 100’000 persons per year[12]. The prevalence and incidence rates of these diseases may vary extensively among different countries. Published epidemiology data are scarce, especially in European Union (EU) where these data are not routinely collected in registries. Moulard *et al.* have assembled the most recent information available on MPNs in European patients, in whom MPNs have the following incidence estimated: PV from 0.4 to 2.8, ET from 0.38 to 1.7 and PMF from 0.1 to 1.0 per 100’000 persons per year[13].

Most recently, Srour *et al.* have assessed MPN's incidence and survival rate in the United States from 2001 to 2012. The incidence rates (IRs) appear to be variable upon aetiologies and/or susceptible populations. In particular, during the analysis period IRs were highest for PV (IR=10.9) and ET (IR=9.6) rather than PMF (IR=3.1), with significantly lower IR in Hispanic white and in Asians/Pacific Islanders. Additionally, the overall IR of each MPN was variable by gender. Excluding ET, which predominated among females, all the other MPNs were associated with higher IR among males, with the following ratio of the incidence rate man/woman: PV 1.64, ET 0.80 and PMF 1.82. Furthermore, most patients with these disorders were older than 60 years at the initial diagnosis, with median age of 65 years for PV, 68 for ET and 70 for PMF[14]. There are also very few cases reported in the pediatric age group; in this age range MPN's incidence is in fact really low (0.003 per 1'000'000 people)[15]. In general, a poor prognosis corresponds to an early onset of the disease [16,17].

Moreover, a Swedish population-based study has shown that although MPN patients overall have reduced life expectancy compared to the general population, the relative survival rate is lower in PMF compared to PV, and in PV compared with ET[18].

Limited information is available about the aetiology and risk factors of MPNs. That is because it requires an extensively investigated large cohort of individuals followed for long periods of time. Among the already identified risk factors can be included: diet, smoking, alcohol, allergies and body mass index[19].

Nevertheless, there has been a clear improvement in the patient's survival rate in the last years, partially due to the improvement of diagnosis and stratification techniques of these patients, but mainly because of the decreased probability of dying as a result of the disease complications[12].

1.3 Pathobiology and clinical manifestations

As described above, MPNs are clonal diseases of hematopoietic stem cells (HSCs) that induce excessive proliferation of the three main myeloid lineages: erythroid, granulocytic/monocytic and megakaryocytic. For this reason, even if MPNs are currently described as heterogenous disorders, they have been ranked into three main disorders: Polycytemia Vera (PV) with prevalent erythroid proliferation, Essential Thrombocythemia (ET) with predominant megakaryocytic hyperplasia, and Primary Myelofibrosis (PMF) related with myelofibrosis and hyperproliferation of granulocytes and megakaryocytes.

The hyperproliferation leads to the expansion of the hematopoietic compartment in BM, but also in other tissues such as spleen and liver. MPNs are characterized by

various degrees of extramedullary hematopoiesis (EMH), by high risk of thrombotic and hemorrhagic events and by spontaneous transformation into acute myeloid leukemia (AML)[7]. Evolution to AML occurs in 15-20% of PMF and 10% of PV/ET cases[20], and this phenomenon raised the hypothesis that MPNs can be considered as shades of biological continuum[21,22].

Nevertheless, despite the common origin from mutated hematopoietic progenitors, these disorders represent different clinical outcomes, as shown from patients' bone marrow biopsies (**Figure 1**)[12]. A discussion of the clinical manifestations, natural history and prognosis of PV, ET and PMF follows separately.

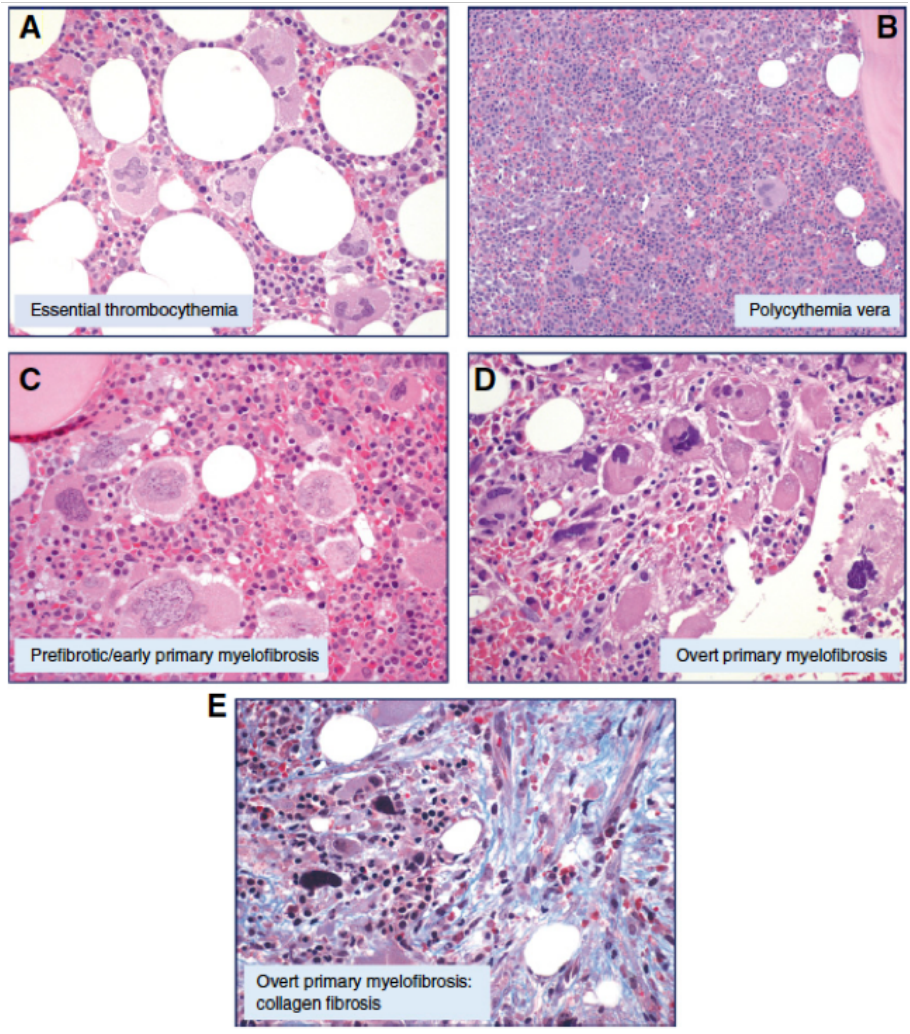

Figure 1: *Bone marrow biopsies from MPNs patients by Boveri from IRCCS Pavia (Hematoxylin and eosin H&E).* ***(A)*** *ET: Normocellular marrow with giant megakaryocytes.* ***(B)*** *PV: Hypercellular marrow with erythroid proliferation and some pleomorphic megakaryocytes.* ***(C)*** *PMF: Hypercellular marrow with granulocytic proliferation and large megakaryocytes with atypical bulbous nuclei.* ***(D)*** *Overt PMF: Hypercellular marrow, proliferation of atypical megakaryocytes forming dense clusters, and dilated vessels with intraluminal hematopoiesis.* ***(E)*** *Overt PMF (collagen fibrosis): Bands of collagen fibrosis within hematopoietic lacunae* (RUMI ET AL., BLOOD, 2017)[12].

***Polycythemia Vera (PV)*:** PV is the most common disease among the MPNs[12,13]. PV patients are characterized by an increased proliferation of red blood cells, granulocytes and platelets in the peripheral blood[23]. This condition, defined as Erythrocytosis, is mainly caused by hypersensitivity of PV erythroid precursors to Erythropoietin (EPO) accompanied by low serum EPO levels.

The EPO hypersensitivity was also demonstrated *in vitro*; PV hematopoietic stem/progenitor cells (CD34+) grow in the absence of any stimulus with EPO, generating endogenous erythroid colonies (EEC)[24,25]. EPO acts by binding to the erythropoietin receptor (EpoR) on the red cell progenitors surface and activating JAK2 signalling cascade, leading to the maturation of erythroblast cells[26].

The discovery in 2005 of the somatic mutation JAK2V617F, associated with almost all PV patients (96%), helped to explain the molecular mechanism and pathogenesis of this disorder[27,28]. In fact, the JAK2 gain of function mutation is able to activate erythropoietin receptor in a cytokine-independent manner. In addition, Tefferi *et al.* also demonstrated a positive correlation between the presence of this mutation and an increase in hemoglobin levels observed in patients[29]. Beyond the high level of hemoglobin and hematocrit, PV patients can show other asymptomatic manifestations among which pruritus, headache, dizziness and asthenia. Other disease features include leukocytosis, splenomegaly, bleeding, thrombosis and microcirculatory symptoms.

In a small subset of patients, PV may progress into myelofibrosis, with the presence of blasts in peripheral blood (PB) and/or Bone Marrow (BM)(10-20% in PB/BM)[30] and enlargement of the secondary hematopoietic sites, i.e. spleen and liver[31]. Progression of PV in post Polycythemia Vera Myelofibrosis (post-PV MF) increases the complication in terms of thrombosis and may be potentially fatal[32].

***Essential Thrombocythemia (ET)*:** ET is characterized by a persistent non-reactive thrombocytosis with high platelets count ($\geq 450 \times 10^9$)[33] due to the presence of a malignant and highly proliferating megakaryocyte (MK) clone[34,35]. ET patients usually display an elevated number of bone marrow MK with bizarre morphologies and hyperlobulated nuclei[36,37]. Even though the production of platelets is regulated by thrombopoietin (TPO), TPO serum levels in ET patients are usually normal, suggesting that this cytokine is not involved in a pathogenetic role[38].

Beyond thrombocytosis, in ET patients there are no specific symptoms, among these headache, light-headedness and blurred vision. The extremely high platelet count causes the increased in the risk of thrombosis, typically arterial, and bruising[39]. Paradoxically, despite the elevated number of circulating platelets, ET patients may

suffer from major hemorrhagic events, probably linked to the sequestration of Von Willebrand Factor (VWF) for the plasma[40].

Furthermore, the extramedullary hematopoiesis and the medullary fibrosis in ET patients is slight; splenomegaly is seen in about 20-25% of cases while hepatomegaly is seen in 15-20% of patients[41]. Fibrotic and leukemic transformation are considered rare events that occur in less than 5% of patients[42]. However, the risk of progression to more aggressive neoplasms may depend on the mutational profile of the disease. While JAK2V617F-mutant and MPL-mutant ET patients have been associated with a high risk to progress to PV or MF, CALR mutation is associated with a lower risk of fibrotic progression and a better prognosis[12,42].

***Primary myelofibrosis (PMF)*:** PMF, the most aggressive among MPNs[12,43,44], is characterized by stem cell-derived clonal myeloproliferation with the presence of dysplastic and hyperplastic megakaryocytes (MK) in the Bone Marrow (BM)[45]. The increase of MKs generate an altered microenvironment[46,47], resulting in abnormal cytokines expression, granulocytic proliferation, angiogenesis, BM stroma disruption, fibrosis, extramedullary hematopoiesis (EMH) that leads splenomegaly and hepatomegaly[45]. Moreover, in PMF peripheral blood cell counts may change during the progression, passing from a thrombocytotic state to a severe cytopenia[45]. Other disease features include anemia, leucocytosis and increased LDH serum level[48]. Additional constitutional symptoms include cachexia, fever, fatigue and weight loss[45].

Therefore, it is evident that PMF is a very heterogeneous disorder. Indeed, PMF is also characterized by the presence of CD34+ cells and circulating blasts in the peripheral blood. More than 20% of circulating blasts reflect a leukemic transformation[49]. Below is a more detailed discussion of the various clinical manifestations of PMF:

- *Bone marrow fibrosis*: An important hallmark of PMF is the excessive production and subsequent deposition of matrix fibers in the BM[50]. According to the grade of BM fibrosis, four stages of myelofibrosis (MF) have been defined, ranging from a non-fibrotic stage to a completely fibrotic marrow: MF-0, MF-1, MF-2, MF-3 (**Figure 2**)[51,52].The MF-0 and MF-1 stages are characterized by the absence of deposition of matrix fibers. On the other hand, in the MF-2 and MF-3 stages diffuse Reticulin deposition is observed which is afterwards replaced by Collagen (especially type I, IV), to finally induce the deposition of Fibronectin, Laminin, and Vitronectin[53].

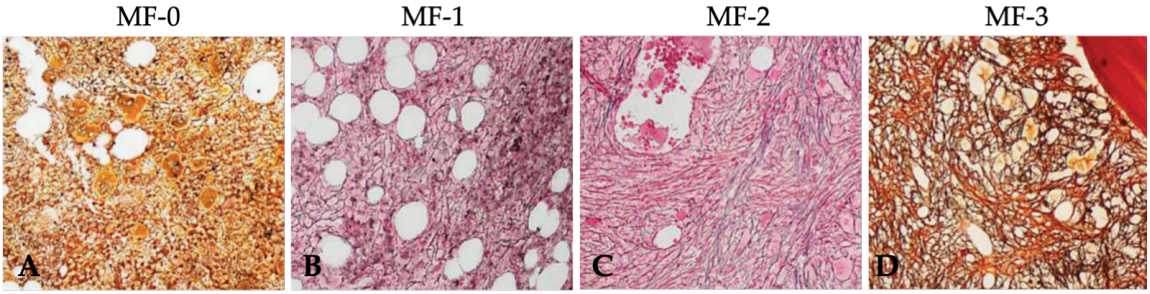

Figure 2**: Gomori staining of bone marrow biopsies used to mark matrix fibers adapted from Gianelli et al. A and B pictures represent a BM without fibrosis while C and D represent a late stage of fibrotic hypocellular BM in which reticulin and collagen fibers are overexpressed.* ***(A) *MF-0 stage.* ***(B)*** *MF-1 stage.* ***(C)*** *MF-2 stage.* ***(D)*** *MF-3 stage* (GIANELLI ET AL., MODERN PATHOLOGY, 2017)[52].

The molecular mechanisms involved in the deposition of matrix fibers have been extensively analyzed. PMF fibroblasts, responsible for collagen production, are completely functional[54]. However, they are secondarily stimulated to overproduce collagen by several pro-inflammatory cytokines and growth factors secreted by megakaryocytes and neutrophils in the BM niche[55]. In fact, it has been observed a massive release of various profibrogenic cytokines by the work of malignant megakaryocytes (MK) and monocytes in PMF patients' plasma, including transforming growth factor β (TGF-β), platelet-derived growth factor (PDGF), basic fibroblast growth factor (bFGF) and Interleukin 1 β (IL-1β)[56]. All these factors may stimulate fibroblasts to depose extracellular matrix[57]. Especially, TGF-β is considered the main regulator of BM fibrosis, because it is stored in platelet cytoplasmic granules and MKs and is able to induce fibroblasts activation[58,59,60]. The proof-of-principle of an effective implication of TGF-β in BM fibrosis was provided by Chagraoui *et al*. They transduced TGF-β Knock-Out (KO) and TGF-β Wild type (WT) BM-derived cells *ex vivo* with a retroviral vector carrying the Thrombopoietin (TPO) gene. Both groups, KO and WT, developed a myeloproliferative disorder, but only the mice WT developed a fibrosis in BM as well[61]. This is in line with the observation that high TGF-β concentrations have been found in BM and plasma of PMF patients with a high grade of fibrosis[62]. Nevertheless, beyond the TGF-β, other factors may take part to the fibrotic process, such as Matrix Metalloproteinases (MMPs). MMPs are a family of endopeptidases that can remodel extracellular matrix. In PMF patients MMPs are downregulated[63,64], suggesting that MMPs deregulation can lead to an increase accumulation of extracellular matrix components. Furthermore, in a recent work by ours research group it was demonstrated that MAF (V-Maf Avian Musculoaponeurotic Fibrosarcoma Oncogene Homolog) upregulation in PMF patients increased SPP1 (Secreted Phosphoprotein 1) plasma levels. SPP1 promotes fibroblasts and mesenchymal stromal cells proliferation and collagen production. Interestingly, clinical

correlation analysis uncovered that higher SPP1 plasma levels in PMF patients correlate with a more severe fibrosis degree and a shorter overall survival[65]. However, more studies will be necessary to better define the molecular mechanisms underlying the BM fibrosis.

- *Hyperplastic and dysplastic megakaryopoiesis*: Megakaryocytes (MKs) play a pivot role in the development of BM fibrosis[66]. MKs from PMF patients are of variable size and show nuclei with a bulbous aspect[67]. In particular, in the early stages of PMF, BM is characterized by an increased number of atypical micro-MKs or giant-MKs, especially located in the trabecular zone[68] and with an aberrant nuclear-cytoplasmic ratio[69]. In the following stages of fibrosis, the BM cellularity decreases and there is the development of enormous clusters of irregular MKs[46,47,53]. Moreover, in the BM of PMF patients it has been observed the phenomenon called emperipolesis, which consists in the transit of different cell types though the cytoplasm of MKs, including neutrophils and eosinophils[70]. During the transit of these cells, there may be the release of proteolytic enzymes, granules and growth factors involved in myelofibrosis pathogenesis[71].
- *Neoangiogenesis*: Another feature of PMF is the neoangiogenesis which consists in the formation of new blood vessels[72]. This process is regulated by Vascular Endothelial Growth Factor (VEGF), which has been reported as increased in the serum of PMF patients[73]. Of note, Rosti *et al.* demonstrated that endothelial cells obtained from splenic capillaries harboring the JAK2V617F mutation, suggesting that angiogenesis is also involved in the process of malignant transformation in myelofibrosis[74].
- *Osteosclerosis*: The osteoclastogenesis is regulated by two different cell types: osteoblasts, which produce the bone matrix, and osteoclasts, which degrade it. Osteosclerosis is a pathological condition characterized by abnormal hardening of bone and an increase in bone density. Bone marrow of PMF patients displays osteosclerosis with an increase of bone trabecules[75]. This condition is the result of the activity of Osteoprogerin (OPG), an inhibitor of osteoclastogenesis which has been found increased in PMF patients[76]. On the other hand, osteosclerosis in PMF is also trigged by the stimulation of osteoblast proliferation, mediated from the high levels of TGF-β present in PMF patients.
- *Inflammation*: Several studies have suggested that PMF is involved in the signaling of inflammatory cytokines, which may increase the risk of leukemic transformation[77]. Tefferi *et al.* identified several circulating pro-inflammatory cytokines in the plasma of PMF patients. Among these, IL-8, IL-2R, IL-12, IL-15 have proved to be predictive of inferior survival[78]. PMF has also been associated with high levels of the inflammation marker CRP (C-Reactive Protein)[79]. Moreover,

inflammation status can enhance the production of ROS, which in turn induce an enhanced inflammation and create a perpetual cycle that may promote the progression of the pathology[80].

- *Extramedullary hematopoiesis (EMH)*: As mentioned before, PMF is characterized by the abnormal presence of circulating hematopoietic CD34+ cells, with consequent migration of stem cells from bone marrow to other sites, among them spleen and liver (**Figure 3**)[56,81]. It has been shown that stem cells moving from the niche in response to proteolytic microenvironment in the BM. Indeed, elevated levels of Metalloprotease-9 (MMP9) and neutrophil elastase have been found in the plasma of PMF patients[82,83]. The increase of these proteolytic factors alter the expression of the chemoattractant molecule for CD34+, Canonical Receptor Chemokine Receptor 4 (CXCR4), expressed on the surface of CD34+ cells[84,85]. In addition, in PMF patients it has also been reported the increase of Vascular Cellular Adhesion Molecule 1 (VCAM-1) that could be involved in the HSCs mobilization[83].

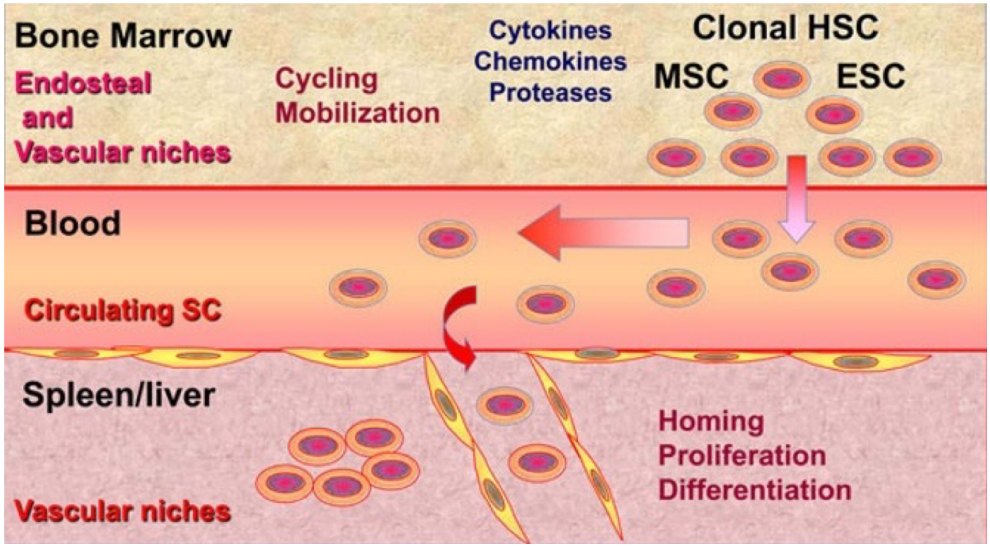

Figure 3: *Extramedullary Hematopoiesis in PMF (EMH). Stem cells move from niche to other sites, such as spleen and liver. The microenvironment in the bone marrow would favor the proliferation and mobilization of these cells from the bone marrow through blood flow. Once they reach these secondary sites, the generation of newly created vascular niches would favor their homing and differentiation resulting in an ECM in these organs* (LE BOUSSE-KERDILES, FIBROGENESIS & TISSUE REPAIR, 2010)[56].

1.4 Diagnosis

For the first time in 2001, the World Health Organization (WHO), in collaboration with hematopathologists, clinicians and scientists specialized in MPNs, attempted to provide an up-to-date classification system of MPNs based on diagnostic guidelines and published data available. This classification has been updated gradually each time new information emerged, the 5th is the most recent edition, to establish more

elaborate diagnostic approaches able to distinguish of various clinical manifestations of MPNs[86]. The WHO classification criteria of MPNs combine both clinical and laboratory features. These features, were subdivided in major and minor criteria [86,87]. Despite the recent progress in the understanding of the molecular pathogenesis of MPNs, an approach taking into consideration clinical, morphologic, and genetic features remains the gold standard for classification and the subsequent diagnosis of these pathologies. The rational for diagnostics has been influenced by two main factors: somatic mutations in the 3 driver genes (JAK2, CALR, MPL) and histologic features correlating with clinical outcome[88].

The 2016 revision of WHO classification has introduced various modifications to better clarify of the defining criteria for MPNs. Compared to last update of 2008, the new edition brings the following improvements[10,89]:

i. the inclusion of driver mutations shown to have an impact on clonality, diagnosis and prognosis, such as the recently discovered CALR mutation;
ii. the reduction of the hemoglobin threshold level and the usefulness of BM morphology as a reproducible criterion for the diagnosis of PV;
iii. the use of other features, including the lack of reticulin fibers in BM, to differentiate "true" ET from pre-PMF;
iv. the standardized morphologic criteria for the BM biopsies.

However, in the future the classification must be reviewed to better define diagnostic criteria for MPNs for the benefit of patients. The major and minor criteria are listed briefly in the following section for each of these disorders: PV, ET, PMF.

- *PV diagnosis:* Diagnosis of PV according to the 2016 WHO criteria is based on composite assessment of multiple parameters[42]. Diagnosis requires all 3 major criteria or the first 2 major and the minor criterion (**Table 2**)[42].

2016 WHO diagnostic criteria for PV

Major criteria:	
1.	Hemoglobin >16.5 g/dL in men or > 16 g/dL in women; or hematocrit >49% in men or > 48% in women or increased red blood cell mass
2.	Bone marrow tri-lineage proliferation with Pleomorphic mature megakaryocytes
3.	Presence of JAK2 mutation
Minor criterion:	
1.	Subnormal serum erythropoietin level
***DIAGNOSIS REQUIRES ALL 3 MAJOR CRITERIA OR THE FIRST 2 MAJOR AND THE MINOR CRITERION**	

Table 2: *2016 revised WHO diagnostic criteria for PV modified by Tefferi et al.* (TEFFERI ET AL., AJH, 2019)[42].

PV patients show an abnormal increase in red blood cells. In fact, erythrocytosis is one of the major diagnostic criteria, associated to reduced levels of Erythropoietin (EPO)[12]. Moreover, the detection of pleomorphic and mature megakaryocytes in bone marrow, in combination with JAK2 mutation, remains the best diagnostic method available[42]. JAK2 mutations play a crucial role in PV diagnosis. Almost all patients harbor JAK2 mutation; approximately 96% displaying somatic mutations in exon 14 (JAK2V617F), and a residual of 3% in exon 12[90,91]. MPL and CALR mutations are rare in PV[81]. The possibility of a false positive or false negative mutation test is rare to obtain nowadays. The mutation detection of JAK2V617 is highly sensitive (97%), however the wrong diagnosis could be caused by the concomitant measurement of serum EPO level which is subnormal in more than 85% of patients with PV[92]. Eventually, some patients with PV develop a PMF-like phenotype over time, referred to as post-PV MF (**Table 3**)[42].

2016 WHO diagnostic criteria for Post-PV MF and Pre-fibrotic PMF

Post-PV MF	**Pre-fibrotic PMF**
Major criteria:	**Major criteria:**
1. Prior documentation of WHO-defined PV 2. Bone marrow fibrosis grade ≥ 2 (Diffuse often coarse fiber network with or without evidence of collagenization, trichrome stain)	1. Typical megakaryocyte changes, a accompanied by ≤grade 1 reticulin/collagen fibrosis 2. Presence of JAK2, CALR or MPL mutations, or presence of other clonal markers, or absence of evidence for reactive bone marrow fibrosis 3. Not meeting WHO criteria for other myeloid neoplasms
Minor criterion:	**Minor criterion:**
1. Anemia or loss of phlebotomy requirement 2. A leukoerythroblastic blood smear 3. Increasing splenomegaly 4. Development of constitutional symptoms	1. Anemia not otherwise explained 2. Leukocytosis ≥ 11 × 109/L 3. Palpable splenomegaly 4. Increased serum lactate dehydrogenase
***DIAGNOSIS REQUIRES ALL 2 MAJOR CRITERIA AND 2 MINOR CRITERION**	***DIAGNOSIS REQUIRES ALL 3 MAJOR CRITERIA AND ONE MINOR CRITERION**

Table 3: *Comparison between the 2016 revised WHO diagnostic criteria for Post-PV MF and Pre-fibrotic PMF modified by Tefferi et al.* (TEFFERI ET AL., AJH, 2019)[42].

- *ET diagnosis*: Diagnosis of ET follows the 2016 WHO criteria and is based on the composite assessment of multiple parameters[42]. Diagnosis requires all 4 major criteria or the first 3 major and the minor criterion (**Table 4**)[42].

2016 WHO diagnostic criteria for ET

Major criteria:	
1.	Platelets ≥450 × 109/L
2.	Bone marrow megakaryocyte proliferation and loose clusters
3.	Not meeting WHO criteria for other myeloid neoplasms
4.	JAK2/CALR/MPL mutated
Minor criterion:	
1	Other clonal marker present or no evidence of reactive thrombocytosis
***DIAGNOSIS REQUIRES ALL 4 MAJOR CRITERIA OR THE FIRST 3 MAJOR AND THE MINOR CRITERION**	

Table 4: *2016 revised WHO diagnostic criteria for ET modified by Tefferi et al.* (TEFFERI ET AL., AJH, 2019)[42].

Thrombocytosis is a major diagnostic criterion for ET. JAK2V617F is also found in ET (55%), while exon12 mutations are very rare. CALR mutations occur in 15-24% and MPL mutation in 4%. Furthermore, up to 20% of patients with ET might be negative for all 3 mutations (triple-negative patients)[42]. It is also important to consider that myelodysplastic syndrome MDS/MPS can mimic ET in their manifestation[93]. Since most patients with pre-fibrotic PMF (pre-PMF) present thrombocytosis similar to ET[94], BM histology is the most important criterion for distinguishing pre-PMF from ET. For this reason, the 2016 new criteria include bone marrow examination, a very important feature in order to make an accurate ET diagnosis and distinguish it from pre-PMF (**Table 5**)[42]. Megakaryocytes in ET are large and form loose clusters, while in pre-PMF display hypercellularity with hyperchromatic and irregular nuclei and form tight clusters[42].

2016 WHO diagnostic criteria for Post-ET MF and Pre-fibrotic PMF

Post-ET MF	**Pre-fibrotic PMF**
Major criteria:	**Major criteria:**
1. Prior documentation of WHO-defined ET 2. Bone marrow fibrosis grade ≥ 2 (Diffuse often coarse fiber network with or without evidence of collagenization, trichrome stain)	1. Typical megakaryocyte changes, a accompanied by ≤grade 1 reticulin/collagen fibrosis 2. Presence of JAK2, CALR or MPL mutations, or presence of other clonal markers, or absence of evidence for reactive bone marrow fibrosis 3. Not meeting WHO criteria for other myeloid neoplasms
Minor criterion:	**Minor criterion:**
1. Anemia and ≥ 2 g/dL decrease in hemoglobin level 2. A leukoerythroblastic blood smear 3. Increasing splenomegaly 4. Development of constitutional symptoms 5. Increased serum lactate dehydrogenase	1. Anemia not otherwise explained 2. Leukocytosis ≥ 11 × 109/L 3. Palpable splenomegaly 4. Increased serum lactate dehydrogenase
***DIAGNOSIS REQUIRES ALL 2 MAJOR CRITERIA AND 2 MINOR CRITERION**	***DIAGNOSIS REQUIRES ALL 3 MAJOR CRITERIA AND ONE MINOR CRITERION**

Table 5: *Comparison between the 2016 revised WHO diagnostic criteria for Post-ET MF and Pre-fibrotic PMF modified by Tefferi et al.* (TEFFERI ET AL., AJH, 2019)[42].

- *PMF diagnosis*: Diagnosis of PMF follows the 2016 WHO criteria and is based on composite assessment of multiple parameters (**Table 6**)[45]. The PMF is a very heterogeneous disorder. Diagnosis of PMF is mainly based on bone marrow morphology. Presence of driver mutations (JAK2, CALR, MPL) aids but is not essential for diagnosis. The non-driver mutations (ASXL1, SRSF2, U2AF1) might contribute to development of disorder[45]. The diagnosis may be complicated by the fact that almost 30% of patients are asymptomatic at the beginning of the pathology[95]. In addition, it is necessary to distinguish two categories of patients: prefibrotic PMF (pre-PMF) and overt PMF. Pre-PMF BM biopsy shows hypercellularity with an increased number of neutrophils and granulocytes and atypical megakaryocytes with "cloud-like" and "balloon-like" nuclei[12]. In overt PMF, megakaryocytic proliferation and atypia are combined with deposition of fibrotic matrix in the bone marrow (reticulin and/or collagen)[12,45]. In table 6 diagnostic criteria for pre-PMF and overt PMF are reported according to 2016 WHO revision (**Table 6**)[45].

2016 WHO diagnostic criteria for overtly fibrotic and pre-fibrotic PMF

Overtly fibrotic PMF	Pre-fibrotic PMF
Major criteria:	**Major criteria:**
1. Typical megakaryocyte changes, a accompanied by ≥grade 2 reticulin/collagen fibrosis 2. Presence of JAK2, CALR or MPL mutations, or presence of other clonal markers, or absence of evidence for reactive bone marrow fibrosis 3. Not meeting WHO criteria for other myeloid neoplasms	1. Typical megakaryocyte changes, a accompanied by ≤grade 1 reticulin/collagen fibrosis 2. Presence of JAK2, CALR or MPL mutations, or presence of other clonal markers, or absence of evidence for reactive bone marrow fibrosis 3. Not meeting WHO criteria for other myeloid neoplasms
Minor criterion:	**Minor criterion:**
1. Anemia not otherwise explained 2. Leukocytosis ≥ 11 × 109/L 3. Palpable splenomegaly 4. Increased serum lactate dehydrogenase 5. A leukoerythroblastic blood smear	1. Anemia not otherwise explained 2. Leukocytosis ≥ 11 × 109/L 3. Palpable splenomegaly 4. Increased serum lactate dehydrogenase
***DIAGNOSIS REQUIRES ALL 3 MAJOR CRITERIA AND ONE MINOR CRITERION**	***DIAGNOSIS REQUIRES ALL 3 MAJOR CRITERIA AND ONE MINOR CRITERION**

Table 6: *Comparison between the 2016 revised WHO diagnostic criteria for Overtly fibrotic and Pre-fibrotic PMF modified by Tefferi et al.* (TEFFERI ET AL., AJH, 2018)[45].

1.5 Prognosis

Although PV, ET and PMF are chronic malignancies, the overall survival for these pathologies is short. It is influenced by several risk factors, including advanced age, transfusion dependency, thrombosis, leukocytosis, circulating blasts and karyotype.

- *PV prognosis*: Different prospective studies revealed that the mean age for PV diagnosis to occurs is 60 years and PV patients have a relatively long median survival (14 years than extend to 24 years for younger patients). Leukemic transformation rates at 10 years are low and estimated at 3% of cases[42].
- *ET prognosis*: ET is the most indolent among the MPNs since it has been demonstrated that the relative survival is higher in ET as compared with PMF or PV and is approximately 20 years (33 years for the younger patients). Leukemic transformation rates at 10 years are very rare, estimated at less than 1% of cases[18,42,96].
- *PMF prognosis*: PMF is the most severe disorder among MPNs with the worst prognosis. A recent study demonstrated that the median survival in PMF patients is approximately 6 years[43,44], while the median age at clinical presentation is 70[12,13]. In the last years, several prognostic models for PMF have been introduced and have allowed to determine the most appropriate therapy for the individual patient[97]. The initial strategy developed in 2009 was the International Prognostic Scoring System (IPSS). IPSS is applicable to the patients at the time of diagnosis and use five clinically derived risk variables: age > 65 years, hemoglobin < 10 g/dl, leukocyte count > $25x10^9$/l, circulating blasts ≥ 1% and constitutional symptoms. IPSS defined 4 risk categories: low, intermediate-1, intermediate-2 and high, with corresponding median survivals of 11.3, 7.9, 4 and 2.3 years respectively[98]. In 2010, IPSS was upgraded to time–depending prognostic model DIPSS (Dynamic International Prognostic Scoring System). Unlike the IPSS, this model can be used at any time during the clinical course of the pathology[99]. DIPSS was subsequently modified into DIPSS-plus, in order to include other risks factors such as unfavourable karyotype (e.g. inv(3), +8, -7/7q-, 12p-). DIPSS-plus identifies four risk categories, low (no risk factors), intermediate-1 (one risk factor), intermediate-2 (2 or 3 risk factors) and high (4 or more risk factors) with respective median survivals of 15.4, 6.5, 2.9 and 1.3 years[100]. Moreover, Vannucchi *et al.* have included in DIPSS-plus high-risk mutations for survival in PMF, such as the ones involving ASXL1, SRSF2, EZH2, IDH1/2. These mutations are associated with to shorter overall survival and increased risk of leukemic transformation[101]. On the other hand, Tefferi *et al.* identified several circulating cytokines (i.e. IL-8, IL-2R, IL-12, IL-15) in PMF patients which have been considered an independent prognostic criterion and for this reason included in the DIPPS plus[78]. MIPSS70 (Mutation-enhanced International Prognostic Scoring System for transplant-age patients), and its updated versions MIPSS70 plus[102] and MIPSS70 version 2.0[103], is the newest prognostic system for PMF which includes clinical risk, additional mutations and karyotype, adjusting for sex and severity. MIPSS70 has been mainly developed in

order to be directly relevant for transplant decision making[97]. More recently, Grinfield and colleagues developed a new prognostic model for predicting outcomes in PMF patients. In particular, they created a multistage prognostic model, integrating 63 clinical and genomic variables, capable of generating personally tailored predictions of clinical outcomes, improving predictive accuracy[104].

1.6 Treatments

In recent years new and improved treatments have changed survival patterns in some MPNs[19]. However, drug therapy in MPNs is neither curative nor capable of preventing disease progression so far. The only curative approach is allogenic hematopoietic stem cell transplant (HSCT), which is currently the first treatment of choice for high-risk patients[105,106,107].

- *PV and ET therapy:* Some clinical trials have shown an increased risk of acute leukemia evolution, fibrotic transformation and arterial thrombosis correlated with use of some drugs[108,109,110]. Therefore, one has to be careful when in introducing new drugs[81]. The primary aim of current therapy in PV and ET includes thrombosis prevention and symptoms alleviation. For this reason, treatments with Aspirin, Hydroxyurea and Phlebotomy have shown to be effective alleviating symptoms. In addition, cytoreductive therapies include the use using of Interferon-α, for younger patients, and Busulfan, for older patients[81].
- *PMF therapy:* In myelofibrosis, HSCT is the only curative option for PMF patients. Current drug therapies for PMF are mostly palliative, to alleviate symptoms such as: anemia, splenomegaly and EMH-associated pulmonary hypertension. Anemia is mainly treated using Lenalidomide, Thalidomide and Prednisone[111]. Instead, Hydroxyurea is the drug of choice for splenomegaly[112]. After the discovery of JAK2 mutation, JAK2 inhibitors (JAK2i) have substituted conventional therapy. Ruxolitinib is the first JAK2i approved by FDA for the treatment of PMF[113]. This drug acts by binding and stabilizing the active conformation of the kinase[114]. Clinical trials highlight its ability to reduce constitutional symptoms, splenomegaly and levels of inflammatory cytokines. Moreover, Ruxolitinib plays a significant role in improving the overall survival[111,115]. However, several trials are trying to test combinatorial protocols, in association with Ruxolitinib or new drugs, to try to improve the treatment of PMF.

1.7 Driver mutations

In the last years, several somatic mutations have been described in MPNs. The discovery and characterization of oncogenic driver mutations in MPNs has revolutionized our understanding of these complex and heterogeneous disorders. Driver mutation in PV, ET and PMF are often mutually exclusive and hit the genes Janus Kinase 2 (JAK2), Calreticulin (CALR) and Myeloproliferative Leukemia Virus Oncogene (MPL)(**Figure 4**)[116].

These mutations have been called drivers because of their key role in leading the clonal expansion. JAK2 is the most frequently mutated gene in MPNs, while CALR and MPL mutations are absent in PV, except for rare reports[43]. This difference may be partially explained by the molecular mechanisms related to the different mutations; in fact, JAK2V617 activates the 3 main cytokine receptors, Erythropoietin Receptor (EpoR), Thrombopoietin Receptor (TpoR/MPL) and Granulocyte Colony-Stimulating Factor Receptor (G-CSF-R); whereas CALR and MPL mutants are restricted to MPL activation[117]. Below is an overview of the most characterized mutation so far.

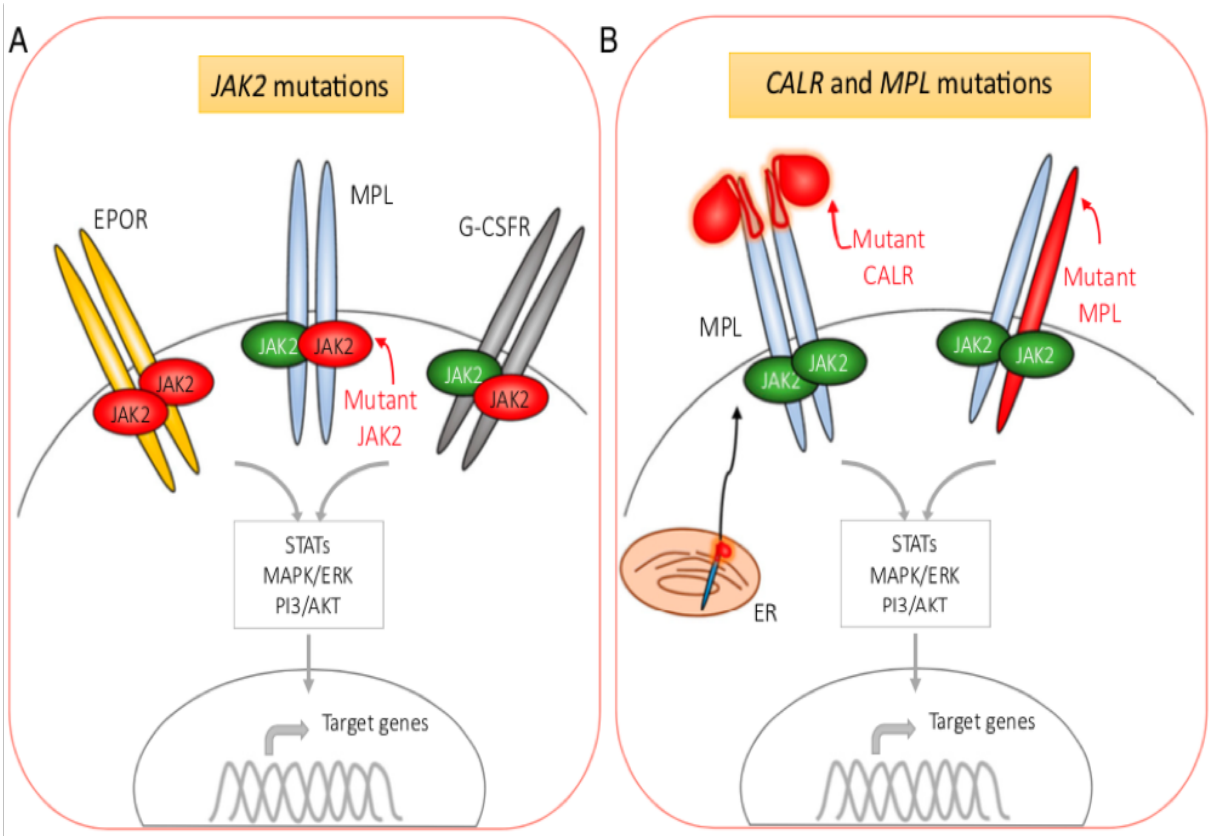

Figure 4: *Mutation in JAK2, CALR, and MPL drive excessive myeloproliferation via constitutively activation of JAK2 downstream signaling.* ***(A)*** *JAK2 mutant, shown in red, is constitutively active and leads to variable levels of erythroid, megakaryocytic and granulocytic proliferation and differentiation.* ***(B)*** *Mutations in CALR and MPL result in aberrant activation of signaling downstream of the MPL receptor. Both mutations in CALR and MPL result in receptor dimerization and activation of JAK2-STAT pathway* (NANGALIA ET AL., BLOOD, 2017)[116].

***JAK2 mutation*:** In 2005, the identification of a point mutation in JAK2 gene paved the way for greater knowledge of the pathophysiology of MPNs[27,28,118,119,120]. JAK2V617F consists a G to T somatic mutation at nucleotide 1894 in exon 14, resulting in the substitution from Valine (V) to Phenylalanine (F) at codon 617. This mutation can be found in around 95% of PV cases and 50% to 60% of ET and PMF cases[117]. A transition from heterozygosity to homozygosity is not unusual, due the occurrence of mitotic recombination along the short arm of chromosome 9 (9pLOH)[121]. From the phenotypic point of view, JAK2 mutations are generally associated with older age, leukocytosis, risk of thrombocytosis, higher hemoglobin level and lower platelet count[122].

JAK2 is a member of the Janus kinase (JAK) family. Its gene is located on the short arm of chromosome 24 and contains twenty five exons, while JAK2 protein is a tyrosine kinase which takes part in several signaling pathways, including the cytokine signaling[123]. As shown in figure 5, protein structure of JAK contains 2 kinase domains at the C-terminus. The first one, JH1, shows catalytically activity upon cytokine stimuli, while the second one, JH2, is a catalytically inactive pseudo-kinase that prevents self-activation of the kinase domain. At the N-terminus, a SH2 domain is present an able to mediate the association with the cytoplasmic tail of other cytokines receptors. In the same region is located the FERM domain, that avoids the noncovalent binding at of JAKs to cytokine receptors (**Figure 5**)[77].

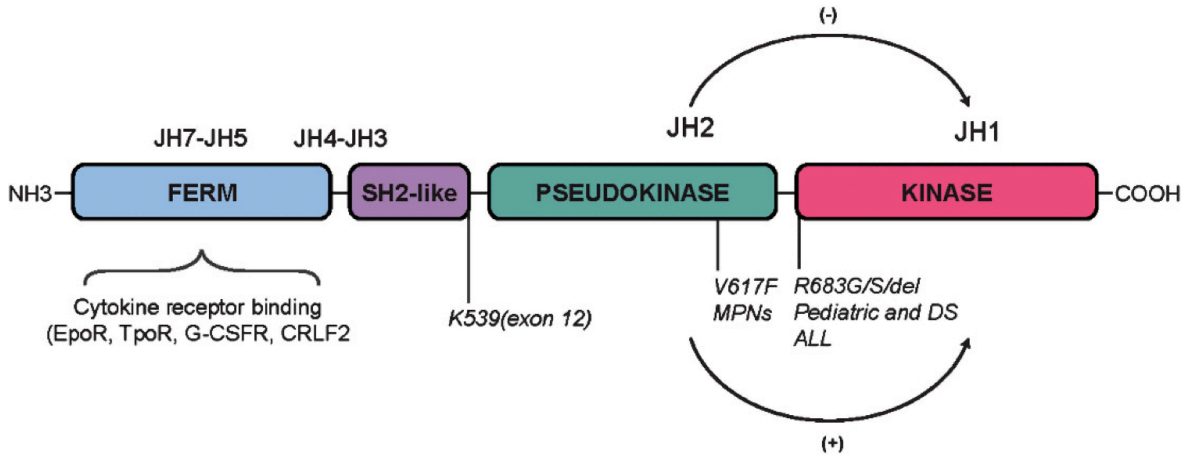

Figure 5: Structural and functional domains of JAK2 protein (VAINCHENKER ET AL., ONCOGENE, 2013)[77].

In physiological conditions, the association of JAKs with different receptors, among which EpoR, TpoR/MPL and G-CSF-R, induce conformation changes of these receptors with consequent activation of JAKs by trans-phosphorylation. Once activated, JAKs can phosphorylate other substrates, including the transducer and

activator of transcription (STAT). Subsequently, phosphorylated STATs migrate to the nucleus and activates the transcription of their target genes[117].

The mechanism of action of JAK2 mutants is not completely understood and differs depending on the type of the mutations, but it has been demonstrated that the V to F substitution in JAK2 induces cytokine independence or hypersensitivity[28], and subsequently constitutive activation of STATs proteins[124].

In addition, some evidences have revealed that JAK2V617F acts like an epigenetic modifier, affecting chromatin accessibility through the phosphorylation of histone 3 at the Tyrosine 41 (H3Y41)[125,126]. However, the role of these modification in MPNs pathogenesis of MPNs is not well known.

Interestingly, other JAK2 mutations in exon 12 have been identified in around 2-4% of JAK2V617F-nonmuted PV patients. The most common mutations in exon 12 are N542-E543 and E543-D544 deletions[127].

In order to understand the pathogenetic role of JAK2 mutation, several mouse models have been development through several approaches: retroviral transduction of HSCs followed by bone marrow transplantation, transgenic mice and constitutive or inducible knock-in (KI) mice[128,129,130]. In each of these models, JAK2 mutations induced a myeloproliferative disorder that may also evolve to a ET-like or PV-like phenotype, depending on the expression level of JAK2V617F[131].

Indeed, it also been shown that MPNs phenotype in humans may be related with JAK2V617F allele burden. A more severe fibrotic phenotype is in fact associated with a higher burden[91]. Moreover, transgenic mice with JAK2 exon 12 mutation have developed isolated erythrocytosis[132].

However, all these murine models seem to originate from several hematopoietic stem cells, while the human MPNs are monoclonal disorders deriving from the alteration of a single hematopoietic stem cell[133]. For this reason, it has been hypothesized that JAK2V617F might not be the initiating molecular event and that additional mutations could precede the acquisition of JAK2 mutation[134,135].

***MPL mutation*:** Somatic MPL mutation was described for the first time in 2006[90,136]. MPL gene is located on chromosome 1p34 and is composed of twelve exons. It encodes for the TPO receptor and is related to the development and survival of megakaryocytes.

The most frequent mutation MPLW515L consists of a G to T transition at nucleotide 1544 resulting in a Tryptophane (W) to Leucine (L) substitution at codon 515 of the transmembrane region (exon 10).

However, several other mutations have been described[137]. A number of non-canonical mutations of MPL has also been found in triple-negative ET[138,139]. These mutations are generally in a heterozygous state but can be homozygous during progression of the pathology[137]. Mutations are restricted to patients with ET or PMF at a frequency of approximately 3% and 5%, respectively[140]. Interestingly, in a small number of patients MPL mutations can co-occur alongside with JAK2 mutations, thus increasing the degree of complexity[141].

Under physiological conditions, the binding of Thrombopoietin (TPO) to the receptor induces its homodimerization and, subsequently, activation of the JAK2/STAT signaling pathway. In light of this, all these mutations lead to the constitutive activation of MPL and JAK2[142].

Studies on a murine model of MPLW515L recapitulate many phenotypic features of myelofibrosis in patients, including splenomegaly, megakaryocytic hyperplasia and bone marrow fibrosis[136].

CALR mutation: At the end of 2013 two independent groups have discovered a new somatic mutation in CALR gene in approximately 50-60% of ET and 75% of PMF patients[143,144].

In particular, Klampfl and colleagues performed whole-exome sequencing to identify somatic mutations acquired in 6 PMF patients without mutations in JAK2 or MPL. Surprisingly, they have detected insertions or deletions in exon 9 of CALR in all analyzed patients. Next, a screening for mutation in CALR exon 9 was performed on a largest cohort of samples by means of polymerase chain reaction (PCR). They discovered that CALR mutations are mutually exclusive in ET and PMF patients, while absent in PV patients[143].

Simultaneously, exome sequencing was carried out by Nangalia *et al.* on 151 MPNs patients. They have found somatic CALR mutations in about 80% of samples with nonmutated JAK2 or MPL. However, in this study, 3 patients carrying double mutations (JAK2 and CALR) were found[144].

About 80% of MPN patients harbor one of two variants in exon 9: a 52-bp deletion (type 1: c.1092_1143del52) and a 5-bp insertion (type 2: c.1154_1155insTTGTC)[117]. However, more than 40 different types of mutations have been reported, which are classified into Type 1-like and Type 2-like variants on the basis of their structural similarities to type 1 and type 2 CALR variants respectively[145]. CALR mutations are typically heterozygous, although a few cases of homozygous mutations can occur[146]. Interestingly, variant allele frequency (VAF) for mutants CALR in ET is relatively high

compared to JAK2, suggesting that CALR mutants may give an enhanced clonal advance[147].

The clinical course in CALR patients appear to be more indolent than the one of JAK2-mutated patients. Moreover, CALR mutations are generally associated with younger age, male sex, leukocytosis, higher platelet count and lower hemoglobin levels[145]. In ET, CALR type 2 mutations were associated with significantly higher platelet count[148] while, in PMF they were correlated with higher risk category, large amount of circulating blasts, higher leukocyte count and inferior survival[145].

The identification of such mutations was surprising because, in contrast with JAK2 and MPL, this gene is neither a cytokine receptor nor a signaling molecule known as a participant in JAK-STAT signaling. CALR gene encodes for a multifunctional Endoplasmic Reticulum (ER) chaperone.

Recent studies have established that CALR mutants can activate MPL and subsequently JAK-STAT pathway[149,150]. However, the precise mechanism of action of CALR mutants hasn't been fully elucidated.

In particular several questions remain to be addressed: what are the relationships between CALR mutation and the Unfolded Protein Response (UPR)? CALR mutations could be affecting the sensitivity to oxidative stress and ROS production? And if so, can oxidative stress induce genomic instability and increase DNA damage observed in MPNs? A detailed overview regarding CALR follows in the next chapters.

1.8 Non-driver mutations

The 3 main driver mutations do not explain the entire heterogeneity of MPNs. The genomic landscape of these disorders is more complex than initially thought and involves several mutant genes[117].

Thanks to High-resolution genome analysis it has been allowed the identification of several additional mutated genes in MPNs, including epigenetic regulators (i.e. TET2, DNMT3, ASXL1, EZH2, IDH1/IDH2), splicing factors (i.e. SRSF2, SF3B1, U2AF1, ZRSR2) and transcriptional factors (i.e. TP53, RUNX1, FOXP1)[151,152].

Most of these mutations are loss of function and act as dominant-negative or complete homozygous loss. However, none of these mutations is restricted to MPNs, underscoring the continuum between the different myeloid malignancies.

Moreover, it has been shown that the genomic landscape and the order of acquisition of additional mutations may affect prognosis (**Figure 6**)[117].

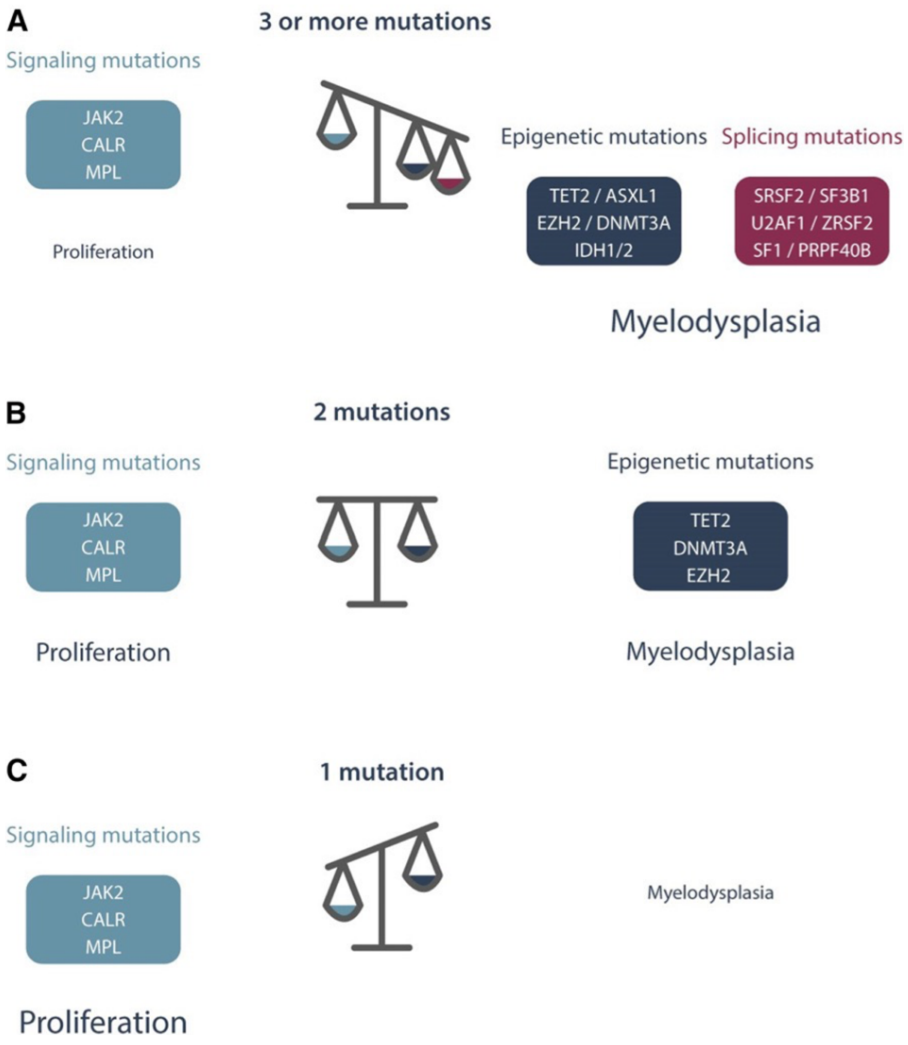

Figure 6: *Genetic and epigenetic landscape in MPNs by Somersault.* ***(A-C)*** *The 3 drivers mutations lead to a myeloproliferative phenotype. All of the additional mutations in genes involved in epigenetics and splicing modify the differentiation and confer a myelodysplastic phenotype. Moreover, some of them, such as TET2, DNMT3A and EZH2, clearly play an important role in pathology initiation. On the other hand, additional mutations involved in splicing induce myelodysplastic features leading to MF, cytopenia, and eventually progression to leukemia* (VAINCHENKER ET AL., BLOOD, 2017)[117].

The number of detected mutations, representing an indirect measure of genetic complexity, allowed to identified the high-risk patients[101]. In most of cases of PV and ET only one mutation in driver genes is found, while in the majority of PMF cases 3 or more somatic mutations are present, suggesting their role in MPN progression. In fact, the presence of addition mutations, as well as the 3 drivers mutations, increases the myelodyspalstic features and severity of these disorders[117].

2. CALRETICULIN

2.1 Gene

Calreticulin (CALR) gene is located in the short arm of chromosome 19 (19p13.2) and contains nine exons for a length of about 3,6 Kbp[147].

This gene is highly conserved in different species of vertebrates and invertebrates[154]. cDNA encoding CALR have been isolated from human, mouse, rabbit, rat, *Xenopous*, *Aplysia*, *Drosophila*, *S. mansoni*, *C. elegans* cDNA libraries[155,156,157,158,159,160,161,162]. For instance, the nucleotide sequences of the mouse and the human gene show 70% identity. With the exception of introns 3 and 6, the organizations of these genes are almost the same[153,118]. This high degree of gene and nucleotide conservation is in agreement with earlier observations that the amino acid sequences of CALR of mouse and human share 95% similarity, especially in N-terminal sequence[164].

Several putative regulatory elements are found in the promoter region of CALR gene such as binding sites to transcription factors AP-1 and AP-2, typically present in genes that are active during cellular proliferation. In addition, the presence of multiple GC-rich sites in the promoter, including Sp1-binding site, H4TF-1-binding site and four CCAAT sequences, suggests that its protein product may have a housekeeping function[155,153,163,165]. Interestingly, multiple poly G sequences are present in the human glucose-regulated protein Grp78 and Grp94 involved in Endoplasmic Reticulum (ER) stress response[166]. These data indicate that these sequences may regulate the protein level in the ER lumen and be responsible for the ER stress-induced activation of CALR gene[163].

Indeed, different stimuli can trigger CALR gene expression. It has been demonstrated that depletion of intracellular Ca^{2+} stores is involved with its activation[157]. An interesting observation is that Calreticulin promoter is also activated by Zinc[167], heat shock[168], viral infection[169] and amino acid starvation[170].

There is no evidence regarding the possible alternative splicing phenomena. Currently, two mRNA isoforms have been identified but only one encoding the protein (1.9 Kbp); the function of the second one is yet unknown[155].

2.2 Protein

Calreticulin (CALR) protein was first isolated in the 1974 from sarcoplasmic reticulum as a high affinity calcium-binding protein by MacLennan group[171]. It is a 46 kDa

protein[155,172] and it's one of the five main members of the family of abundant Endoplasmic Reticulum (ER) resident proteins[164].

CALR is a multifunctional protein, these distinct functional properties may be associated to each of the three structural domains of CALR. In fact, structural analysis of the amino acid sequence of CALR indicates that the protein can be divided into at least three distinct domains: N-domain (exons 1, 2, 3, 4), P-domain (exons 5, 6, 7) and C-domain (exons 8, 9)(**Figure 7**)[164,155,173].

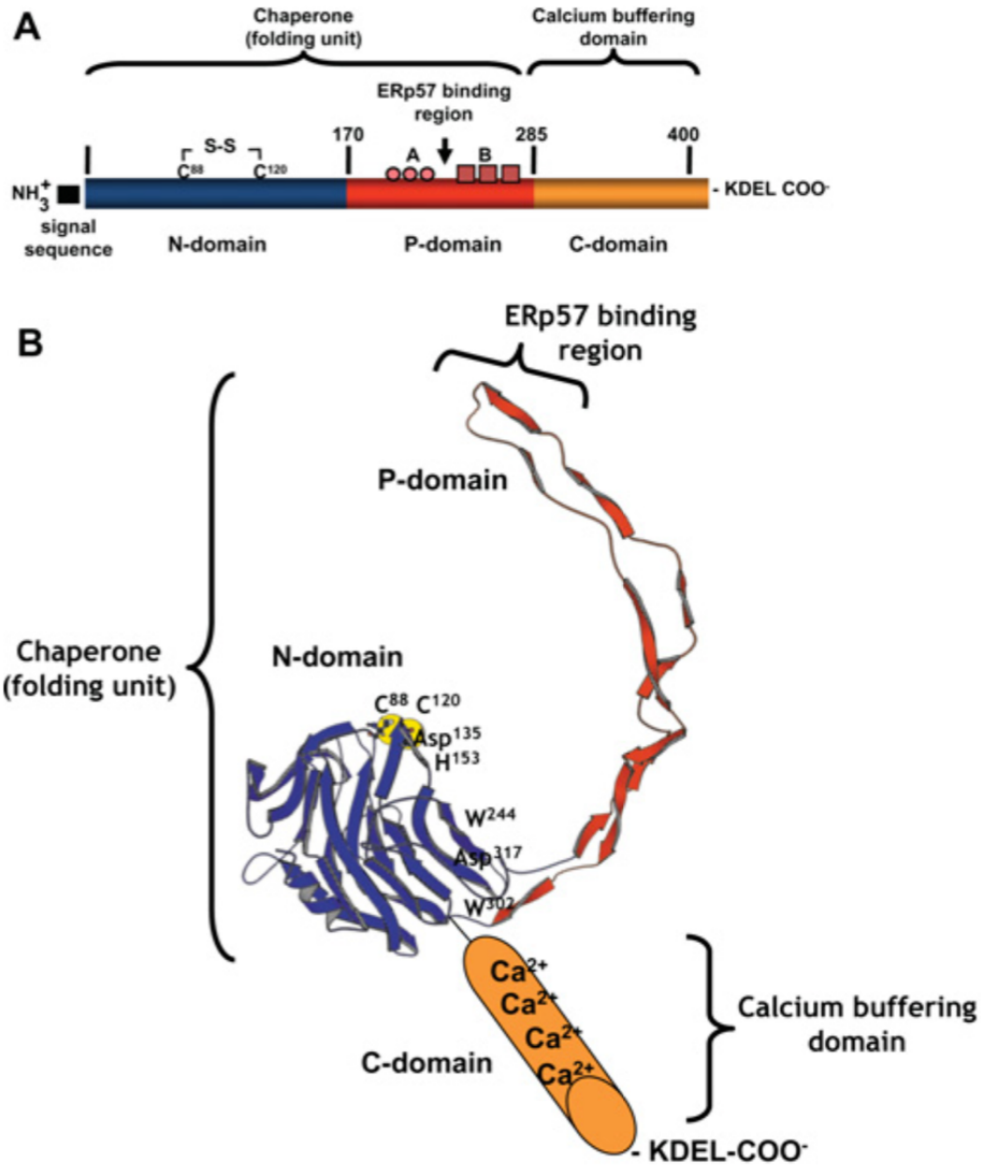

Figure 7: ***(A)*** *Linear representation of CALR domains;* ***(B)*** *Three-dimensional model of the N- and P-domain of CALR based on NMR studies by Ellgaard et al. CALR contains a globular N-domain (in blue) and central proline-rich domain (in red) which forms a characteristic loop. The C-domain contains a large number of negatively charged amino acids and is involved in high-capacity Ca^{2+} storage (in orange). Yellow balls represent the cysteine residues which form a thiol bridge in CALR (Cys^{88} and Cys^{120})*(MICHALAK ET AL., BIOCHEM J, 2009)[174].

The N-terminal region is a highly conserved globular domain containing eight antiparallel β-strands. The N-domain of CALR includes the polypeptide- and carbohydrate-binding site[175,176], a Zn^{2+}-binding site[177] and a disulfide-linkage site[178]. This domain can interact with α-integrins[153] and DNA-binding site of steroid receptor[180]. The disulfide bond composed by cysteine residues in the N-domain can interact with P-domain to generate important chaperone function of CALR[175,181]. *In vitro* studies indicate that the polypeptide- and oligo-saccharide-binding regions are located in the N- and P-domain of CALR[175]. Oligosaccharide binding by this region induces conformational change in the chaperone, thereby influencing polypeptide binding[182]. There is a requirement for both the N-domain, with the oligosaccharide- and polypeptide-binding regions, as well as the P-domain, containing the secondary binding sites, to generate full chaperone function of CALR.

The P-domain is a highly plastic region that acts as a structural backbone taking part in chaperone activity[183]. Nuclear magnetic resonance (NMR) studies reveal that the structure of P-domain of CALR contains an extended region stabilized by three antiparallel β-sheets[172]. This domain is proline-rich, contains three sets of two repetitive regions which are responsible for the protein-folding function of CALR. These repeated amino acid sequences are important for the lectine-like function of the protein[185]. Moreover, *in vitro* analysis indicate that this region of CALR binds Ca^{2+} with a relatively high affinity (K_d = 1 μM) but low capacity (1 mol of Ca^{2+} per mol of protein)[186,187].

The C-terminal domain is very interesting because is highly acidic and responsible for Ca^{2+} buffering activity. Its terminal portion ends with ER KDEL (Lys-Asp-Glu-Leu) retention/retrieval signal. C-domain binds over 50% of ER luminal Ca^{2+} with high capacity (25 mol of Ca^{2+} per mol of protein) and low affinity manner (K_d = 2 μM)[188]. It has been reported that C-domain is important for CALR retrotranslocation from ER lumen to the cytosol[189]. Further study also indicates that this retrotranslocation process is triggered by ER Ca^{2+} depletion[190].

In summary, C-domain of CALR is involved in determining Ca^{2+} storage and the N domain, in conjunction with P-domain, may form a functionally important folding unit responsible for chaperone function of CALR.

2.3 Localization

It's now well known that Calreticulin (CALR) is a resident Endoplasmic Reticulum (ER) protein that is involved in regulation of intracellular Ca^{2+} homoeostasis and in the folding of newly synthesized proteins. At the same time, CALR has been implicated in a number of cytoplasmic and nuclear processes as demonstrated by Afshar *et al*. In

fact, CALR is located in the cytoplasm, at the cell membrane and extracellular matrix. The ability of CALR to retrotranslocate from the ER lumen to the cytosol explains how CALR can change compartments and modulate cell adhesion, transcription, and translation[189].

2.4 Physiological functions of Calreticulin

Calreticulin (CALR) has been implicated to play a role in many biological processes, including functions inside and outside the Endoplasmic Reticulum (ER).

It's involved in the control of protein folding interacting with various other ER chaperones. CALR also plays a crucial role in regulating intracellular Ca^{2+} homeostasis and cellular stress response.

The role of CALR outside the ER is also extensive, including functions in immunity, development and differentiation, cell migration and adhesion. Taken together, CALR may be defined as a multifunctional protein (**Figure 8**)[191].

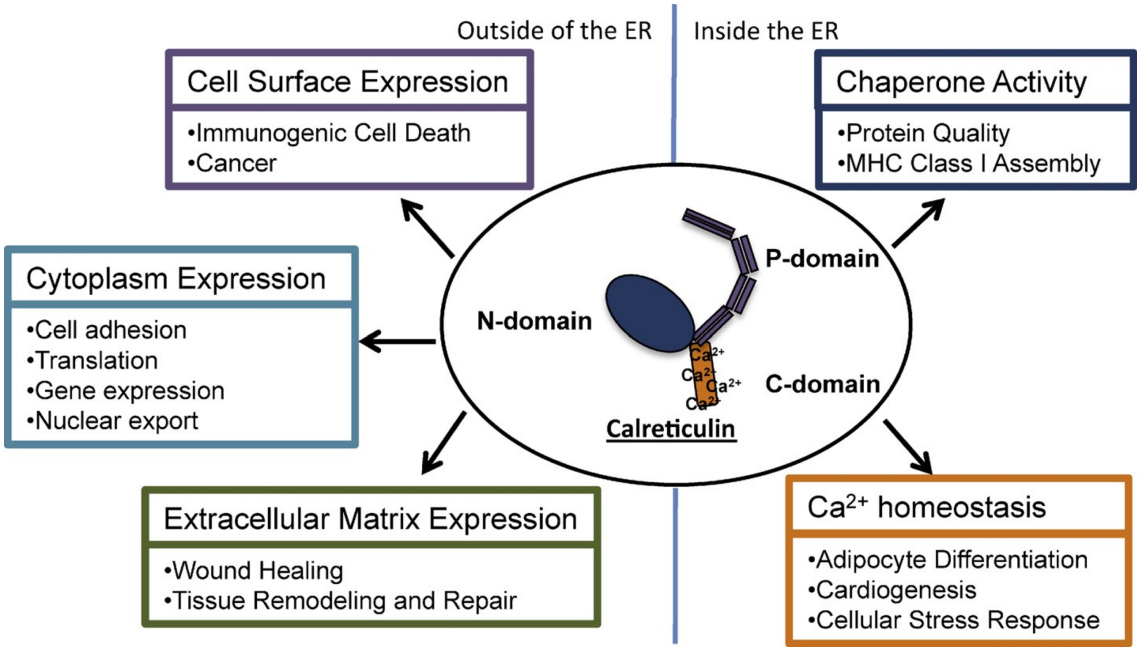

Figure 8: A summary of the functions of Calreticulin and their effects on health and disease related system (WANG ET AL., INT J BIOCHEM CELL BIOL, 2012)[191].

Protein Chaperone: Protein synthesis is an extremely complex process. The correct three-dimensional structure of proteins is essential for their functionality. Failure to fold into native structure generally produces inactive proteins, with impaired or toxic functionality. Correct folding is determined in large part by the sequence of the protein, but it is also assisted by interaction with enzymes and chaperones of the Endoplasmic Reticulum (ER). In this regard, chaperone activity is necessary for a

protein to obtain functional shape. Within the ER, nascent unfolded proteins interact with different molecules involved in this quality control system, including Calreticulin[192].

CALR is one of the well-characterized lectin-like ER chaperons. In combination with Calnexin (CNX), is involved in folding of newly synthesized glycoproteins that traverse through the ER. In particular, CALR and CNX bind monoglucosylated carbohydrates on newly synthesized glycoprotein and establish a cycle of de-glucosylation and repro-glucosylation, which can be repeated several times before a newly synthesized glycoprotein is properly folded end enters the secretory pathway. If the protein is unable to fold properly it is targeted for degradation[193].

The chaperone function of CALR is also involved in proper conformation of major histocompatibility complex (MHC) class I molecule, essential for processing and presenting exogenous antigens to activate $CD4^+$ T cells[194]. In CALR-deficient fibroblasts, MHC I molecules display unusually rapid export from the ER, impaired T-cell recognition and inefficient peptide loading[195]. Therefore, these results demonstrated a crucial role of CALR in context of immunity.

***Calcium Homeostasis*:** Ca^{2+} performs an important role in the cell since it takes part in many processes, such as gene expression, protein synthesis and stress signalling. Lumen of Endoplasmic Reticulum (ER) is a major site for Ca^{2+} storage, in concentrations largely exceeding that of cytosol (C = 400 μM)[196]. The Ca^{2+} present in the ER serves as a source of easily releasable Ca^{2+}, but is also important as a regulator of a number of enzymes and proteins.

Ca^{2+} oscillations are triggered by opening of the inositol 1,4,5-trisphosphate receptor ($InsP_3R$) channel and the Ryanodine Receptor (RyR), whereas reuptake of the cation into the ER lumen is due to the activity of the Sarco/Endoplasmic Reticulum Ca^{2+}-ATPase (SERCA) pump[174]. Fluctuations of the ER luminal Ca^{2+} concentration results in altered ER-Golgi trafficking[197], hindered transport of molecules across the nuclear pore[198] and disrupted chaperone function[199].

The important role of maintaining Ca^{2+} homeostasis within the cell is dependent upon Ca^{2+}-binding chaperones, including CALR. More than 50% of Ca^{2+} stored in ER lumen associates with CALR. As mentioned before, CALR contains two Ca^{2+}-binding sites in the P-domain (high-affinity, low capacity) and C-domain (low-affinity, high-capacity)[188]. Not surprisingly, higher levels of CALR may lead to increase intracellular Ca^{2+} storage[200,201]. In contrast, CALR-deficient cells have a lower capacity for Ca^{2+} storage in the ER lumen[188].

There are several mechanisms responsible for refilling the ER stores after Ca^{2+} signaling, called SOCI (Store Operated-Ca^{2+} Influx). A protein located at the membrane of the ER, Stim1 (stromal cell-surface molecule 1), has been identified as ER luminal Ca^{2+} levels sensor. This information is then transmitted to a protein at the plasma membrane, Orai1, a Ca^{2+} transporter that regulates SOCI[202]. CALR-overexpressing fibroblasts deregulate Stim1 protein, owing to a decrease in ER Ca^{2+} release, demonstrating the involvement of CALR in the regulation of SOCI[201].

Moreover, it has been demonstrated that CALR inhibits Ca^{2+} oscillations through the direct regulation of SERCA pump. At high Ca^{2+} levels, in fact, N-domain of CALR recruits molecular chaperone ERp57 to target SERCA 2b, promoting intra/inter disulfide bond formation thus reducing pump activity. Vice versa, at low Ca^{2+} levels SERCA 2b favors ER store refilling (**Figure 9**)[203]. These findings further support that CALR plays important roles during Ca^{2+} homeostasis.

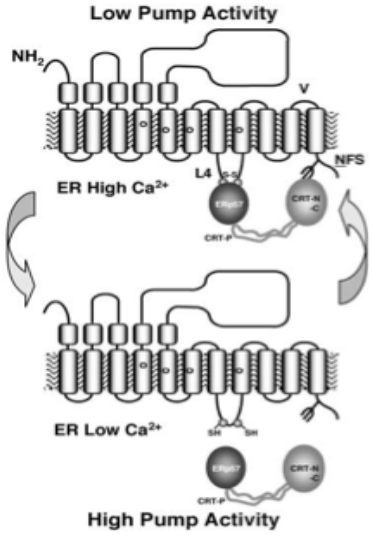

Figure 9: *Functional model of the interaction between ERp57-CALR with SERCA 2b. At high Ca^{2+} levels, N-domain of CALR recruits molecular chaperone ERp57 to target SERCA 2b, promoting intra/inter disulfide bond formation thus reducing pump activity. At low Ca^{2+} levels SERCA 2b favors ER store refilling* (LI ET AL., J CELL BIOL, 2004)[203].

***Stress response*:** Calreticulin expression is typically induced to protect cells against various toxic insults. Under stress conditions, Reactive Oxygen Species (ROS) alter physiological cell processes, especially calcium signaling. Fluctuations of the ER luminal Ca^{2+} concentrations result in deregulation of calcium homeostasis and are widely studied as a cell death signal[204].

As previously mentioned, CALR, due to its Ca^{2+}-binding sites, is able to regulate the calcium homeostasis and its storage capacity. Different studies have shown the involvement of CALR in stress response.

Dihazi *et al.* have demonstrated a downregulation of CALR in response to high osmotic stress, allowing release of free Ca^{2+} to counterbalance this stress[205]. Conversely,

CALR overexpression impairs cells viability since it generates hyperosmotic environment[206].

Ihara *et al*. have studied the role of CALR in cardiac tissue, being that oxidative stress is a main cause of myocardial apoptosis in the ischemic heart. In H9C2 cells, overexpression of CALR has been shown to increase susceptibility to H_2O_2-induced apoptosis. Moreover, the levels of cytoplasmic free Ca^{2+} were significantly increased by H_2O_2, suggesting the important role of calcium homeostasis in H_2O_2-mediated oxidative stress-induced apoptosis[207].

To further investigate the correlation between CALR and ROS-induced apoptosis, Zhang *et al*. have shown that intracellular and surface CALR levels increased in a time-dependent manner in human immortalized melanocytes exposed to H_2O_2-induced oxidative stress[208]. Indeed, translocation of CALR to cell surface act as an "eat me" signal in apoptotic cells as we will discuss later[209].

However, CALR overexpression in other cellular contexts confers resistance to stress-induced apoptosis[210,211]. Therefore, CALR role in apoptosis regulation may vary depending on different cellular types.

Additionally, CALR is also implicated in the regulation of Endoplasmic Reticulum (ER) stress. In association with Calnexin (CNX), CALR promotes proper folding and quality control in the ER. Nakamura *et al*. have shown that CALR overexpression induced an increased sensitivity of HeLa cells to Thapsigargin-induced apoptosis, suggesting a potential role of CALR in the reticulum-mitochondrial axis[212].

***Immunity*:** Several studies revealed that Calreticulin is localized on the cell surface of many mammalian cells[213,214,215], where it may play a role as marker for phagocytosis of apoptotic cells in immune response. Indeed, CALR exposure on cellular membrane has been implicated in recognition and removal of apoptotic cells, in a process called Efferocytosis. In association with Phosphatidylserine, CALR acts as "eat me" signal by binding and activating LDL-receptor-related protein (LRP) on the professional (e.g. macrophages and neutrophils) and non-professional phagocytes (e.g. fibroblasts)[209]. It has been demonstrated that this clearance can be blocked by Plasminogen activator (PAI-1)[216].

The proper functioning of this pathway is very important. In fact, inefficient clearance of dying cells can contribute to the pathogenesis of autoimmune diseases[217]. Autoantibodies against CALR have been found in sera from patients with Systemic Lupus Erythematosus (SLE), coeliac and rheumatic disease[218]. Furthermore, Ca^{2+} concentration regulated by CALR concurs to the modulation of the T cell adaptive

immune response[219]. In addition, CALR co-localizes with Perforin in the secretory granules of Cytotoxic T-Lymphocytes (CTL) and is required for targeting and contact of the CTL to the target cell[177].

CALR has also been described to be involved in Immunogenic Cell Death (ICD). Obeid *et al.* demonstrated that chemotherapy treatment with Anthracyclines or inhibitors of protein phosphatase 1/GADD34 cause translocation of CALR to the cell surface, followed by T cell-mediated phagocytosis. Conversely, downregulation of CALR expression inhibits Anthracycline-induced phagocytosis[192]. In particular, it has been shown that the exposure of CALR on the membrane is regulated by intracellular calcium levels[222]. Moreover, pharmacological enforcement of endogenous CALR to the cell surface, by means of PP1/GADD34 inhibitors, can induce immunogenic cell death, in patients with acute myeloid leukemia (AML)[223,224]. These findings suggest that CALR could ameliorate the efficacy of chemotherapy by stimulating an anti-tumor immune response.

The mechanism by which CALR translocates to the cell surface is not fully elucidate. One major hypothesis, formulated by Panaretakis *et al.*, could be that ER stress response induces PERK and eIF2 phosphorylation and their subsequent activation. Following this, apoptotic activation may induce co-translocation of CALR/ERp57 complex on cell surface and activate immunogenic cell death (**Figure 10**)[66]. Finally, it was demonstrated that intracellular pathogens can be modulating the host's complement system to evade immune response[225].

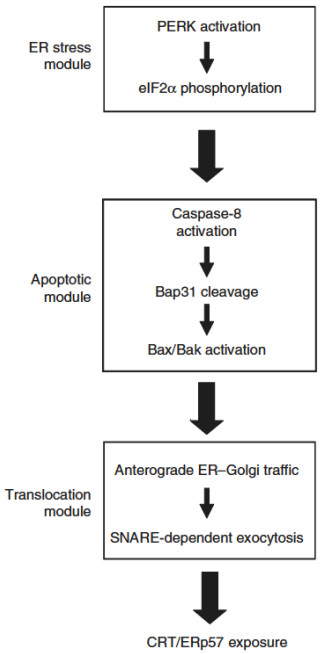

Figure 10: *Hypothetical scheme of the pathway of CALR/ERp57 exposure by Panaretakis et al. ER stress response induces PERK and eIF2 phosphorylation and their subsequent activation. Following this, apoptotic activation may induce translocation of CALR/ERp57 complex on cell surface* (PANARETAKIS ET AL., EMBO J, 2009)[66].

***Development and differentiation*:** Many studies have shown the role of Calreticulin in development and cellular differentiation. Below is a list of the various processes in which CALR is involved.

- *Adipogenesis*: CALR is a transcriptional regulator of peroxisome proliferator-activated receptor (PPAR)[226] and CCAAT enhancer-binding protein α (C/EBPα)[227], both essential factors in the development of adipocyte. In fact, intra- and extra-cellular Ca^{2+} levels are important during the adipocyte differentiation process[228]. It has been shown that the inhibition of SERCA pump by Thapsigargin blocks early stages of adipogenesis[229]. In this context, CALR can act as a Ca^{2+} regulator for adipocyte differentiation.
- *Skeletogenesis*: CALR influences osteocyte and chondrocyte differentiation through the regulation of Calcineurin[230]. In the MC3T3-E1 cell line, expression of CALR is decreased during the first 14 days of osteoblast differentiation. Indeed, CALR overexpression experiments show that the protein inhibits calcium deposition into the extracellular matrix and bone mineralization[231].
- *Cardiogenesis*: CALR plays a pivotal role in cardiac development. *In vitro* and *in vivo* studies shown that CALR deficiency compromises cardiac myofibrils formation[232,233]. CALR Knockout (KO) is lethal in mouse embryonic development[234], and its lethality can be rescued by over-expression of Calcineurin[235]. Calcineurin activity depends upon $InsP_3R$ mediated release of Ca^{2+} from ER[234]. As previously mentioned, CALR is involved in Ca^{2+} homeostasis, it follows that absence of CALR may compromise InsP3R functionality[156,188]. Unexpectedly, CALR levels in adult cardiac tissue are very low[236]. Overexpression of CALR in the adult heart causes bradycardia, heart block and sudden death in mouse model by decreased protein level of MEF2C, a cardiac-specific transcriptional factor[237,238].
- *Neurogenesis*: CALR is abundant in retina, cerebral and cerebellar cortex of mouse embryonic[239]. Rauch *et al.* demonstrated that CALR-deficient embryos exhibited defective neural tube closure. CALR KO mouse exhibited embryonic lethality with significant defects in the brain, suggesting a potential role of CALR in the development of the nervous system[240].
- *Angiogenesis*: Vasostatin, the N-terminal fragment of CALR, regulates VEGF expression (Vascular Endothelial Growth Factor)[241], a well-known proangiogenic factor[242]. Calreticulin/Vasostatin inhibits endothelial cell proliferation, angiogenesis and tumor growth[243]. In particular, Vasostatin stops endothelial cell attachment to laminin and extracellular matrix[244]. Since the inhibition of angiogenesis decreases tumor growth, several studies have tested the efficacy of

Calreticulin/Vasostatin treatment[245,246,247,248]. Unfortunately, gene transfer of Vasostatin can cause some problems in some cell/tissue types[249].

- *Hematopoiesis*: Some works highlight the potential role of CALR in hematopoietic differentiation. Immunostaining using specific CALR antibody revealed a preferential expression of CALR in megakaryocyte progenitors, phenomenon may be related to CALR role in platelet activation[250]. On the other hand, it has been shown a decrease of CALR expression during granulocyte differentiation[251]. In my thesis project, instead, I have demonstrated that CALR overexpression is able to enhance erythroid and megakaryocyte (MK) differentiation of hematopoietic stem/progenitor cells (HPSCs).

***Adhesion and cell migration*:** CALR is implicated in the control of adhesiveness through different molecular mechanisms. It is involved in the regulation of N-cadherin, Viniculin and other adhesion proteins[,253,254].

Furthermore, it has been shown that CALR can regulate cell adhesion through its bonds with Integrin[179]. Integrins are transmembrane proteins that mediate adhesion to the extracellular matrix (ECM) thanks to their connection to the cytoskeleton. Interactions between intracellular CALR and Integrin $\alpha 2\beta 1$ can regulate the affinity state of integrin to type I collagen[255]. In particular, this interaction is modulated by integrins phosphorylation and dephosphorylation status[256].

Papp *et al.* have demonstrated that CALR can regulate fibronectin expressions and increase focal contacts formation through Ca^{2+} levels and c-SRC activity regulation[257].

As for migration, it has been proposed the role of CALR in focal contacts[258]. In fact, cell surface CALR interacts with Thrombospondin (TSP-1)-LDL receptor-related protein 1 (LRP1) complex to disassemble focal adhesions through phosphoinositide 3-kinase activation[213,240]. CALR is involved in migration processes of human keratinocytes, fibroblasts and the ones of THP-1 hematopoietic cell line[239].

2.5 Functional role of Calreticulin mutants

As mentioned before, Philadelphia-negative MPNs are characterized by three mutually exclusive drivers mutations involving JAK2, MPL and CALR gene[117].

CALR mutations were simultaneously discovered by Nangalia *et al.*[144] and Klampfl *et al.*[143] in approximately 60-80% of JAK2 and MPL unmutated Essential Thrombocythemia (ET) and Primary Myelofibrosis (PMF) patients. Ever since these mutations have been discovered, the clinical and molecular roles of mutants CALR mutants have been the novel topics of interest in the field of hematology.

All the mutations identified so far are located in exon 9 of CALR gene and the two most common mutations correspond to a 52-bp deletion (type 1: c.1092_1143del52) and a 5-bp insertion (type 2: c.1154_1155insTTGTC)[259].

The occurrence of such mutations causes shifting of the reading frame and leads to the generation of a new C terminus devoid of the KDEL motif. Moreover, the negative charges required for Ca^{2+} binding are partially lost in type 2 CALR mutants and completely lost in type 1, hypothesizing that the mutations types of CALR may be associated with different phenotypes of MPNs (**Figure 11**)[143].

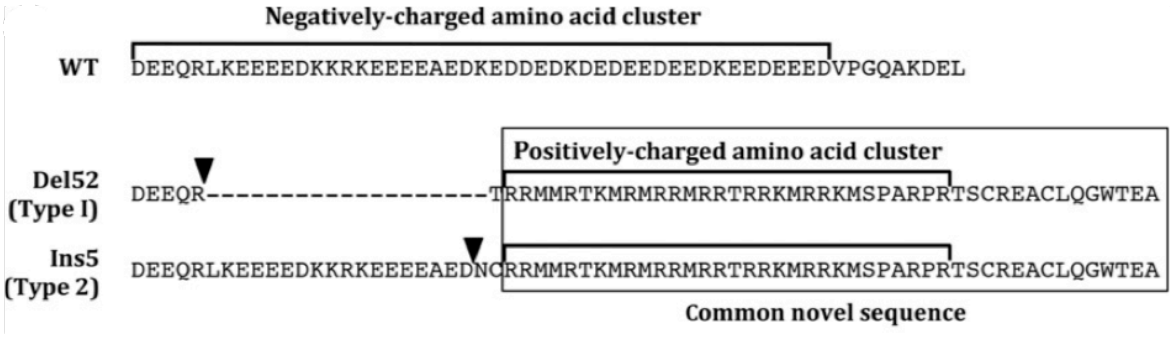

Figure 11: *C-terminal amino acid sequence of CALR Wild-Type and mutants CALR, type1 and type2. These mutations cause a frameshift that encodes a novel C-terminal domain lacking KDEL sequence and gaining a novel positively charged amino acid tail (*ARAKI ET AL., CANCER SCI, 2017*)*[260].

To understand how CALR mutants cause or contribute to the development of MPNs, several groups have performed *in vivo* and *in vitro* experiments. Although the two pioneering articles were in agreement with the types of mutations and protein alterations involved, different controversies were present regarding the role of CALR in MPNs pathogenesis, clinical progression and the optimal treatment strategies.

In particular, regarding clinical outcome both research groups observe that CALR mutations induce an increase in the platelet counts and a decrease of hemoglobin levels. However, while Klampfl argues that patients with somatic mutation of CALR have longer overall survival, Nangalia shows increased susceptibility to leukemic progression.

Another controversial item, at the molecular level, is the localization of CALR mutants. Klampfl detected a translocation of CALR to cytosol and in the cellular membrane, while for Nangalia the mutant protein localized on cell surface. Supporting this evidence a study revealed that retention in the Endoplasmic Reticulum (ER) may be linked to an acid CALR region (aa 351-359) involved in protein retrotranslocation into the cytoplasm[261]. Therefore, the absence of this domain in CALR mutants could lead to its secretion despite the presence of the KDEL fragment.

JAK-STAT signaling pathway: Since MPNs are associated with constitutive activation of JAK2/STAT signaling, this pathway has been one of the first mechanisms hypothesized as involved in the pathogenic function of CALR mutants. Klampfl *et al.* observed that overexpression of CALRdel52 induces cytokine-independent growth mediated by JAK-STAT pathway in the murine cell line Ba/F3 mediated by JAK-STAT pathway. In fact, they detected increased STAT5 phosphorylation in absence of interleukin-3 (IL3). Moreover, CALRdel52 confers hypersensitivity to cytokines. In accordance with this finding, the growth of cells expressing nonmutant and mutant CALR was suppressed equally on treatment with a JAK inhibitor[143]. These results have further been confirmed in hematopoietic progenitors (EMC and EEC) derived from bone marrow of patients with ET harboring CALR mutations. CALR mutants progenitors showed a significant growth of endogenous megakaryocyte colonies, ability attributed to the activation of the MPL receptor[262].

To understand how CALR mutants induce MPNs development, several research groups have carried out *in vitro* and *in vivo* experiments using systems expressing the two mutated forms of CALR, del52 and ins5.

Marty *et al.* demonstrated that ectopic expression of CALR mutants is able to induce MPN-like phenotype in hematopoietic stem and progenitors cells[263]. *In vivo* experiments demonstrate that mutant CALR is able to induce a similar MPN phenotype (thrombocytosis and megakaryocytic hyperplasia). In addition, it seems that CALRdel52 possesses a stronger oncogenic property than ins5 in vivo. Type 1 CALR-mutants mice develop myelofibrosis at 6 months after transplantation[225,149]. CALR mutants induce ligand-independent activation of PI-3K and MAP kinase by activating the thrombopoietin receptor (MPL)[263].

Consistent with these observations, Chachoua *et al*. showed that only MPL is able to maintain long-term cytokine-independent cell growth in Ba/F3 cells. No such effects were detected with other type I and II cytokine receptors, like EpoR (Erythropoietin Receptor) or GCSFR (Granulocyte Colony-Stimulating Factor Receptor), in the presence of CALR mutants[263,149,264]. The proliferation properties of mutant CALR were also confirmed by other groups in UT-7/TPO[264], UT-7[149] and 32D cells[265]. Conversely, the silencing of MPL or JAK2 led to the inhibition MPL-independent megakaryocytic progenitors growth, which is a hallmark of CALR-mutated MPNs[264,263,149].

Altogether, a first model has been proposed providing for the interaction between the extracellular domain of MPL and mutant CALR (**Figure 12**)[260,266].

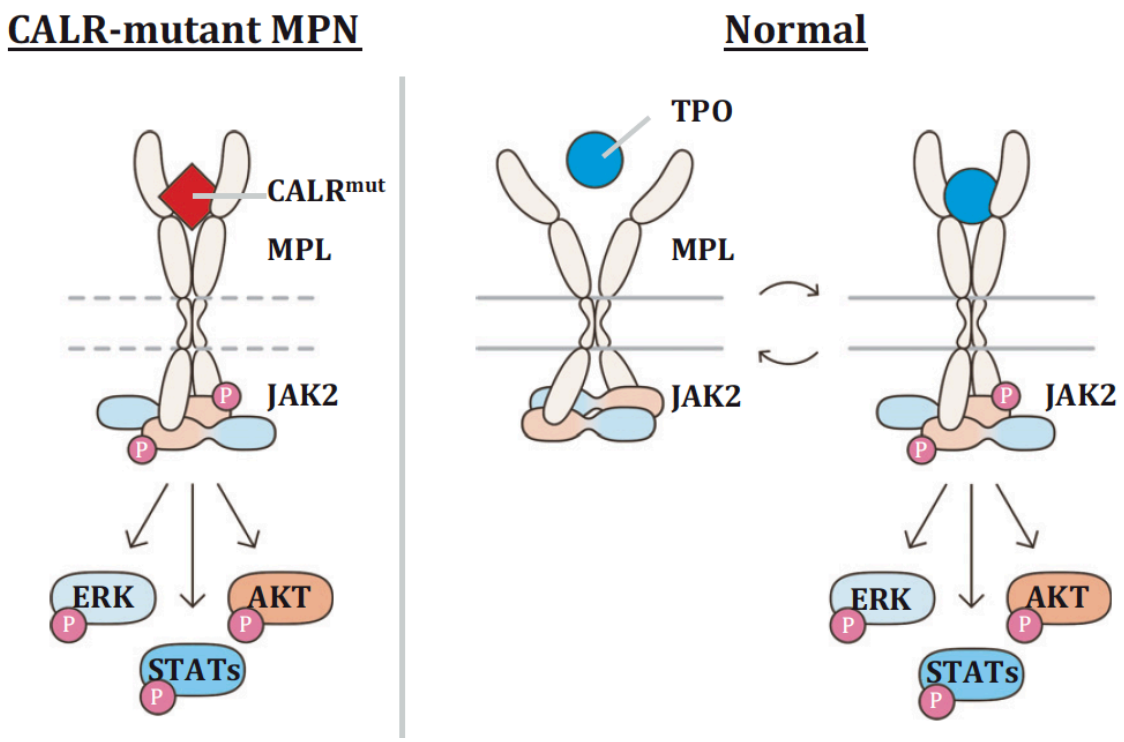

*Figure 12: Functioning mechanism of mutated CALR. CALR mutant interacts with MPL receptor and activates the downstream pathways (*ARAKI ET AL., INT J HEMATOL, 2017)[260].

Based on this hypothetical model, several studies have attempted to identify the molecular mechanism underlying the activation of MPL in the presence of CALR mutants. In physiological conditions, TPO binding to MPL induces receptor dimerization and subsequent activation of JAK2/STAT pathway[267]. Yet it appears that CALR mutants do not promote homodimerization of the receptor. Instead, the extracellular domain of MPL is indispensable for mutant CALR-dependent downstream activation[266]. The interaction between mutant CALR and the extracellular domain of MPL induces structural changes in the MPL-JAK2 complex that are required for receptor activation[268,269,270].

Afterwards, it has been hypothesized that the novel C-terminal tail of the mutant CALR is required for MPL activation[266]. The physical interaction between MPL and CALR mutants has been demonstrated[149]. However, CALR mutant C-terminus is necessary but not sufficient for oncogenic transformation[149]. Interestingly, it has been shown that the N-domain, and not the C-terminus domain, is able to interact with MPL. In particular, the P domain of unmutated CALR prevents the interaction between the N-terminal domain and MPL, while this repressive activity is lost after the acquisition of CALR mutations. In fact, the mutant-specific C-terminal domain interferes with P-domain, allowing interaction between the N-domain and MPL receptor (**Figure 13**)[264,271].

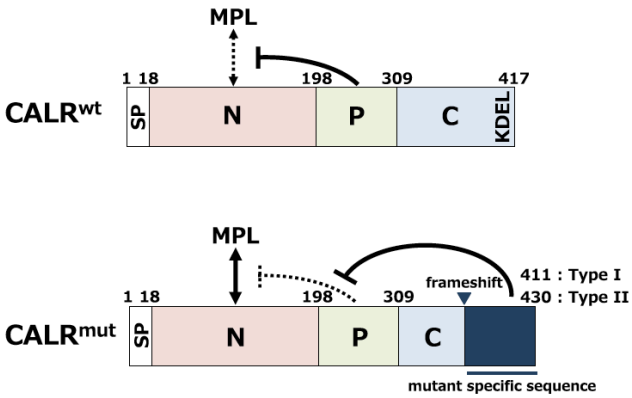

Figure 13: *Domain structure of Wild-Type or mutant CALR and model for MPL binding. While the P-domain blocks binding of the N-domain to MPL in Wild-Type protein, the mutant C domain interferes with P-domain and induces interaction between the N-domain and MPL for activation* (IMAI ET AL., INT J HEMATOL, 2017)[271].

Since CALR can bind to N-glycosylated residues of several proteins[174], site-directed mutagenesis experiments have been performed on glycosylated sites of MPL. Activation of MPL by CALR mutants is dependent on MPL N-glycosylated residues, especially at Asparagine 117 residue (N117)[266].

Interestingly, a recent study has shown that the novel CALR tail can generate a complex between CALR and immature MPL. Pecquet *et al.* demonstrated that oncogenic MPL activation requires interaction, stabilization and cell surface localization of MPL-CALR mutant complex. Mass spectrometry further revealed that CALR mutants bind partially immature MPL through a hydrophobic site near the N117. Only binding and stabilization of the receptor can induce cell surface localization of this complex and activation of cellular transformation (**Figure 14**)[272]. For these reasons, even though mutant CALR is expressed on cell surface and secreted out of the cell, CALR mutants lack paracrine capacity for MPL activation, just as previous studies suggested[264,265].

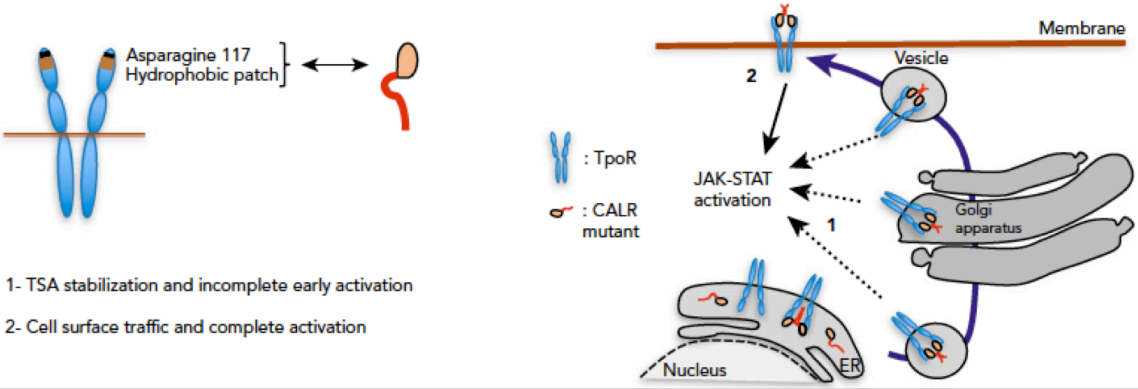

Figure 14: *Mechanisms of action of CALR mutants. CALR mutants bind partially immature MPL through a hydrophobic site near the Asparagine 117, travel through the Golgi, arrive at the cell surface and activate MPL signaling* (PACQUET ET AL., BLOOD, 2019)[272].

In addition, novel C-terminal of CALR can interact with other mutant CALR proteins. In fact, CALR mutants, but not Wilde-Type, were detected as molecules with significantly larger size, suggesting that mutant CALR might form trimeric or tetrameric complex. It has also been demonstrated that interaction and activation of MPL may be mediated by CALR homomultimers. Deletion of mutant C-terminal sequence results in a loss of CALR homomultimerization, MPL binding and JAK2/STAT pathway activation (**Figure 15**)[150]. Furthermore, physical interaction between MPL and mutant CALR is not enough for MPL activation[273].

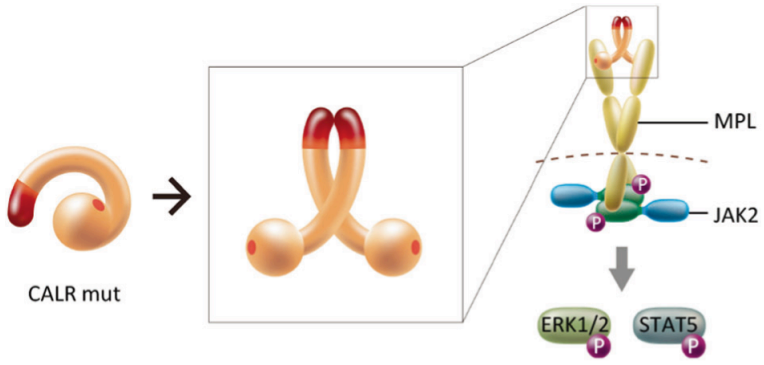

Figure 15: *CALR homomultimer. Homomultimer CALR induces presumptive structural change that induces binding to MPL* (ARAKI ET AL., LEUKEMIA, 2019)[150]

***Hematopoietic differentiation*:** CALR mutations play a fundamental role in hematopoietic differentiation. We have extensively discussed about molecular mechanism through which mutant CALR induces constitutive activation of MPL, thus explaining how it can induce megakaryocytes (MK) differentiation.

Indeed, in pathological conditions an increase platelet count and a decrease in hemoglobin level are observed in the peripheral blood, associated with an increase in megakaryocytes at the expense of erythroid lineage. Concordant with this clinical outcome, somatic mutations of CALR were detected in most patients with ET, post-ET or PMF, while they were absent in PV[144,227].

Furthermore, in mouse transplantation models, type 1 and type 2 CALR mutants are sufficient to induce a ET-like phenotype[263]. As extensively described before, this phenotype may be explained by hypersensitivity to TPO and constitutive ligand-independent activation of MPL, observed in CALR mutant mice.

The immunohistochemistry analysis, using specific antibodies against CALR mutations or Wild-Type CALR, revealed its localization in megakaryocytes suggesting a preferential expression of CALR in MK lineage[250].

Recently, have also been shown a premature commitment to megakaryocytic differentiation have also been shown in iPSCs (induced pluripotent stem cells) generated from ET patient harboring a CALRins5 mutation[274].

Interestingly, CALR can generate a set of protein-to-protein interactions and act as an important modulator of the regulation of gene transcription[275,276]. Affinity chromatography coupled with mass spectrometry proteomics demonstrated that CALR mutations promote abnormal protein complexes. In particular CALRdel52 promote the preferential binding of megakaryocyte transcription factor Fli1 and ERp57 to the MPL promoter to enhance transcription, contributing to the pathogenic phenotype[277].

Moreover, in megakaryocytes from patients with mutations in CALR gene it has been shown a defective interaction between CALR, ERp57 and STIM, associated with abnormal activation of Store Operated Calcium Entry (SOCI) machinery. This activation induces an increase of cytosolic Ca^{2+} flows and results in abnormal megakaryocyte proliferation[278].

***Other oncogenic mechanisms*:** In a retrospective analysis of CALR-mutant patients it has been demonstrated that only 16.8% of them exhibited a CALR allele-burden reduction after Ruxolitinib treatment[279]. In fact, recent studies demonstrated that additional pathogenic mechanisms mediated by CALR mutants and independent from JAK-STAT signaling pathway exist.

It has been shown that CALR-mutant MARIMO cells, derived from an ET patient and devoid of JAK2 and MPL mutations, are unresponsive to JAK2 inhibitors. It has been observed that CALR mutations are able to activate MAPK signaling[280]. These results are in agreement with previous observations that TPO activates MAP kinase cascade in megakaryocytic cell lines[281,282]. Conversely, inhibition of the TPO inhibits megakaryocytic differentiation of CD34+ progenitors[283]. Hence, it seems that CALR mutations can also induce MK differentiation in a JAK-STAT signaling independent manner.

Moreover, Wild-Type CALR acts as the dominant pro-phagocytic signal, promoting macrophage activity. It can therefore be easily hypothesized how this activity is impaired in the presence of CALR mutants[284].

For this reason, in my PhD thesis project I decided to study the role of CALRdel52 and CALRins5 play in the ER, independent of MPL expression, in order to identify additional pathways whose alterations might cooperate with cellular transformation mediated by MPL activation.

2.6 Animal models

Different mouse models were generated to investigate the involvement of mutant CALR in MPN development. So far, three types of murine models generated with different genetic approaches are available: a retroviral mouse model, a transgenic mouse model and a knock-in mouse model.

- *Retroviral*: in 2016 Marty *et al.* generated the first CALR-mutant mouse model, using a retroviral transduction system. In particular, lineage negative (Lin-) cells transduced with retrovirus expressing one of human CALR-mutated variants (CALRdel52, CALRins5) or CALRdelex9 (lacking the entire exon 9) were injected into a lethally irradiated mouse. CALR mutant-expressing mice developed thrombocytosis at higher levels in the presence of del52 than in presence of ins5. However, although CALR type 1 and CALR type 2 exhibited different phenotypes, the expression of any of these CALR-mutants led the ET phenotype. In contrast, CALR delex9 mice did not develop a disease, suggesting that the mutant C-terminal tail plays a central role in the MPNs pathophysiology[263]. Consistent with these results, Elf *et al.* demonstrated that the oncogenicity of mutant CALR is dependent on the positive electrostatic charge of C-terminal domain of CALR-mutants, which is required the interaction between CALR and MPL[149]. Moreover, after 6 months from transplantation, CALRdel52 mice showed a decrease in blood count associated with an increase in spleen weight, bone marrow fibrosis and osteosclerosis, suggesting that CALRdel52 confers growth advantage and PMF-like phenotype[263].
- *Transgenic*: similar to the retroviral model, the transgenic mouse expressing a CALRdel52 showed ET-like phenotype, with an increase in platelet count, but not white blood count or hemoglobin level. In addition, it was observed an increase in mature megakaryocytes in bone marrow, even though CALRdel52 mice did not drive myelofibrosis progression. However, the hematopoietic stem cells of CALRdel52 mice did not outgrow compared to retrovirally transduced bone marrow transplantation model. This discrepancy might be due to the differential strength of the promoter or, alternatively, by different levels of expression of mutant CALR; the expression of CALRdel52 in transgenic mice was near physiological levels, in contrast to the overexpression of retroviral transgenes[285].
- *Knock-In*: Li *et al.* generated a conditional knock-In mouse model of CALRdel52 mutation, under the control of the full complement of endogenous CALR regulatory elements. Heterozygous CALRdel52 mice ($CALR^{del/+}$) develop a transplantable ET-like disease, comparable to the mouse models listed above (with

thrombocytosis, morphologically abnormal megakaryocytes and increase of hematopoietic stem cells). On the other hand, homozygous CALRdel52 mice ($CALR^{del/del}$) developed extreme thrombocytosis accompanied by features of myelofibrosis, including reduced hemoglobin levels, splenomegaly, leukocytosis and increased bone marrow reticulin. The myelofibrosis was seen only in homozygous mice, perhaps reflecting the high levels of CALRdel52 expression achieved by these mice[286]. Recent studies demonstrated that a homozygous state of CALRdel52 mutation is lethal at a late embryonic development stage, showing narrowed ventricular myocardium walls, suggesting that the C terminus of CALR is crucial for heart development[287].

3. OXIDATIVE STRESS

3.1 ROS and oxidative stress

Reactive Oxygen Species (ROS) are high reactive chemical species containing oxygen. They are generated as a consequence of metabolic reactions that mainly occur inside the mitochondria.

More than 90% of oxygen consumed by living organisms is reduced directly to water by cytochrome oxidase in electron- transport chain (ETC), without ROS release. The remaining part is subsequently reduced to superoxide anion radical ($O_2^{\cdot -}$), which is converted to hydrogen peroxide (H_2O_2). H_2O_2 is chemically more active than molecular oxygen. Accepting one more electron H_2O_2 generates hydroxyl radical (HO·) and hydroxyl anion (OH^-). Finally, HO· may interact with one more electron and proton resulting in formation of two water molecules. Superoxide radical ($O_2^{\cdot -}$), Hydrogen peroxide (H_2O_2) and hydroxyl radical (HO·) are collectively called ROS (Figure 16)[288].

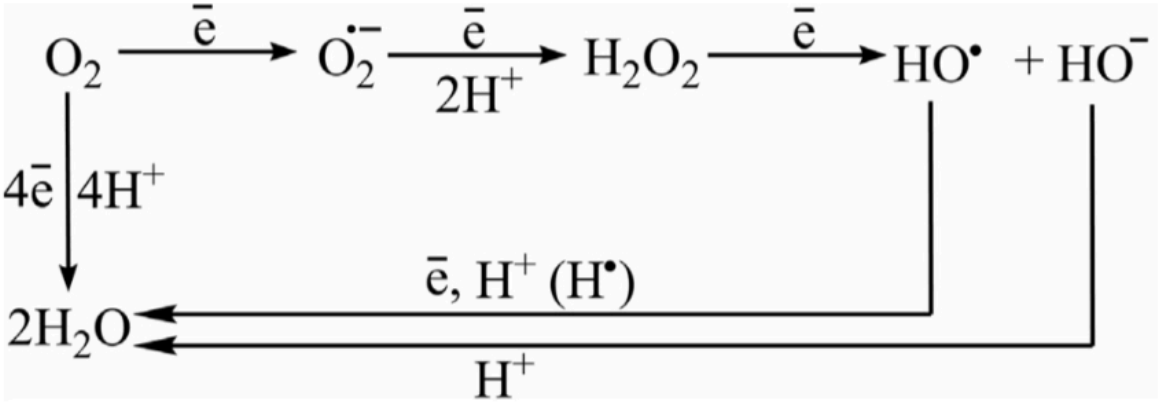

Figure 16: *Series of reactions which lead to the reduction of molecular oxygen and to ROS production* (LUSHCHAK, CHEMICO-BIOLOGICAL INTERASTIONS, 2014)[288].

ROS are mainly produced by mitochondria as a result of electron transport chain[289]. In addition, ROS are also produced in Endoplasmic Reticulum (ER) and nuclear membranes following hydroxylation processes mediated by cytochrome P450 family enzymes[288].

An imbalance between ROS production and the ability of the antioxidant systems to readily detoxify these reactive intermediates results in oxidative stress. This imbalance can be caused by endogenous sources, such as inactivation or reduction of antioxidant enzymes, depletion of nutritional antioxidant reserves and increased self-oxidation of different compounds. Additionally, ROS formation can be induced by exogenous

sources such as UV light, ionizing radiation, lifestyle, diet, stress and smoking[288]. ROS are involved in many biological processes, including cellular signaling, inflammation and tissue damage[290,291]. Furthermore, ROS impair proteins', lipids' and nucleic acids' structures[292].

3.2 Antioxidant systems

To maintain a low steady-state ROS level, cells possess finely regulated antioxidant systems. These compounds act as inhibitor of oxidation process even at relatively small concentration, thus having diverse physiological role in the body[293]. The antioxidant systems can be both enzymatic and non-enzymatic classified in low and high molecular weight.

The low molecular weight antioxidants are mainly found in dietary sources like fruits and vegetables. Among these can be listed Vitamin C (Ascorbic Acid), Vitamin A (Retinol), Vitamin E (Tocopherols, Tocotrienols), Uric Acid, Carotenoid and a wide class of Flavonoids such as Anthocyanins. Recently, it has also been discovered the role of melatonin in preventing ROS accumulation[294].

In addition to these molecules, another important antioxidant is Glutathione (GSH). GSH is a tripeptide with multiple functions. As a carrier of an active thiol group in the form of a cysteine residue, it acts as an antioxidant by directly interacting with ROS or functioning as a cofactor for various enzymes. GSH exists in two forms: reduced (GSH) and oxidized (GSSG). The oxidized form consists of two residues of GSH that have been oxidized in such a fashion as to be connected by an intermolecular disulfide bond. The former counteracts oxidative stress preventing the reducing thiol proteins, through the block of the disulfide bridge, and oxidizing in turn. The latter consists of two residues of oxidized GSH connected by an intermolecular disulfide bond. The glutathione couple GSH/GSSG, adjusting the balance between NADP+/NADPH, plays a critically role in maintaining homeostatic redox state and restoring the pool of reduced glutathione[295]. Moreover, GSH counteracts oxidative stress by interacting with glutathione peroxidase, which in his oxidated state is able to decrease the concentration of H_2O_2 present in the cell[296]. Therefore, GSH/GSSG ratio is a marker of cell oxidative stress.

The high molecular weight antioxidants include several enzymes, such as Thioredoxin (TRX). TRX is a small multifunctional protein that functions as regulator of oxidative stresses through the reduction oxidation of protein cysteine residues[297]. In particular, TRX catalyze a reversible reduction of protein disulfide bonds, and TRX active-site cysteines are regenerated by TRX reductase and NADPH.

Indeed, NADPH is the electron donor involved in the restoration of GSH and TRX redox status. Pyridine nucleotides (which comprise NADH/NAD+ and NADPH/NADP+) in addition to ATP production are also linked to oxidative stress defense and redox regulation[298].

Another antioxidative high molecular weight enzyme is Superoxide Dismutase (SOD) which catalyzes the dismutation of superoxide radical ($O_2^{\bullet -}$) to molecular oxygen (O_2) and hydrogen peroxide (H_2O_2)[299]. The H_2O_2 is further dismutated by SOD in in water (H_2O) and molecular oxygen (O_2)[300]. Alternatively, H_2O_2 can be reduced by several lipid peroxidases[301]. These different antioxidant systems are activated differently based on the extent of stress. For mild or moderate stress Nrf2/Keap1 signaling is activated, which in turn regulates SOD, peroxidase, catalase and GST-transferase. Whether stress is moderate, the pathways of NF-kB, AP-1 and MAPK are activated. Conversely, in acute stress situations, ROS are released outside of the cell which can even lead to apoptosis[288].

3.3 Markers and approaches to measure oxidative stress

Biomarkers of oxidative stress are important tools in the assessment both of disease status and of the health-enhancing effects of antioxidants in humans[302]. Over the years have been discovered different biomarkers and methodologies to measure the level of oxidative stress.

One way to estimate the cellular levels of ROS is through the use of fluorogenic probes[303,304,305]. ROS can be measured after staining with 5-(and -6)-carboxy-2,7-dichlorodihydrofluorescein diacetate (DCFDA). This membrane-permeable probe diffuses into the cells where it becomes hydrolyzed by intracellular esterase to DCFH. The latter reacts with H_2O_2, generating the fluorescent 2,7-dichlorofluorescein (DCF). Therefore, the amount of peroxide produced by the cells can be estimated by the fluorescence intensity of DCF and analyzed by Flow Cytometry[303].

Direct measurement of ROS levels with high accuracy and precision is difficult due to their short lifespan and high reactivity. Therefore, indirect measurement of ROS by examining the oxidative damage these radicals cause to nucleic acids of the cells is a promising alternative approach to assess oxidative stress[306]. Among the DNA modifications induced by oxidative stress there are nucleotides oxidation, strand break, loss of bases and formations of adducts. The $HO^{\bullet}$ radical can react with the nitrogenous bases and generate different products. 8-Hydroxy-2-deoxyguanosine (8-OHdG) is one of the major DNA oxidative modifications that can be generated by

hydroxylation of the deoxyguanosine residues. Levels of 8-OHdG can be detected by enzyme-linked immunosorbent assay (ELISA)[307].

Moreover, H2AX phosphorylation is considered an oxidative stress marker. It is considered involved in DNA repair, cell cycle checkpoints, regulation of gene recombination events, and tumor suppression. It has been demonstrated that phosphorylation at serine 139 of histone H2AX (γ-H2AX) serves to concentrate DNA repair/signaling factors on the sites of injury, acting as damage response amplifier[308].

In particular, γ-H2AX is chronologically the first DNA damage marker[309]. γ-H2AX foci are formed rapidly at the cutting site facilitating the anchoring of damage repair proteins: MRN, 53BPI, MDC and RAD51[310]. Thus, γ-H2AX formation is a rapid and sensitive cellular response to the presence of DNA double-strand breaks.

Superoxide dismutase (SOD) is a family of antioxidant enzymes that regulate ROS levels by catalyzing the conversion of superoxide to hydrogen peroxide and molecular oxygen[311]. Three superoxide dismutases isoforms have been biochemically and molecularly characterized to date. SOD1 is zinc-containing homodimer that is found almost exclusively in cytoplasmic spaces. SOD2, instead, exists as a tetramer and is founds exclusively in mitochondria. SOD3, the most recently characterized, exists as a copper and zinc-containing tetramer and is found exclusively in extracellular spaces[312].

SOD activity can be measured using indirect methods, in which a unit of SOD is generally defined as the amount of the enzyme causing the inhibition of an oxidation reaction (autoxidation of adrenaline, autoxidation of pyrogallol, or tetrazolium reduction)[313].

3.4 Oxidative stress in myeloproliferative neoplasms

Maintaining equilibrium between the reducing and oxidizing states is crucial for proper physiological functions. It's now well known that most risk factor associated with various disorders, including cancer, interact with cells through the generation of ROS. However, under physiologic conditions a moderate amount of ROS is required for intracellular cell signaling and homeostasis, gene expression, cell death, immune defense against pathogens, and induction of mitogenic response[314,315]. On the other hand, the accelerated metabolism, typical of tumor cells, induce high ROS production which support their high proliferation rate[316,317].

Therefore, ROS overproduction is involved in cancer development both in solid tumors and hematological malignancies[80,318,319,320,321].

ROS are involved in many biological processes during tumorigenesis, including inflammation, tissue damage and genomic instability. In particular, DNA damage is

seen as a consequence of increased ROS levels in hematopoietic stem cells, thus contributing to the genetic instability and the consequent acquisition of additional mutations. ROS create a vicious self-perpetuating circle: ROS activate proinflammatory pathways which in turn generate more ROS[322,323].

In MPNs several studies shown that patients are characterized by elevated ROS levels[320,324]. It has been demonstrated in various cell line models that JAK2V617F mutation trigger downstream signaling pathways including STAT5, starting a cycle of genomic instability with increased ROS production[325,326]. The excessive production of ROS and increased genomic instability seem to favor the expansion of the JAK2 positive clone in mouse model, underlining the importance of oxidative stress in MPN pathogenesis [80,327].

Marty *et al.* have demonstrated that ROS overproduction, that occurs in presence of JAK2V617F mutation, induce DNA damages that promote disease progression[80]. The release of ROS and pro-inflammatory cytokines is also favored by granulocytes, megakaryocytes and stromal cells, which contribute to the creation of a pro-oxidant environment[328]. The researchers hypothesized that the constitutive activation of the PI3K/AKT pathway mediated by JAK2 mutation may inhibit FOXO activity, blocking the antioxidant enzyme catalase. Treatment with antioxidant N-acetylcysteine (NAC) in JAKV617F Knock-in (KI) mice reduces DNA damage and restore normal parameters, suggesting that ROS play a crucial role in MPN. The potential pathogenic mechanism hypothesized by the authors is reported in following figure[80].

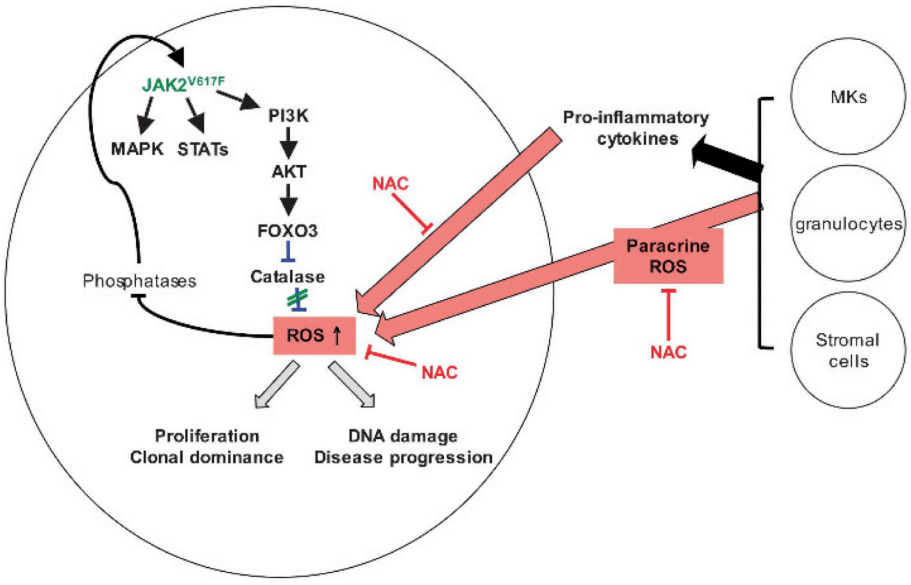

Figure 17: *Role of ROS in JAK2V617F myeloproliferative neoplasms progression. High ROS levels induce a decrease in the detoxifying enzyme Catalase via activation of the PI3K/AKT pathway. In addition, the microenvironment cells release pro-inflammatory cytokines (such as TNF alpha, TGF beta, interleukins). In turn, ROS increase might inhibit phosphatase activities leading to a prolonged phosphorylation-dependent JAK/STAT signaling* (MARTY ET AL., LEUKEMIA, 2013)[80].

High ROS levels induce a decrease in the detoxifying enzyme Catalase via activation of the PI3K/AKT pathway. In addition, the microenvironmental cells release pro-inflammatory cytokines (such as TNF alpha, TGF beta, interleukins). In turn, ROS augmentation might inhibit phosphatase activities leading to a prolonged phosphorylation-dependent JAK/STAT signaling (**Figure 17**)[80].

Moreover, MPNs transcriptional profiling showed that several oxidative stress and anti-oxidative stress genes are significantly deregulated. In particular, Nrf2 gene (Nuclear factor erythroid 2-related factor 2) was found significantly downregulated in all MPNs, suggesting a key role in the regulation of the oxidative stress response[329].

In addition, oxidative stress can also induce chronic inflammation that, in combination with proinflammatory microenvironment, would alter DNA and the function of hematopoietic stem cells, leading fibrosis[330].

Finally, in PMF patients, vitamin B12 depletion correlates with increased levels of homocysteine and oxidative stress. This tendency to develop a pro-oxidant environment has been observed in patients with worse prognosis[320].

3.5 Oxidation resistance 1 gene

Oxidation resistance 1 (OXR1) gene plays a critical role in protecting the cell against oxidative stress. There are several isoforms of OXR1: shorter isoforms are mostly located in the mitochondrial membrane, while the longer isoforms show a cytosolic localization. It has been observed that the deregulation of these isoforms can alter mitochondrial morphology[331].

Yang *et al.* demonstrated that OXR1 induces the expression of antioxidant genes through the p21 pathway. p21 is a cell cycle inhibitor capable of activating the transcription factor Nrf2, which favors the transcription of genes coding for antioxidant enzymes, including glutathione peroxidase, heme-oxygenase 1 and HADH quinone oxide reductase. Therefore, in cells in which the expression of OXR1 is reduced, these antioxidant systems are not activated with the consequent inability to counteract oxidative stress[332].

RNA sequencing experiments showed that OXR1 depletion resulted in deregulation of various genes including transcription factors, antioxidant genes and numerous genes of the p53 signaling pathway involved in cell-cycle arrest and apoptosis. In particular, OXR1 upregulates the transcription of four antioxidant genes (CYGB, PTGS1, HO-1, GPX2), resulting in inhibition of ROS production and modulation of early stress response genes. When OXR1 is downregulated, ROS levels increase, leading to oxidative damage, especially DNA damage, that triggers cell cycle arrest in

G2/M and apoptosis via regulation of RPRM, CASP9 and several other genes in the p53 pathway (**Figure 18**)[333].

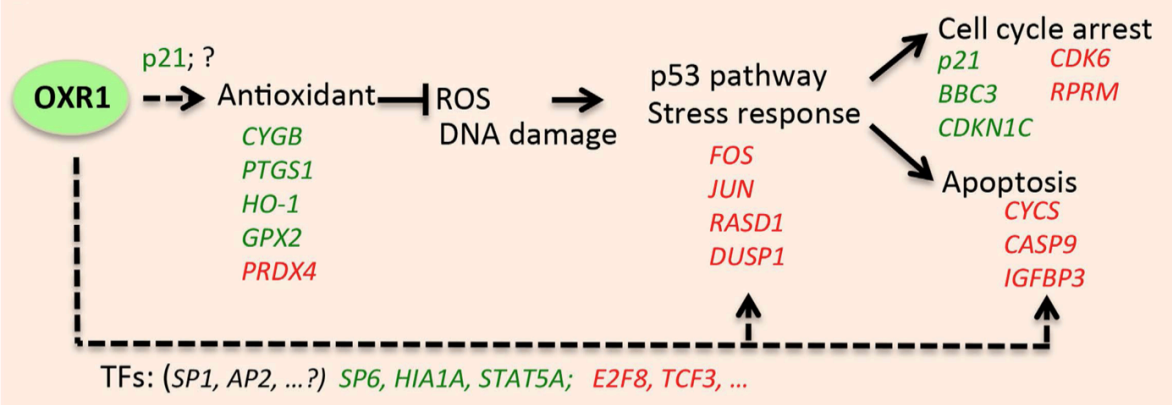

Figure 18: *Model of OXR1 mediated regulation of antioxidant defense, early stress response, cell cycle and apoptosis by Yang et al.; genes labeled in red or green are up- or down-regulated, respectively* (YANG ET AL., SCIENTIFIC REPORTS, 2015).

Finally, it was shown that OXR1 downregulates the expression of pro-apoptotic cytochrome C genes, whose release is stimulated by ROS and Caspase 9[334]. Collectively, OXR1 gene would seem to be an oxidative stress and regulator of the key transcriptional factors of this metabolic process.

4. ENDOPLASMIC RETICULUM STRESS

4.1 Unfolded protein response

Endoplasmic Reticulum (ER) is a eukaryotic organelle that plays multiple cellular functions including the synthesis, folding, sorting and transport of proteins. Moreover, ER is optimized to carry out these processes because it provides highest Ca^{2+} levels and an oxidizing microenvironment which supports the formation of disulfide bonds during protein folding[335].

Physiological or pathological disruptions in the normal functions of the ER cause accumulation of unfolded proteins, triggering chronic stress. Hypoxia, nutrients deprivation, viral infections, proteasome dysfunctions and Ca^{2+} levels imbalances are just few disturbances that can lead to the ER stress and subsequent Unfolded Protein Response (UPR)[335,336,337,338].

UPR initially induces translation arrest and the production of specific factors able to compensate the damage induced by accumulation of misfolded proteins and reestablish normal ER function. These adaptative mechanisms involve transcriptional factors that induce increased protein folding or ER-associated degradation (ERAD) to ensure cell survival. In order to reduce the influx of newly synthesized proteins, in the early stages of UPR translation of mRNA is also inhibited. When the adaptation is fails UPR induces an alarm signal through the activation of NF-kB and other transcriptional factors related to host defense. Eventually, if the stress is too severe and prolonged, UPR triggers cell suicide by apoptosis[335].

4.2 Signaling pathway of unfolded protein response

ER lumen is rich in molecular chaperones such as Grp78/BIP, Grp94, Calnexin and Calreticulin, which are responsible for proofreading newly synthesized proteins and UPR activation[339].

In mammalian cells, UPR is mainly controlled by three ER transmembrane proteins: IRE1 (Inositol-Requiring Enzyme 1 α), PERK (PRK-like ER kinase) and ATF6α (Activating Transcriptional Factor 6 α). Each of these proteins contains an ER luminal domain which can act like a sensor of misfolded proteins[340]. During homeostasis condition, the N-terminal domain of these three proteins is maintained inactive the ER chaperone Grp78, also known as Binding immunoglobulin Protein (BiP). Under ER stress conditions BiP/Grp78 is released due to its higher affinity for misfolded proteins, allowing the UPR activation. In particular, the dissociation of BiP/Grp78 from these

transmembrane proteins allows their aggregation and the subsequent activation of their downstream pathways[341]. In figure 19 are represented the three branches able to mediate UPR signaling (**Figure 19**)[338].

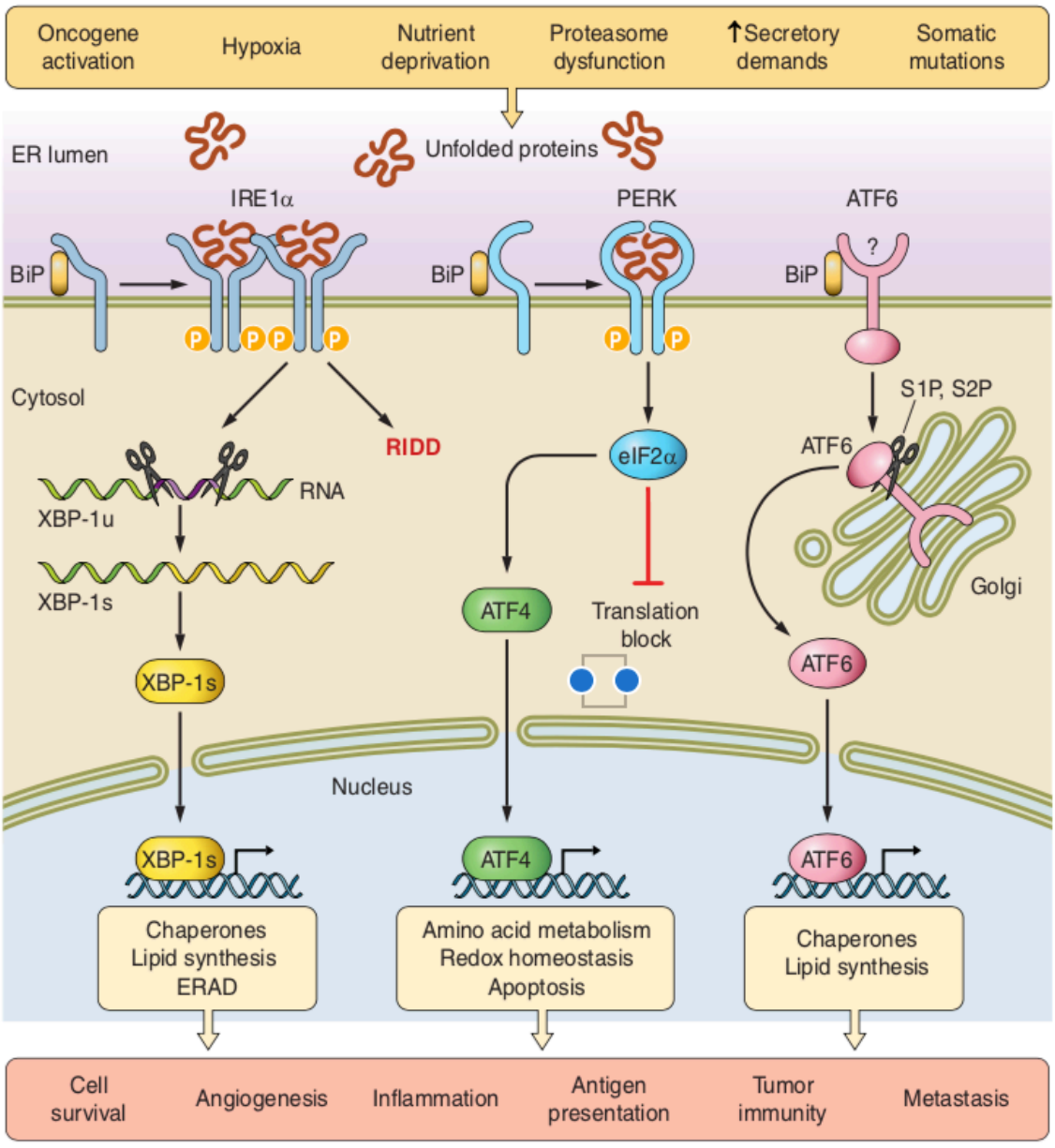

Figure 19: *Key axes of UPR modified by Oakes from Osorio et al. Extrinsic stresses compromise protein folding in the ER. In response to this accumulation, UPR is activated by three transmembrane ER proteins: IRE1, PERK and ATF6. At low levels of ER stress, IRE1 kinase dimerizes/tetramerizes to cleave a nonconventional intron from XBP1 mRNA, resulting in the production of a spliced XBP1 form (XBP1s) that upregulates ER protein-folding and quality control systems to promote adaptation to the stress condition. However, if the stress is too severe, IRE1 oligomerizes, and its RNase activity degrades many mRNAs causing cell death (RIDD process). On the other hand, PERK is able to phosphorylate eIF2α, a phenomenon that promotes the expression of ATF4, which induces CHOP upregulation. CHOP upregulates GADD34 transcription, which in turn induces eIF2α dephosporylation and reduces protein folding. Moreover, ATF6, another protein controlling the third branch of UPR, can translocate to the Golgi during ER stress and is cleaved to release the relative transcription factors (ATF6N) into the cytoplasm before migrating to the nucleus. Taken together, XBP1, ATF6 and ERAD increase the transcription of targets genes that regulate protein-folding capacity or trigger cell suicide by apoptosis.* (OAKES, AMP-CELL PHYSIOL, 2017)(OSORIO ET AL, NATURE IMMUNOLOGY, 2014)[337,342].

- *IRE1*: IRE1 pathway is the most evolutionarily conserved branch of the UPR. IRE1 gene can generate two isoforms: IRE1α and IRE1β. IRE1α is a type I transmembrane protein that oligomerizes during ER stress and acts as kinase and endoribonuclease (RNase). At low ER stress levels, IRE1α kinase dimerizes/oligomerizes and autophosphorylates. This phenomenon triggers its endonuclease activity which catalyzes XBP1 mRNA splicing, generating XBP1 protein. XBP1 activity upregulates several genes involved in ER protein-folding and quality control systems to promote adaptation to stress[343]. XBP-1 can also heterodimerize with NF-Y protein (Nuclear transcription Factor Y) and bind various *cis*-acting elements in gene promoters, including ERSE (ER Stress Enhancer) and UPRE (Unfolded Protein Response Element)[344]. However, if the stress is too severe, IRE1α oligomerizes, and its RNase activity degrades many mRNAs to cause cell death. This process is termed Regulated IRE1-Dependent Decay (RIDD). Moreover, IRE1α also interacts with TRAF2 (TNF-Receptor-Associated Factor 2) to lead the upregulation of ASK1 (Apoptosis Signal-regulation Kinase 1)[345] and JNK (JUN N-terminal Kinase)[346] which promotes apoptosis. In summary, XBP1s is linked to the promotion of cell survival, while RIDD activation induces cell apoptosis[347].
- *PERK*: Similarly, PERK is a protein kinase that oligomerizes in ER membranes when is released by BiP/Grp78. Its catalytic domain shares homologies with other kinases of eIF2α family (eukaryotic translation Initiation Factor 2 α)[348]. PERK is able to phosphorylate eIF2α, promoting cells cycle arrest[349]. PERK phosphorylates and inactivates eIF2*α*, thereby globally shutting off mRNA translation and reducing the protein load on the ER. However, certain mRNAs gain a selective advantage for translation under these conditions, including ATF4-encoding (Activating Transcription Factor 4) mRNA[350]. ATF4 triggers the expression of the pro-apoptotic gene CHOP[351]. Moreover, CHOP upregulates transcription of GADD34 and other related genes, which in turn induce the dephosporylation of eIF2*α* and reduce protein folding[352].
- *ATF6*: ATF6 is a type II transmembrane protein that has two homologous forms: ATF6α and ATF6β. ATF6α can move to the Golgi during ER stress and is cleaved from resident proteases. In particular, site 1 and site 2 proteases cleave ATF6α at a juxtamembrane site to release the transcription factors (ATF6N) into the cytoplasm before migrating to the nucleus to regulate gene expression[353]. ATF6N increases transcription of its targets (e.g., BiP, Grp94, p58IPK/DNAJC3) that increase ER protein-folding capacity and ERAD activity[354]. In fact, a study shows that ATF6*α* regulates the transcription of ERAD components[355]. Moreover, ATF6 induces upregulation of XBP-1 mRNA and IRE1's endoribonuclease activity, collaborating with IRE1 to produce the spliced form of XBP-1 protein[335]. In addition, activation

of ATF6 is also associated with an increase in the expression of the pro-apoptotic gene CHOP by binding regulatory elements on its promoter[356].

4.3 Endoplasmic reticulum stress inductors

UPR is part of the proteostasis network so any event that affects protein homeostasis can ultimately induce UPR. In this contest, hypoxia is the main UPR-inducing factor. Indeed, severe hypoxic exposure causes ER stress and regulates several UPR downstream effector pathways that promote hypoxia tolerance[357].

However, different compounds are able to induce ER stress in a non-specific or specific manner. The three chemical agents classically used to this purpose are: Thapsigargin, Tunicamycin and Brefaldin. All of these drugs induce UPR, but also have other non-UPR related effects.

In particular, Tunicamycin causes accumulation of unfolded proteins in the Endoplasmic Reticulum (ER) by inhibiting proteins N-glycosylation in this organelle[358]. Moreover, it has been demonstrated that Tunicamycin upregulates the expression of STAT3 and CHOP in a time- and concentration-dependent manner[359]. On the other hand, Thapsigargin acts to block the activity of the SERCA Ca^{2+}-ATPase pump, involved in calcium homeostasis[360]. Overall, both of these molecules cause strong ER stress by promoting autophagy and apoptosis, activating PERK, ATF4 and CHOP pathways.

Other ER stress inductors include Disulfide bond Disrupting Agents (DDAs). It has been demonstrated that DDAs irreversibly break disulfide bonds, thus altering protein folding. DDAs are able to activate all UPR branches through the increase of XBP1 transcriptional levels and BiP/Grp78 production[361]. Finally, also the Dithiothreitol (DTT) is widely used to reduce disulfide bonds and induce ER stress[362].

4.4 Role of the unfolded protein response in cancer

It is well proven that ER stress and subsequent UPR activation are involved in the development of both solid and hematological malignancies[343,350].

Tumors are characterized by a highly hypoxic environment in which a nutrient deprivation is observed due to the rapid growth of the tumor mass[363]. In particular, hypoxia impacts directly on the post-translational formation of disulfide bonds[364] and, indirectly, by increasing ATF4 stability[365]. Furthermore, genomic instability and somatic mutations can induce ER stress[366]. However, to survive in this hostile microenvironment, cancer cells have developed different resistance mechanisms,

including increased dependence on UPR. Consistent with this, UPR is overeractivated in a wide range of primary human tumors[367]. UPR favors angiogenesis thanks to the direct binding of ATF4 and XBP1 on the promoter of the Vascular Endothelial Growth Factor A (VEGF)[368]. In addition, UPR can confer resistance to anti-cancer treatments[336].

Most of the published works demonstrated that UPR supports tumor growth by: increasing protein folding capacity thanks to the synthesis of protein chaperones, and promoting the ER-Associated Degradation (ERAD) pathways to alleviate ER stress[338]. Moreover, UPR can be impact on inflammatory stimuli. In fact, ER stress can strongly induced the transcription of NF-kB, the master regulator of multiple inflammatory pathways[369].

Although several lines of evidence suggest that UPR promotes proliferation of cancer cells, the role of ER stress and UPR pathways in cancer development is complicated. It has been developed anti-cancer drugs that target ER stress and UPR. In fact, as it was previous said, if ER stress is prolonged UPR induces an apoptosis-mediated cell death[338]. Studies show that combining Tunicamycin or Thapsigargin with chemotherapeutic drugs enhances their efficacy suggesting the anti-cancer effects of ER inhibitors[370].

Somatic mutations in IRE1a and PERK have been rarely found in tumors[371]. UPR has been mostly studied in Myeloma[372]. Myelomas patients show unusually high levels of XBP1[373], but the role of XBP1 in this cancer is not yet fully understood.

Hematopoietic stem cells (HSC) have a high self-renewal capacity that can lead to ER stress and subsequently UPR. HSCs are prone to apoptosis through PERK pathway activation, exhibiting an adaptive response leading to their survival[374]. It has been shown that inhibition of ER stress-associated IRE1/XBP1 signaling reduces leukemic cell survival, suggesting that targeting XBP1 could be a potential therapeutic strategy not only for myeloma but also for leukemia and lymphoma[375].

5. HEMATOPOIESIS

5.1 Physiological hematopoiesis

Blood is one of the most regenerative and dynamic tissues of body, old blood cells are replaced each second during the life. The blood system contains different cell types (lineages) with various specialized functions, however all blood cell types arise from hematopoietic stem cells (HSCs) that reside mainly in the Bone Marrow (BM)[376].

The HSCs are characterized by their abilities of long-term, self-renewal and differentiation potential[377]. Hematopoiesis is the physiological process responsible for the formation of blood cells. HSCs are at the apex of hierarchy of numerous progenitor cells stages with an increasingly potential to generate lineages that give rise to all blood cells (**Figure 20**)[378].

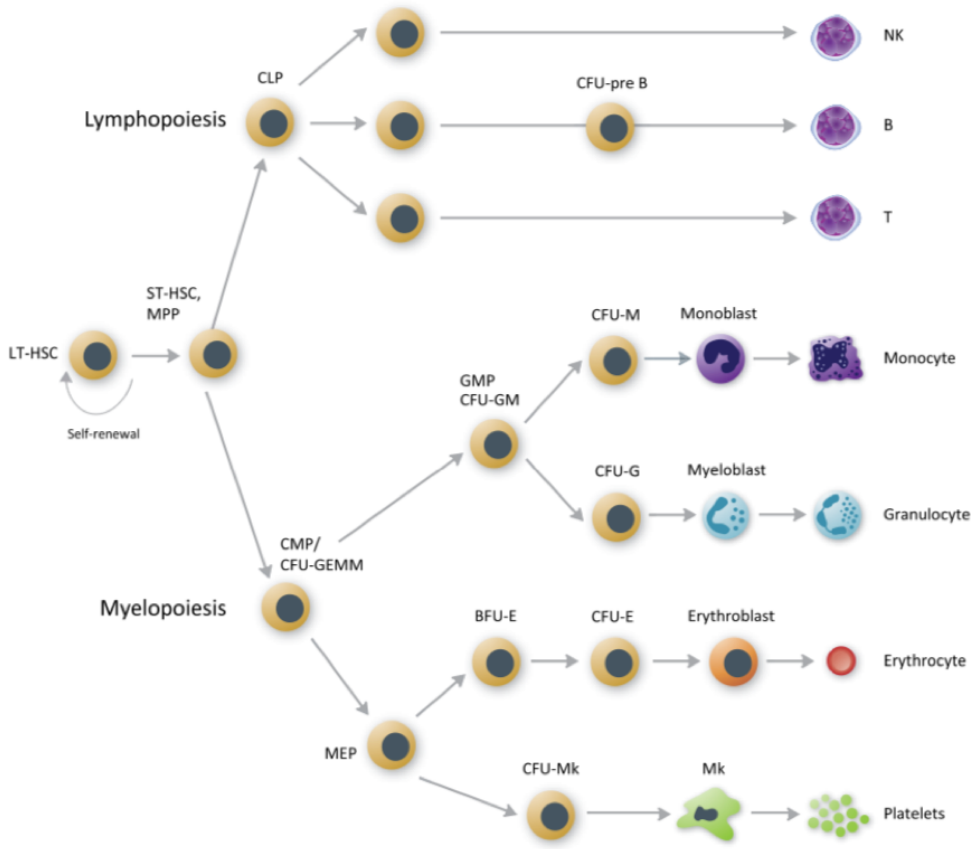

Figure 20: *Schematic representation of the production of mature blood cells through hematopoietic stem cell proliferation and differentiation. Intermediate stages are also depicted. Abbreviations: LT-HSC, Long-Term Hematopoietic Stem Cell; ST-HSC, Short-Term Hematopoietic Stem Cell; MPP, Multipotential Progenitor; CMP, Common Myeloid Progenitor; CLP, Common Lymphoid Progenitor; CFU-GEMM, Colony-Forming Unit - Granulocyte/Erythrocyte/Macrophage/ Megakaryocyte; BFU-E, Burst-Forming Unit - Erythroid; CFU-E, Colony-Forming Unit – Erythroid; CFU-MK, Colony-Forming Unit - Megakaryocyte; CFU-GM, Colony-Forming Unit - Granulocyte/Macrophage; CFU-G, Colony-Forming Unit – Granulocyte; CFU-M, Colony-Forming Unit – Macrophag Adapted from Wognum et al.* (DOCUMENT #29068 VERSION 6.0.0 APRIL 2015, STEMCELL TECHNOLOGIES INC.)[378].

The loss of the self-renewal capacity precedes lineages commitment, in fact LT-HSC generate multipotent progenitors (MPPs) with a finite self-renewal potential[376]. HSCs differentiate into a cascade of progenitor cell stages that progressively lose multilineage potential until unilineage commitment[379]. In particular, lineage decisions occur through stepwise bifurcations: the first one separates myeloid and lymphoid breaches originating common lymphoid progenitors (CLPs) and common myeloid progenitors (CMPs). Afterwards, CLPs give rise to B cell precursors and the earliest thymic progenitors (ETPs) committed to the NK and T lineages. CMPs give rise to granulocyte-monocyte progenitors (GMP), therefore become committed to the granulocyte or monocyte fate, ot megakaryocyte-erythroid progenitors (MEPs), which only produce erythroid and MK cells[380]. The HSC's choice between differentiation and self-renewal is regulated by both intrinsic and extrinsic mechanism. The intrinsic mechanisms involve genetic and epigenetic regulation, involving both transcriptional factors and chromatin modifiers. Moreover, the environment of blood system regulates HSC behavior, including cell-cell interactions, cytokines release and extracellular matrix associated ligand. The stepwise identification of multiple surface markers was able to define stem and progenitor cell populations by Flow Cytometry. The correlation of surface markers expression patterns with functional tests examining self-renewal capacity, clonogenicity and lineage potentials, leads to enrichment of distinct HSCs populations[376,380].

5.2 Megakaryocytic differentiation

Megakaryocytes (MK) generate platelets for blood clotting and wound healing. MKs, residing within the bone marrow, are large cells characterized by the presence of a single, multilobulated and polyploid nucleus originated by endomitosis process. These cells derive from megakaryocyte-erythroid progenitors (MEPs), which can originate from CMPs or, directly, from HSCs. Bipotent megakaryocyte and granulocyte progenitors give rise to unipotent progenitors that ultimately give rise to a fully mature progeny[381]. The transcriptional factor MYB plays a crucial role in megakaryocytopoiesis due to its ability to influence the fate decision of MEPs. In fact, high MYB levels favor erythroid development, vice versa its low expression is required for MK differentiation[382]. However, megakaryocyte precursors are one of the most debated subjects so far. Recent studies have suggested non classical megakaryocytic differentiation pathways. It seems that megakaryocytes can be generated from multiple pathways and that some differential pathways do not require transit through a multipotent or bipotent megakaryocyte-erythrocyte progenitor stage[383].

5.3 Erythroid differentiation

Erythrocytes are pivotal to healthy of organisms because they provide O_2 and CO_2 transport. Red blood cells derive from erythroid progenitors and precursors which reside in the BM and have very short lifespan. Development studies show that there are two types of red blood cells: embryonic and adult cells. They develop from distinct hematopoietic progenitors in different anatomic sites[384].

The first erythroid progenitor originated from MEPs is the burst-forming unit erythroid (BFU-E) which in turn differentiate in the late progenitor colony-forming unit erythroid (CFU-E). Subsequently CFU-E become increasingly dependent on EPO and undergo terminal differentiation[385].

It has been shown that GATA1 is a master regulator of erythroid cell development[386]. Ectopic expression of GATA-1 in erythroleukemia cells eliminates their differentiation block to their differentiation and leads to terminal cell division[387].

5.4 Granulocytic and monocytic differentiation

Granulocytes are a category of leukocytes (white blood cells) characterized by the presence of granules in their cytoplasm. Therefore, they are also called polymorphonuclear leukocytes or polymorphonuclear neutrophils because of the various shapes of their nucleus. Neutrophil granulocytes are the most form abundant of the granulocytes. The other cell types (eosinophils, basophils, and mast cells) are fewer in peripheral blood. Monocytes are another type of white blood cell. They can differentiate into macrophages and myeloid lineage dendritic cells. Monocytes influence the process of adaptive immunity.

Granulocytes and monocytes are produced in the bone marrow from common myeloid progenitors (CMPs). CMPs generates several types of myeloid progenitors with proliferative and differentiative potential. The first progenitors are CFU-GM (granulo-monocyte colony-forming unit) that in turn give rise to CFU-M (monocyte colony-forming unit) or GFU-G (granulocytic colony-forming unit). These progenitors generate precursors increasingly more differentiated until reaching mature granulocytes and monocytes[388].

It has been shown that cell cycle inhibition mediated by C/EBPα is required for the terminal phases of granulocytic differentiation[389]. C/EBPα also binds the endogenous PU.1 promoter[390]. In fact, C/EBPα and PU.1 are essential for the generation of granulocyte-macrophage progenitors. C/EBPα expression in committed lymphoid cells (B and T cells) instructs the development of macrophages. Furthermore, committed T cells transdifferentiate into myeloid dendritic cells upon ectopic PU.1

expression[391,392]. Activation of the PU.1 promoter by C/EBPα helps account for the finding that myeloid cells show increased levels of PU.1 compared with B-lineage cells[393].

EXPERIMENTAL DESIGN

Myeloproliferative neoplasms (MPNs), a category of diseases that include Polycytemia Vera (PV), Essential Thrombocythemia (ET) and Primary Myelofibrosis (PMF)[1], are clonal hematopoietic stem cell disorders characterized by an increase in the proliferation of terminally differentiated myeloid cells. Among the MPNs, PMF carries the worst prognosis and is defined by the presence of Bone Marrow (BM) fibrosis, extramedullary hematopoiesis and short overall survival[117]. Moreover, PMF patients are characterized by increased numbers of dysplastic megakaryocytes (MK) in the BM and is also associated with granulocytic proliferation[45]. Of note, patients suffering from PMF show increased pro-inflammatory cytokines and Reactive Oxygen Species (ROS) levels, which play a pivotal role in the disease progression[78,322].

The molecular pathogenesis of MPNs has been extensively investigated after the discovery of the somatic gain-of-function mutations involving JAK2 and MPL in the majority of MPNs patients[119,135]. Furthermore, the discovery of mutations in the gene encoding CALR in 2013 has improved the knowledge of these complex disorders[143,144]. Indeed, it has been demonstrated that CALR mutations generate a novel C-terminal domain that enables the N-terminal domain of CALR to interact with the extracellular domain of MPL, inducing constitutive activation of JAK-STAT signalling[148,264]. Although extensive studies have demonstrated that all these driver mutations are able to directly or indirectly induce the activation of JAK/STAT pathway, their presence alone does not fully explain the heterogenous pathological features observed in MPNs.

In this regard, current therapeutic approaches, mainly targeting JAK-STAT signalling pathway[394], have been found to provide only a little modulation on the symptoms and prognosis of myeloid malignancies[45]. In a retrospective analysis of CALR-mutant patients it has been demonstrated that only 16.8% of them exhibited a CALR allele-burden reduction after Ruxolitinib treatment[135]. In fact, recent studies shown that additional pathogenic mechanisms mediated by CALR mutants and independent from JAK-STAT signalling pathway exist. Moreover, clinical reports show a preferential expression of CALR in the megakaryocyte (MK) compartment, leading to the hypothesis that CALR mutations could preferentially affect the human megakaryocytic lineage compared to the other myeloid cell types[250].

For this reason, in my PhD thesis project I planned to study: 1) the role of Wild-Type (WT) CALR during physiological hematopoiesis, 2) the role of CALR mutations that could arise in an MPL-independent manner in order to identify additional pathways

whose alterations might cooperate with cellular transformation mediated by MPL activation.

***1) Wild-Type CALR*:** CALR is an Endoplasmic Reticulum (ER) chaperone responsible for calcium homeostasis and protein folding. CALR is also able to perform different functions outside the ER, such as responses to cellular stress, cell adhesion, immunity and cell differentiation. However, no data are available on the physiological function played by CALR during normal hematopoiesis.

To shed light on the role of CALR in the proliferation and differentiation of Hematopoietic Stem/Progenitor Cells (HPSCs), in first part of my thesis, we performed overexpression and gene silencing experiments in Cord Blood (CB) CD34+ cells from healthy subjects.

To this end, CD34+ cells have been transduced with the retroviral LXIDN vector expressing the full-length CALR cDNA and DLNGFR as reporter gene, in the bicistronic transcript derived by the viral LTR[395]. After purifying the transduced cells by immunomagnetic separation for the NGFR marker, we evaluated the biological effects exerted by CALR overexpression by means of various *in vitro* assays (**Figure 21**).

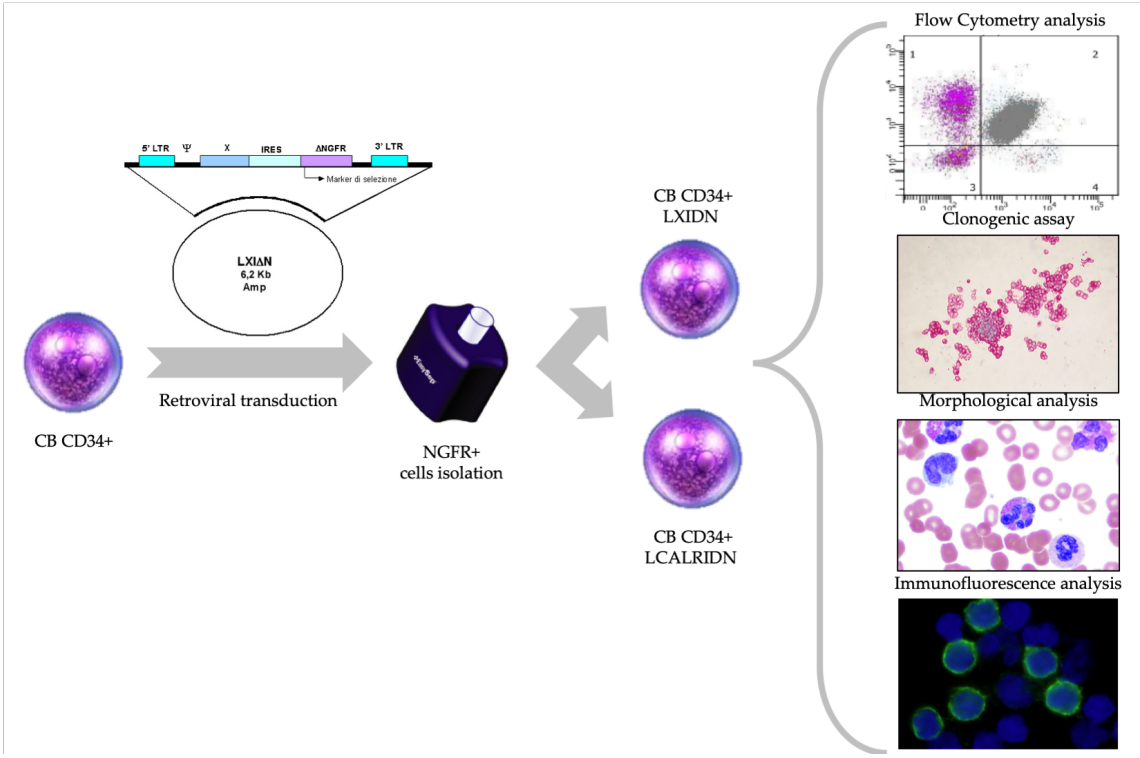

Figure 21: *Functional validation of LXIDN and LCALRIDN was carried out by their overexpression in healthy CB CD34+ cells. We performed different analysis to evaluate the expression of lineage markers: Flow Cytometry analysis, Collagen-based clonogenic assay, Methylcellulose-based clonogenic assay, Morphological analysis of May-Grünwald-Giemsa-stained slides and Immunofluorescent analysis.*

The effect of WT CALR expression has been evaluated both in liquid and semisolid culture, through the Flow Cytometric evaluation of the expression of the lineage differentiation markers and Colony-Forming Unit (CFU) assay. Moreover, we also performed morphological analysis of May-Grünwald-Giemsa-stained samples and Immunofluorescent analysis of lineages markers on different days. Furthermore, to better characterize the molecular mechanisms underlying the observed biological effects, we performed Gene Expression Profiling (GEP) of LCALRIDN and LXIDN cells by using Affymetrix HG-U219 Array Strips®. GEP data were processed with Partek Genomic Suite Software®, while Differentially Expressed Gene (DEG) evaluation was carried out by means of Ingenuity Pathway Analysis software (IPA)® (**Figure 22**).

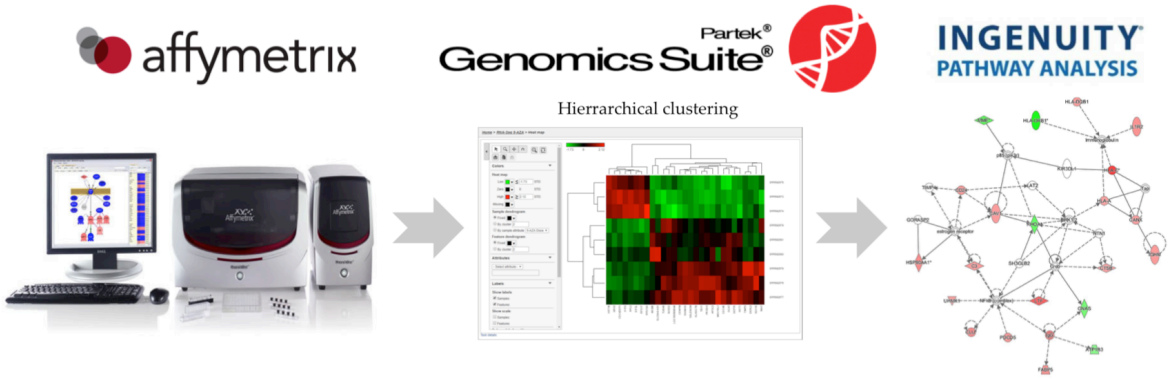

Figure 22: *Gene Expression Profiling (GEP) was performed in order to identify the molecular mechanism underlying the biological effect of CALR overexpression using Affymetrix HG-U219 Array Strips®. GEP data were processed with Partek Genomic Suite Software®, Differentially Expressed Gene (DEG) evaluation was carried out by means of Ingenuity Pathway Analysis software (IPA)®.*

Next, to confirm the role played by CALR in the regulation of megakaryocytopoiesis and erythropoiesis, CALR silencing was performed and the same parameters was evaluated to assess its effect on differentiation. To this end, CB CD34+ cells were electroporated with a siRNA directed against CALR. Its effects were compared to non-targeting control siRNA (NT-siRNA)(**Figure 23**).

In order to better characterize the molecular mechanisms underlying the observed biological effects, we again performed Gene Expression Profiling (GEP) of CALR siRNA and NT siRNA cells by using Affymetrix HG-U219 Array Strips®. GEP data were processed with Partek Genomic Suite Software®, while Differentially Expressed Gene (DEG) evaluation was carried out by means of Ingenuity Pathway Analysis software (IPA)®.

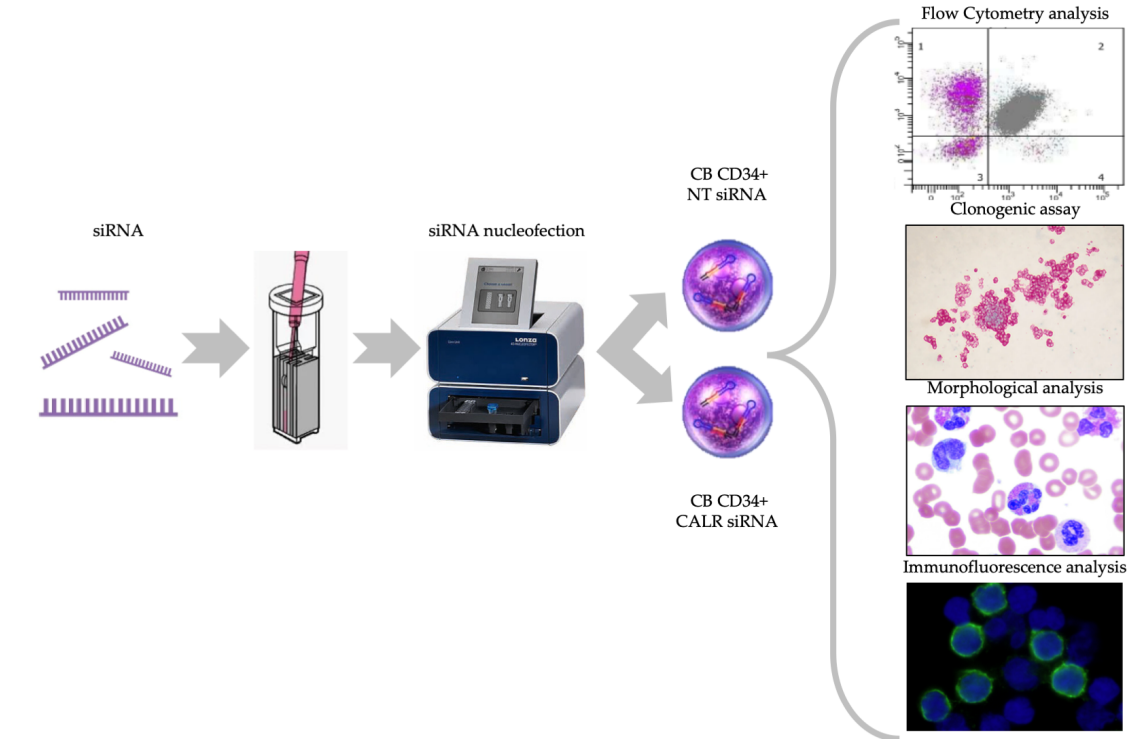

Figure 23: *Functional validation of NT siRNA and CALR siRNA was carried out by nucleofection in healthy CB CD34+ cells. We performed different analysis to evaluate the expression of lineage differentiation markers: Flow Cytometry analysis, Collagen-based clonogenic assay, Methylcellulose-based clonogenic assay, Morphological analysis of May-Grünwald-Giemsa-stained slides and Immunofluorescent analysis.*

***2) CALR mutants*:** Mutations in exon 9 of Calreticulin (CALR) consist of insertions and/or deletions that induce a frameshift, resulting in the formation of a stop codon that induce the loss of the C-terminal portion domain and the KDEL sequence. Moreover, the negative charges required for Ca^{2+} binding are partially or completely lost in CALR mutants. Recent studies have established that the interaction between mutant CALR and the extracellular domain of MPL induces structural changes in the MPL-JAK2 complex that are required for receptor activation[263,264,266]. However, the effect of CALR mutants on the functionality of Endoplasmic Reticulum (ER) hasn't been elucidated so far.

Moreover, CALR plays a pivotal role in the quality control of protein folding[335]. It has been demonstrated that CALR overexpression increases cell sensitivity to H_2O_2-induced cytotoxicity[207], suggesting that CALR can be involved in oxidative stress-induced apoptosis. However, no report has described the role of CALR mutants in Unfolded Protein Response (UPR) and oxidative stress response.

Therefore, in the second part of my thesis, in order to characterize the MPL-independent mechanisms underlying the effect of CALR mutations in myeloproliferative neoplasms, we analysed the transcriptional changes induced by

CALR mutants, either CALRdel52 or CALRins5, in the K562 cell line, devoid of MPL expression. K562 cells have been transduced with the retroviral LXIDN vector expressing the WT CALR (LCALRwtIDN) or one of the two commonest CALR mutated variants (LCALRins5IDN, LCALRdel52IDN), in association with NGFR marker necessary for the purification of these transduced cell lines. After purification, we have evaluated the Gene Expressions Profiling (GEP) of these three cell lines by means of Affymetrix HG-U219 Array Strips® and, subsequently, we performed the unsupervised analysis of these data through the Principal Component Analysis (PCA). In order to characterize the interactions between Differentially Expressed Genes (DEGs) and determine their role in MPN pathogenesis, we performed a functional analysis with Ingenuity Pathway Analysis (IPA)®(**Figure 24**).

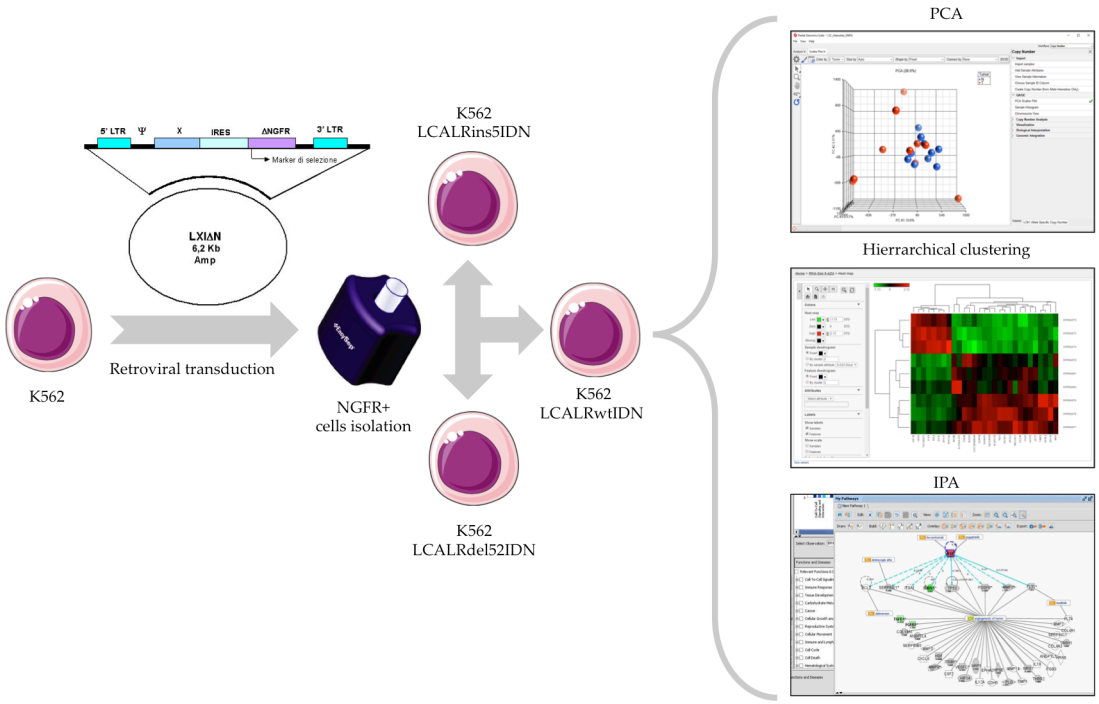

Figure 24: *Gene Expression Profiling (GEP) was performed in order to identify MPL-independent mechanisms underlying the biological effect of CALR mutations in K562 transduced cell lines by using Affymetrix HG-U219 Array Strips®. GEP data were processed with Partek Genomic Suite Software®, that has enabled us to carry out the Principal Component Analysis (PCA). Differentially Expressed Gene (DEG) evaluation was performed by means of Ingenuity Pathway Analysis software (IPA)®.*

As mentioned before, severe hypoxic exposure causes ER stress and regulates several UPR downstream effector pathways in a non-specific manner[357]. Thus, in order to analyze the effect of CALR mutations on the response to ER stress, K562-WT and K562 CALR-mutant cells were cultured in hypoxic environment. Activation of UPR response was evaluated by measuring the expression levels of the different UPR pathways components: Grp78, CHOP, ATF4, GADD34 for the PERK pathways and ERDJ4, XBP1(Spliced)/XBP1(Unspliced) for IRE1 signalling. To further assess the

effects of CALR mutants on the response to ER stress, K562 cells were treated with specific ER stress inductors: Tunicamycin (Tm) and Thapsigargin (Tg). In particular, Tm causes the accumulation of unfolded proteins in the Endoplasmic Reticulum (ER) by inhibiting proteins N-glycosylation[358], while Tg blocks the activity of the SERCA Ca^{2+}-ATPase pump, involved in calcium homeostasis[360]. We evaluated UPR activation, both at the transcriptional and at the protein level, by RT-qPCR and Western Blot analysis. Moreover, to investigate whether CALR mutations confer a different resistance to ER stress, we treated K562 cells with Tm and evaluated apoptosis levels by Annexin V/PI staining.

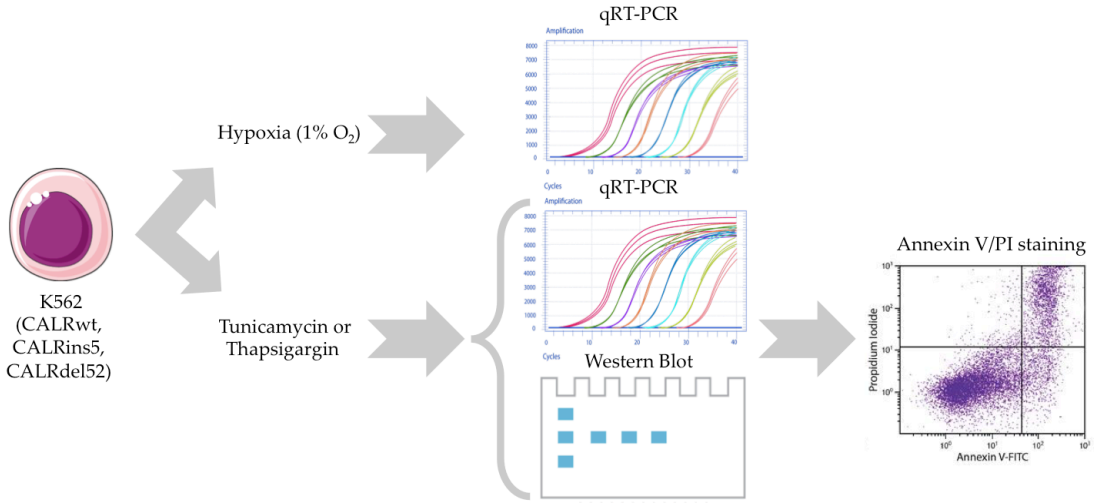

Figure 25: *Analysis of ER stress response in the K562-WT and K562 CALR-mutant cells. ER stress was induced in different ways: by generating a hypoxic environment or by Tunicamycin (Tm) and Thapsigargin (Tg) treatment. Stress-induced effects were evaluated by RT-qPCR and Western Blot analysis. Moreover, we measured the apoptosis levels of Tm treated K562 cells by Annexin V/PI staining.*

Next, in order to assess whether CALR mutations are also able to impact on oxidative stress levels and the associated genomic instability, we treated K562 cells expressing either the WT or the mutated variants of CALR with Melittin or Mitirone. Melittin (MEL) is the main constituent of bee venom involved in the induction of oxidative stress and DNA damage[396], while Miltirone (MILT) is a diterpene quinine compound isolated from *Salvia miltiorrhiza* that induces oxidative stress through the increase of ROS production[397]. The effects of these treatments on the DNA damage was measured through different oxidative stress markers, after 24 hours of treatment and after 24 additional hours in culture without the damaging agent in order to repair the damage. First of all, we measured the levels of genetic markers involved in oxidative stress-induced DNA damage, including γ-H2AX and 8-OHdG. Then, after having shown that DNA damage was specifically induced by oxidative stress, we have assessed the

intracellular levels of ROS and the activity of antioxidant enzymes, such as Superoxide Dismutase (SOD) or Glutathione Reductase (GSR)(**Figure 26**). In fact, enhanced ROS production has been already associated to DNA damage in hematopoietic stem cells[398].

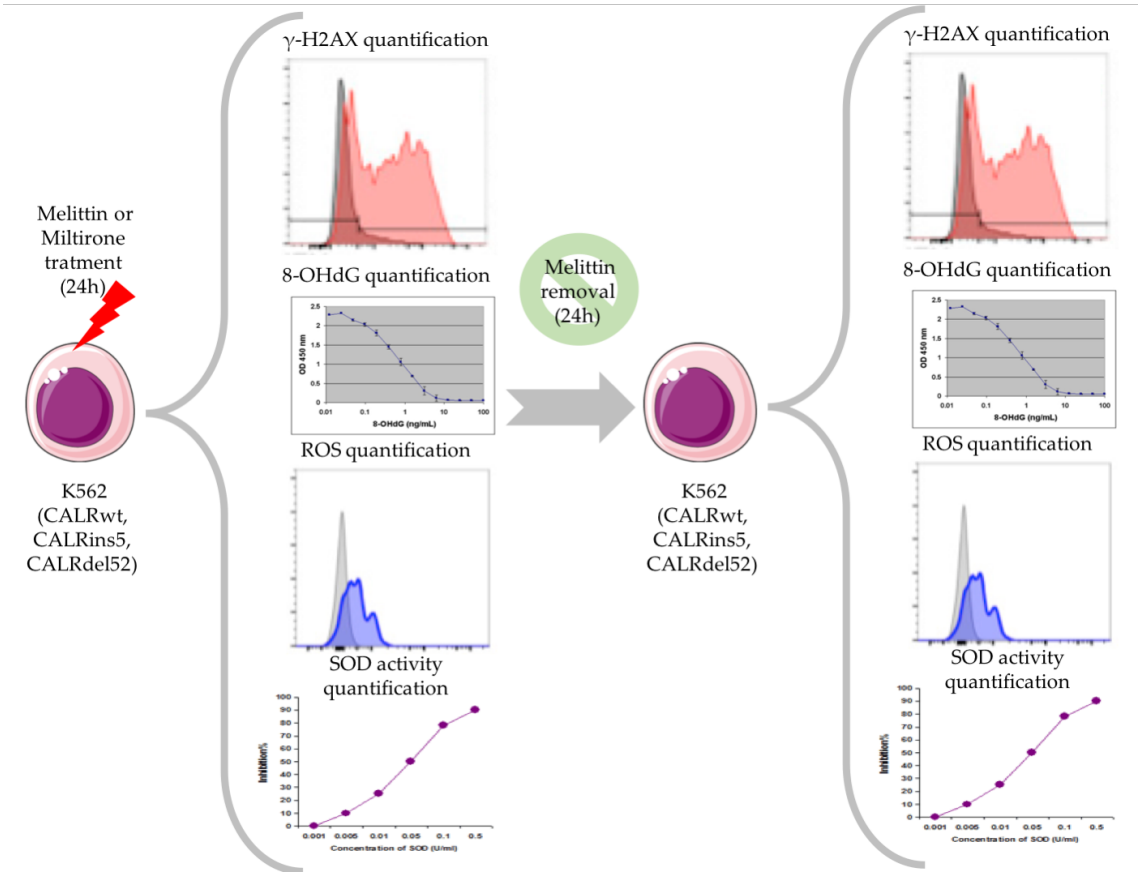

Figure 26: *Analysis of oxidative stress on the K562-WT and K562 CALR-mutation cells. Oxidative stress was induced in different ways: by Melittin (MEL) and Miltirone (MILT) treatment. The oxidative stress-induced effects on DNA was evaluated by quantification of γ-H2AX and 8-OHdG. Moreover, we measured the intracellular levels of ROS and the activity of antioxidant enzymes, such as SOD or GSR.*

Finally, to unravel the potential molecular mechanisms responsible for the increased of oxidative stress-induced DNA damage in K562 cells carrying CALR mutations, we investigated the biological function of Oxidation Resistance gene 1 (OXR1) deregulation. OXR1 was found deregulated in the comparison between CALR mutated and WT K562 cells. Previous data demonstrated that this gene seems to affects the capability of mutant cells to counterbalance ROS accumulation through the p21 pathway[332,333]. To this end, we performed OXR1 silencing in CB CD34+ cells from healthy subjects, which are the target cells involved in the development of myeloproliferative disorders. After having confirmed the downregulation of mRNA levels in OXR1siRNA sample, we assessed the effects of this knockdown on the response to the oxidative stress by measuring ROS and γ-H2AX levels, at 24 hours after Melittin treatment and at 24 hours in culture after treatment removal (**Figure 27**).

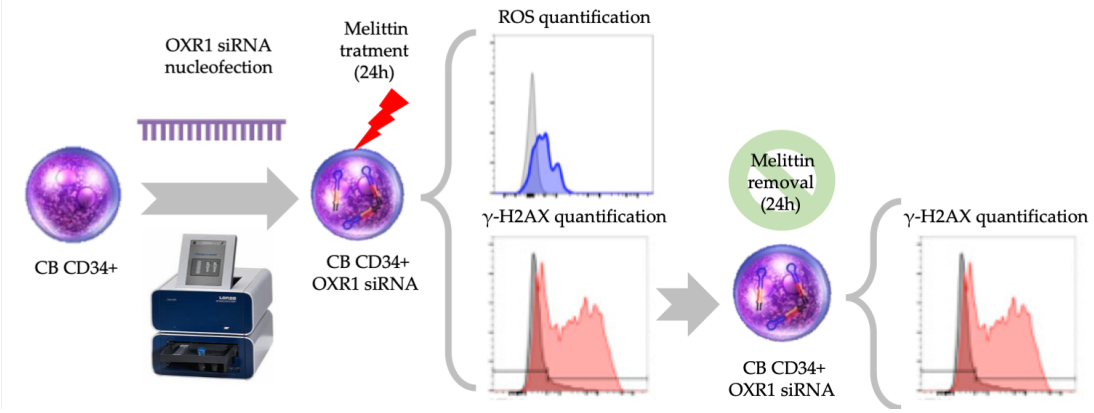

Figure 27: *Functional studies following OXR1 gene silencing in CD34+ cells. To evaluate the regulation of oxidative stress response we treated OXR1 silenced cells with Melittin and have evaluated the levels of ROS and γ-H2AX during and after treatment.*

Collectively, in my PhD thesis I attempted to define how mutants CALR mutants play a role in the pathogenesis of myeloproliferative neoplasms in a MPN-independent manner and how endogenous Wild-Type CALR can regulate hematopoietic stem/progenitor cell fate.

MATERIALS AND METHODS

1. SAMPLES

1.1 Ethics statements

Human Cord Blood (CB) samples, used for in vitro experiments, were collected after normal deliveries, according to the institutional guidelines for discarded material (Clearance of Ethical Commitee for Human experimentation of Florence: Comitato Etico Area Vasta dell'Azienda Ospedaliero-Universitaria Careggi, approval date:April 22, 2011, approval file number # 2011/ 0014777).

1.2 CD34+ HSPC isolation and cell culture conditions

Human CD34+ cells were purified from CB by density gradient separation using Lympholyte®-H Cell Separation (CEDARLANE) Media according to the manufacturer's instructions. Briefly, CB was diluted 1:4 with Phosphate-Buffered Saline (PBS) with 1 mM EDTA and 2% Fetal Bovine Serum (FBS) and centrifuged at 800xg for 20 minutes at room temperature (RT) in a swinging-bucket rotor without brake. The monocuclear cell (MNC) ring was then recovered and washed thrice with PBS. MNCs were further processed through the immunomagnetic CD34 positive selection (CD34 MicroBead Kit UltraPure, MILTENYI BIOTEC).

After immunomagnetic separation, CD34+ cells were seeded in 24-well plates at the concentration of $5x10^5$ cells/ml in Iscove's modified Dulbecco's medium (IMDM)(GIBCO) containing 20% Human Serum (HS)(BIO-WHITTAKER), SCF (50ng/ml), Flt3-ligand (Flt3 L)(50ng/ml), THPO (20ng/ml), IL-6 (10ng/ml), and IL-3 (10ng/ml)(all from MILTENYI BIOTEC) and transduced with the retroviral vector or electroporated 24 hours later.

- *Oxidative stress*: To induce oxidative stress, CD34+ cells were seeded at $5x10^5$ cells/ml in IMDM, as described above, and exposed to Melittin 5μg/ml (SIGMA-ALDRICH)(SANTA CRUZ BIOTECHNOLOGY) for 24 hours at 37 °C in a humidified atmosphere with 5% CO_2. To assess the capacity of CD34+ cells to repair the oxidative damage induced by MEL exposure, 24 hours after treatment cells were washed twice with PBS and then seeded at $5x10^5$ cells/ml in fresh culture medium for additional 24 hours.

1.3 K562 cell culture conditions

K562 cell line originated from Human Caucasian Chronic Myelogenous Leukemia (CML) and was previously purchased by our laboratory. K562 cells were seeded at $3x10^5$ cells/ml in RPMI-1640 medium (EUROCLONE) supplemented with 10% FBS (SIGMA-ALDRICH). Subsequent passages were performed when cells reached 70-80% confluency.

- *Hypoxia*: To provide a hypoxic environment (1% O_2), cells were cultured and treated in sealed incubators calibrated for a constant hypoxic environment: 1% O_2, 94% N_2 and 5% CO_2, at a temperature of 37 °C. For physiological oxygenation or normoxia (N), cells were cultured in an incubator calibrated to 21% O_2.
- *ER stress*: To induce ER stress, K562 cells were seeded at $5x10^5$ cells/ml in RPMI-1640 supplemented with 10% FBS and exposed to Tunicamycin (Tm)(SIGMA-ALDRICH) 2.5µg/ml for 4 and 6 hours, or to Tunicamycin 20µg/ml for 24 hours, or to Thapsigargin (Tg)(SIGMA-ALDRICH) 0.1µM or 1µM for 4 and 6 hours.
- *Oxidative stress*: To induce oxidative stress, K562 cells were seeded at $5x10^5$ cells/ml in RPMI-1640 supplemented with 10% FBS and exposed to Melittin (MEL) 5µg/ml (SIGMA-ALDRICH) or to Miltirone (MILT) 10µM (SANTA CRUZ BIOTECHNOLOGY) for 24 hours at 37 °C in a humidified atmosphere with 5% CO_2. To assess the capacity of K562 cells to repair the oxidative damage induced by MEL exposure, 24 hours after treatment cells were washed twice with PBS and then seeded at $5x10^5$ cells/ml in fresh culture medium for additional 24 hours.

2. OVEREXPRESSION AND DOWNREGULATION GENE EXPERIMENTS

2.1 CD34+ Retroviral vectors packaging

The human CALR cDNA (NM_004343) was synthesized and cloned into the retroviral vector LXIDN (**Figure 28**)[395,]. Packaging line for LCALRIDN was generated by transinfection in the ecotropic Phoenix and amphotropic GP+envAm12 cells, as previously described[395,65].

Viral titers were assessed by Flow Cytometry analysis of a truncated version of low-affinity Nerve Growth Factor Receptor (DeltaNGFR, DNGFR) expression percentage upon infection of CD34+ cells.

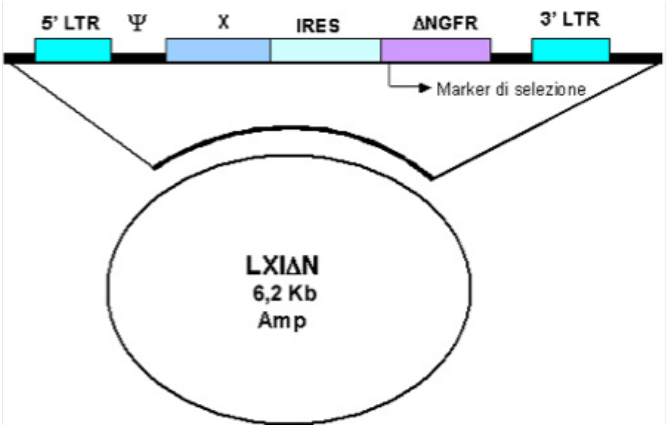

Figure 28: *Schematic representation of LXIDN retroviral vector used for the in-vitro experiments* (GRANDE ET AL., BLOOD, 1999)[395]

2.2 CD34+ HSPC transduction and purification

Transduction of CB CD34+ cells was performed 24 hours after isolation. Retroviral transduction was performed by four cycles of infection (one every 12 h) with viral supernatant with the addition of Polybrene (8mg/ml), 20% HS, and human cytokines (SCF, Flt3-l, THPO, IL-6, and IL-3 as described above) in retronectin-coated plates. Untreated 24-well plates were coated with Retronectin (10μg/cm^2)(TAKARA BIO INC) following the manufacturer's protocol. To achieve optimal expansion and infection of primary CD34+ cells, the retronectin-coated plates were preincubated with retroviral supernatant for 4 hours, and then CD34+ cells were seeded in 24-well plates at 3x10^5 cells/ml (1ml/well) in fresh viral supernatant. After transduction, CB CD34+ cells were maintained in the above described liquid culture conditions for additional 36 hours.

Transduced CD34+ cells were subsequently purified by means of immunomagnetic selection (EasySep ''Do-It-Yourself'' Selection Kit, STEMCELL TECHNOLOGIES) using the anti-human p75-NGFR mouse monoclonal antibody (BD BIOSCIENCES). Purity of the NGFR+ cell fraction was assessed by flow cytometry after labeling with PE-conjugated anti-NGFR monoclonal antibody (MILTENYI BIOTEC) 48 hours post purification and was always >90%. Moreover, cells were analyzed 24 and 48 hours after the last infection for both cell viability and CALR mRNA and protein expression.

2.3 CD34+ nucleofection

Human CD34+ cells were transfected by using the 4DNucleofector™ System (LONZA). Briefly, each sample was electroporated three times once every 24 hours with a small interfering RNA (siRNA) targeting human CALR mRNAs (siRNA ID s115, LIFE TECHNOLOGIES) or human OXR1 mRNAs (siRNA ID s115, LIFE

TECHNOLOGIES), starting from the day after CD34+ cell purification. For each electroporation, $4x10^5$ CD34+ cells were resuspended in 100µl of P3 Primary Cell Solution (LONZA), containing 3mg of siRNA, and pulsed with the program DS112.

To exclude nonspecific effects caused by interfering RNA (RNAi) nucleofection, a sample transfected with a non targeting siRNA (NT siRNA, LIFE TECHNOLOGIES) was included. Cells were analyzed 24 and 48 hours after the last nucleofection for both cell viability and expression of OXR1 or CALR mRNA and protein.

2.4 K562 Retroviral vectors packaging

The cDNAs coding for human CALR (NM_004343) and the two commonest CALR mutated variants (CALRdel52/type I and CALRins5/type II) were synthesized (service from ORIGENE TECHNOLOGIES) and cloned into the retroviral vector LXIDN(**Figure 28**)[395].

Packaging line for LCALRwtIDN, LCALRdel52IDN, LCALRins5IDN were generated by transfection in the ecotropic Phoenix and amphotropic GP+ envAm12 cells, as previously described[395,65].

2.5 K562 transduction and purification

Transduction of K562 cells was performed by four cycles of infection (one every 12 hours) with viral supernatant with the addition of Polybrene (8mg/ml), and 20% FBS (SIGMA-ALDRICH) in retronectin-coated plates. Untreated 24-well plates were coated with Retronectin (10µg/cm^2)(TAKARA BIO INC) following the manufacturer's protocol. Then K562 cells were seeded in 24-wells plates at $3x10^5$ cells/ml (1ml/well) in fresh viral supernatant. After transduction, K562 cells were maintained in Roswell Park Memorial Institute medium (RPMI-1640, EUROCLONE) supplemented with 20% FBS for additional 36 hours.

Transduced K562 cells were subsequently purified by means of immunomagnetic selection (EasySep "Do-It-Yourself" Selection Kit; STEMCELL TECHNOLOGIES) using the anti-human p75-NGFR mouse monoclonal antibody (BD BIOSCIENCES). Purity of the NGFR+ cell fraction was assessed by flow cytometry after labeling with PE-conjugated anti-NGFR monoclonal antibody (MILTENYI) 48 hours post-purification and was always >90%. Moreover, cells were analyzed 24 and 48 hours after the last nucleofection for both cell viability and CALR protein expression.

3. TRANSCRIPTOMIC ANALYSIS

3.1 RNA extraction

Total cellular RNA was harvested from $1x10^5$ cells from each sample using the miRNeasy Micro RNA isolation kit (QIAGEN), according to the manufacturer's instructions. RNA samples concentration and purity (assessed as 260/280nm and 260/230nm ratios) were evaluated by NanoDrop ND-1000 spectrophotometer (NANODROP TECHNOLOGIES), while RNA integrity was assessed by using the Agilent 2100 Bioanalyzer (AGILENT TECHNOLOGIES).

3.2 Quantitative reverse transcription polymerase chain reaction

Total RNA (100ng) was reverse transcribed to cDNA using a High Capacity cDNA Reverse Transcription Kit (LIFE TECHNOLOGIES). TaqMan PCR was carried out using the TaqMan Fast Advanced PCR master mix and TaqMan gene expression assays (all reagents from LIFE TECHNOLOGIES) by means of a 7900HT Fast Real-Time PCR System (APPLIED BIOSYSTEMS). Assays were performed in triplicate.

Gene expression profiling (GEP) was achieved using the comparative cycle threshold (CT) method of relative quantitation using Glyceraldehyde-3-phosphate dehydrogenase (GAPDH) as housekeeping genes. To normalize data, $\Delta\Delta$CT was calculated for each sample using the mean of its ΔCT values subtracted from the mean ΔCT value measured in the control sample, set as a calibrator; relative quantitation (RQ) value was expressed as $2^{-\Delta\Delta CT}$.

3.3 Gene expression profiling

GEP was performed on RNA samples isolated from NGFR-positive cells (CD34+ or K562) purified after retroviral transduction from the samples expressing empty control vector LXIDN (LXIDN) and from the samples expressing carrying CALRwt cDNA (LCALRwtIDN, also called LCARLIDN), CALRdel52 cDNA (LCALRdel52IDN), CALRins5 cDNA (LCALRins5IDN), obtained from three independent experiments.

Biotin-labeled cRNA synthesis was performed using the GeneAtlas® 3'IVT Express Kit according to the protocol supplied by Affymetrix. The HG-U219 Array Strips (AFFYMETRIX) hybridization, staining, and scanning were performed by using the GeneAtlas Platform.

Robust Multiarray Average (RMA) procedure was used to perform probe-level normalization and conversion into expression values. Differentially Expressed Genes

(DEGs) were then selected following a supervised approach with the analysis of variance (ANOVA) module supplied by the Partek GS. 6.6 Software Package (www.partek.com).

We consider as differentially expressed all the probesets with a fold change contrast ≥1.5 in the pairwise comparison between LCALRIDN, LCALRdel52IDN, LCALRins5IDN versus LXIDN samples and a P-value ≤0.05.

In the same way, GEP was performed on RNA samples isolated from CALR-silenced (CALRsiRNA sample) and non-targeting negative control siRNA-transfected (NTsiRNA sample) CD34+ cells 24 hours after last nucleofection from three independent experiments.

GEP data were analyzed by using the Partek GS 6.6 Software Package as reported above, by selecting the probesets with a fold change contrast ≥1.5 (P<0.05) as DEGs in the pairwise comparison between CALR siRNA and NTsiRNA samples.

Raw and normalized GEP data have been submitted to the NCBI's Gene Expression Omnibus (GEO) public repository (www.ncbi.nlm.nih.gov/geo; series GSE97809 for CD34+ cells, series GSE114414 for K562 cells).

To construct the regulatory interaction networks of the deregulated genes interactions, functional analysis was performed using Ingenuity Pathway Analysis (IPA) software (IPA, version 8.6)(www.ingenuity.com).

4. PROTEIN ANALYSIS

4.1 Western Blot

Protein levels were assessed by means of Western Blot analysis in K562 and CD34+ cells overexpressing or downregulating CALR (CALRwt, CALRins5, CALRdel52).

Briefly, cells were harvested at different times after drugs treatment or transduction/nucleofection, washed twice with cold PBS and lysed in 50mM Tris (tris(hydroxymethyl) aminomethane)-Cl (pH 7.4), 150 mM NaCl, 1% Nonidet P-40, 10 mM KCl, 1 mM EDTA, 20 mM NaF, 0.25% Na Doexycholate, 5 mM Dithiothreitol (DTT). Protease inhibitors (ROCHE) and phosphatase inhibitors (THERMOFISHER SCIENTIFIC) were added to the lysis buffer. Samples were centrifugated at 10'000xg for 15 minutes at 4°C. Protein concentration was determined by the Pierce™ Coomassie Plus (Bradford) Assay Kit (THERMO FISHER).

Total cellular lysates (30μg for each samples) were loaded and separated on 10% or 12,5% SDS-polyacrylamide gel, based on the MW of proteins, and then transferred on

a Nitrocellulose membrane 0,45μm (BIORAD) by electroblotting procedure in TGM buffer (25mM Tris pH 8.3, 250mM Glycine, 20% Methanol). To monitor the electroblotting efficiency, the membrane was stained in 0.2% Red Ponceau – 3% TCA and destained in 3% TCA (Dichloroacetic acid).

Membranes were then pre-blocked in a blocking solution of 0,1% TBST containing 5% non-fat dry milk (NFDM) or 0,1% TBST containing 2.5% bovine serum albumin (BSA), according to the antibodies manufacturer's instructions.

Then membranes were incubated with the following primary antibodies: rabbit polyclonal anti-CALR antibody (Co. ab2907, 1:250 dilution, ABCAM), mouse monoclonal anti-GRP78 antibody (Co. sc-376768, 1:500 dilution, SANTA CRUZ BIOTECHNOLOGY), mouse monoclonal anti-CHOP antibody (Co. sc-7351, 1:100 dilution, SANTA CRUZ BIOTECHNOLOGY), mouse monoclonal anti-ATF4 antibody (Co. sc-390063, 1:50 dilution, SANTA CRUZ BIOTECHNOLOGY), rabbit polyclonal anti-eIF2α antibody (Co. 9722, 1:200 dilution, CELL SIGNALING TECHNOLOGY), rabbit polyclonal anti-Phospho-eIF2α antibody (Co. 9721, 1:200 dilution, CELL SIGNALING TECHNOLOGY) and rabbit polyclonal anti-βACTIN antibody (Co. PA1-16889, 1:2'000 dilution, THERMO FISHER).

The blots were washed three times with 0,1% TBST and then incubated with 1:1000 dilution of HRP-conjugated goat anti-rabbit secondary antibody (Co. 32460, THERMO FISHER) or with 1:2000 dilution HRP-conjugated donkey anti-mouse secondary antibody (Co. sc-2314, SANTA CRUZ BIOTECHNOLOGY) for 1 hour at RT. After three washes with 0,1% TBST, SuperSignal West Pico Plus Chemiluminescent Substrate (THERMO FISHER) was used for protein detection.

5. IMMUNOPHENOTYPIC AND MORPHOLOGICAL ANALYSIS

5.1 Liquid culture differentiation assay

For liquid culture differentiation assays, 24h after the nucleofection or after NGFR-positive cell isolation, CD34+ cells were plated ($5x10^5$cells/ml) in the following conditions:

- *Multilineage differentiation medium*: IMDM added with 20% BIT serum substitute (Bovine Serum Albumin, Insulin, and Transferrin; STEMCELL TECHNOLOGIES), supplemented with SCF (50ng/ml), Flt3L (50ng/ml), THPO (20ng/ml), IL-6 (10ng/ml), and IL-3 (10ng/ml).

- *MK differentiation medium*: serum-free medium SYN-H (AB CELL-BIO) supplemented with SCF (5ng/ml), THPO (50ng/ml), IL11 (4ng/ml), IL3 (2ng/ml), and IL6 (1ng/ml).
- *Erythroid differentiation medium*: IMDM added with 20% BIT serum substitute (STEMCELL TECHNOLOGIES) supplemented with Erythropoietin (EPO; 0.4U/ml; R&D SYSTEMS) and SCF (50ng/ml; MILTENYI BIOTEC); (all cytokines from MILTENYI BIOTEC).

The medium was routinely replaced every 3 days or anytime it appeared to be consumed.

5.2 Flow Cytometry analysis

Differentiation of CD34+ cells under different culture conditions was monitored by Flow Cytometry analysis of Myeloperoxidase (MPO) as an intracellular antigen, CD15, CD66b, for erythroid differentiation, CD14 and CD163 for monocyte/macrophage differentiation, Glycophorin A (GPA) for erythroid differentiation, CD41 and CD42b for MK differentiation. These analyses were performed from 3 to 17 days of liquid culture post NGFR-positive cells purification, in case of overexpression experiment and post the last nucleofection, in case of gene-silencing experiments.

The following monoclonal antibodies (MoAbs) were used for Flow Cytometry analysis: FITC-conjugated mouse antihuman CD41 MoAb, PE-conjugated mouse antihuman CD42b MoAb, PE-conjugated mouse anti-human GPA MoAb (all from DAKO), FITC-conjugated mouse antihuman MPO MoAb (BECTON DICKINSON), FITC-conjugated mouse antihuman CD15 MoAb, FITC-conjugated mouse antihuman CD66b MoAb, PE-conjugated mouse anti-human CD14 MoAb, APC-conjugated mouse anti-human CD163 MoAb (all from MILTENYI BIOTEC).

Briefly, after a PBS wash cell samples were incubated in the presence of Fc receptor (FcR) blocking reagent (1:100)(MILTENYI BIOTEC) for 30 minutes at 4°C and the indicated MoAbs (1:100 or 1:50 according to the antibodies manufacturer's instructions) for 30 minutes at 4°C o RT (according to the antibodies manufacturer's instructions).

After staining, cells were analyzed by using a BD FACSCanto II (BD BIOSCIENCES). At least 10'000 events were counted for each sample to ensure statistical relevance.

5.3 May-Grünwald-Giemsa staining

Differentiation of CD34+ cells was monitored by morphological analysis of May-Grünwald-Giemsa-stained cytospins on day 7 (erythroid differentiation) or 13 (MK differentiation) after the last nucleofection or retroviral infection.

An aliquot of suspended cells was used to prepare cytospin slides, by means of Shadon Cytospin 4 Cytocentrifuge (THERMO FISHER). Almost 50'000-80'000 cells per cultured sample were harvested and centrifuged. The obtained cell spot was then fixed and stained according to the May-Grünwald-Giemsa staining protocol. The spot was finally included with DPX Mountant for Histology (FLUKA ANALYTICAL).

Images were captured by using an Ax10scopeA1 microscope equipped with AxioCam ERc 5S Digital Camera and Axion software 4.8 (all CARL ZEISS MICROIMAGING). The images were then processed with Adobe Photoshop 7.0 software.

5.4 Immunofluorescence staining

An aliquot of suspended CD34+ cells was used to prepare cytospin slides as mentioned above.

Cytospins were fixed with 4% paraformaldehyde (PFA) and permeabilized using 0.3% Triton X-100 in PBS for 20 minutes at room temperature.

After blocking with 5% FBS, 2% BSA, and 0.1% Triton X-100 in PBS for 30 minutes at 37°C, slides were incubated with mouse anti-human CD41a (1:200 in blocking solution, BD) or mouse anti-human Glycophorin A (clone JC159, 1:100 in blocking solution; DAKO) overnight at 4°C.

This was followed by incubation with horseradish peroxidase-conjugated goat anti-mouse IgG (1:1,000 in blocking, Co. sc2005; SANTA CRUZ BIOTECHNOLOGY) for 30 minutes at 37°C. All incubations were followed by three washes with PBS solution. Nuclear counterstaining was performed with 4',6-diamino-2-phenylindole (DAPI). The slides were mounted with the DakoCytomation fluorescent mounting medium (DAKO).

Finally, fluorescence imaging was performed using Zeiss LSM 510 Meta Confocal Microscope (ZEISS) and digital images of representative areas were taken. To ensure random sampling, 50images/slide were captured and cells positive for GPA or CD41 were scored.

6. CLONOGENIC ASSAYS

6.1 Methylcellulose-based clonogenic assay

To assess variations in erythroid and myeloid lineage commitment of CD34+ cells during overexpression and nucleofection experiments, the methylcellulose clonogenic assay was performed. Briefly, 300 CD34+ cells were plated in triplicate in MethoCultTM GF H4434 "Complete" Methylcellulose Medium (STEMCELL TECHNOLOGIES) containing a cocktail of recombinant human cytokines: SCF (50ng/ml), granulocytemacrophage colony-stimulating factor (GM-CSF; 10ng/ml), IL-3 (10ng/ml), and erythropoietin (EPO; 3U/ml).

After 14 days of culture at 37°C in a humidified atmosphere with 5% CO2, colonies were scored as Erythroid Burst-Forming Units (BFU-E), Erythroid (CFU-E), Granulocyte (CFU-G), Macrophage (CFU-M), Granulocyte/Macrophage (CFU-GM) and Granulocyte/Erythrocyte/ Macrophage/Megakaryocyte (CFU-GEMM). MK Colony Forming Units (CFUMK) were assayed in collagen-based medium, using a commercial MK assay as reported below.

6.2 Collagen-based clonogenic assay

To assess variations in MK lineage commitment of CD34+ cells during overexpression and nucleofection experiments, the collagen-based clonogenic assay was performed. To this end, a commercial Mk assay detection kit (MegaCult-C, STEMCELL TECHNOLOGIES) was employed.

Briefly, 2'500 CD34+ cells were cultured in a volume of 0.75ml and seeded in a chamber of a double-chamber slide. The collagen-based system contains a medium supplemented to a final concentration with 1.1mg/ml Collagen, 1% BSA, 0.01mg/ml bovine pancreatic Insulin, 0.2mg/ml human iron saturated Transferrin and the human recombinant cytokines: 50ng/ml TPO, 10ng/ml IL-3 and 10ng/ml IL-6.

The chamber slides were incubated at 37°C for 11 days and then fixed for 20 minutes in 1:3 Methanol/Acetone. Megakaryocyte colonies were stained using a primary monoclonal anti-CD41 (GPIIb/IIIa) antibody and then identified by using an alkaline phosphatase detection system (all from STEMCELL TECHNOLOGIES).

Nuclei of all the cells regardless of lineage were counterstained with Evans Blue. CD41-positive colonies were scored as CFU-Mk; Mixed CD41-positive and CD41-negative colonies were scored as CFU-Mix; CD41-negative colonies were scored as CFU-nonMK. CFUMKs were scored according to the manufacturer's protocol as small

(3–21 cells, deriving from more mature megakaryocyte progenitors), medium (21–49 cells), and large (>50 cells, arising from more primitive MK progenitors) colonies based on their size, which reflects the maturation stage of the progenitor cells giving rise to each colony.

7. DNA DAMAGE MEASUREMENT

7.1 γ-H2AX assay

The phosphorylation of Histone H2AX at serine 139 (γ-H2AX) was evaluated in CD34+ and K562 cells after treatment with MEL 5μg/mL for 24 hours, after 24 hours of repair or after treatment with MILT 10μM for 24 hours by means of Flow Cytometry analysis.

Briefly, $1x10^5$ cells were fixed and permeabilized with Cell Signaling Buffer Set A (MILTENYI BIOTEC) and then stained with the Anti-H2AX pS139-FITC (clone: REA502, MILTENYI BIOTEC) for 30 minutes in the dark at room temperature.

After staining, cells were analyzed by using a BD FACSCanto II (BD BIOSCIENCES). At least 10'000 events were counted for each sample to ensure statistical relevance.

7.2 8-OHdG assay

Oxidative DNA damage was detected in K652 cells by means of OxiSelect Oxidative DNA Damage ELISA Kit (CELL BIOLABS).

Briefly, Genomic DNA was extracted from K652 cells carrying either CALRwt, CALRins5 or CALRdel52 after treatment with MEL 5μg/mL for 24 hours, after 24 hours of repair or after treatment with MILT 10μM for 24 hours by means of DNeasy Blood and Tissue kit (QIAGEN).

Genomic DNA was extracted from treated/untreated cells following a standard molecular biology protocol and re-suspended in 100 μL water.

The same amount of genomic DNA (3μg) was used for the detection of 8-OHdG, following the manufacturer's instructions.

8. APOPTOSIS DETECTION

8.1 Annexin V/PI staining

Apoptosis rate was evaluated in K562 cells after Tm treatment 20µg/ml for 24 hours by Annexin V-FITC Kit (TREVIGEN INC) following manufacturer protocol.

Briefly, $5x10^5$cells were washed with cold PBS and incubated in 100µL Annexin V Incubation Reagent for 15 minutes at RT in the dark.

After staining, cells were analyzed by using a BD FACSCanto II (BD BIOSCIENCES). At least 10'000 events were counted for each sample to ensure statistical relevance.

9. OXIDANT AND ANTIOXIDANT MOLECULES MEASUREMENT

9.1 Detection of ROS level

Intracellular ROS production has been evaluated in K562 or CD34+ cells after treatment with MEL 5µg/mL for 24 hours, after 24 hours of repair or after treatment with MILT 10µM for 24 hours using the redox-sensitive fluorochrome 5-(and 6)-chloromethyl-2',7'-dichlorodihydroflurescein diacetate dye (CM-H_2DCFDA, INVITROGEN).

CM-H_2DCFDA is a Chloromethyl derivative of H_2DCFDA, useful as an indicator of reactive oxygen species (ROS) in cells. CM-H_2DCFDA passively diffuses into cells, where its acetate groups are cleaved by intracellular Esterases and its Thiol-reactive Chloromethyl group reacts with intracellular Glutathione and other Thiols. Subsequent oxidation yields a fluorescent adduct that is trapped inside the cell, thus facilitating long-term studies.

Briefly, cells were loaded with 2µM CM-H_2DCFDA for 20 minutes at 37 °C. Before analysis by Flow Cytometry, the cells were removed from loading buffer and incubated in growth medium for 1 hours at 37 °C, as suggested by manufacturer's instructions.

Data acquisition and analysis was performed using a BD FACSCanto II (BD BIOSCIENCES). At least 10'000 events were detected for each sample to guarantee the statistical significance.

9.2 Measurement of SOD activity

SOD activity was measured in K562 cells after treatment with MEL 5μg/mL for 24 hours, after 24 hours of repair or after treatment with MILT 10μM for 24 hours using Superoxide Dismutase Assay Kit (TREVIGEN) following manufacturer's instructions.

Superoxide Dismutase Assay Kit is a colorimetric assay based on the ability of SOD to form H_2O_2 from Superoxide Radicals (O_2^-) generated by an exogenous reaction involving Xanthine and Xanthine Oxidase that can convert Nitroblue Tetrazolium (NBT) to NBT-Diformazan, which absorbs light at 550nm.

Since SODs reduce superoxide ion concentration, the reduction in NBT-diformazan is a measure of total SOD activity in U/ml, defined as the amount of enzyme needed to catalyze the dismutation of 50% of the superoxide radicals. The reduction of NBT to NBT-Diformazan induced by the Superoxide Radical (O_2^-) was monitored with a spectrophotometer by reading the absorbance at 550 nm.

Briefly, $1x10^6$ cells were lysed in 5 volumes cold 1X Cell Lysis Solution provided by the company. Total 15μg of protein/sample were used to perform the assay.

9.3 Measurement of GSR activity

GSR activity was measured in CD34+ and K562 cells after treatment with MEL 5μg/mL for 24 hours, after 24 hours of repair or after treatment with MILT 10μM for 24 hours using Glutathione Reductase Assay Kit (TREVIGEN) following manufacturer's instructions.

Glutathione reductase activity is defined as 1 unit of enzyme reducing 1 μmole oxidized glutathione (GSSG) per minute at pH 7.6 and 25°C. The kit employs a simple enzymatic recycling reaction for glutathione quantification where the reduction of a chromagen is correlated to glutathione reductase enzymatic activity.

Briefly, $1x10^6$ cells were lysed in 5 volumes cold 1X Tissue Homogenization. Total 15μg of protein/sample were used to perform the assay.

10. STATISTISTICAL ANALYSIS

The statistic used for data analysis was based on 2-tailed Student t-tests for average comparisons in paired samples (equal variance). Data were analyzed with Microsoft Excel (MICROSOFT OFFICE, 2011 release) and are reported as mean ± standard error of the mean (SEM). A p-value < 0.05 was considered significant. $p<0.05$ (*), $p<0.01$ (**), $p<0.001$ (***).

RESULTS

1. BIOLOGICAL EFFECTS OF WT CALR OVEREXPRESSION IN CD34+ HSPCs

1.1 CALR overexpression

In order to characterize the role of CALR in the proliferation and differentiation of Hematopoietic Stem/Progenitor Cells (HSPCs), we decided to investigate the effects of CALR overexpression in Cord Blood (CB) CD34+ cells isolated from healthy donors.

To this aim, CD34+ cells have been transduced with the retroviral vector LCALRIDN, expressing Wild-Type (WT) CALR cDNA, or LXIDN empty vector. Each vector contained DLNGFR as a reporter gene.

We performed a set of five independent experiments. No differences were identified in terms of viability (data not shown), assessed by trypan blue. Gene transfer efficiency was evaluated by Flow Cytometric analysis of DLNGFR (a truncated version of low-affinity Nerve Growth Factor Receptor) positivity and transduced cells were purified by immunomagnetic separation for NGFR (Nerve Growth Factor Receptor).

Afterwards, we performed Real Time qPCR (RT-qPCR) and Western Blot analyses on transduced/NGFR-purified cells in order to confirm CALR overexpression.

The results show there is a marked increase in both mRNA (RQ±SEM, 5.7±1.4, $p<0.05$, *)(**Figure 29, panel A**) and protein levels (**Figure 29, panel B**) in LCALRIDN-transduced cells compared to the control at 24 and 48 hours after the last transduction respectively.

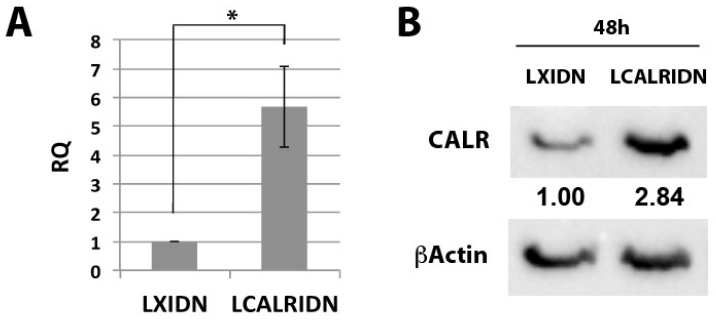

*Figure 29: CALR overexpression on CB CD34+ cells. (**A**) The expression levels of CALR were evaluated at 24h after the last infection by means of RT-qPCR. Data are reported as RQ±SEM of three independent experiments. $p<0.05$ (*). (**B**) Western Blot analysis of CALR protein levels was performed in whole cell lysates collected after 48h after the last transduction. The protein levels in LCALRIDN cells were compared with the control LXIDN empty vector. β-actin was included as loading control.*

1.2 Flow Cytometry and morphological analysis

In order to investigate the effects of CALR overexpression during hematopoietic differentiation, we firstly performed Flow Cytometry analysis of LCALRIDN and LXIDN samples.

We observed that in multilineage culture conditions CALR overexpression did not influence monocyte/macrophage or granulocyte differentiation, as demonstrated by the unchanged expression of CD14, CD163, CD66b, CD15, MPO respectively (**Figure 30, panel A and B**).

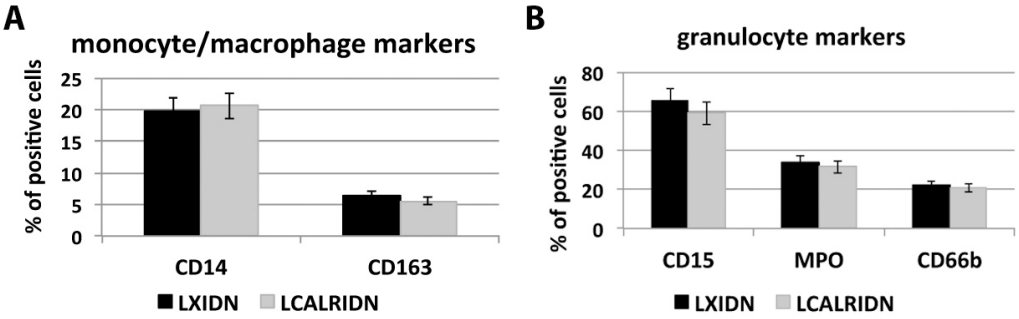

Figure 30: *Flow Cytometry analysis of monocyte and granulocyte markers in CALR overexpressing cells. (**A**) Bar graphs representing the statistical analysis of the percentages of positivity to the monocyte/macrophages CD14 and CD163 markers in CB CD34+ cells overexpressing CALR (LCALRIDN, grey bars) and control (LXIDN, black bars). (**B**) Bar graphs representing the statistical analysis of the percentages of positivity to the granulocyte CD15, MPO and CD66b markers in CB CD34+ cells overexpressing CALR (LCALRIDN, grey bars) and empty vector control (LXIDN, black bars).*

Since the presence of Human Serum (HS) inhibits erythroid and megakaryocyte (MK) differentiation of HSPCs *in vitro*, we also tested the effects of CALR overexpression on these two lineages in serum-free multilineage conditions. In particular, we evaluated the expression of the erythroid marker GPA, as well as the MK markers CD41 and CD42b at different time points after the last transduction by means of Flow Cytometry analysis.

We observed a statistically significant increase in the percentage of GPA-positive cells associated with CALR overexpression (**Figure 31**).

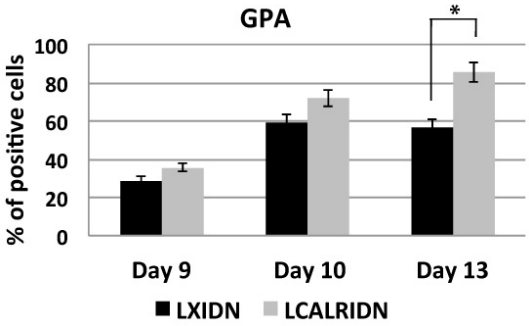

Figure 31: *Flow Cytometry analysis of the erythroid marker GPA in CALR overexpressing cells. Bar graphs representing the statistical analysis of the percentages of positivity to the erythroid marker GPA in CB CD34+ cells overexpressing CALR (LCALRIDN, grey bars) and empty vector control (LXIDN, black bars). $p<0.05$ (*).*

Moreover, we also show a significant increase in the percentage of CD41 (**Figure 32, panel A**) and CD42b (**Figure 32, panel B**) positive cell fraction in LCALRIDN samples compared to the control.

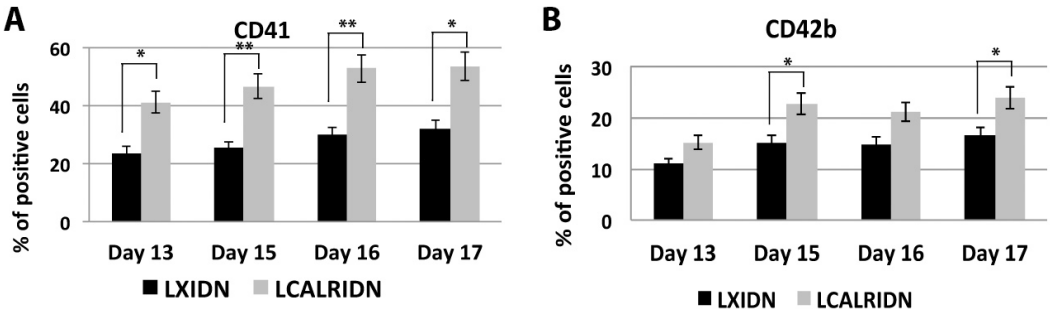

*Figure 32: Flow Cytometry analysis of megakaryocytic markers in CALR overexpressing cells. (**A**) Bar graphs representing the statistical analysis of the percentages of positivity to the megakaryocytic CD41 marker in CB CD34+ cells overexpressing CALR (LCALRIDN, grey bars) and control (LXIDN, black bars). CD41 has been evaluated at day 13, 15, 16, 17 after the last infection. (**B**) Bar graphs representing the statistical analysis of the percentages of positivity to the megakaryocytic CD42b marker in CB CD34+ cells overexpressing CALR (LCALRIDN, grey bars) and control (LXIDN, black bars). CD42b has been evaluated at day 13, 15, 16, 17 after the last infection. p<0.05 (*), p<0.01 (**).*

In agreement with Flow Cytometry results, morphological analysis of May-Grünwald-Giemsa-stained samples (**Figure 33**) and immunofluorescence analysis (**Figure 34**) performed at the different time points of liquid culture confirmed a strong enrichment in erythroid and MK precursors at different stages of maturation.

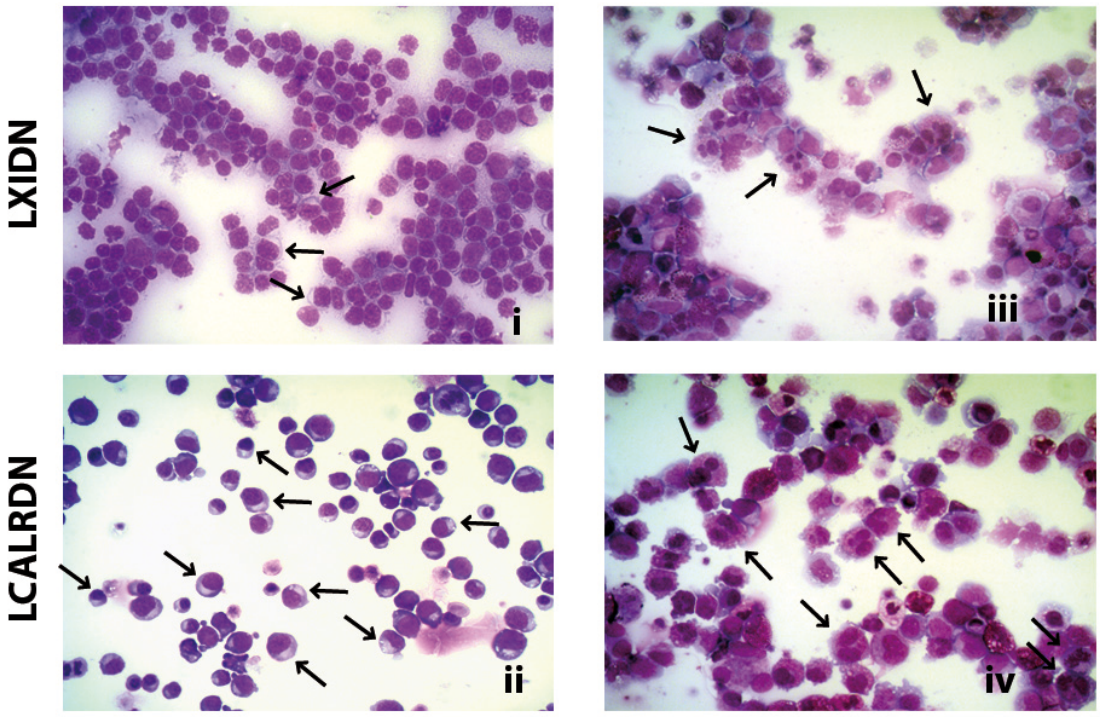

*Figure 33: Morphological analysis of CALR overexpressing cells by May-Grünwald-Giemsa-stained. Representative morphological analyses of LXIDN (**i**) and LCALRIDN (**ii**) samples on day 7 of erythroid unilineage culture, arrows point to orthochromatic and polychromatic erythroblasts. In addition, representative morphological analyses of LXIDN (**iii**) and LCALRIDN (**iv**) samples on day 13 of serum-free multilineage culture, arrows point to megakaryoblasts. Magnification x400.*

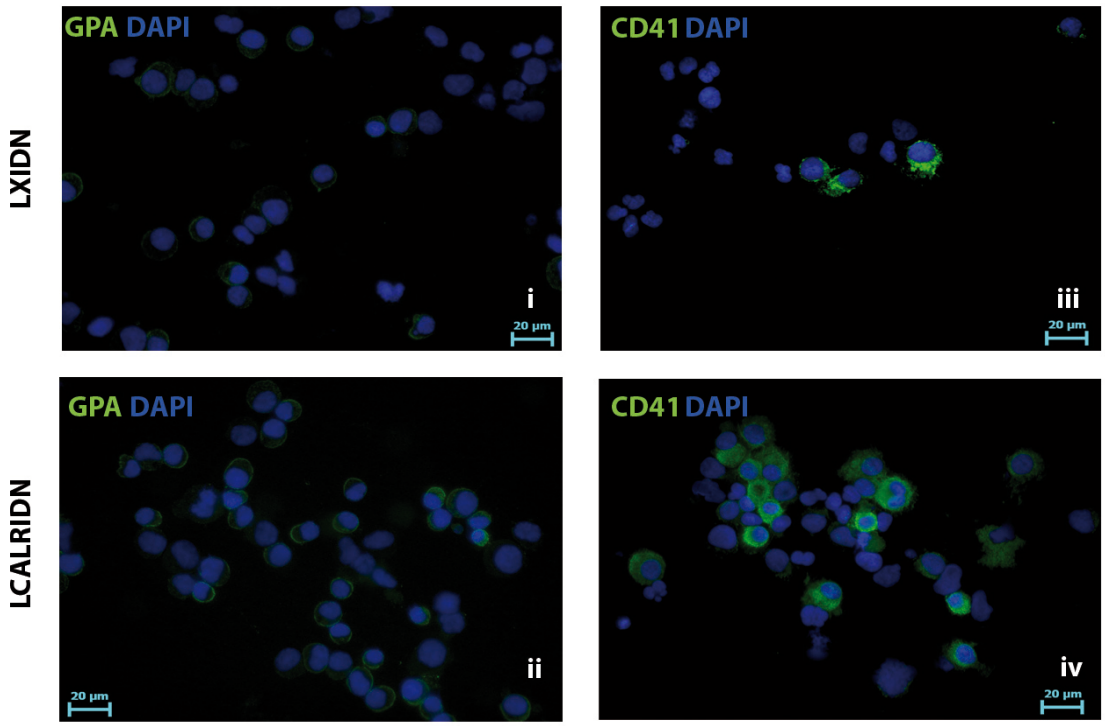

*Figure 34: Immunofluorescent analysis of CD41 and GPA antigens on CALR overexpressing cells. LXIDN (**i**) and LCALRIDN (**ii**) cells were labelled with anti-human GPA antibody (green fluorescence) or anti-human CD41 antibody (green fluorescence)(LXIDN: **iii**; LCALRIDN: **iv**). Nuclear counterstaining was performed with DAPI (blue fluorescence). Magnification x400.*

1.3 Clonogenic assays

In order to further clarify the role of CALR overexpression in HSPCs commitment, methylcellulose and collagen-based clonogenic assays were performed on LCALRIDN and LXIDN samples.

In agreement with the results obtained in liquid culture, methylcellulose-based semi-solid culture showed a significant increase in the percentage of erythroid colonies (CFU-E and BFU-E) upon CALR overexpression. Conversely, no difference in myeloid colonies was observed between samples (CFU-G, GFU-M and CFU-GM)(**Figure 35**).

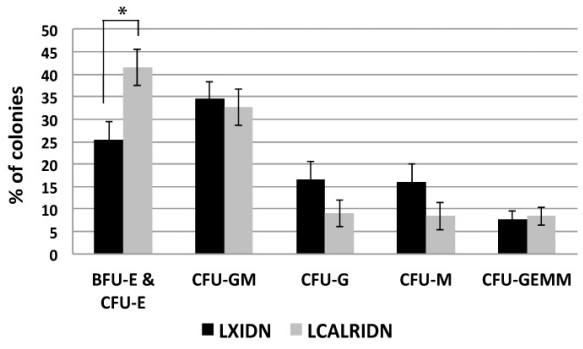

Figure 35: Methylcellulose-based clonogenic assay of CALR overexpressing cells. LXIDN and LCALRIDN cells were plated in triplicate 24 hours after the last infection and colonies were scored on day 14. Results are reported as percentage of colonies

and statistical analysis is indicated as mean±SEM, p<0.05 (*). Abbreviations: CFU, colony-forming unit; BFU, burst-forming unit; E, erythroid; GM, granulo-monocyte; G, granulocyte; M, monocyte; GEMM, granulocyte, erythrocyte, macrophage, megakaryocyte.

Furthermore, we performed collagen-based semi-solid culture in order to assess the ability of MK colony formation.

The data showed a significant increase in the percentage of CFU-MK colonies in association with a decrease in the non-MK colonies in the LCALRIDN compared to the LXIDN cells (**Figure 36**).

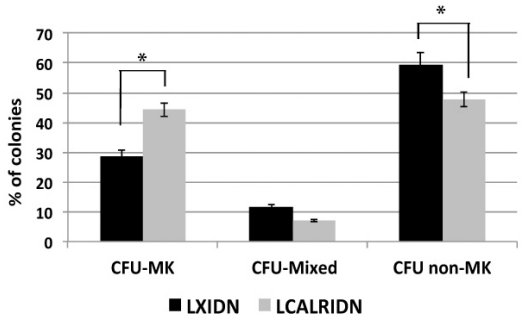

Figure 36: *Collagen-based clonogenic assay of CALR overexpressing cells. LXIDN and LCALRIDN cells were plated in triplicate 24 hours after the last infection and colonies were scored on day 11. Results are reported as percentage of colonies and statistical analysis was indicated as mean±SEM, p<0.05 (*). Abbreviations: CFU, colony forming unit; MK, megakaryocyte; MIX, mixed, non-MK, other than megakaryocyte.*

Altogether, our data demonstrated that CALR overexpression is able to induce MK and erythroid differentiation of HSPCs.

1.4 Gene expression profile

To better characterize the molecular mechanisms underlying the biological effects exerted by CALR overexpression on erythroid and megakaryocytic (MK) differentiation, we performed Gene Expression Profiling (GEP) on NGFR-positive cells purified after retroviral transduction in order to compare CALR-overexpressing cells (LCALRIDN) to control cells (LXIDN). Microarray analysis on three independent experiments was performed 24 hours after the last infection by means of Affymetrix HG-U219 Array Strips®.

Gene expression profile analysis generated a list of 54 Differentially Expressed Genes (DEGs) in the CALR overexpressing cells compared to control (**Table 7**).

	Probeset ID	Gene Symbol	FC	P-value
1.	11724589_s_at	MMP12	3,98937	0,0019503
2.	11716384_at	CCL2	3,15337	0,0405495
3.	11728717_at	CXCL5	3,07483	0,0222313
4.	11728679_a_at	CD163	3,02099	0,0047603
5.	11728715_at	CXCL5	3,01707	0,0289971

6.	11731422_s_at	FCGR3A	2,96491	0,0122365
7.	11754026_a_at	IL8	2,82482	0,0408867
8.	11757650_s_at	FN1	2,76000	0,0267112
9.	11725332_a_at	CTSL1	2,73482	0,0040945
10.	11728716_x_at	CXCL5	2,72653	0,0459167
11.	11721630_at	MAFB	2,55705	0,0021851
12.	11735095_at	LEP	2,54255	0,0008432
13.	11741520_x_at	CD14	2,52327	0,0008911
14.	11734549_s_at	TGFBI	2,50404	0,0113935
15.	11715374_a_at	CALR	2,44935	0,0002744
16.	11747010_a_at	VSIG4	2,39145	0,0120103
17.	11716818_a_at	VSIG4	2,38178	0,0047230
18.	11755730_x_at	SPP1	2,37515	0,0051191
19.	11734550_x_at	TGFBI	2,34911	0,0078528
20.	11737944_x_at	SPP1	2,28989	0,0053759
21.	11737943_a_at	SPP1	2,24138	0,0060207
22.	11734548_a_at	TGFBI	2,23438	0,0099515
23.	11741519_s_at	CD14	2,19796	0,0012422
24.	11746264_a_at	PPAP2A	2,17533	0,0011156
25.	11751647_a_at	IL7R	2,17247	0,0133998
26.	11748750_a_at	GPNMB	2,16311	0,0170143
27.	11723665_a_at	PPAP2A	2,10732	0,0001203
28.	11746506_a_at	SPP1	2,08985	0,0040997
29.	11754801_x_at	PPAP2A	2,02696	0,0000780
30.	11719366_s_at	CXCL1	2,01874	0,0349887
31.	11754604_x_at	SPP1	1,99592	0,0045182
32.	11720994_x_at	CCL3	1,98578	0,0271307
33.	11733187_a_at	IL7R	1,97088	0,0012843
34.	11734051_a_at	TRAT1	1,96971	0,0249079
35.	11726129_at	HBZ	1,96656	0,0149835
36.	11758095_s_at	FPR1	1,94741	0,0017139
37.	11734035_a_at	FPR2	1,94619	0,0121860
38.	11727797_at	NDFIP2	1,94357	0,0016858
39.	11763854_a_at	CD9	1,91875	0,0245312
40.	11725888_at	C19orf59	1,91623	0,0039146
41.	11726554_at	C1orf186	1,91006	0,0417766
42.	11721092_a_at	THBS1	1,90493	0,0460568
43.	11736538_s_at	RHCE /// RHD	1,88269	0,0366951
44.	11723804_a_at	AKAP12	1,88008	0,0001773
45.	11723803_a_at	TREM2	1,83271	0,0658946
46.	11715931_s_at	SGK1	1,83147	0,0442424
47.	11717565_s_at	EMP1	1,77192	0,0355244
48.	11727473_at	CLC	1,75075	0,0010397
49.	11758069_s_at	C1orf186	1,73185	0,0096746
50.	11721099_at	C3AR1	1,70714	0,0138575
51.	11719827_a_at	QPCT	1,61905	0,0301447
52.	11736739_at	CLEC5A	1,59734	0,0120578
53.	11757625_s_at	CD200	-2,03914	0,0036603
54.	11754354_s_at	PROM1/CD133	-1,85015	0,0003416

Table 7: *List of Differentially Expressed Genes (DEGs) in the comparison between CALR-overexpressing cells versus LXIDN-transduced cells.*

Based on this list, we performed hierarchical clustering of LXIDN and LCALRIDN samples (**Figure 37, panel A**). As expected, we showed that LCALRIDN clustered together and were clearly separated from LXIDN samples.

In addition, DEGs' functional analysis by means of Ingenuity Pathway Analysis (IPA)® software identified several categories of genes involved in pro-inflammatory pathways (i.e. CCL2, CCL4, CXCL5), platelet activation (i.e. SGK1, CD9, ANXA5, THSB1), erythrocyte differentiation (i.e. RDH, HBZ) and several cancer markers already described in both solid and hematological neoplasms (i.e. EMP1, VSIG4, LEP)(**Figure 37, panel B**).

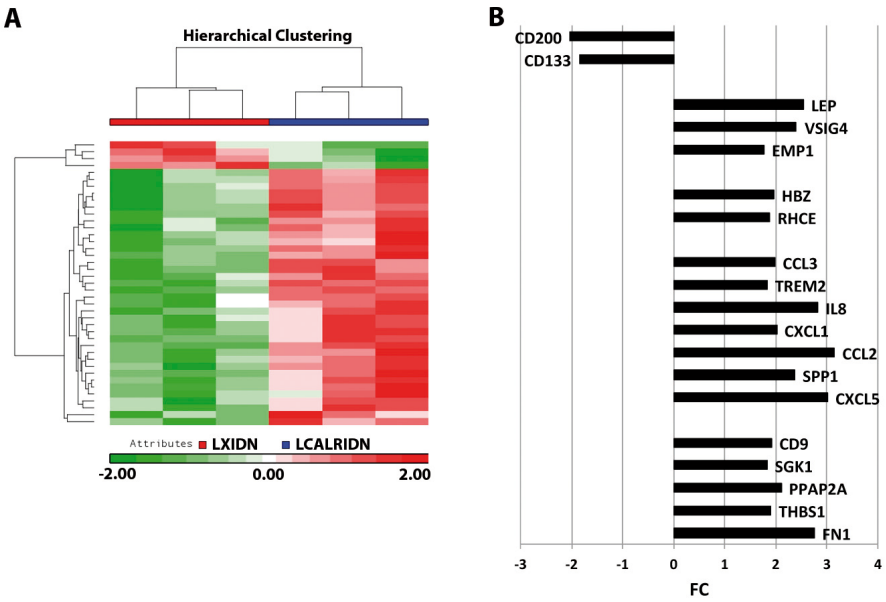

Figure 37: *Gene Expression Profile (GEP) performed upon CALR overexpression. (**A**) Hierarchical clustering and Heatmap of LXIDN and LCALRIDN samples based on the list of 54 differentially expressed transcripts. The statistical analysis was performing using a gene list having an unadjusted p-value<0.01 in the ANOVA analysis. Red bar indicate relatively high signal intensity, while green bars represent lower intensity and black intermediate. (**B**)Histogram chart of a selection of the major relevant different expressed genes between LCALRIDN and LXIDN.*

These results suggest that CALR overexpression in HSPCs is able to induce the expression of several genes involved in development of MPNs. Furthermore, we also have validated a selection of DEGs by means of RT-qPCR (**Figure 38**).

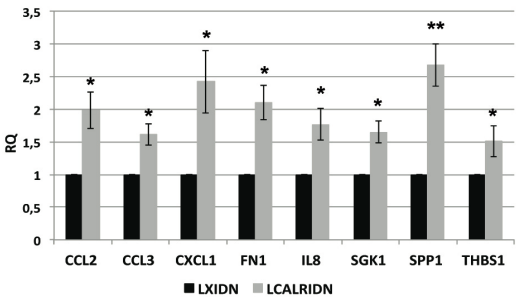

Figure 38: *Validation of mRNA differential expression levels induced by CALR overexpression. The expression levels of these genes were evaluated 24h after the last infection by means of RT-qPCR in LCALRIDN vs LXIDN. Data are reported as RQ±SEM of three independent experiments, using GAPDH as housekeeping gene. p<0.05 (*), p<0.01 (**).*

2. BIOLOGICAL EFFECTS OF WT CALR DOWNREGULATION IN CD34+ HSPCs

2.1 CALR silencing

Afterwards, in order to confirm the role of CALR overexpression-driven megakaryocytopoiesis and erythropoiesis, we decided to perform CALR silencing experiments in Cord Blood (CB) CD34+ cells isolated from healthy donors.

To this end, CD34+ cells were nucleofected with a siRNA specifically directed against CALR gene or a non-targeting siRNA (NT siRNA) negative control.

We performed a set of three independent experiments. No differences were identified in terms of viability assessed by trypan blue (data not shown).

Real Time qPCR (RT-qPCR) and Western Blot analyses allowed us to confirm the successful silencing of CALR in terms of RNA and protein levels.

In fact, we showed CALR downregulation both at the mRNA (RQ±SEM, 0.12±0.01, p<0.001, ***)(**Figure 39, panel A**) and protein level (**Figure 39, panel B**) at 24 and 48 hours respectively after the last transfection.

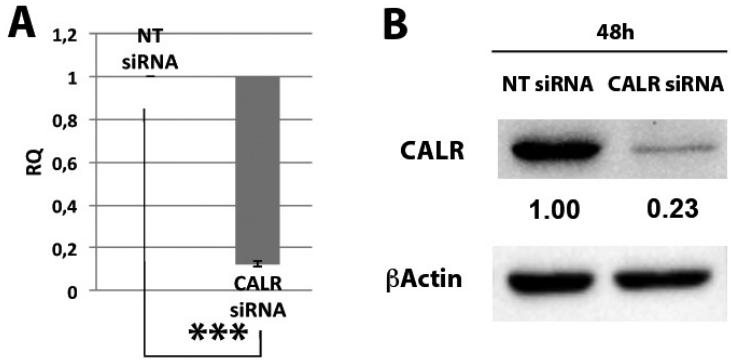

Figure 39: *CALR downregulation in CB CD34+ cells. (**A**) CALR expression levels were evaluated 24h after the last infection by means of RT-qPCR. Data are reported as RQ±SEM of three independent experiments. p<0.001 (***). (**B**) Western Blot analysis of CALR protein levels was performed in whole cell lysates collected after 48h after last transduction. The protein levels in CALR siRNA cells were compared with NT siRNA negative control. β-actin was included as loading control.*

2.2 Flow Cytometry and morphological analysis

In order to assess whether CALR silencing affects hematopoietic differentiation, we then performed an immunophenotypic analysis of liquid cultured-cells by means of Flow Cytometry in NT siRNA and CALR-silenced samples.

Our results demonstrated that CALR silencing did not influence monocyte/macrophage (**Figure 40, panel A**) or granulocyte (**Figure 40, panel B**) differentiation in multi-lineage conditions.

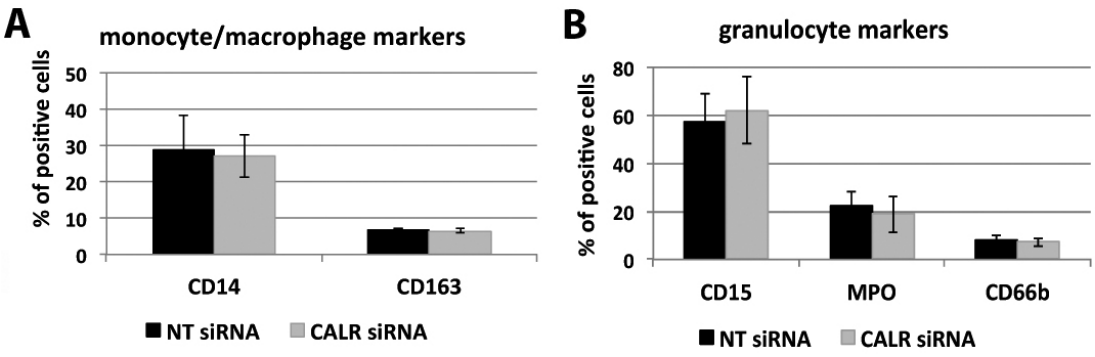

Figure 40: *Flow Cytometry analysis of monocyte and granulocyte markers in CALR silenced cells. (**A**) Bar graphs representing the statistical analysis of the percentages of positivity to the monocyte/macrophages CD14 and CD163 markers in CB CD34+ cells upon CALR silencing (CALR siRNA, grey bars) or in control cells (NT siRNA, black bars). (**B**) Bar graphs representing the statistical analysis of the percentages of positivity to the granulocyte CD15, MPO and CD66b markers in CB CD34+ cells upon CALR silencing (CALR siRNA, grey bars) or in control cells (NT siRNA, black bars).*

Moreover, we evaluated the expression of the erythroid marker GPA, as well as of the MK markers CD41 and CD42b by means of Flow Cytometry analysis, in serum-free multilineage and EPO-treated cultures.

We observed a steady decrease in the percentage of the erythroid marker GPA in CALR silenced cells (**Figure 41**).

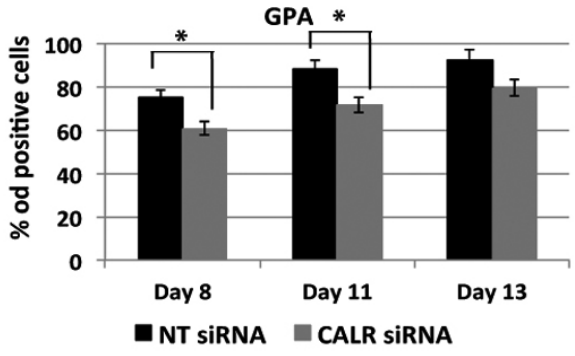

Figure 41: *Flow Cytometry analysis of erythroid marker in CALR silenced cells. Bar graphs representing the statistical analysis of the percentages of positivity to the erythroid marker GPA in CB CD34+ cells upon CALR silencing (CALR siRNA, grey bars) or in control cells (NT siRNA, black bars). $p<0.05$ (*).*

Moreover, we detected a significant decrease in the expression of the MK markers CD41 (**Figure 42, panel A**) and CD42b (**Figure 42, panel B**) in CALR silenced cells compared to the negative control (NT siRNA) samples.

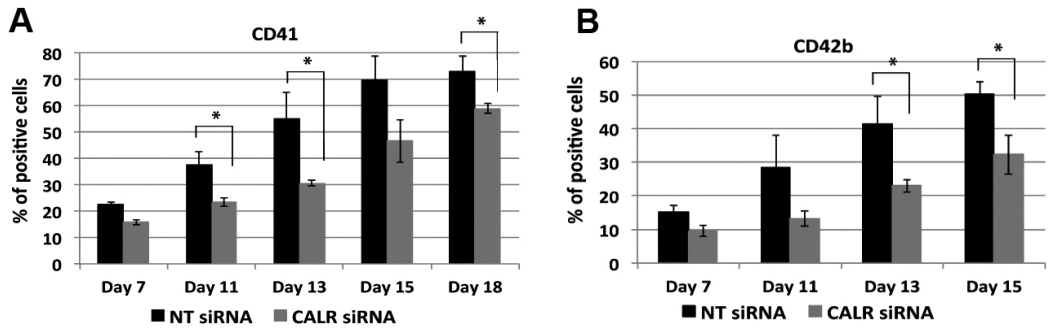

*Figure 42: Flow Cytometry analysis of megakaryocytic markers in CALR silenced cells. (**A**) Bar graphs representing the statistical analysis of the percentages of positivity to the megakaryocytic CD41 marker in CB CD34+ cells upon CALR silencing (CALR siRNA, grey bars) or in control cells (NT siRNA, black bars). CD41 has been evaluated at day 7, 11, 13, 15, 18 after the last nucleofection. (**B**) Bar graphs representing the statistical analysis of the percentages of positivity to the megakaryocytic CD42b marker in CB CD34+ cells upon CALR silencing (CALR siRNA, grey bars) or in control cells (NT siRNA, black bars). CD42b has been evaluated at day 7, 11, 13, 15 after the last infection. p<0.05 (*).*

In agreement with the Flow Cytometry results, morphological analysis of May-Grünwald-Giemsa-stained slides (**Figure 43**) and immunofluorescence analysis (**Figure 44**), performed on different times of liquid culture confirmed a strong downregulation in erythroid and MK precursors at different stages of maturation.

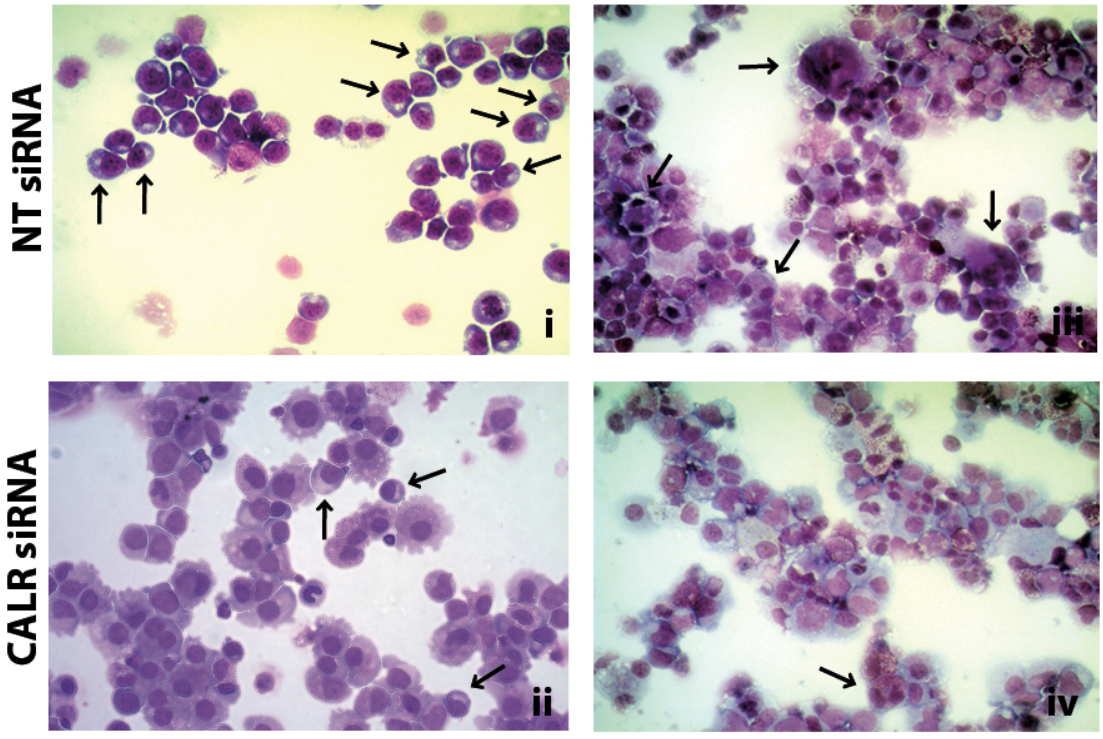

*Figure 43: Morphological analysis of CALR silenced cells by May-Grünwald-Giemsa-stained. Representative morphological analyses of NT siRNA (**i**) and CALR siRNA (**ii**) samples on day 7 of erythroid unilineage culture, arrows point to orthochromatic and polychromatic erythroblasts. Magnification x40. In addiction representative morphological analyses of NT siRNA (**iii**) and CALR siRNA (**iv**) samples on day 13 of serum-free multilineage culture, arrows point to megakaryoblasts. Magnification x400.*

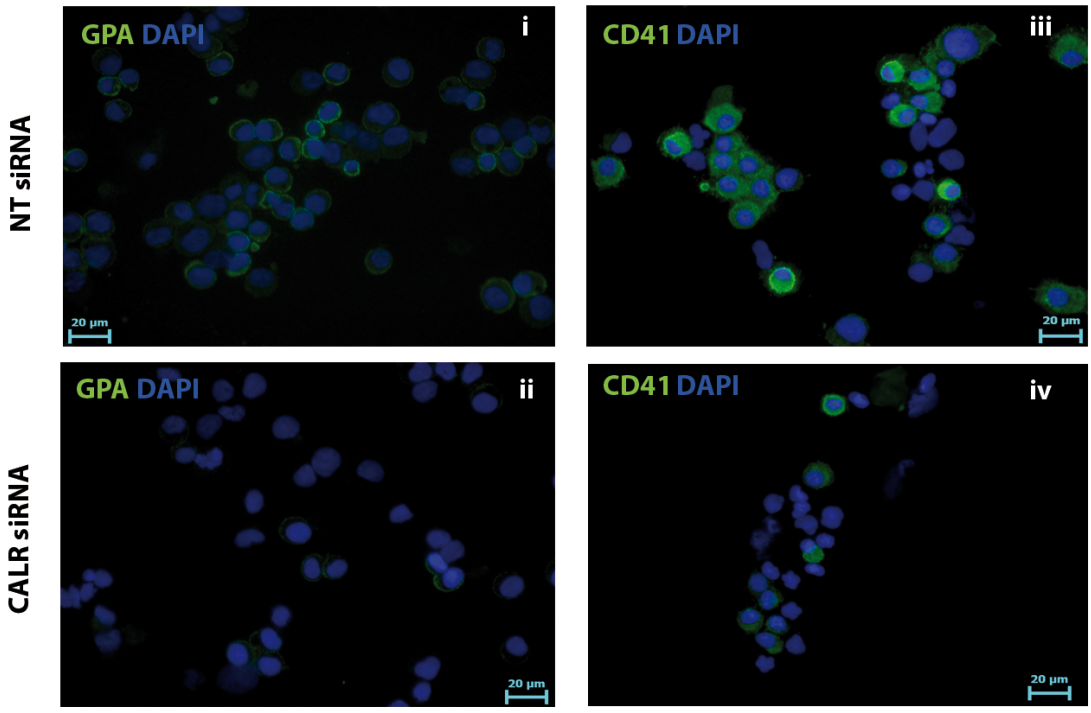

Figure 44: *Immunofluorescent analysis of CD41 and GPA antigen on CALR silenced cells. NT siRNA (**i**) and CALR siRNA (**ii**) cells were labelled with anti-human GPA antibody (green fluorescence) or anti-human CD41 antibody (green fluorescence)(NT siRNA: **iii**, CALR siRNA: **iv**). Nuclear counterstaining was performed with DAPI (blue fluorescence). Magnification x400.*

Altogether, our data demonstrated that CALR silencing led to the inhibition of MK and erythroid differentiation of HSPCs, in agreement with previous results obtained in CALR overexpression experiments.

2.3 Clonogenic assays

To better characterize the role of CALR silencing in HSPCs commitment, methylcellulose and collagen-based clonogenic assays were performed on CALR siRNA and NT siRNA samples.

Methylcellulose-based semi-solid culture showed no difference in the percentage of myeloid colonies (CFU-G, CFU-GM, CFU-M and GFU-GEMM) in CALR silenced cells compared to negative control. On the other hand, CALR silencing promoted a significant reduction of the erythroid lineage as demonstrated by the decrease of erythroid colonies (BFU-E and CFU-E)(**Figure 45**).

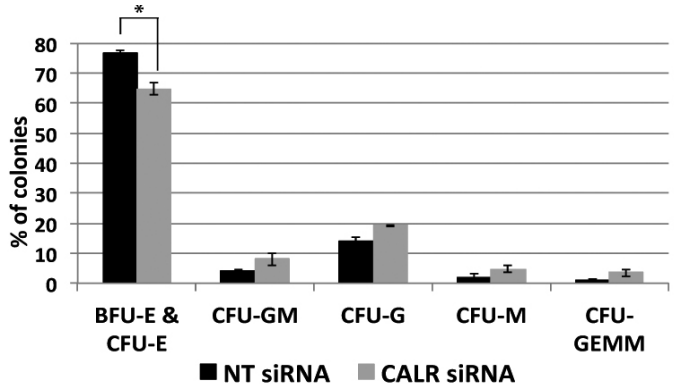

Figure 45: *Methylcellulose-based clonogenic assay of CALR silenced cells. NT siRNA and CALR siRNA cells were plated in triplicate 24 hours after the last nucleofection and colonies were scored on day 14. Results are reported as percentage of colonies and statistical analysis is indicated as mean±SEM, p<0.05 (*).Abbreviations: CFU, colony-forming unit; BFU, burst-forming unit; E, erythroid; GM, granulo-monocyte; G, granulocyte; M, monocyte; GEMM, granulocyte, erythrocyte, macrophage, megakaryocyte.*

Additionally, we performed collagen-based semisolid culture in order to assay the *in vitro* MK colony formation.

We have shown a significant increase in the percentage of CFU-Mixed and CFU non-MK colonies together with a parallel decrease in the CFU-MK colonies in the CALR siRNA cells compared to the NT siRNA control cells (**Figure 46**).

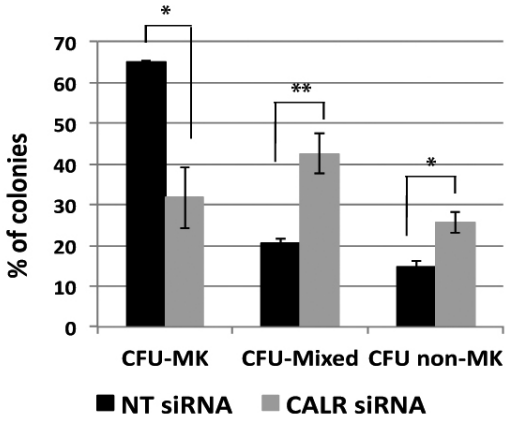

Figure 46: *Collagen-based clonogenic assay of CALR silenced cells. NT siRNA and CALR siRNA cells were plated in triplicate 24 hours after the last infection and colonies were scored on day 11. Results are reported as percentage of colonies and statistical analysis is indicated as mean±SEM, p<0.05 (*), P<0.01 (**). Abbreviations: CFU, colony forming unit; MK, megakaryocyte; MIX, mixed, non-MK, other than megakaryocyte.*

2.4 Gene expression profile

Moreover, to better characterize the molecular mechanisms leading the biological effects of CALR silencing on erythroid and megakaryocytic (MK) differentiation, we also performed a Gene Expression Profiling (GEP) on CALR silenced cells (CALR siRNA) and non-targeting negative control siRNA-transfected cells (NT siRNA).

Microarray analysis of three independent experiments was performed 24 hours after the last infection through Affymetrix HG-U219 Array Strips®.

Gene expression profile analysis generated a list of 154 Differentially Expressed Genes (DEGs) in the CALR silenced cells compared to control (**Table 8**).

	Probeset ID	Gene Symbol	FC	P-value
1.	11718201_at	HEY1	3,05265	0,0071044
2.	11758779_at	TMEM50B	2,71064	0,0008647
3.	11716329_s_at	GJA1	2,51530	0,0126090
4.	11717523_x_at	TMEM50B	2,45439	0,0002155
5.	11718591_at	SDF2L1	2,26563	0,0000119
6.	11717522_at	TMEM50B	2,24878	0,0035714
7.	11719327_a_at	CRELD2	2,23531	0,0009940
8.	11733115_a_at	CA2	2,22429	0,0265056
9.	11725931_at	HSPA5	2,14953	0,0207499
10.	11724275_s_at	TMEM158	2,14271	0,0146135
11.	11754545_x_at	PLAT	2,11461	0,0010719
12.	11755207_a_at	NT5E	2,08213	0,0144064
13.	11715795_at	MANF	2,04755	0,0103857
14.	11732321_a_at	PLAT	2,02834	0,0011920
15.	11756570_a_at	TMEM50B	2,01064	0,0000886
16.	11718873_a_at	ATP2A2	1,98962	0,0492951
17.	11733953_x_at	GBP4	1,98546	0,0239928
18.	11754593_x_at	TUBB3	1,97422	0,0304525
19.	11754973_x_at	MANSC1	1,94662	0,0264837
20.	11758027_s_at	HOOK1	1,94600	0,0340667
21.	11757775_s_at	C6orf120	1,92329	0,0032521
22.	11718874_s_at	ATP2A2	1,91708	0,0317641
23.	11741912_a_at	HSP90B1	1,87432	0,0232922
24.	11723655_a_at	DNAJB11	1,86275	0,0034194
25.	11743440_at	PDIA3	1,84938	0,0054142
26.	11741550_a_at	OSBPL6	1,82223	0,0095071
27.	11740030_s_at	CREM	1,81905	0,0037633
28.	11734874_x_at	PPFIBP1	1,75902	0,0001984
29.	11742143_s_at	RHCE /// RHD	1,75553	0,0469542
30.	11716587_at	AXL	1,75254	0,0138857
31.	11716580_s_at	CYSTM1	1,72472	0,0374404
32.	11719827_a_at	QPCT	1,71674	0,0193382
33.	11719202_a_at	MORN2	1,68828	0,0146830
34.	11716579_a_at	CYSTM1	1,68758	0,0089231
35.	11743441_s_at	PDIA3	1,68360	0,0440062
36.	11720574_s_at	ATP8B1	1,67955	0,0069214
37.	11756961_a_at	HYOU1	1,67719	0,0092466
38.	11748094_a_at	FAM3C	1,66379	0,0254570
39.	11753981_a_at	VEPH1	1,65763	0,0202812
40.	11744880_a_at	ZNF165	1,65424	0,0132287
41.	11723578_a_at	SMIM13	1,65011	0,0345601
42.	11731027_s_at	CREM	1,64705	0,0079818

43.	11750599_a_at	OSBPL6	1,64457	0,0096547
44.	11754608_x_at	HSP90B1	1,64297	0,0217249
45.	11717099_at	HIST1H2BK	1,63887	0,0282222
46.	11753260_x_at	HSP90B1	1,63406	0,0430355
47.	11723008_s_at	CCPG1	1,63367	0,0041831
48.	11733781_a_at	RAB18	1,63314	0,0123811
49.	11740680_s_at	RHCE /// RHD	1,63101	0,0252645
50.	11754693_a_at	AHI1	1,62643	0,0228392
51.	11747376_s_at	CCPG1	1,62304	0,0005329
52.	11739937_a_at	DYRK3	1,62163	0,0455634
53.	11715435_s_at	TIMP3	1,61592	0,0142193
54.	11728733_at	ZBTB38	1,61474	0,0452078
55.	11724787_s_at	KIF3A	1,60603	0,0104305
56.	11763293_at	ZSCAN9	1,60411	0,0309104
57.	11763987_a_at	VEPH1	1,59902	0,0242844
58.	11758842_at	THBS1	1,59235	0,0419123
59.	11756246_s_at	TTC28	1,58716	0,0051879
60.	11758670_s_at	STK3	1,57135	0,0443373
61.	11716119_x_at	PDIA4	1,57095	0,0026784
62.	11750442_s_at	LMNB1 /// PCIF1	1,56807	0,0369996
63.	11745327_a_at	ARL13B	1,56679	0,0342495
64.	11755110_a_at	LRIG1	1,56655	0,0155909
65.	11720431_s_at	COL15A1	1,56328	0,0373286
66.	11758570_s_at	CDADC1	1,56088	0,0229546
67.	11716945_s_at	TWF1	1,55998	0,0350778
68.	11723007_a_at	CCPG1 /// DYX1C1-CCPG1	1,55107	0,0207933
69.	11759016_at	MAN1A2	1,55021	0,0183827
70.	11754606_a_at	HSP90B1	1,54933	0,0478331
71.	11720158_a_at	WDR19	1,54858	0,0391601
72.	11718770_a_at	SELK	1,54699	0,0029208
73.	11760463_at	MED6	1,53631	0,0287801
74.	11740338_a_at	AGFG1	1,53281	0,0206850
75.	11718771_x_at	SELK	1,53242	0,0052441
76.	11724264_a_at	IFT22	1,52923	0,0067407
77.	11741913_s_at	HSP90B1	1,52842	0,0207656
78.	11716786_s_at	TRAK2	1,52841	0,0322379
79.	11730111_a_at	DEPDC1	1,52823	0,0490344
80.	11735453_at	NHLRC1	1,52791	0,0143830
81.	11735275_at	IL18R1	1,52527	0,00222729
82	11716118_a_at	PDIA4	1,51963	0,0169141
83.	11754607_s_at	HSP90B1	1,51847	0,0310818
84.	11721726_a_at	IFT88	1,51806	0,0302239
85.	11715514_a_at	HERPUD1	1,51186	0,0075518
86.	11727262_at	ENTPD7	1,50890	0,0498355
87.	11715847_x_at	PLAT	1,50872	0,0042051
88.	11743773_s_at	LZTFL1	1,50791	0,0419328
89.	11743609_a_at	FAM3C	1,50372	0,0334963
90.	11733950_at	GBP4	1,50101	0,0290635
91.	11754458_a_at	ACRBP	1,50041	0,0054262
92.	11753264_x_at	C3orf17	-1,50959	0,0271996

93.	11727473_at	CLC	-1,51782	0,0041537
94.	11716020_s_at	RAD23A	-1,51910	0,0075101
95.	11721598_a_at	EFS	-1,52190	0,0323673
96.	11726148_a_at	PPIP5K2	-1,53007	0,0051231
97.	11715245_s_at	IGLL1	-1,53577	0,0147551
98.	11736240_a_at	AAED1	-1,55185	0,0191761
99.	11724516_s_at	GPD1L	-1,55913	0,0078069
100.	11756080_s_at	NUS1 /// NUS1P3	-1,56569	0,0139858
101	11736633_at	AAK1	-1,56681	0,0086451
102.	11717115_at	CERK	-1,57107	0,0203721
103.	11744165_a_at	PPME1	-1,57607	0,0475320
104.	11728191_x_at	CXCR4	-1,59911	0,0131130
105.	11755245_x_at	C3orf17	-1,59987	0,0079955
106.	11729686_x_at	LYRM7	-1,60428	0,0081516
107.	11751454_x_at	MEST	-1,60948	0,0364415
108.	11725471_a_at	MAN2A1	-1,61606	0,0301041
109.	11719689_a_at	TWSG1	-1,61956	0,0337850
110.	11732135_a_at	ADCK3	-1,62307	0,0333107
111.	11739094_a_at	CXCR4	-1,63056	0,0036538
112.	11728646_at	NUCKS1	-1,63621	0,0084812
113.	11760228_s_at	KLHL23 /// PHOSPHO2-KLHL23	-1,63663	0,0194626
114.	11716308_s_at	CYBRD1	-1,64128	0,0096584
115.	11748315_s_at	PRNP	-1,64291	0,0054475
116.	11728189_a_at	CXCR4	-1,65875	0,0051904
117.	11748000_a_at	C3orf17	-1,67257	0,0116884
118.	11728393_a_at	BLOC1S5 /// EEF1E1-BLOC1S5	-1,68095	0,0174223
119.	11728649_s_at	NUCKS1	-1,69094	0,0002130
120.	11757946_s_at	CPNE3	-1,69230	0,0326451
121.	11733701_a_at	FKBP11	-1,69879	0,0022320
122.	11750783_a_at	GALNT1	-1,70416	0,0049021
123.	11743290_at	GALNT1	-1,71358	0,0027887
124.	11722213_at	NPM3	-1,73141	0,0008881
125.	11758583_s_at	TMEM154	-1,73154	0,0147015
126.	11729685_at	LYRM7	-1,73525	0,0214331
127.	11749950_a_at	C3orf17	-1,73832	0,0047460
128.	11717435_a_at	CDCA7L	-1,73841	0,0091517
129.	11719647_a_at	CASP7	-1,76625	0,0169172
130.	11750198_a_at	CASP7	-1,76728	0,0194114
131.	11724515_a_at	GPD1L	-1,78346	0,0468036
132.	11716309_a_at	CYBRD1	-1,80066	0,0002603
133.	11737765_a_at	C3orf17	-1,82329	0,0083822
134.	11729688_s_at	LYRM7	-1,85076	0,0375034
135.	11729156_a_at	SLC25A32	-1,86006	0,0429173
136.	11743292_at	GALNT1	-1,86917	0,0038180
137.	11743724_a_at	MFSD1	-1,87019	0,0012962
138.	11715375_x_at	CALR	-1,89197	0,0083430
139.	11748128_a_at	SLC25A32	-1,89921	0,0012725
140.	11731603_at	TMEM154	-1,90060	0,0214660
141.	11753263_a_at	C3orf17	-1,94600	0,0169935
142.	11743251_s_at	MMP2	-1,96924	0,0310706

143.	11743291_a_at	GALNT1	-1,98689	0,0039804
144.	11719690_at	TWSG1	-1,99838	0,0052579
145.	11719691_x_at	TWSG1	-2,01826	0,0030255
146.	11751783_a_at	MFSD1	-2,03756	0,0001371
147.	11717116_at	CERK	-2,03795	0,0150931
148.	11719229_s_at	URI1	-2,05491	0,0029601
149.	11729687_at	LYRM7	-2,12342	0,0234564
150.	11726470_s_at	PLS1	-2,14129	0,0046993
151.	11743725_s_at	MFSD1	-2,22629	0,0010197
152.	11727093_s_at	UBE2V2	-2,71777	0,0003071
153.	11754112_a_at	UBE2V2	-3,18651	0,0002316
154.	11715374_a_at	CALR	-3,33756	0,0018033

Table 8: *List of Differentially Expressed Genes (DEGs) between CALR-silenced and NT siRNA cells.*

Based on this list, we performed hierarchical clustering of NT siRNA and CALR siRNA samples (**Figure 47, panel A**). As expected, we showed that CALR siRNA samples clustered together and were clearly separated from NTsiRNA samples, which in turn clustered together.

In addition, functional analysis of the deregulated gene by means of Ingenuity Pathway Analysis (IPA)® software identified several categories of DEGs. In particular, among upregulated genes we found genes involved in UPR and ER stress response (i.e. HSP90B1, HSPA5, SELK) and in the regulation of self-renewal of hematopoietic stem cells (i.e. cAMP, CREM, KIF3A, MANSC1, CA2). Conversely, among downregulated genes we found genes involved in DNA repair (i.e. NUCKS1, UBE2 V2)(**Figure 47, panel B**).

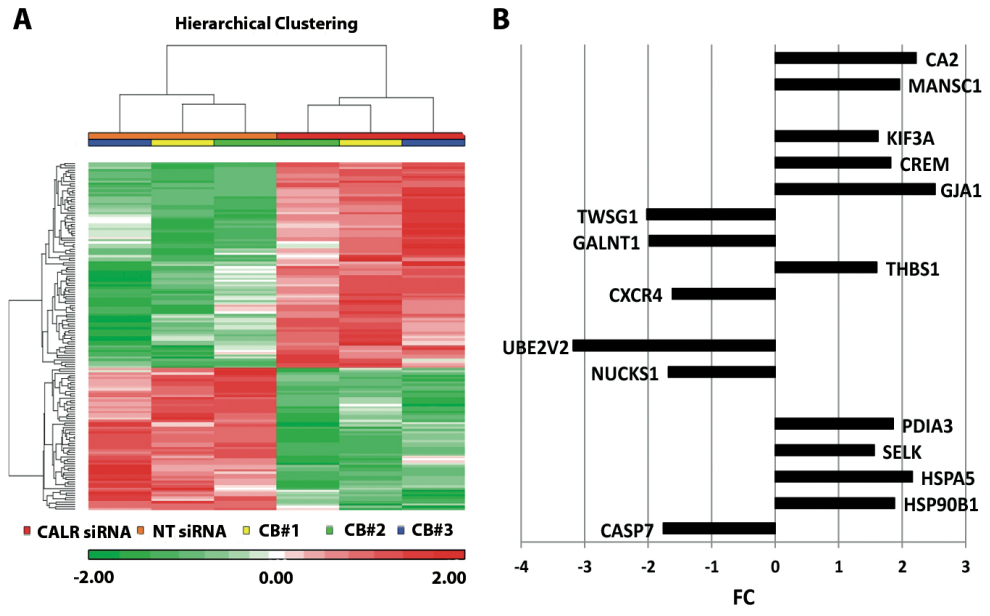

Figure 47: *Gene Expression Profile (GEP) upon CALR silencing. (**A**) Hierarchical clustering and Heatmap of NT siRNA and CALR siRNA samples based on the list of 154 differentially expressed transcripts. The statistical analysis was performing using a gene list having an unadjusted p-value<0.01 in the ANOVA analysis. Red bar indicates relatively high signal intensity,*

*while green bars represent lower intensity and black intermediate. (**B**)Histogram chart of a selection of the major relevant different expressed genes in the comparison between CALR siRNA and NT siRNA.*

Furthermore, we also have validated selected DEGs by RT-qPCR (**Figure 48**).

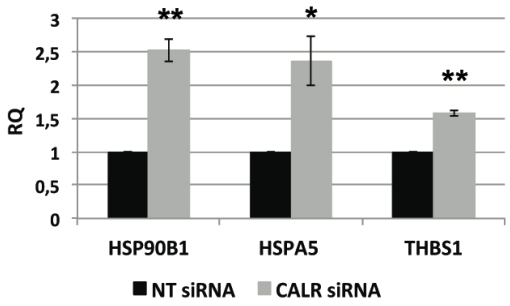

Figure 48: *Validation of mRNA differential expression levels transcripts induced by CALR silencing. The expression levels of these genes were evaluated 24h after the last infection by means of RT-qPCR in CALR siRNA vs NT siRNA. Data are reported as RQ±SEM of three independent experiments, using GAPDH as housekeeping gene. p<0.05 (*), p<0.01 (**).*

Collectively, GEP data suggested a role for CALR in several biological processes, including ER stress, UPR and DNA repair. The downregulation of CALR might impair the role of chaperone that CALR plays in the ER, while the role that CALR plays in the DNA repair or HSC self-renewal is not yet well known. For this reason, in the second part of my thesis I decided to investigate the role of CALR mutants in these biological pathways.

3 GENE EXPRESSION PROFILE OF CALR-MUTANT K562 CELLS

3.1 CALR del52 and ins5 overexpression

Recent data demonstrated that CALR mutants interact with the thrombopoietin receptor (MPL), then inducing the constitutive activation of JAK-STAT pathway. However, the precise mechanism of action through which CALR mutants contribute to the development of MPNs has only been partially clarified.

In order to evaluate MPL-independent mechanisms underlying the effect of CALR mutations on myeloproliferative disorders, we overexpressed CALR mutations in the K562 cell line, devoid of MPL expression.

To this end, K562 cells were transduced with vectors expressing one of the two commonest CALR mutated variants, either CALRdel52 or CALRins5. In three independent experiments, K562 were transduced with the retroviral vector LXIDN expressing cDNA of either CALRdel52 mutation type 1 (LCALRdel52IDN, CALRdel52), CALRins5 mutation type 2 (LCALRins5IDN, CALRins5) or Wild-Type CALR (LCALRwtIDN, CALRwt) as control. Transduced K562 cells were subsequently

purified by means of immunomagnetic selection for NGFR marker expressed by the retroviral vector LXIDN. Gene transfer efficiency was checked through Flow Cytometry analysis while CALR protein levels were assessed by Western Blot analysis.

Flow Cytometry analysis (**Figure 49, panel A**) as well as Western Blot analysis (**Figure 49, panel B**) confirmed the retroviral vectors' and CALR overexpression in these cells.

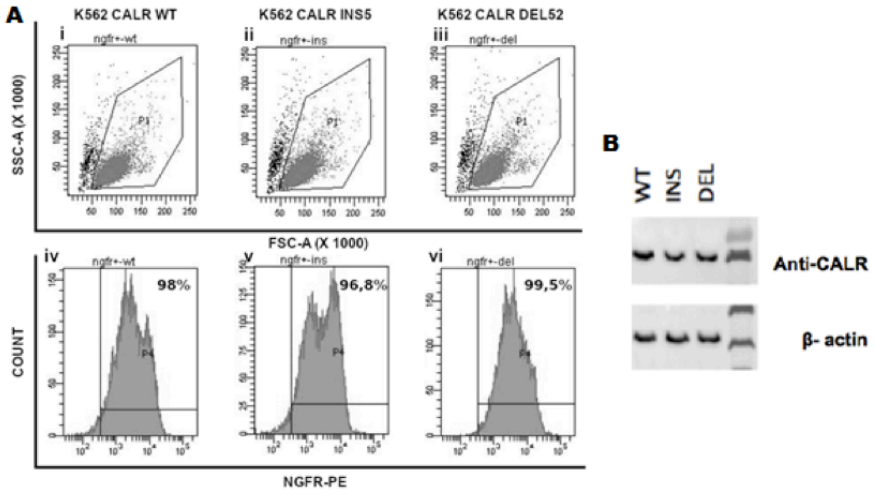

*Figure 49: WT and mutant CALR overexpression in K562 cells. (**A**) The NGFR-positivity levels of transduced cells were evaluated at 48 hours after the purification by means of Flow Cytometry. Data are reported as percentage of NGFR positive cells of three independent experiments. (**B**) Western Blot analysis of CALR protein levels was performed in whole cell lysate collected 48 hours after last transduction. β-actin was included as loading control.*

3.2 Gene expression profile

In order to investigate the mechanisms underlying the effects of CALR mutations overexpression in K562 cell line, we performed Gene Expression Profiling (GEP) on NGFR-positive cells to compare the phenotypic effect of overexpression of CALR mutation type 1 (LCALRdel52IDN) and type 2 (LCALRins5IDN) versus Wild-Type control (LCALRwtIDN).

Microarray analysis on three independent experiments was performed 24 hours after the last infection through Affymetrix HG-U219 Array Strips®.

The unsupervised analysis of the microarray dataset through the Principal Component Analysis (PCA) showed that CALRdel52 and CALRins5-overexpressing samples clustered together and were separated from CALRwt-transduced control (**Figure 50**).

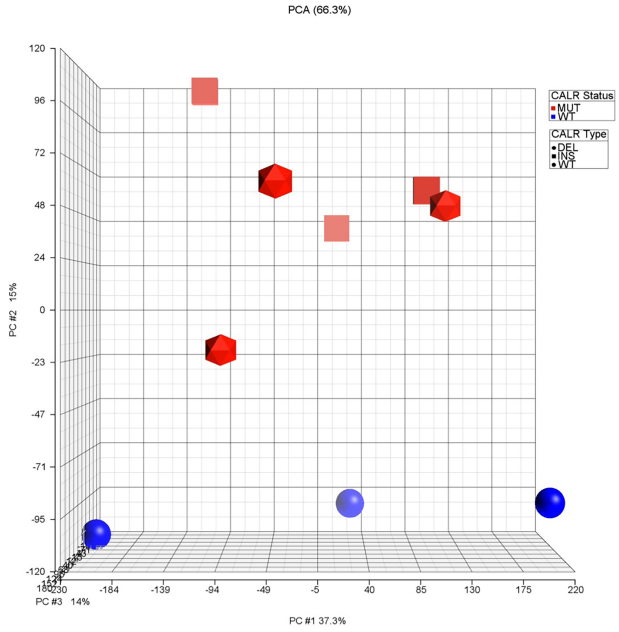

Figure 50: *Principal Component Analysis (PCA) based on gene expression profiling of CALRwt, CALRdel52 and CALRins5-transduced K562 cells. CALRwt samples are showed in blue, while CALRdel52 and CALRins5-expressing cell lines are shown in red. Mutational status (i.e. CALRwt, CALRdel52 and CALRins5) is indicated by using different shapes (sphere represents CALRwt, squares represent CALRins5 and polyhedrons represents CALRdel52)*

Next, we performed the analysis of variance (ANOVA) to characterize the Differentially Expressed Genes (DEGs).

Figure 51 shows the hierarchical clustering of both CALRdel52 and CALRins5 K562 cells compared to CALRwt (**Figure 51**).

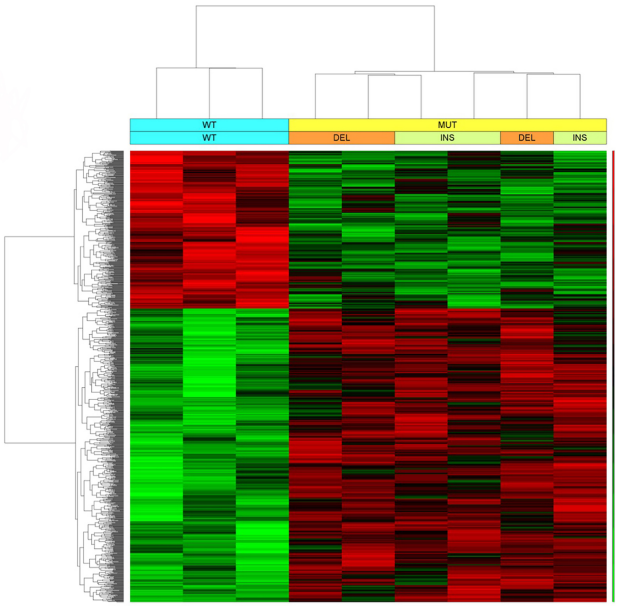

Figure 51: *Hierarchical clustering and Heatmap of the differentially expressed transcripts differentially in both CALRdel52 and CALRins5 K562 cells compared to CALRwt. The statistical analysis was performed using a gene list with an unadjusted p-value<0.01 in the ANOVA analysis. Red bars indicate relatively high signal intensity, while green bars represent lower intensity and black intermediate.*

Moreover, we performed a functional analysis of DEGs by means of Ingenuity Pathway Analysis software (IPA)®.

IPA analysis showed that the categories "Unfolded Protein Response", "Endoplasmic Reticulum Stress Pathway", "HIF1a Signaling", "GADD45 Signalling", "NRF2-mediated Oxidative Stress Response" are significantly decreased in CALR-mutant K562 cells (**Table 9**), suggesting a potential role of CALR mutants in UPR and oxidative stress response.

Pathway name	*Z-score*
Unfolded protein response	-1,890
ATM Signaling	-0,816
Production of Nitric Oxide and Reactive Oxygen species	-2,449
DNA Double-Strand Break Repair by Homologous Recombination	-2,449
Role of BRCA1 in DNA Damage Response	-2,236
DNA damage	-2,236
DNA Double-Strand Break Repair by Non-Homologous End Joining	-1,633
NRF2-mediated Oxidative Stress Response	-0,816
EIF2 Signaling	-1,134
Endoplasmic Reticulum Stress Pathway	-2,449
UVB-Induced MAPK Signaling	-2,236
PTEN signaling	-2,828
Protein Ubiquitination Pathway	-1,342
HIF1α Signaling	-2,449
Chronic Myeloid Leukemia Signaling	-2,236
Hereditary Breast Cancer Signaling	-2,146
p53 Signaling	-2,447
Erythropoietin Signaling	-2,000
GADD45 Signaling	-2,236
FLT3 Signaling in Hematopoietic Progenitor Cells	-2,236
Myc Mediated Apoptosis Signaling	-2,236
Regulation of eIF4 and p70S6K Signaling	-2,000
PDGF Signaling	-2,236
Acute Myeloid Leukemia Signaling	-2,236
mTOR Signaling	-2,449
IL-6 Signaling	-2,449
Thrombin Signaling	-2,121
Gα12/13 Signaling	-2,449
VEGF Signaling	-2,236
VEGF Family Ligand-Receptor Interactions	-2,000
Cell cycle: G2/M DNA damage Checkpoint regulation	0,707
ERK/MAPK Signaling	-0,816
Paxillin Signaling	-2,000
Signaling by Rho Family GTPases	-2,449

Table 9: *Canonical Pathways significantly represented in the list of decreased genes in mutated versus WT K562 cells.*

4 BIOLOGICAL EFFECTS OF CALR MUTATIONS IN ER STRESS RESPONSE IN K562 CELL LINE

4.1 UPR activation induced by hypoxia treatment

In order to discover whether CALR mutations could affect ER stress and then UPR activation we cultured K562 in hypoxic environment.

As previously described, hypoxia is a strong ER stress inducer. In particular, hypoxia causes the activation of PERK and IRE1 pathways, two important branches of UPR.

After 24 hours under hypoxic conditions (1% O_2), we collected the cells and we analyzed the expression levels of different genes involved in the UPR, such as GRP78, CHOP, ATF4, GADD34, ERDJ4 and XBP1 spliced variants.

Our results show that in hypoxic conditions the mRNA expression of CHOP, ATF4, GRP78 and GADD34 in CALR-mutated cells decrease when compared to the CALRwt (**Figure 52, panel A, C, E, F**). Conversely, no statistical differences in expression were observed in IRE1 pathway players in both CALRwt and CALR-mutant cells (**Figure 52, panel B**). Moreover, XBP1 (S) (spliced variant), associated with activation of IRE1 pathway, was downregulated in response to hypoxia in all samples (**Figure 52, panel D**).

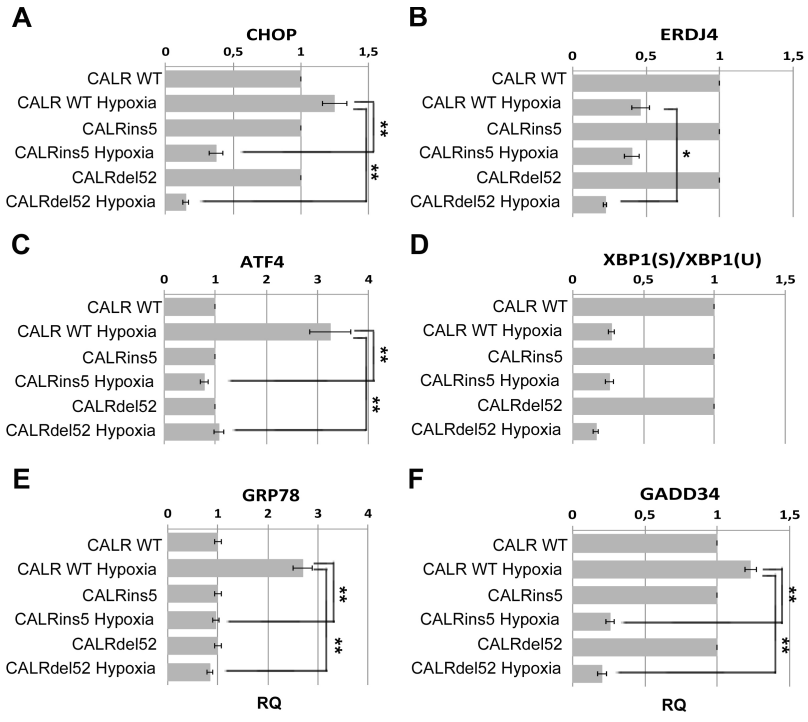

*Figure 52: The expression levels of UPR components were evaluated after 24h of hypoxia by of means RT-qPCR. (**A**) CHOP. (**B**) ERDJ4. (**C**) ATF4. (**D**) XBP1(Spliced)/XBP1(Unspliced). (**E**) GRP78. (**F**) GADD34. Results were normalized to each CALR variant sample cultured in normoxic conditions Data are reported as RQ±SEM of three independent experiments. p <0.05 (*), p<0.01 (**).*

4.2 UPR activation induced by Thapsigargin and Tunicamycin treatment

Since hypoxic conditions seem to impair PERK pathway in CALR mutants, we decided to test the response to more specifics treatments, including Thapsigargin (Tg) and Tunicamycin (Tm). In fact, hypoxia activates several pathways, while Tg and Tm specifically induce UPR, such as PERK pathway. As previously described, Tg disrupts calcium homeostasis in the ER and Tm inhibits protein N-glycosylation.

After treating the cells with these compounds, we have again quantified the levels of UPR components by means of RT-qPCR and Western Blot.

Treatment with Tg (C=0.1μM) for 4 hours resulted in upregulation of UPR genes in K562 cells expressing either WT or mutated CALR, with no statistically significance between the two variants of CALR (**Figure 53**)

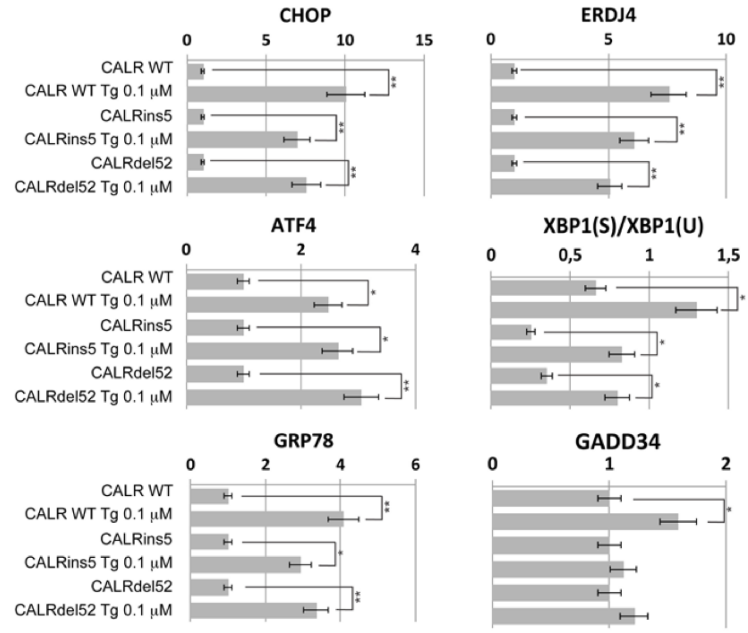

Figure 53: The expression levels of UPR components were evaluated after treatment with Thapsigargin (Tg)(C=0.1μM, 4h). Expression of CHOP, ERDJ4 ATF4, XBP1(Spliced)/XBP1(Unspliced), GRP78 and GADD34 was measured by means of RT-qPCR. Results were normalized to each CALR variant sample cultured in normoxic conditions Data are reported as RQ±SEM of three independent experiments. p <0.05 (*), p<0.01 (**).

Vice versa, treatment with Tm (C=2.5g/ml) for 4 hours confirmed the lack of activation of PERK pathway in CALR-mutated compared to CALRwt cells, as it previously demonstrated in hypoxic environment.

In particular, we observed increased expression levels of ERDJ4, GRP78 and other molecules specifically involved in PERK pathway (i.e. ATF4, CHOP, P-eIF2α) in CALRwt compared to CALR-mutant K562 cells (**Figure 54, panel A**). Moreover, Western Blot analyses indicate that GRP78, ATF4, CHOP and P-eIF2α are downregulated in CALR-mutant K562 cells compared to control cells (**Figure 54, panel B**).

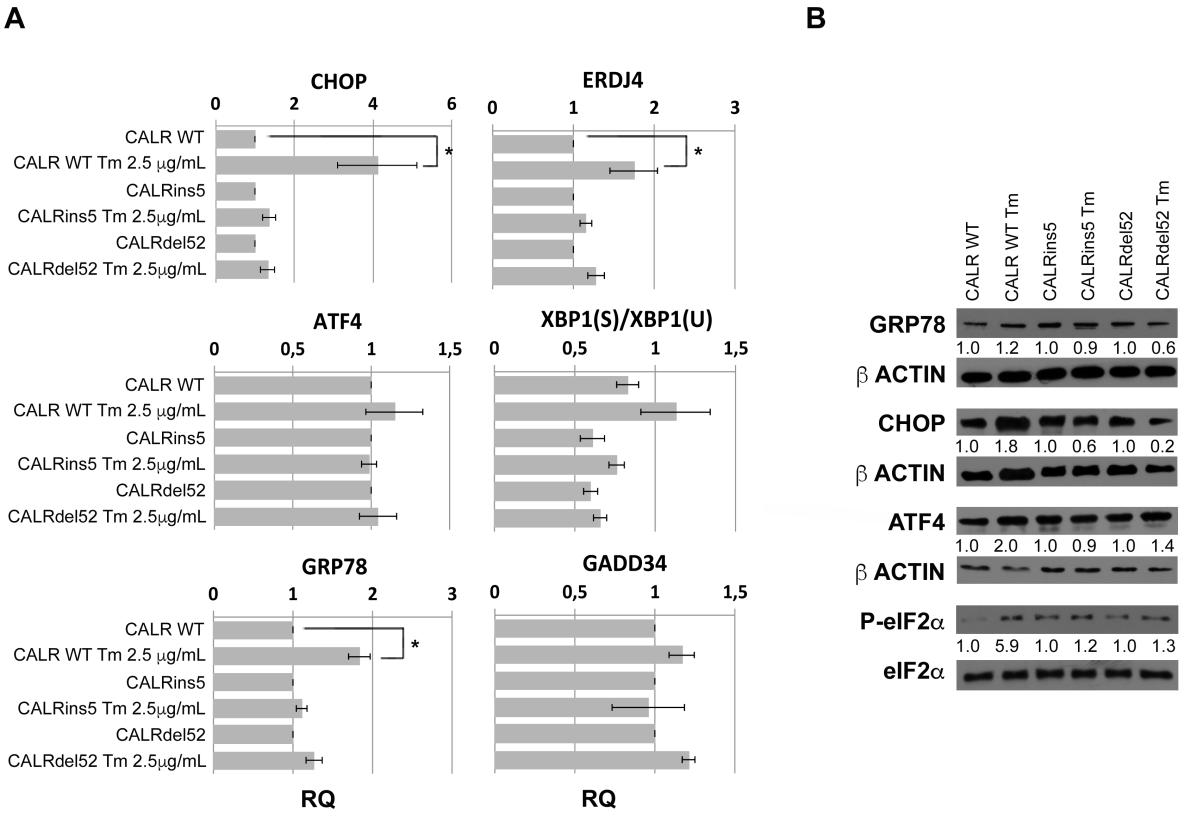

Figure 54: *Activation of UPR after Tunicamycin (Tm) treatment in both CALRdel52 and CALRins5 K562 cells compared to CALRwt. (**A**) The expression levels of UPR components were evaluated after treatment with Tm (C=2.5g/ml, 4h). Expression of CHOP, ERDJ4 ATF4, XBP1(Spliced)/XBP1(Unspliced), GRP78 and GADD34 was measured by means of RT-qPCR. Results were normalized to each CALR variant sample cultured in normoxic conditions Data are reported as RQ±SEM of three independent experiments. p <0.05 (*). (**B**) Western Blot analysis of GRP78, CHOP, ATF4, P-eIF2α protein levels were performed in whole cell lysates collected 48 hours after treatment. The protein levels in CALR-mutant cells were compared with control cells. β-actin was included as loading control for GRP78, CHOP and ATF4. Total eIF2α was included as loading control for P-eIF2α.*

In order to investigate whether this differential activation of the PERK pathway involves a distinct ability to induce apoptosis, K562 cells were treated with Tm (20μg/ml) for 24 hours and apoptosis levels were evaluated by means of Annexin V/ PI staining.

Flow Cytometry analysis showed that CALR-mutant cells show a reduced apoptosis rate compared to CALRwt cells (CALRins5: 9.2±1.08% vs 16.43±1,63%, p<0.05; CALRdel52: 9.56±0.58% vs 16.43±1.63%, p<0.05)(**Figure 55, panel A and B**).

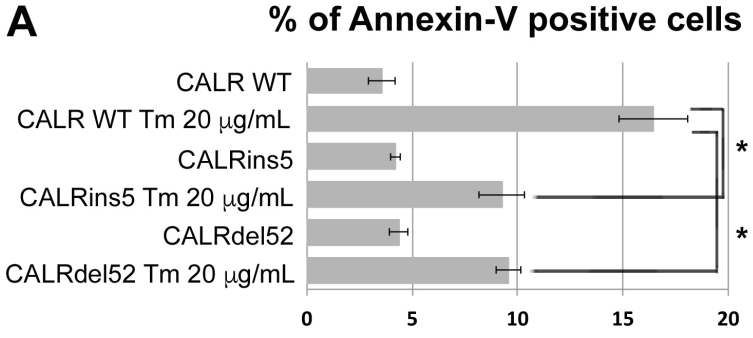

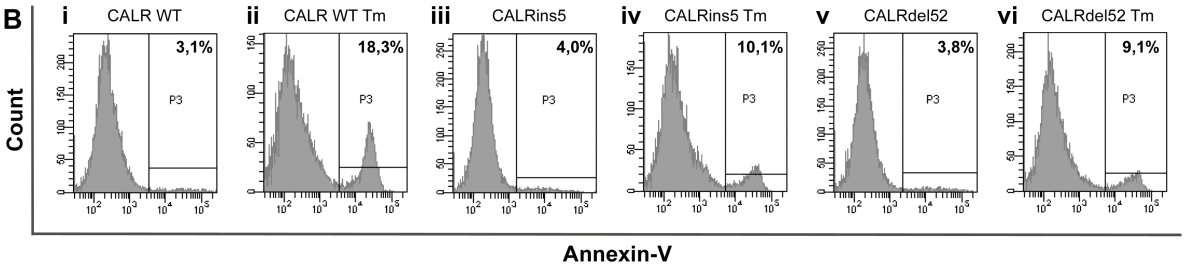

Figure 55: *Flow Cytometry analysis of Annexin V/PI staining on K562 cells 24 hours after Tm treatment (C=20μg/ml). (**A**) Bar charts representing the percentages of Annexin V-positive cells. Data are reported as mean±SEM of three independent experiments. (**B**) Representative histograms for Annexin V staining on K562 cells (**i**: CALRwt not treated, **ii**: CALRwt Tm, **iii**: CALRins5 not treated, **iv**: CALRins5 Tm, **v**: CALRdel52 not treated, **v**: CALRdel52 Tm).*

Collectively, our results confirmed the correlation between CALR mutations and the impairment of PERK response. More specifically, CALR mutations affect cell ability to induce the expression of pro-apoptotic components of the UPR, thus allowing the cells to become resistant to ER stress-induced apoptosis.

5 BIOLOGICAL EFFECTS OF CALR MUTATIONS IN OXIDATIVE STRESS IN K562 CELLS

5.1 DNA damage induced by Melittin and Miltirone treatment

In order to evaluate whether CALRins5 and CALRdel52 mutations are able to impact on the capacity to repair DNA damage induced by oxidative stress, K562 cells were treated with Melittin (C=5μg/ml) for 24 hours.

As mentioned above, Melittin (MEL) is the main constituent of bee venom involved in the induction of DNA damage including oxidative DNA damage.

To assess DNA damage, we decided to measure the levels of phosphorylation at serine 139 of histone H2AX (γ-H2AX), which is considered an early DNA damage marker, both after MEL treatment and after 24 hours of repair.

Flow Cytometry analysis revealed that MEL is able to enhance the DNA damage in CALRdel52 and CALRins5 cells. However, only K562 cells expressing CALRdel52 show statistically significant higher levels of γ-H2AX compared to CALRwt (48.5±2.6% vs 36.9±1.4%, $p<0.05$). These differences are even more strong 24 hours after treatment removal. In fact, after 24 hours after the removal CALRdel52 and CALRins5 were not able to efficiently repair the DNA damage as shown by the percentage of γ-H2AX-positive cells (CALRdel52: 24.5±2.7% vs 11.5±1.8, $p<0.05$; CALRins5: 26.1±2.9% vs 11.5±1.8%, $p<0.05$)(**Figure 56**).

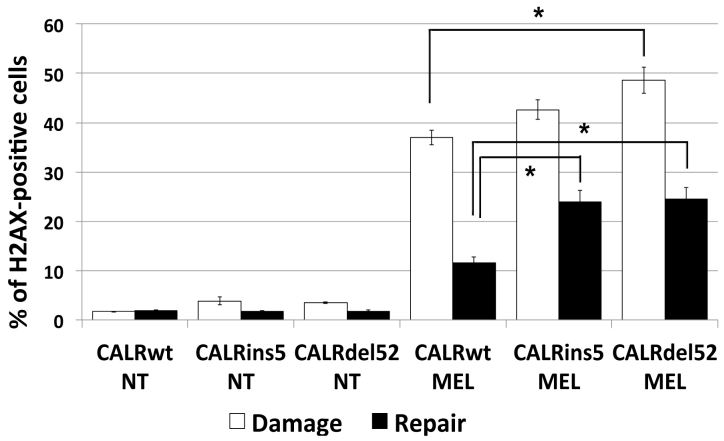

Figure 56: *Flow Cytometry analysis of γ-H2AX staining on K562 cells expressing either WT or mutated CALR. White bars represent the percentage of γ-H2AX-positive cells after 24 hours of MEL treatment (C=5μg/ml), while black bars measure the staining percentage after 24 hours of repair. Data are reported as mean±SEM of three independent experiments. P<0.05 (*). Abbreviations: NT, not treated; MEL, Melittin.*

To further validate our results on DNA damage induced by oxidative stress, we treated the CALRwt, CALRins5 and CALRdel52 K562 cells with Miltirone (MILT), an another agent able to induce oxidative stress.

Even after MILT treatment (C=10μM, 24 hours), we demonstrated that K562 cells expressing either CALRins5 or CALRdel52 show statistically significant higher levels of γ-H2AX compared to CALRwt (CALRins5: 36.6±5.2% vs 22.25±3.6%, p<0.05; CALRdel52: 35.9±6.1% vs 22.25±3.6%, p<0.05)(**Figure 57**). However, we were not able to generate data after 24 hours of repair due to the major toxicity of this treatment.

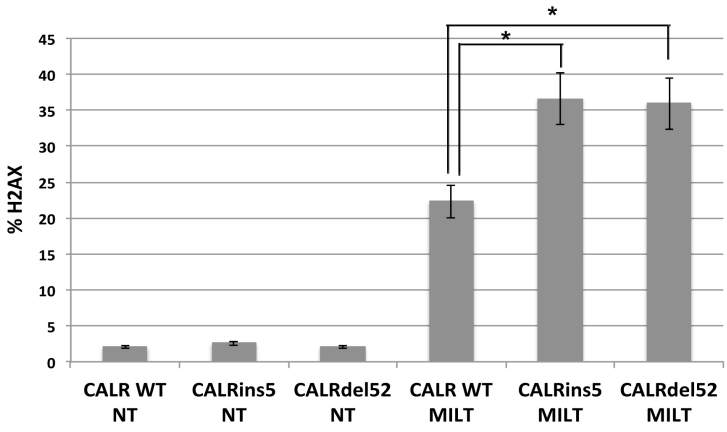

Figure 57: *Flow Cytometry analysis of γ-H2AX staining on K562 cells expressing either WT or mutated CALR after 24 hours of MILT treatment (C=10μM). Data are reported as mean±SEM of three independent experiments. P<0.05 (*). Abbreviations: NT, not treated; MILT, Miltirone.*

Next, to assess whether the DNA damage response was specifically induced by oxidative stress, we measured the levels of a ubiquitous marker of oxidative DNA damage: 8-Hydroxy-2-deoxyguanosine (8-OHdG). 8-OHdG is one of the major DNA

oxidative modifications that can be generated by hydroxylation of the deoxyguanosine residues.

To this end, K562 cells expressing either the Wild-Type or mutated variants of CALR were treated with MEL (C=5μg/ml) for 24 hours. Levels of 8-OHdG have been detected by means of OxiSelect Oxidative DNA Damage ELISA kit, both after MEL treatment and after 24 hours of repair.

Our results demonstrated that there are no statistically significant differences in 8-OHdG levels between K562wt and K562 mutated cells after 24 hours of MEL exposure. However, after 24 hours of repair, K562 cells expressing Wild-Type CALR showed statistically significant lower levels of 8-OHdG compared to CALRdel52 and CALRins5 K562 cells (CALRdel52: 5.8±0.64ng/ml vs 3.8±0.23ng/ml, $p<0.05$; CALRins5: 4.9±0.28ng/ml vs 3.8±0.23ng/ml, $p<0.05$)(**Figure 58**).

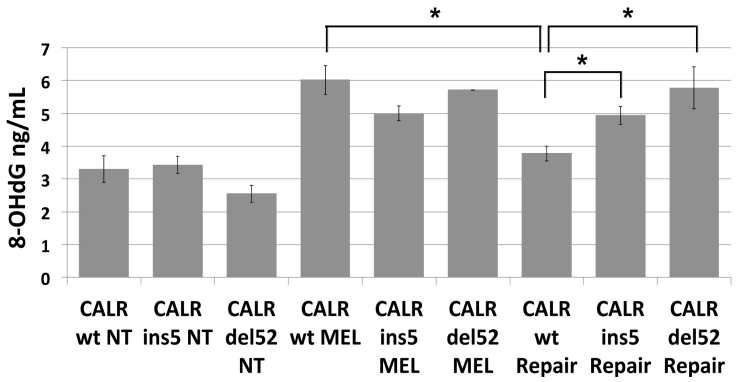

Figure 58: ELISA analysis of 8-OHdG levels in K562 cells expressing either WT or mutated CALR after 24 hours of MEL treatment (C=5μg/ml) and after 24 hours of repair. Data are reported as mean of 8-OHdG levels (expressed in ng/ml)±SEM of three independent experiments. P<0.05 (*). Abbreviations: NT, not treated; MEL, Melittin.

Even in this case we performed the same experiment using MILT. K562 CALRdel52 treated with MILT (C=10μM) for 24 hours showed statistically significant higher levels of 8-OHdG compared to CALRwt cells (0.59±0.02ng/ml vs 0.37±0.01ng/ml, $p<0.05$)(**Figure 59**).

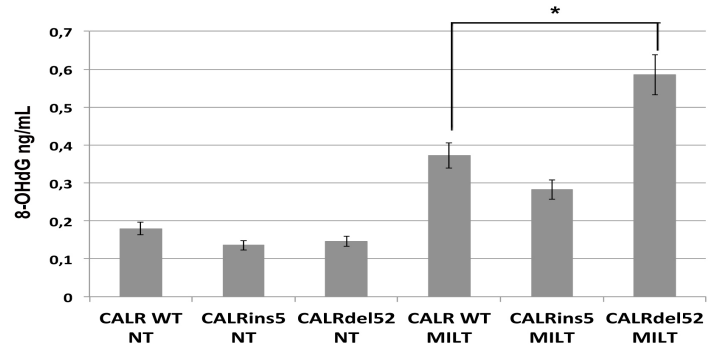

Figure 59: ELISA analysis of 8-OHdG levels in K562 cells expressing either WT or mutated CALR after 24 hours of MILT treatment (C=10μM). Data are reported as mean of 8-OHdG levels (expressed in ng/ml)±SEM of three independent experiments. P<0.05 (*). Abbreviations: NT, not treated; MILT, Miltirone.

Overall, these data suggest that CALRdel52 and CALRins5 mutations negatively impact the capability of cells to respond to DNA damage induced by oxidative stress.

5.2 ROS production induced by Melittin and Miltirone treatment

As mentioned before, enhanced Reactive Oxygen Species (ROS) production has been already associated to DNA damage in hematopoietic stem cells. For this reason, we evaluated ROS level after treatment with MEL (C=5μg/ml) for 24 hours and 24 hours after repair.

The effects of CALRdel52 and CALRins5 on the response to oxidative stress were assessed by measuring the levels of intracellular ROS through CM-H_2DCFDA staining detected by Flow Cytometry analysis.

We detected a significant accumulation of ROS in CALR-mutant cells compared to CALRwt K562 cells after treatment (CALRins5: 30.2±0.7% vs 24.5±0.4%, $p<0.05$; CALRdel52: 29.9±0.6% vs 24.5±0.4%, $p<0.05$). These differences are more striking if the cells are left for 24 additional hours in culture to counteract ROS accumulation induced by treatment. Indeed, after 24 additional hours in culture, CALRins5 and CALRdel52 K562 cells were unable to reduce ROS levels induced by MEL, while CALRwt K562 cells were able to reduce efficiently ROS accumulation (CALRins5: 29.8±0.6% vs 20.4±0.36%, $p<0.5$; CALRdel52: 28.5±0.55% vs 20.4±0.36%, $p<0.5$)(**Figure 60**).

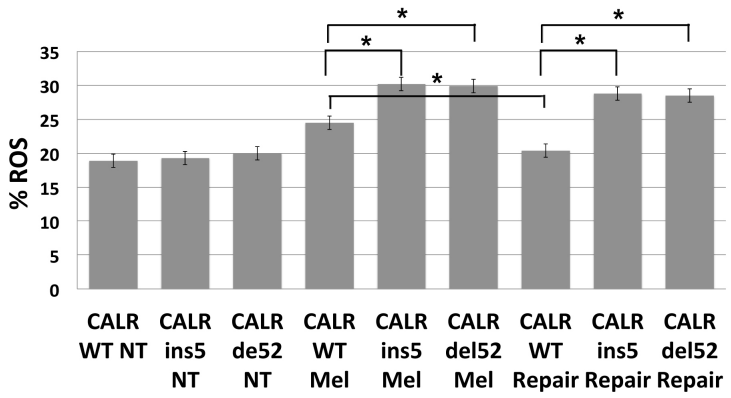

Figure 60: *Percentage of intracellular ROS levels measured by means of Flow Cytometry analysis in K562 cells expressing either WT or mutated CALR. The levels have been measured after 24 hours of MEL treatment (C=5μg/ml) and after 24 hours of repair. Data are reported as percentage of ROS-positive cells±SEM of three independent experiments. P<0.05 (*). Abbreviations: NT, not treated; MEL, Melittin.*

To further validate our results on ROS accumulation in CALR mutants, we treated CALRwt, CALRins5 and CALRdel52 K562 cells with MILT (C=10μM) for 24 hours.

In agreement with previous data, ROS levels measured after MILT treatment showed a significant increase in K562 CALR-mutant cells compared to WT control (CALRins5: 48.5±5.1% vs 23.2±3.3%, p<0.05; CALRdel52: 44.5±3.1% vs 23.2±3.3%, p<0.05)(**Figure 61**).

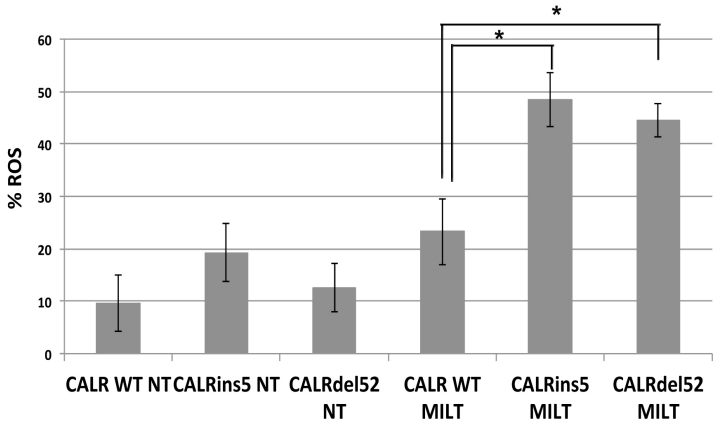

Figure 61: *Percentage of intracellular ROS levels measured by means of Flow Cytometry analysis in K562 cells expressing either WT or mutated CALR. The levels have been measured after 24 hours of MILT treatment (C=10μM). Data are reported as percentage of ROS-positive cells±SEM of three independent experiments. P<0.05 (*). Abbreviations: NT, not treated; MILT, Miltirone.*

Our results suggest that CALR mutants negatively affect cell ability to respond to ROS intracellular accumulation.

5.3 Activity of antioxidant enzymes after Melittin and Miltirone treatment

To better understand the molecular mechanisms responsible for the increased oxidative stress-induced DNA damage in K562-mutant cells, we measured the activity of different antioxidant enzymes after treatment with MEL and MILT, including Superoxide Dismutase (SOD) and Glutathione Reductase (GSR).

SOD is an antioxidant enzyme responsible for the dismutation of superoxide radical anion into hydrogen peroxide. Since SOD plays a pivotal role in defense against the toxicity of reactive oxygen species, we decided to evaluate SOD activity by means of Superoxide Dismutase Assay Kit.

After treatment with MEL (C=5μg/ml) for 24 hours, CALRwt K562 cells showed an increase of SOD activity, while CALRins5 and CALRdel52 K562 cells demonstrated a significant lower SOD activity after MEL exposure compared to WT control (**Figure 62**).

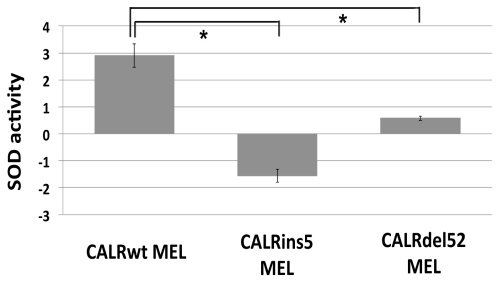

Figure 62: *SOD activity measured by means of Superoxide Dismutase Assay Kit in K562 cells expressing either WT or mutated CALR. SOD activity has been measured after 24 hours of MEL treatment (C=5μg/ml) and normalized to the SOD activity of the sample collected before MEL treatment. Data are reported as mean±SEM of three independent experiments. P<0.05 (*). Abbreviations: MEL, Melittin.*

These data have been confirmed even after treatment with MILT (C=10μM) for 24 hours (**Figure 63**).

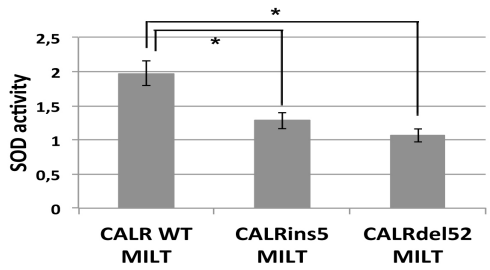

Figure 63: *SOD activity measured by means of Superoxide Dismutase Assay Kit in K562 cells expressing either WT or mutated CALR. The SOD activity has been measured after 24 hours of MILT treatment (C=10μM) and normalized to the SOD activity of the sample collected before MILT treatment. Data are reported as mean±SEM of three independent experiments. P<0.05 (*). Abbreviations: MILT, Miltirone.*

Another important enzyme able to counteract oxidative stress is Glutathione Reductase (GSR), which acts as an antioxidant by directly interacting with ROS or functioning as a cofactor for other enzymes. We have also assessed the activity of GSR upon 24 hours of MILT (C=10μM) treatment by means of Glutathione Reductase Assay Kit.

Our results revealed that GSR was less active in K562 cells carrying either CALRins5 or CALRdel52 mutated variants compared to CALRwt control K562 cells (**Figure 64**), suggesting that failure to activate antioxidant systems may be a cause of the increased oxidative stress in mutated CALR cells.

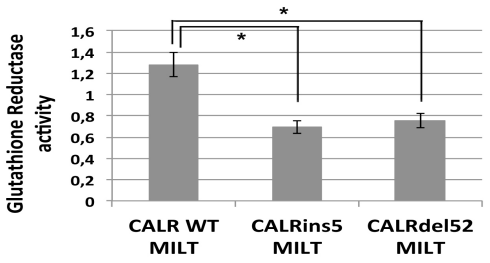

Figure 64: *GSR activity measured by means of Glutathione Reductase Assay Kit in K562 cells expressing either WT or mutated CALR. The GSR activity has been measured after 24 hours of MILT treatment (C=10μM) and normalized to the GSR activity of the sample collected before MILT treatment. Data are reported as mean±SEM of three independent experiments. P<0.05 (*). Abbreviations: MILT, Miltirone.*

6 BIOLOGICAL EFFECTS OF OXR1 SILENCING ON OXIDATIVE STRESS IN CD34+ HSPC

6.1 OXR1 silencing

Finally, in order to identify potential molecular mechanisms that could be responsible for the increased sensitivity to oxidative stress mediated by CALR mutants, we analyzed the Differentially Expressed Genes (DEGs) arising from the comparison K562 mutated vs WT cells. Among these, we identified Oxidation resistance 1 (OXR1) gene. As described above, OXR1 plays a critical role in protecting the cell against oxidative stress and the consequent oxidative stress-induced cell death.

After the validation by means of RT-qPCR of the OXR1 downregulation in CALR-mutants K562 cells compared to control (**Figure 65, panel A**), we performed OXR1 silencing in CB CD34+ cells from healthy subjects, which are the target cells involved in the development of myeloproliferative neoplasms.

Our results confirmed the downregulation of OXR1 expression level after the last siRNA nucleofection compared to non-targeting siRNA (NT siRNA) negative control (RQ±SEM 0.3328±0.0231, $p<0.01$, **)(**Figure 65, panel B**).

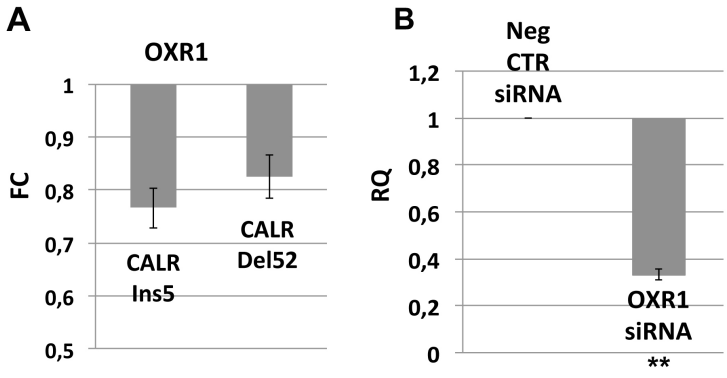

*Figure 65: OXR1 downregulation. (**A**) Expression levels of OXR1 mRNA in the comparison between CALR mutated and WT K562 cells. Data are reported as RQ±SEM of three independent experiments. (**B**) Expression levels of OXR1 mRNA in the comparison CD34+ OXR1 siRNA vs NTsiRNA. Expression levels were measured 24h after the last infection by means of RT-qPCR. Data are reported as RQ±SEM of three independent experiments. p<0.01 (**).*

6.2 Activity of antioxidant enzymes after Melittin treatment

Next, in order to assess the effects of OXR1 downregulation on the capacity of CD34+ cells to respond to oxidative stress, we treated OXR1 siRNA and NT siRNA-transduced CD34+ cells with Melittin (MEL)(C=5µg/ml) for 24 hours and measured the levels of intracellular ROS.

Flow Cytometry analysis showed a striking increase of ROS in OXR1 siRNA samples versus negative control (NegCTR siRNA)(17.15±2.25% VS 10.1±0.36%, p<0.01)(**Figure 66**), suggesting that OXR1 silencing impairs the capacity to counteract the accumulation of intracellular ROS.

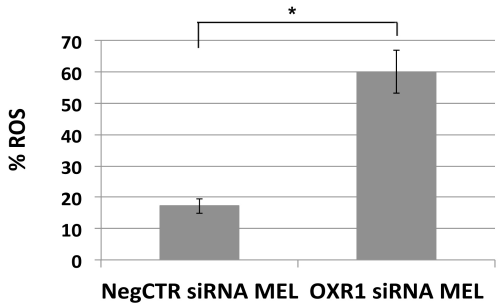

Figure 66: *Percentage of intracellular ROS levels measured by means of Flow Cytometry analysis in OXR1 siRNA and NegCTR siRNA-transduced CD34+ cells. The levels have been measured after 24 hours of MEL treatment (C=5μg/ml). Data are reported as percentage of ROS-positive cells±SEM of three independent experiments. P<0.01 (**). Abbreviations: MEL, Melittin.*

6.3 DNA damage induced by Melittin treatment

Finally, to evaluate whether OXR1 knockdown is able to impact on the capacity to repair the DNA damage induced by oxidative stress, OXR1 siRNA and NegCTR siRNA-transduced CD34+ cells were treated with MEL (C=5μg/ml) for 24 hours.

Flow Cytometry analysis revealed that OXR1 siRNA samples show statistically significant higher levels of γ-H2AX compared to negative control (16.1±0.6% vs 10.1±0.36%, p<0.05)(**Figure 67**). Moreover, these differences are even more strong 24 hours after treatment removal. In fact, at this time point OXR1 siRNA samples were not able to efficiently repair the DNA damage as evidenced by the high percentage of γ-H2AX-positive cells (15.3±0.4% vs 5.3±0.3, p<0.05)(**Figure 67**).

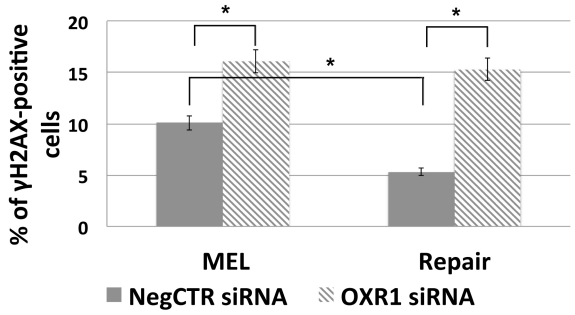

Figure 67: *Flow Cytometry analysis of γ-H2AX staining on OXR1 siRNA or NegCTR siRNA-transduced CD34+ cells after 24 hours of MEL treatment (C=5μg/ml)(left) and after 24 hours of repair (right). Data are reported as mean±SEM of three independent experiments. P<0.05 (*). Abbreviations: MEL, Melittin.*

These data suggest that OXR1 knockdown negatively impacts on the capability of cells to respond to DNA damage and could be a potential mechanism mediating the effect on oxidative stress response in CALR mutated celsl. The inability to repair DNA damage might lead to genomic instability which can induce the accumulation of further mutations underlying molecular pathogenesis of MPNs.

All the results obtained in this study were included in the following papers:

- "*Calreticulin affects hematopoietic stem/progenitor cell fate by impacting erythroid and megakaryocytic differentiation*" Stem Cells Dev. 27, 225–236 (2018)[399];
- "*Calreticulin Ins5 and Del52 mutations impair unfolded protein and oxidative stress responses in K562 cells expressing CALR mutants*" Sci. Rep. 9, 10558 (2019)[400];

DISCUSSION

The term "Myeloproliferative disorders" was used for the first time by William Dameshek in 1951 to describe a group of hematological disorders defined by excessive production of mature blood cells[1]. However, very little was known about the pathogenesis of these disorders until 2005 when a somatic mutation in the JAK2 kinase (JAK2V617F) was discovered in these malignancies[27,28,118,119,120]. Since then, a number of stem cell derived mutations have been identified, leading to a better understanding of the molecular pathogenesis of these neoplasms.

Myeloproliferative neoplasms (MPNs), a category of diseases that include Polycytemia vera (PV), Essential Thrombocythemia (ET) and Primary Myelofibrosis (PMF), are clonal hematopoietic stem cell disorders characterized by increased proliferation of terminally differentiated myeloid cells[2]. Among them, PMF is the most severe disorder with the worst prognosis, characterized by bone marrow fibrosis, abnormal cytokine expression and shortened survival[45].

The discovery of three driver mutations in JAK2, MPL and CALR has improved patients' stratification. In PMF, mutations involving JAK2 occurs in approximately 50-60% of ET and PMF patients, mutations in MPL are restricted to around 5% while CALR abnormalities have been reported in 60-80% of JAK2 and MPL unmutated patients[117].

In particular, the discovery in 2013 of CALR gene mutations has filled the gap in the knowledge of molecular pathogenesis of MPNs. Moreover, it would appear that this mutation plays a key role in the first stages of MPNs' development; in fact several evidence suggests that CALR mutation is acquired early in the clonal history of these diseases[117,401,402].

The majority of CALR mutated cases harbor one of two mutations in exon 9: a 52-bp deletion (type 1) or a 5-bp insertion (type 2)[117]. So far, more than 40 different types of CALR mutants have been reported in MPNs[143,144]. All these different mutations induce a frameshift, resulting in the formation of a stop codon that causes the loss of the C-terminal portion and, subsequently, the partially or completely loss of the negative charges required for Ca^{2+} binding. Indeed, CALR protein is composed of three structural domains[143]. C-domain is involved in determining Ca^{2+} storage while the N-domain, in conjunction with P-domain, may form a functionally important folding unit responsible for chaperone function of CALR[174].

As extensively described above, CALR is a multifunctional Endoplasmic Reticulum (ER) chaperone responsible for intracellular calcium regulation and protein folding. Apart from these functions, CALR is also able to perform different functions outside the ER, including functions in immunity, development and differentiation, cell migration and adhesion[191].

In the last decade many research groups tried to explain the molecular mechanisms underlying MPN pathogenesis caused by CALR mutation. The main tumorigenic mechanism demonstrated as triggered by CALR mutations is based on the interaction of mutant CALR with Thrombopoietin receptor (MPL). Mutated CALR homomultimers may binds MPL, through the glycosylated residues of the latter and subsequently activate the JAK-STAT pathway[149,150,263,266].

Even though the mechanism by which CALR mutants can activate JAK-STAT signalling has been well described, no data are available on the effects exerted by these mutants on the physiological functions that CALR plays in the ER. For this reason, we decided to study the pathological role of CALR mutations that could arise in an MPL-independent manner in order to identify additional pathways whose alterations might cooperate with cellular transformation mediated by MPL activation.

Moreover, recent clinical parameter assessment on ET and PMF patients highlighted a strong correlation between CALR mutations and higher platelet count associated with lower white blood cells count[42,403,404]. In addition, a preferential expression of CALR in megakaryocyte (MK) compartment it has been demonstrated. Starting from these observations, we wondered how Wild-Type (WT) CALR takes part in physiological hematopoiesis.

Our overexpression and gene silencing experiments in CD34+ HSPCs unraveled a new and unexpected role of CALR in CD34+ Hematopoietic Stem/Progenitor cells (HSPCs).

In particular, immunophenotypic analysis clearly showed that CALR overexpression in CD34+ cells enhanced the expression of both erythroid and MK lineage markers (**Figures 31, 32 and 34**), which is also supported by morphological analysis (**Figure 33**). In agreement with these data, clonogenic assays showed an increase in the percentage of erythroid and MK colonies, BFU-E/CFU-E and CFU-MK respectively (**Figures 35 and 36**). Furthermore, Gene Expression Profiling (GEP) analysis revealed the up-regulation in CALR-overexpressing CD34+ cells of several genes involved in erythroid differentiation (i.e. RHCE, HBZ) and platelet activation (i.e. SGK1, FN1, CD9, THBS1), as well as proinflammation (i.e. IL8, CXCL5, CCL2, CCL3) and markers already described in hematological malignancies (i.e. EMP1, VSIG4, LEP)(**Table 7 and figure 37**). These data suggest that CALR overexpression in CD34+ HSPCs is able to enhance

erythroid and MK differentiation together with the induction of several genes already described to play a role in MPNs' development.

In agreement with these data, CALR silencing displays a significant decrease in the expression of the MK markers CD41 and CD42b markers as well as the erythroid marker GPA (**Figures 41, 42 and 44**). The inhibition of erythroid and MK differentiation was also confirmed by morphological analysis, which evidences a decrease in the number of megakaryoblasts in MK culture and a reduction in polychromatic and orthochromatic erythroblasts in erythroid culture (**Figure 43**). In agreement with liquid culture differentiation assay data, semisolid cultures showed a significant decrease in the percentage of MK and erythroid colonies upon CALR silencing compared to control (**Figures 45 and 46**). Additionally, GEP analysis showed that CALR silencing modulated several signaling pathways such as DNA repair (i.e. NUCKS1 and UBE2 V2), regulation of self-renewal of HSCs (i.e. CREM and KIF3A), ER stress response and Unfolded Protein Response (UPR)(i.e. SELK, HSP90B1 and HSPA5)(**Table 8 and figure 47**). Therefore, our findings support a role of CALR knockdown in the reduction of the MK and erythroid lineages in CD34+ HSPCs. Moreover, these data also suggest a potential role of CALR in DNA repair, essential in cell transformation and MPNs' development. In fact, DNA damage accumulation and proinflammation environment have been suggested as causes of the increase of cancer incidence and aging[405,406].

Even though the mechanism by which CALR mutants can activate JAK-STAT signalling has been well described, this pathway may not be the only one involved in the progression of the pathology, also considering that only 16,7 % of CALR-mutated patients show a reduction in CALR allele burden after Ruxolitinib treatment[407]. Moreover, recent data showed that CALR mutants promote the abnormal interaction and mislocalization of its binding partners. In particular, it has been shown that CALR type 1 and type 2 mutations preferentially bind UPR proteins or megakaryocytic transcriptional factors, suggesting that aberrant CALR protein complexes can contribute to the pathogenic phenotype[408].

In order to investigate the impact of CALR mutations in additional pathways whose alterations might cooperate with cellular transformation mediated by MPL activation, we transduced K562 cells with vectors expressing one of the two commonest CALR mutated variants, either CALRdel52 or CALRins5. We chose to perform experiments in the K562 cell line, devoid of MPL expression.

To better characterize the genetic program activated by CALR mutants, we performed Gene Expression Profiling (GEP) analysis on K562 cells transduced with retroviral vectors expressing CALRwt, CALRins5 or CALRdel52. The unsupervised analysis of

the microarray data through the Principal Component Analysis (PCA) showed that CALRdel52 and CALRins5-overexpressing samples clustered together and were separated from CALRwt-transduced controls (**Figure 50**). Moreover, functional analysis performed by means of Ingenuity Pathway Analysis (IPA)® software allowed us to identify several categories of Differentially Expressed Genes (DEGs) modulated by CALR mutants versus Wild-Type, such as "Unfolded Protein Response", "Endoplasmic Reticulum stress", HIF1a Signaling", "GADD45 Signalling", "NRF2-mediated Oxidative Stress Response" (**Table 9**). Starting from these findings, we decided to take advantage of this new cellular model to study the involvement of mutated CALR in oxidative stress response and to clarify if this could represent an additional pathogenetic mechanism involved in CALR-mediated myeloproliferative disease.

Activation of Unfolded Protein Response (UPR) is needed to induce adaptation of the cell to ER stress or to initiate apoptosis[409]. UPR initially induces translation arrest and the production of specific factors able to compensate the damage induced by accumulation of misfolded proteins and reestablish normal ER function. When the adaptation fails UPR induces an alarm signal through the activation of various transcriptional factors related to host defense. Eventually, if the stress is too severe and prolonged, UPR triggers cell suicide by apoptosis[335]. Therefore, the activation of UPR has a bivalent function: the promotion of protein synthesis or the activation of apoptosis. Recent works have demonstrated a correlation between transcriptional activation of UPR and upregulation of the NF-kB pathway in CALR-mutant MPNs[410,411]. Our data demonstrated the upregulation of important branches of UPR upon ER stress induction in K562 CALRwt, whereas we showed a downregulation of UPR-target genes (i.e. GRP78 and ERDJ4), especially target genes of PERK pathways (i.e. CHOP, ATF4 and P-eIF2α) in CALR-mutant K562 cells (**Figure 52 and 53**). In agreement with these results, the failure to activate PERK pathway induces a downregulation of apoptosis levels in K562-mutant cells (**Figure 55**). Taken together, these results demonstrated that CALR mutations are able to inhibit apoptosis because of the failed activation of UPR, suggesting that mutations might impact on CALR chaperone activity.

Next, we investigated how CALR mutations could affect cell response to oxidative stress. Oxidative stress is considered as an imbalance between pro- and antioxidant species, which results in molecular and cellular damage[412]. Indeed, intracellular Reactive Oxygen Species (ROS) accumulation impairs proteins', lipids' and nucleic acids' structures[292]. Previous works demonstrated the involvement of oxidative stress in the pathogenesis of MPNs: oxidative stress would seem to favor the formation of

fibrosis following the accumulation of DNA damage. Moreover, high cell turnover contributes to the production of ROS with consequent genetic instability[80,327].

Our results demonstrate that, following treatment with different substances which induce oxidative stress, CALR-mutant cells show higher levels of γ-H2AX, considered an early marker of DNA damage (**Figures 56 and 57**). Moreover, K562 CALRdel52 and CALRins5 cells were not able to efficiently repair the DNA damage compared to CALRwt-expressing K562 cells (**Figure 56**). To further validate that DNA damage is actually caused by oxidative stress, we also evaluated 8-Hydroxy-2-deoxyguanosine (8-OHdG) levels. 8-OHdG is one of the major DNA oxidative modifications that can be generated by hydroxylation of the deoxyguanosine residues. In agreement with previous results, K562 cells expressing CALRdel52 and CALRins5 showed statistically higher levels of 8-OHdG compared to CALRwt after 24 hours of repair (**Figures 58 and 59**). Overall, these data suggest that CALR-mutant cells negatively impact on the capability to response to oxidative stress-induced DNA damage.

To assess whether the increase in DNA damage in K562-mutant cells correlated with an increase in Reactive Oxygen Species (ROS) we measured their levels after the treatment with Melittin and Miltirone. Our data showed higher levels of intracellular ROS in K562 cells expressing CALR mutations compared to control (**Figures 60 and 61**). In addition, mutated K562 cells are unable to counteract ROS accumulation after 24 from the removal of DNA-damaging agent; on the contrary, this reduction is observed in the CALRwt control samples (**Figures 60 and 61**).

In order to understand the molecular mechanism underlying ROS accumulation in CALR-mutant cells, we evaluated the levels of different antioxidant molecules in our samples. In agreement with these findings, the results showed a decreased levels of Superoxide Dismutase (SOD) and Glutathione Reductase (GSR) activity when K562-mutant cells are exposed to oxidative stress (**Figures 62, 63 and 64**). Thus, the observed DNA damage correlates with increased formation of ROS and a parallel reduction of SOD and GSR activity, showing that CALR-mutant cells are more sensitive to oxidative stress.

Finally, in order to identify the molecular mechanisms involved in CALR mutants-mediated increased sensitivity to oxidative stress, we analyzed the Differentially Expressed Genes (DEGs) between CALR-mutant and WT K562 cells. Among downregulated genes in mutated K562 cells, preliminary data have been collected through *in vitro* experiments on the Oxidation Resistance 1 (OXR1) gene, described to exert protective effects against oxidative stress. Moreover, OXR1 is involved in the modulation of cell cycle and apoptosis[332]. To get new insights into the potential role played by this gene during the MPN progression, we performed gene silencing

experiments in primary human CD34+ cells and treated these cells with a stress-inducing substance. Our preliminary data demonstrated that OXR1 silencing in CD34+ cells induces the increase of intracellular ROS (**Figure 66**) and significant high levels of DNA damage, measured as percentage of γ-H2AX positive-cell (**Figure 67**), suggesting that OXR1 is involved in the counteraction of ROS accumulation and response to oxidative stress-induced DNA damage even in hematopoietic stem progenitor cells.

Collectively, these data suggest a role of WT CALR in hematopoietic stem/progenitor cell fate determination by impacting on erythroid and megakaryocytic differentiation, which are the two main lineages affected in MPNs. Moreover, we also demonstrated a role for WT CALR in several biological processes, including regulation of proinflammatory cytokines, DNA damage and UPR.

Finally, we demonstrated that CALR mutation negatively impact on the ability of cells to respond to oxidative stress-induced DNA damage. This in turn will lead to genomic instability and to susceptibility of CALR-mutant cells to acquire additional mutations, therefore contributing to the MPN phenotype onset.

BIBLIOGRAPHY

1. Dameshek, W. Editorial: Some Speculations on the Myeloproliferative Syndromes. *Blood* **6**, 372–375 (1951).

2. Fialkow, P. J. Cell lineages in hematopoietic neoplasia studied with glucose-6-phosphate dehydrogenase cell markers. *J. Cell. Physiol. Suppl.* **1**, 37–43 (1982).

3. Vardiman, J. W., Harris, N. L. & Brunning, R. D. The World Health Organization (WHO) classification of the myeloid neoplasms. *Blood* **100**, 2292–2302 (2002).

4. Nowell, P. C. & Hungerford, D. A. Chromosome studies on normal and leukemic human leukocytes. *J. Natl. Cancer Inst.* **25**, 85–109 (1960).

5. Rowley, J. D. A New Consistent Chromosomal Abnormality in Chronic Myelogenous Leukaemia identified by Quinacrine Fluorescence and Giemsa Staining. *Nature* **243**, 290–293 (1973).

6. Tefferi, A. & Gilliland, G. Classification of chronic myeloid disorders: From Dameshek towards a semi-molecular system. *Best Pract. Res. Clin. Haematol.* **19**, 365–385 (2006).

7. Delhommeau, F. *et al.* Oncogenic mechanisms in myeloproliferative disorders. *Cell. Mol. Life Sci.* **63**, 2939–2953 (2006).

8. De Keersmaecker, K. & Cools, J. Chronic myeloproliferative disorders: a tyrosine kinase tale. *Leukemia* **20**, 200–205 (2006).

9. Tefferi, A. & Barbui, T. Polycythemia vera and essential thrombocythemia: 2017 update on diagnosis, risk-stratification, and management: TEFFERI and BARBUI. *Am. J. Hematol.* **92**, 94–108 (2017).

10. Arber, D. A. *et al.* The 2016 revision to the World Health Organization classification of myeloid neoplasms and acute leukemia. *Blood* **127**, 2391–2405 (2016).

11. Barbui, T. *et al.* Survival and Disease Progression in Essential Thrombocythemia Are Significantly Influenced by Accurate Morphologic Diagnosis: An International Study. *J. Clin. Oncol.* **29**, 3179–3184 (2011).

12. Rumi, E. & Cazzola, M. Diagnosis, risk stratification, and response evaluation in classical myeloproliferative neoplasms. *Blood* **129**, 680–692 (2017).

13. Moulard, O. *et al.* Epidemiology of myelofibrosis, essential thrombocythemia, and polycythemia vera in the European Union. *Eur. J. Haematol.* **92**, 289–297 (2014).

14. Srour, S. A. *et al.* Incidence and patient survival of myeloproliferative neoplasms and myelodysplastic/myeloproliferative neoplasms in the United States, 2001-12. *Br. J. Haematol.* **174**, 382–396 (2016).

15. Craft, A., Amineddine, H., Scott, J. & Wagget, J. The Northern region Children's malignant disease registry 1968-82: incidence and survival. *Br. J. Cancer* **56**, 853–858 (1987).

16. Wolanskyj, A. P., Schwager, S. M., McClure, R. F., Larson, D. R. & Tefferi, A. Essential Thrombocythemia Beyond the First Decade: Life Expectancy, Long-term Complication Rates, and Prognostic Factors. *Mayo Clin. Proc.* **81**, 159–166 (2006).

17. Cervantes, F. *et al.* Improving Survival Trends in Primary Myelofibrosis: An International Study. *J. Clin. Oncol.* **30**, 2981–2987 (2012).

18. Hultcrantz, M. *et al.* Patterns of Survival Among Patients With Myeloproliferative Neoplasms Diagnosed in Sweden From 1973 to 2008: A Population-Based Study. *J. Clin. Oncol.* **30**, 2995–3001 (2012).

19. Anderson, L. A. & McMullin, M. F. Epidemiology of MPN: What Do We Know? *Curr. Hematol. Malig. Rep.* **9**, 340–349 (2014).

20. Yogarajah, M. & Tefferi, A. Leukemic Transformation in Myeloproliferative Neoplasms. *Mayo Clin. Proc.* **92**, 1118–1128 (2017).

21. Campbell, P. J. *et al.* Definition of subtypes of essential thrombocythaemia and relation to polycythaemia vera based on JAK2 V617F mutation status: a prospective study. *The Lancet* **366**, 1945–1953 (2005).

22. Spivak, J. L. Myeloproliferative Neoplasms. *N. Engl. J. Med.* **376**, 2168–2181 (2017).

23. Bilgrami, S. & Greenberg, B. R. Polycythemia rubra vera. *Semin. Oncol.* **22**, 307–326 (1995).

24. Prchal, A. Bone-Marrow Responses in Polycythemia Vera. *N. Engl. J. Med.* **290**, 1382–1382 (1974).

25. Green, A. R. Pathogenesis of polycythaemia vera. *The Lancet* **347**, 844–845 (1996).

26. Miyake, T., Kung, C. K. & Goldwasser, E. Purification of human erythropoietin. *J. Biol. Chem.* **252**, 5558–5564 (1977).

27. Baxter, E. J. *et al.* Acquired mutation of the tyrosine kinase JAK2 in human myeloproliferative disorders. *The Lancet* **365**, 1054–1061 (2005).

28. James, C. *et al.* A unique clonal JAK2 mutation leading to constitutive signalling causes polycythaemia vera. *Nature* **434**, 1144–1148 (2005).

29. Tefferi, A., Dingli, D., Li, C.-Y. & Dewald, G. W. Prognostic diversity among cytogenetic abnormalities in myelofibrosis with myeloid metaplasia. *Cancer* **104**, 1656–1660 (2005).

30. Cerquozzi, S. & Tefferi, A. Blast transformation and fibrotic progression in polycythemia vera and essential thrombocythemia: a literature review of incidence and risk factors. *Blood Cancer J.* **5**, e366–e366 (2015).

31. Tefferi, A. Polycythemia vera and essential thrombocythemia: 2012 update on diagnosis, risk stratification, and management. *Am. J. Hematol.* **87**, 284–293 (2012).

32. Passamonti, F. *et al.* A dynamic prognostic model to predict survival in post–polycythemia vera myelofibrosis. *Blood* **111**, 3383–3387 (2008).

33. Barbui, T. *et al.* Practice guidelines for the therapy of essential thrombocythemia. A statement from the Italian Society of Hematology, the Italian Society of Experimental Hematology and the Italian Group for Bone Marrow Transplantation. *Haematologica* **89**, 215–232 (2004).

34. Fialkow, P. J., Faguet, G. B., Jacobson, R. J., Vaidya, K. & Murphy, S. Evidence that essential thrombocythemia is a clonal disorder with origin in a multipotent stem cell. *Blood* **58**, 916–919 (1981).

35. Schafer, A. I. Thrombocytosis and thrombocythemia. *Blood Rev.* **15**, 159–166 (2001).

36. Thiele, J. *et al.* Bone Marrow Fibrosis and Diagnosis of Essential Thrombocythemia. *J. Clin. Oncol.* **27**, e220–e221 (2009).

37. Thiele, J. *et al.* European Bone Marrow Working Group trial on reproducibility of World Health Organization criteria to discriminate essential thrombocythemia from prefibrotic primary myelofibrosis. Haematologica 2012;97(3):360-5 - Comment. *Haematologica* **97**, e5–e6 (2012).

38. Harrison, C. N., Gale, R. E., Machin, S. J. & Linch, D. C. A large proportion of patients with a diagnosis of essential thrombocythemia do not have a clonal disorder and may be at lower risk of thrombotic complications. *Blood* **93**, 417–424 (1999).

39. Michiels, J. J., Berneman, Z. N., Schroyens, W. & Van Vliet, H. H. D. M. Pathophysiology and treatment of platelet-mediated microvascular disturbances, major thrombosis and bleeding complications in essential thrombocythaemia and polycythaemia vera. *Platelets* **15**, 67–84 (2004).

40. Elliott, M. A. & Tefferi, A. Thrombosis and haemorrhage in polycythaemia vera and essential thrombocythaemia. *Br. J. Haematol.* **128**, 275–290 (2005).

41. Finazzi, G. & Harrison, C. Essential Thrombocythemia. *Semin. Hematol.* **42**, 230–238 (2005).

42. Tefferi, A. & Barbui, T. Polycythemia vera and essential thrombocythemia: 2019 update on diagnosis, risk-stratification and management. *Am. J. Hematol.* **94**, 133–143

(2019).

43. Tefferi, A. *et al.* Long-term survival and blast transformation in molecularly annotated essential thrombocythemia, polycythemia vera, and myelofibrosis. *Blood* **124**, 2507–2513 (2014).

44. Vannucchi, A. M., Guglielmelli, P. & Tefferi, A. Advances in Understanding and Management of Myeloproliferative Neoplasms. *CA. Cancer J. Clin.* **59**, 171–191 (2009).

45. Tefferi, A. Primary myelofibrosis: 2019 update on diagnosis, risk-stratification and management. *Am. J. Hematol.* **93**, 1551–1560 (2018).

46. Thiele, J., Hoeppner, B., Zankovich, R. & Fischer, R. Histomorphometry of bone marrow biopsies in primary osteomyelofibrosis/-sclerosis (agnogenic myeloid metaplasia) - correlations between clinical and morphological features. *Virchows Arch. A Pathol. Anat. Histopathol.* **415**, 191–202 (1989).

47. Thiele, J., Kuemmel, T., Sander, C. & Fischer, R. Ultrastructure of bone marrow tissue in so-called primary (idiopathic) myelofibrosis-osteomyelosclerosis (agnogenic myeloid metaplasia). I. Abnormalities of megakaryopoiesis and thrombocytes. *J. Submicrosc. Cytol. Pathol.* **23**, 93–107 (1991).

48. Pardanani, A. & Tefferi, A. Prognostic relevance of anemia and transfusion dependency in myelodysplastic syndromes and primary myelofibrosis. *Haematologica* **96**, 8–10 (2011).

49. Orvain, C. *et al.* Circulating Cd34+ cell count differentiates primary myelofibrosis from other Philadelphia-negative myeloproliferative neoplasms: a pragmatic study. *Ann. Hematol.* **95**, 1819–1823 (2016).

50. Zahr, A. A. *et al.* Bone marrow fibrosis in myelofibrosis: pathogenesis, prognosis and targeted strategies. *Haematologica* **101**, 660–671 (2016).

51. Thiele, J. *et al.* European consensus on grading bone marrow fibrosis and assessment of cellularity. *Haematologica* **90**, 1128–1132 (2005).

52. Gianelli, U. *et al.* The European Consensus on grading of bone marrow fibrosis allows a better prognostication of patients with primary myelofibrosis. *Mod. Pathol.* **25**, 1193–1202 (2012).

53. Mesa, R. A., Hanson, C. A., Rajkumar, S. V., Schroeder, G. & Tefferi, A. Evaluation and clinical correlations of bone marrow angiogenesis in myelofibrosis with myeloid metaplasia. *Blood* **96**, 3374–3380 (2000).

54. Castro-Malaspina, H. Pathogenesis of myelofibrosis: role of ineffective megakaryopoiesis and megakaryocyte components. *Prog. Clin. Biol. Res.* **154**, 427–454 (1984).

55. Schmitt, A. *et al.* Pathologic interaction between megakaryocytes and polymorphonuclear leukocytes in myelofibrosis. *Blood* **96**, 1342–1347 (2000).

56. Le Bousse-Kerdilès, M.-C. Primary myelofibrosis and the 'bad seeds in bad soil' concept. *Fibrogenesis Tissue Repair* **5**, S20 (2012).

57. Le Bousse-Kerdilès, M.-C., Martyré, M.-C. & Samson, M. Cellular and molecular mechanisms underlying bone marrow and liver fibrosis: a review. *Eur. Cytokine Netw.* **19**, 69–80 (2008).

58. Badalucco, S. *et al.* Involvement of TGF 1 in autocrine regulation of proplatelet formation in healthy subjects and patients with primary myelofibrosis. *Haematologica* **98**, 514–517 (2013).

59. Le Bousse-Kerdilès, M. C., Martyré, M. C. & French INSERM research network on Idiopathic Myelofibrosis. Involvement of the fibrogenic cytokines, TGF-beta and bFGF, in the pathogenesis of idiopathic myelofibrosis. *Pathol. Biol. (Paris)* **49**, 153–157 (2001).

60. Zingariello, M. *et al.* Characterization of the TGF-β1 signaling abnormalities in the Gata1low mouse model of myelofibrosis. *Blood* **121**, 3345–3363 (2013).

61. Chagraoui, H. *et al.* Prominent role of TGF-β1 in thrombopoietin-induced myelofibrosis in mice. *Blood* **100**, 3495–3503 (2002).

62. Martyré, M. C. *et al.* Transforming

growth factor-β and megakaryocytes in the pathogenesis of idiopathic myelofibrosis. *Br. J. Haematol.* **88**, 9–16 (1994).

63. Wang, J. C., Novetsky, A., Chen, C. & Novetsky, A. D. Plasma matrix metalloproteinase and tissue inhibitor of metalloproteinase in patients with agnogenic myeloid metaplasia or idiopathic primary myelofibrosis. *Br. J. Haematol.* **119**, 709–712 (2002).

64. Lin, P.-S. *et al.* Transforming growth factor beta 1 increases collagen content, and stimulates procollagen I and tissue inhibitor of metalloproteinase-1 production of dental pulp cells: Role of MEK/ERK and activin receptor-like kinase-5/Smad signaling. *J. Formos. Med. Assoc.* **116**, 351–358 (2017).

65. Ruberti, S. *et al.* Involvement of MAF/SPP1 axis in the development of bone marrow fibrosis in PMF patients. *Leukemia* **32**, 438–449 (2018).

66. Panaretakis, T. *et al.* Mechanisms of pre-apoptotic calreticulin exposure in immunogenic cell death. *EMBO J.* **28**, 578–590 (2009).

67. Balduini, A. *et al.* In Vitro Megakaryocyte Differentiation and Proplatelet Formation in Ph-Negative Classical Myeloproliferative Neoplasms: Distinct Patterns in the Different Clinical Phenotypes. *PLoS ONE* **6**, e21015 (2011).

68. Thiele, J., Kvasnicka, H. M., Diehl, V., Fischer, R. & Michiels, J. J. Clinicopathological Diagnosis and Differential Criteria of Thrombocythemias in Various Myeloproliferative Disorders by Histopathology, Histochemistry and Immunostaining from Bone Marrow Biopsies. *Leuk. Lymphoma* **33**, 207–218 (1999).

69. Thiele, J. *et al.* Initial (prefibrotic) stages of idiopathic (primary) myelofibrosis (IMF) – a clinicopathological study. *Leukemia* **13**, 1741–1748 (1999).

70. Cashell, A. W. & Buss, D. H. The frequency and significance of megakaryocytic emperipolesis in myeloproliferative and reactive states. *Ann. Hematol.* **64**, 273–276 (1992).

71. Schmitt, A. *et al.* Polymorphonuclear Neutrophil and Megakaryocyte Mutual Involvement in Myelofibrosis Pathogenesis. *Leuk. Lymphoma* **43**, 719–724 (2002).

72. Medinger, M. *et al.* Angiogenesis and vascular endothelial growth factor-/receptor expression in myeloproliferative neoplasms: correlation with clinical parameters and *JAK2-V617F* mutational status. *Br. J. Haematol.* **146**, 150–157 (2009).

73. Di Raimondo, F. *et al.* Retrospective study of the prognostic role of serum thymidine kinase level in CLL patients with active disease treated with fludarabine. *Ann. Oncol.* **12**, 621–625 (2001).

74. Rosti, V. *et al.* Spleen endothelial cells from patients with myelofibrosis harbor the JAK2V617F mutation. *Blood* **121**, 360–368 (2013).

75. Ward, H. P. & Block, M. H. THE NATURAL HISTORY OF AGNOGENIC MYELOID METAPLASIA (AMM) AND A CRITICAL EVALUATION OF ITS RELATIONSHIP WITH THE MYELOPROLIFERATIVE SYNDROME: *Medicine (Baltimore)* **50**, 357–420 (1971).

76. Bock, O. *et al.* Osteosclerosis in advanced chronic idiopathic myelofibrosis is associated with endothelial overexpression of osteoprotegerin. *Br. J. Haematol.* **130**, 76–82 (2005).

77. Vainchenker, W. & Constantinescu, S. N. JAK/STAT signaling in hematological malignancies. *Oncogene* **32**, 2601–2613 (2013).

78. Tefferi, A. *et al.* Circulating Interleukin (IL)-8, IL-2R, IL-12, and IL-15 Levels Are Independently Prognostic in Primary Myelofibrosis: A Comprehensive Cytokine Profiling Study. *J. Clin. Oncol.* **29**, 1356–1363 (2011).

79. Barbui, T. *et al.* Elevated C-reactive protein is associated with shortened leukemia-free survival in patients with myelofibrosis. *Leukemia* **27**, 2084–2086 (2013).

80. Marty, C. *et al.* A role for reactive oxygen species in JAK2V617F myeloproliferative neoplasm progression. *Leukemia* **27**, 2187–2195 (2013).

81. Tefferi, A. & Pardanani, A. Myeloproliferative Neoplasms: A Contemporary Review. *JAMA Oncol.* **1**, 97 (2015).

82. Janowska-Wieczorek, A. *et al.* Growth Factors and Cytokines Upregulate Gelatinase Expression in Bone Marrow CD34+ Cells and Their Transmigration Through Reconstituted Basement Membrane. *Blood* **93**, 3379–3390 (1999).

83. Xu, M. *et al.* Constitutive mobilization of CD34+ cells into the peripheral blood in idiopathic myelofibrosis may be due to the action of a number of proteases. *Blood* **105**, 4508–4515 (2005).

84. Cho, S. Y. *et al.* The Effect of CXCL12 Processing on CD34+ Cell Migration in Myeloproliferative Neoplasms. *Cancer Res.* **70**, 3402–3410 (2010).

85. Migliaccio, A. R. *et al.* Altered SDF-1/CXCR4 axis in patients with primary myelofibrosis and in the Gata1low mouse model of the disease. *Exp. Hematol.* **36**, 158–171 (2008).

86. Vardiman, J. W. *et al.* The 2008 revision of the World Health Organization (WHO) classification of myeloid neoplasms and acute leukemia: rationale and important changes. *Blood* **114**, 937–951 (2009).

87. Tefferi, A. & Vardiman, J. W. Classification and diagnosis of myeloproliferative neoplasms: The 2008 World Health Organization criteria and point-of-care diagnostic algorithms. *Leukemia* **22**, 14–22 (2008).

88. Thiele, J. & Kvasnicka, H. M. The 2008 WHO diagnostic criteria for polycythemia vera, essential thrombocythemia, and primary myelofibrosis. *Curr. Hematol. Malig. Rep.* **4**, 33–40 (2009).

89. Barbui, T. *et al.* The 2016 WHO classification and diagnostic criteria for myeloproliferative neoplasms: document summary and in-depth discussion. *Blood Cancer J.* **8**, 15 (2018).

90. Pardanani, A., Lasho, T. L., Finke, C., Hanson, C. A. & Tefferi, A. Prevalence and clinicopathologic correlates of JAK2 exon 12 mutations in JAK2V617F-negative polycythemia vera. *Leukemia* **21**, 1960–1963 (2007).

91. Vannucchi, A. M., Antonioli, E., Guglielmelli, P., Pardanani, A. & Tefferi, A. Clinical correlates of JAK2V617F presence or allele burden in myeloproliferative neoplasms: a critical reappraisal. *Leukemia* **22**, 1299–1307 (2008).

92. Mossuz, P. *et al.* Diagnostic value of serum erythropoietin level in patients with absolute erythrocytosis. *Haematologica* **89**, 1194–1198 (2004).

93. Patnaik, M. M. & Tefferi, A. Refractory anemia with ring sideroblasts (RARS) and RARS with thrombocytosis (RARS-T): 2017 update on diagnosis, risk-stratification, and management: PATNAIK and TEFFERI. *Am. J. Hematol.* **92**, 297–310 (2017).

94. Barosi, G. *et al.* Evidence that Prefibrotic Myelofibrosis Is Aligned along a Clinical and Biological Continuum Featuring Primary Myelofibrosis. *PLoS ONE* **7**, e35631 (2012).

95. Tefferi, A. Primary myelofibrosis: 2014 update on diagnosis, risk-stratification, and management. *Am. J. Hematol.* **89**, 915–925 (2014).

96. Chuzi, S. & Stein, B. L. Essential thrombocythemia: a review of the clinical features, diagnostic challenges, and treatment modalities in the era of molecular discovery. *Leuk. Lymphoma* **58**, 2786–2798 (2017).

97. Tefferi, A., Guglielmelli, P., Pardanani, A. & Vannucchi, A. M. Myelofibrosis Treatment Algorithm 2018. *Blood Cancer J.* **8**, 72 (2018).

98. Cervantes, F. *et al.* New prognostic scoring system for primary myelofibrosis based on a study of the International Working Group for Myelofibrosis Research and Treatment. *Blood* **113**, 2895–2901 (2009).

99. Passamonti, F. *et al.* A dynamic prognostic model to predict survival in primary myelofibrosis: a study by the IWG-MRT (International Working Group for Myeloproliferative Neoplasms Research and Treatment). *Blood* **115**, 1703–1708 (2010).

100. Gangat, N. *et al.* DIPSS Plus: A Refined Dynamic International Prognostic Scoring System for Primary Myelofibrosis That Incorporates Prognostic Information From Karyotype, Platelet Count, and Transfusion Status. *J. Clin. Oncol.* **29**, 392–397 (2011).

101. Vannucchi, A. M. *et al.* Mutations and prognosis in primary myelofibrosis. *Leukemia* **27**, 1861–1869 (2013).

102. Guglielmelli, P. *et al.* MIPSS70: Mutation-Enhanced International Prognostic Score System for Transplantation-Age Patients With Primary Myelofibrosis. *J. Clin. Oncol.* **36**, 310–318 (2018).

103. Tefferi, A. *et al.* MIPSS70+ Version 2.0: Mutation and Karyotype-Enhanced International Prognostic Scoring System for Primary Myelofibrosis. *J. Clin. Oncol.* **36**, 1769–1770 (2018).

104. Grinfeld, J. *et al.* Classification and Personalized Prognosis in Myeloproliferative Neoplasms. *N. Engl. J. Med.* **379**, 1416–1430 (2018).

105. Tefferi, A. *et al.* Allogeneic hematopoietic stem cell transplant overcomes the adverse survival effect of very high risk and unfavorable karyotype in myelofibrosis. *Am. J. Hematol.* **93**, 649–654 (2018).

106. Samuelson Bannow, B. T. *et al.* Hematopoietic Cell Transplantation for Myelofibrosis: the Dynamic International Prognostic Scoring System Plus Risk Predicts Post-Transplant Outcomes. *Biol. Blood Marrow Transplant.* **24**, 386–392 (2018).

107. Tefferi, A. Myeloproliferative neoplasms: A decade of discoveries and treatment advances: Myeloproliferative neoplasms. *Am. J. Hematol.* **91**, 50–58 (2016).

108. Berk, P. D., Wasserman, L. R., Fruchtman, S. M. & Goldberg, J. D. Treatment of polycythemia vera: A summary of clinical trials con- ducted by the Polycythemia Vera Study Group. In: Polycythemia Vera and the Myeloproliferative Disorders. **L.R. Wasserman, P.D. Berk & N.I. Berlin**, 166–194 (1995).

109. Kiladjian, J.-J., Chevret, S., Dosquet, C., Chomienne, C. & Rain, J.-D. Treatment of Polycythemia Vera With Hydroxyurea and Pipobroman: Final Results of a Randomized Trial Initiated in 1980. *J. Clin. Oncol.* **29**, 3907–3913 (2011).

110. Harrison, C. N. *et al.* Hydroxyurea Compared with Anagrelide in High-Risk Essential Thrombocythemia. *N. Engl. J. Med.* **353**, 33–45 (2005).

111. Cervantes, F., Mesa, R. & Barosi, G. New and Old Treatment Modalities in Primary Myelofibrosis: *Cancer J.* **13**, 377–383 (2007).

112. Mishchenko, E. & Tefferi, A. Treatment options for hydroxyurea-refractory disease complications in myeloproliferative neoplasms: JAK2 inhibitors, radiotherapy, splenectomy and transjugular intrahepatic portosystemic shunt: Management of disease complications in myeloproliferative neoplasms. *Eur. J. Haematol.* **85**, 192–199 (2010).

113. Mascarenhas, J. & Hoffman, R. Ruxolitinib: The First FDA Approved Therapy for the Treatment of Myelofibrosis. *Clin. Cancer Res.* **18**, 3008–3014 (2012).

114. Bose, P. & Verstovsek, S. JAK2 inhibitors for myeloproliferative neoplasms: what is next? *Blood* **130**, 115–125 (2017).

115. Guglielmelli, P. *et al.* Impact of mutational status on outcomes in myelofibrosis patients treated with ruxolitinib in the COMFORT-II study. *Blood* **123**, 2157–2160 (2014).

116. Nangalia, J. & Green, A. R. Myeloproliferative neoplasms: from origins to outcomes. *Blood* **130**, 2475–2483 (2017).

117. Vainchenker, W. & Kralovics, R. Genetic basis and molecular pathophysiology of classical myeloproliferative neoplasms. *Blood* **129**, 667–679 (2017).

118. Jones, A. V. Widespread occurrence of the JAK2 V617F mutation in chronic myeloproliferative disorders. *Blood* **106**, 2162–2168 (2005).

119. Levine, R. L. *et al.* Activating mutation in the tyrosine kinase JAK2 in polycythemia vera, essential thrombocythemia, and myeloid metaplasia with myelofibrosis. *Cancer Cell* **7**, 387–397 (2005).

120. Kralovics, R. *et al.* A Gain-of-Function Mutation of *JAK2* in Myeloproliferative Disorders. *N. Engl. J. Med.* **352**, 1779–1790 (2005).

121. Kralovics, R. Acquired uniparental disomy of chromosome 9p is a frequent stem cell defect in polycythemia vera. *Exp. Hematol.* **30**, 229–236 (2002).

122. Barbui, T. *et al.* Development and validation of an International Prognostic Score of thrombosis in World Health Organization–essential thrombocythemia (IPSET-thrombosis). *Blood* **120**, 5128–5133 (2012).

123. Darnell, J., Kerr, I. & Stark, G. Jak-STAT pathways and transcriptional activation in response to IFNs and other extracellular signaling proteins. *Science* **264**, 1415–1421 (1994).

124. Ugo, V. Multiple signaling pathways are involved in erythropoietin-independent differentiation of erythroid progenitors in polycythemia vera. *Exp. Hematol.* **32**, 179–187 (2004).

125. Liu, F. *et al.* JAK2V617F-Mediated Phosphorylation of PRMT5 Downregulates Its Methyltransferase Activity and Promotes Myeloproliferation. *Cancer Cell* **19**, 283–294 (2011).

126. Dawson, M. A. *et al.* JAK2 phosphorylates histone H3Y41 and excludes HP1α from chromatin. *Nature* **461**, 819–822 (2009).

127. Scott, L. M. *et al.* JAK2 Exon 12 Mutations in Polycythemia Vera and Idiopathic Erythrocytosis. *N. Engl. J. Med.* **356**, 459–468 (2007).

128. Xing, S. *et al.* Transgenic expression of JAK2V617F causes myeloproliferative disorders in mice. *Blood* **111**, 5109–5117 (2008).

129. Mullally, A. *et al.* Physiological Jak2V617F Expression Causes a Lethal Myeloproliferative Neoplasm with Differential Effects on Hematopoietic Stem and Progenitor Cells. *Cancer Cell* **17**, 584–596 (2010).

130. Hasan, S. *et al.* JAK2V617F expression in mice amplifies early hematopoietic cells and gives them a competitive advantage that is hampered by IFNα. *Blood* **122**, 1464–1477 (2013).

131. Tiedt, R. *et al.* Ratio of mutant JAK2-V617F to wild-type Jak2 determines the MPD phenotypes in transgenic mice. *Blood* **111**, 3931–3940 (2008).

132. Grisouard, J. *et al.* JAK2 exon 12 mutant mice display isolated erythrocytosis and changes in iron metabolism favoring increased erythropoiesis. *Blood* **128**, 839–851 (2016).

133. Wernig, G. *et al.* Expression of Jak2V617F causes a polycythemia vera–like disease with associated myelofibrosis in a murine bone marrow transplant model. *Blood* **107**, 4274–4281 (2006).

134. Kralovics, R. *et al.* Acquisition of the V617F mutation of JAK2 is a late genetic event in a subset of patients with myeloproliferative disorders. *Blood* **108**, 1377–1380 (2006).

135. Campbell, P. J. V617F mutation in JAK2 is associated with poorer survival in idiopathic myelofibrosis. *Blood* **107**, 2098–2100 (2006).

136. Pikman, Y. *et al.* MPLW515L Is a Novel Somatic Activating Mutation in Myelofibrosis with Myeloid Metaplasia. *PLoS Med.* **3**, e270 (2006).

137. Defour, J.-P., Chachoua, I., Pecquet, C. & Constantinescu, S. N. Oncogenic activation of MPL/thrombopoietin receptor by 17 mutations at W515: implications for myeloproliferative neoplasms. *Leukemia* **30**, 1214–1216 (2016).

138. Cabagnols, X. *et al.* Presence of atypical thrombopoietin receptor (MPL) mutations in triple-negative essential thrombocythemia patients. *Blood* **127**, 333–342 (2016).

139. Milosevic Feenstra, J. D. *et al.* Whole-exome sequencing identifies novel MPL and JAK2 mutations in triple-negative myeloproliferative neoplasms. *Blood* **127**, 325–332 (2016).

140. Chaligné, R. *et al.* Evidence for MPL W515L/K mutations in hematopoietic stem cells in primitive myelofibrosis. *Blood* **110**, 3735–3743 (2007).

141. Lasho, T. L. *et al.* Concurrent MPL515 and JAK2V617F mutations in myelofibrosis: chronology of clonal emergence and changes in mutant allele burden over time. *Br. J. Haematol.* **135**, 683–687 (2006).

142. Kaushansky, K. The molecular mechanisms that control thrombopoiesis. *J. Clin. Invest.* **115**, 3339–3347 (2005).

143. Klampfl, T. *et al.* Somatic Mutations of Calreticulin in Myeloproliferative Neoplasms. *N. Engl. J. Med.* **369**, 2379–2390 (2013).

144. Nangalia, J. *et al.* Somatic CALR Mutations in Myeloproliferative Neoplasms with Nonmutated JAK2. *N. Engl. J. Med.* **369**, 2391–2405 (2013).

145. Tefferi, A. *et al.* Type 1 vs type 2 calreticulin mutations in primary myelofibrosis: differences in phenotype and prognostic impact. *Leukemia* **28**, 1568–1570 (2014).

146. Theocharides, A. P. A. *et al.* Homozygous calreticulin mutations in patients with myelofibrosis lead to acquired myeloperoxidase deficiency. *Blood* **127**, 3253–3259 (2016).

147. Rumi, E. *et al.* JAK2 or CALR mutation status defines subtypes of essential thrombocythemia with substantially different clinical course and outcomes. *Blood* **123**, 1544–1551 (2014).

148. Tefferi, A. *et al.* Type 1 versus Type 2 calreticulin mutations in essential thrombocythemia: A collaborative study of 1027 patients: Type 1 vs. type 2 CALR Mutations in ET. *Am. J. Hematol.* **89**, E121–E124 (2014).

149. Elf, S. *et al.* Mutant Calreticulin Requires Both Its Mutant C-terminus and the Thrombopoietin Receptor for Oncogenic Transformation. *Cancer Discov.* **6**, 368–381 (2016).

150. Araki, M. *et al.* Homomultimerization of mutant calreticulin is a prerequisite for MPL binding and activation. *Leukemia* **33**, 122–131 (2019).

151. Rampal, R. *et al.* Genomic and functional analysis of leukemic transformation of myeloproliferative neoplasms. *Proc. Natl. Acad. Sci.* **111**, E5401–E5410 (2014).

152. Stegelmann, F. *et al.* High-resolution single-nucleotide polymorphism array-profiling in myeloproliferative neoplasms identifies novel genomic aberrations. *Haematologica* **95**, 666–669 (2010).

153. McCauliffe, D. P., Yang, Y. S., Wilson, J., Sontheimer, R. D. & Capra, J. D. The 5'-flanking region of the human calreticulin gene shares homology with the human GRP78, GRP94, and protein disulfide isomerase promoters. *J. Biol. Chem.* **267**, 2557–2562 (1992).

154. Nash, P. D., Opas, M. & Michalak, M. Calreticulin: not just another calcium-binding protein. *Mol. Cell. Biochem.* **135**, 71–78 (1994).

155. Fliegel, L., Burns, K., MacLennan, D. H., Reithmeier, R. A. & Michalak, M. Molecular cloning of the high affinity calcium-binding protein (calreticulin) of skeletal muscle sarcoplasmic reticulum. *J. Biol. Chem.* **264**, 21522–21528 (1989).

156. Kennedy, T. E., Kuhl, D., Barzilai, A., Sweatt, J. D. & Kandel, E. R. Long-Term sensitization training in Aplysia leads to an increase in calreticulin, a major presynaptic calcium-binding protein. *Neuron* **9**, 1013–1024 (1992).

157. Liu, N., Fine, R. E. & Johnson, R. J. Comparison of cDNAs from bovine brain coding for two isoforms of calreticulin. *Biochim. Biophys. Acta BBA - Protein Struct. Mol. Enzymol.* **1202**, 70–76 (1993).

158. Rooke, K., Briquet-Laugier, V., Xia, Y.-R., Lusis, A. J. & Doolittle, M. H. Mapping of the gene for calreticulin (Calr) to mouse Chromosome 8. *Mamm. Genome* **8**, 870–871 (1997).

159. Murthy, K. K. *et al.* Structural homology between the rat calreticulin gene product and the *Onchocerca volvulus* antigen Ral-1. *Nucleic Acids Res.* **18**, 4933–4933 (1990).

160. Nakamura, M. *et al.* An Endoplasmic Reticulum Protein, Calreticulin, Is Transported into the Acrosome of Rat Sperm. *Exp. Cell Res.* **205**, 101–110 (1993).

161. Smith, M. J. A C. elegans gene encodes a protein homologous to mammalian calreticulin. *DNA Seq. J. DNA Seq. Mapp.* **2**, 235–240 (1992).

162. Treves, S., Zorzato, F. & Pozzan, T. Identification of calreticulin isoforms in the central nervous system. *Biochem. J.* **287**, 579–581 (1992).

163. Waser, M., Mesaeli, N., Spencer, C. & Michalak, M. Regulation of Calreticulin Gene Expression by Calcium. *J. Cell Biol.* **138**, 547–557 (1997).

164. Smith, M. J. & Koch, G. L. Multiple zones in the sequence of calreticulin (CRP55, calregulin, HACBP), a major calcium binding ER/SR protein. *EMBO J.* **8**, 3581–3586 (1989).

165. Watson, J. D. Molecular Biology of the Gene. in *Molecular Biology of the Gene* (1987).

166. Little, E., Ramakrishnan, M., Roy, B., Gazit, G. & Lee, A. S. The glucose-regulated proteins (GRP78 and GRP94): functions, gene regulation, and applications. *Crit. Rev. Eukaryot. Gene Expr.* **4**, 1–18 (1994).

167. Nguyen, T. Q., Donald Capra, J. & Sontheimer, R. D. Calreticulin is transcriptionally upregulated by heat shock, calcium and heavy metals. *Mol. Immunol.* **33**, 379–386 (1996).

168. Conway, E. M. *et al.* Heat Shock-sensitive Expression of Calreticulin.: *IN VITRO* AND *IN VIVO* UP-REGULATION. *J. Biol. Chem.* **270**, 17011–17016 (1995).

169. Zhu, J. Ultraviolet B irradiation and cytomegalovirus infection synergize to induce the cell surface expression of 52-kD/Ro antigen. *Clin. Exp. Immunol.* **103**, 47–53 (1996).

170. Plakidou-Dymock, S. & McGivan, J. D. Calreticulin — a stress protein induced in the renal epithelial cell line NBL-1 by amino acid deprivation. *Cell Calcium* **16**, 1–8 (1994).

171. Ostwald, T. J. & MacLennan, D. H. Isolation of a high affinity calcium-binding protein from sarcoplasmic reticulum. *J. Biol. Chem.* **249**, 974–979 (1974).

172. Denning, G. M. *et al.* Calreticulin biosynthesis and processing in human myeloid cells: demonstration of signal peptide cleavage and N-glycosylation. *Blood* **90**, 372–381 (1997).

173. Michalak, M., Milner, R. E., Burns, K. & Opas, M. Calreticulin. *Biochem. J.* **285**, 681–692 (1992).

174. Michalak, M., Groenendyk, J., Szabo, E., Gold, L. I. & Opas, M. Calreticulin, a multi-process calcium-buffering chaperone of the endoplasmic reticulum. *Biochem. J.* **417**, 651–666 (2009).

175. Leach, M. R., Cohen-Doyle, M. F., Thomas, D. Y. & Williams, D. B. Localization of the Lectin, ERp57 Binding, and Polypeptide Binding Sites of Calnexin and Calreticulin. *J. Biol. Chem.* **277**, 29686–29697 (2002).

176. Kapoor, M. *et al.* Mutational Analysis Provides Molecular Insight into the Carbohydrate-Binding Region of Calreticulin: Pivotal Roles of Tyrosine-109 and Aspartate-135 in Carbohydrate Recognition †. *Biochemistry* **43**, 97–106 (2004).

177. Baksh, S., Spamer, C., Heilmann, C. & Michalak, M. Identification of the Zn2+ binding region in calreticulin. *FEBS Lett.* **376**, 53–57 (1995).

178. Andrin, C. *et al.* Expression and Purification of Mammalian Calreticulin in Pichia pastoris. *Protein Expr. Purif.* **20**, 207–215 (2000).

179. Rojiani, M. V., Finlay, B. B., Gray, V. & Dedhar, S. In vitro interaction of a polypeptide homologous to human Ro/SS-A antigen (calreticulin) with a highly conserved amino acid sequence in the cytoplasmic domain of integrin .alpha. subunits. *Biochemistry* **30**, 9859–9866 (1991).

180. Burns, K. *et al.* Modulation of gene expression by calreticulin binding to the glucocorticoid receptor. *Nature* **367**, 476–480 (1994).

181. Martin, V. *et al.* Identification by Mutational Analysis of Amino Acid Residues Essential in the Chaperone Function of Calreticulin. *J. Biol. Chem.* **281**, 2338–2346 (2006).

182. Saito, Y. Calreticulin functions in vitro as a molecular chaperone for both glycosylated

and non-glycosylated proteins. *EMBO J.* **18**, 6718–6729 (1999).

183. Krause, K.-H. & Michalak, M. Calreticulin. *Cell* **88**, 439–443 (1997).

184. Ellgaard, L. *et al.* Three-dimensional structure topology of the calreticulin P-domain based on NMR assignment. *FEBS Lett.* **488**, 69–73 (2001).

185. Vassilakos, A., Michalak, M., Lehrman, M. A. & Williams, D. B. Oligosaccharide Binding Characteristics of the Molecular Chaperones Calnexin and Calreticulin †. *Biochemistry* **37**, 3480–3490 (1998).

186. Baksh, S. & Michalak, M. Expression of calreticulin in Escherichia coli and identification of its Ca2+ binding domains. *J. Biol. Chem.* **266**, 21458–21465 (1991).

187. Tjoelker, L. W. *et al.* Human, Mouse, and Rat Calnexin cDNA Cloning: Identification of Potential Calcium Binding Motifs and Gene Localization to Human Chromosome 5. *Biochemistry* **33**, 3229–3236 (1994).

188. Nakamura, K. *et al.* Functional specialization of calreticulin domains. *J. Cell Biol.* **154**, 961–972 (2001).

189. Afshar, N., Black, B. E. & Paschal, B. M. Retrotranslocation of the Chaperone Calreticulin from the Endoplasmic Reticulum Lumen to the Cytosol. *Mol. Cell. Biol.* **25**, 8844–8853 (2005).

190. Labriola, C. A., Conte, I. L., López Medus, M., Parodi, A. J. & Caramelo, J. J. Endoplasmic Reticulum Calcium Regulates the Retrotranslocation of Trypanosoma Cruzi Calreticulin to the Cytosol. *PLoS ONE* **5**, e13141 (2010).

191. Wang, W.-A., Groenendyk, J. & Michalak, M. Calreticulin signaling in health and disease. *Int. J. Biochem. Cell Biol.* **44**, 842–846 (2012).

192. Bedard, K., Szabo, E., Michalak, M. & Opas, M. Cellular Functions of Endoplasmic Reticulum Chaperones Calreticulin, Calnexin, and ERp57. in *International Review of Cytology* vol. 245 91–121 (Elsevier, 2005).

193. Hebert, D. N. & Molinari, M. In and Out of the ER: Protein Folding, Quality Control, Degradation, and Related Human Diseases. *Physiol. Rev.* **87**, 1377–1408 (2007).

194. Elliott, T. & Williams, A. The optimization of peptide cargo bound to MHC class I molecules by the peptide-loading complex. *Immunol. Rev.* **207**, 89–99 (2005).

195. Gao, B. *et al.* Assembly and Antigen-Presenting Function of MHC Class I Molecules in Cells Lacking the ER Chaperone Calreticulin. *Immunity* **16**, 99–109 (2002).

196. Pozzan, T., Rizzuto, R., Volpe, P. & Meldolesi, J. Molecular and cellular physiology of intracellular calcium stores. *Physiol. Rev.* **74**, 595–636 (1994).

197. Ashby, M. C. & Tepikin, A. V. ER calcium and the functions of intracellular organelles. *Semin. Cell Dev. Biol.* **12**, 11–17 (2001).

198. Greber, U. F. Depletion of calcium from the lumen of endoplasmic reticulum reversibly inhibits passive diffusion and signal-mediated transport into the nucleus. *J. Cell Biol.* **128**, 5–14 (1995).

199. Stevens, F. J. & Argon, Y. Protein folding in the ER. *Semin. Cell Dev. Biol.* **10**, 443–454 (1999).

200. Bastianutto, C. Overexpression of calreticulin increases the Ca2+ capacity of rapidly exchanging Ca2+ stores and reveals aspects of their lumenal microenvironment and function. *J. Cell Biol.* **130**, 847–855 (1995).

201. Mery, L. *et al.* Overexpression of Calreticulin Increases Intracellular Ca Storage and Decreases Store-operated Ca Influx. *J. Biol. Chem.* **271**, 9332–9339 (1996).

202. Liou, J. *et al.* STIM Is a Ca2+ Sensor Essential for Ca2+-Store-Depletion-Triggered Ca2+ Influx. *Curr. Biol.* **15**, 1235–1241 (2005).

203. Li, Y. & Camacho, P. Ca^{2+} -dependent redox modulation of SERCA 2b by ERp57. *J. Cell Biol.* **164**, 35–46 (2004).

204. Nicotera, P., Bellomo, G. & Orrenius, S. Calcium-Mediated Mechanisms in Chemically Induced Cell Death. *Annu. Rev. Pharmacol. Toxicol.* **32**, 449–470 (1992).

205. Dihazi, H., Asif, A. R., Agarwal, N. K.,

Doncheva, Y. & Müller, G. A. Proteomic Analysis of Cellular Response to Osmotic Stress in Thick Ascending Limb of Henle's Loop (TALH) Cells. *Mol. Cell. Proteomics* **4**, 1445–1458 (2005).

206. Bibi, A. *et al.* Calreticulin is crucial for calcium homeostasis mediated adaptation and survival of thick ascending limb of Henle's loop cells under osmotic stress. *Int. J. Biochem. Cell Biol.* **43**, 1187–1197 (2011).

207. Ihara, Y., Urata, Y., Goto, S. & Kondo, T. Role of calreticulin in the sensitivity of myocardiac H9c2 cells to oxidative stress caused by hydrogen peroxide. *Am. J. Physiol.-Cell Physiol.* **290**, C208–C221 (2006).

208. Zhang, Y. *et al.* Oxidative Stress–Induced Calreticulin Expression and Translocation: New Insights into the Destruction of Melanocytes. *J. Invest. Dermatol.* **134**, 183–191 (2014).

209. Gardai, S. J. *et al.* Cell-Surface Calreticulin Initiates Clearance of Viable or Apoptotic Cells through trans-Activation of LRP on the Phagocyte. *Cell* **123**, 321–334 (2005).

210. Liu, H., Miller, E., van de Water, B. & Stevens, J. L. Endoplasmic Reticulum Stress Proteins Block Oxidant-induced Ca^{2+} Increases and Cell Death. *J. Biol. Chem.* **273**, 12858–12862 (1998).

211. Hung, C.-C., Ichimura, T., Stevens, J. L. & Bonventre, J. V. Protection of Renal Epithelial Cells against Oxidative Injury by Endoplasmic Reticulum Stress Preconditioning Is Mediated by ERK1/2 Activation. *J. Biol. Chem.* **278**, 29317–29326 (2003).

212. Nakamura, K. *et al.* Changes in Endoplasmic Reticulum Luminal Environment Affect Cell Sensitivity to Apoptosis. *J. Cell Biol.* **150**, 731–740 (2000).

213. Goicoechea, S., Orr, A. W., Pallero, M. A., Eggleton, P. & Murphy-Ullrich, J. E. Thrombospondin Mediates Focal Adhesion Disassembly through Interactions with Cell Surface Calreticulin. *J. Biol. Chem.* **275**, 36358–36368 (2000).

214. Orr, A. W., Pallero, M. A. & Murphy-Ullrich, J. E. Thrombospondin Stimulates Focal Adhesion Disassembly through G_i - and Phosphoinositide 3-Kinase-dependent ERK Activation. *J. Biol. Chem.* **277**, 20453–20460 (2002).

215. Orr, A. W. *et al.* Low density lipoprotein receptor–related protein is a calreticulin coreceptor that signals focal adhesion disassembly. *J. Cell Biol.* **161**, 1179–1189 (2003).

216. Park, Y. *et al.* Refractive index maps and membrane dynamics of human red blood cells parasitized by Plasmodium falciparum. *Proc. Natl. Acad. Sci.* **105**, 13730–13735 (2008).

217. Gaipl, U. S. *et al.* Inefficient Clearance of Dying Cells and Autoreactivity. in *Current Concepts in Autoimmunity and Chronic Inflammation* (eds. Radbruch, A. & Lipsky, P. E.) vol. 305 161–176 (Springer Berlin Heidelberg, 2006).

218. Eggleton & Llewellyn. Pathophysiological Roles of Calreticulin in Autoimmune Disease. *Scand. J. Immunol.* **49**, 466–473 (1999).

219. Porcellini, S. *et al.* Regulation of peripheral T cell activation by calreticulin. *J. Exp. Med.* **203**, 461–471 (2006).

220. Sipione, S., Ewen, C., Shostak, I., Michalak, M. & Bleackley, R. C. Impaired Cytolytic Activity in Calreticulin-Deficient CTLs. *J. Immunol.* **174**, 3212–3219 (2005).

221. Obeid, M. *et al.* Calreticulin exposure dictates the immunogenicity of cancer cell death. *Nat. Med.* **13**, 54–61 (2007).

222. Tufi, R. *et al.* Reduction of endoplasmic reticulum Ca2+ levels favors plasma membrane surface exposure of calreticulin. *Cell Death Differ.* **15**, 274–282 (2008).

223. Chaput, N. *et al.* Molecular determinants of immunogenic cell death: surface exposure of calreticulin makes the difference. *J. Mol. Med.* **85**, 1069–1076 (2007).

224. Wemeau, M. *et al.* Calreticulin exposure on malignant blasts predicts a cellular anticancer immune response in patients with acute myeloid leukemia. *Cell Death Dis.* **1**,

e104–e104 (2010).

225. Ferreira, V., Molina, M. C., Schwaeble, W., Lemus, D. & Ferreira, A. Does Trypanosoma cruzi calreticulin modulate the complement system and angiogenesis? *Trends Parasitol.* **21**, 169–174 (2005).

226. Winrow, C. J. *et al.* Calreticulin modulates the in vitro DNA binding but not the in vivo transcriptional activation by peroxisome proliferator-activated receptor/retinoid X receptor heterodimers. *Mol. Cell. Endocrinol.* **111**, 175–179 (1995).

227. Timchenko, L. T., Iakova, P., Welm, A. L., Cai, Z.-J. & Timchenko, N. A. Calreticulin Interacts with C/EBP and C/EBP mRNAs and Represses Translation of C/EBP Proteins. *Mol. Cell. Biol.* **22**, 7242–7257 (2002).

228. Jensen, B., Farach-Carson, M. C., Kenaley, E. & Akanbi, K. A. High extracellular calcium attenuates adipogenesis in 3T3-L1 preadipocytes. *Exp. Cell Res.* **301**, 280–292 (2004).

229. Shi, H., Halvorsen, Y.-D., Ellis, P. N., Wilkison, W. O. & Zemel, M. B. Role of intracellular calcium in human adipocyte differentiation. *Physiol. Genomics* **3**, 75–82 (2000).

230. Lynch, J. *et al.* Calreticulin signals upstream of calcineurin and MEF2C in a critical Ca^{2+} -dependent signaling cascade. *J. Cell Biol.* **170**, 37–47 (2005).

231. St-Arnaud, R. Constitutive expression of calreticulin in osteoblasts inhibits mineralization. *J. Cell Biol.* **131**, 1351–1359 (1995).

232. Li, J. *et al.* Calreticulin reveals a critical Ca^{2+} checkpoint in cardiac myofibrillogenesis. *J. Cell Biol.* **158**, 103–113 (2002).

233. Lozyk, M. D. *et al.* Ultrastructural analysis of development of myocardium in calreticulin-deficient mice. *BMC Dev. Biol.* **6**, 54 (2006).

234. Mesaeli, N. *et al.* Calreticulin Is Essential for Cardiac Development. *J. Cell Biol.* **144**, 857–868 (1999).

235. Guo, L. *et al.* Cardiac-specific Expression of Calcineurin Reverses Embryonic Lethality in Calreticulin-deficient Mouse. *J. Biol. Chem.* **277**, 50776–50779 (2002).

236. Michalak, M., Guo, L., Robertson, M., Lozak, M. & Opas, M. Calreticulin in the heart. *Mol. Cell. Biochem.* **263**, 137–142 (2004).

237. Nakamura, K. *et al.* Complete heart block and sudden death in mice overexpressing calreticulin. *J. Clin. Invest.* **107**, 1245–1253 (2001).

238. Hattori, K. *et al.* Arrhythmia induced by spatiotemporal overexpression of calreticulin in the heart. *Mol. Genet. Metab.* **91**, 285–293 (2007).

239. Zhang, X., Szabo, E., Michalak, M. & Opas, M. Endoplasmic reticulum stress during the embryonic development of the central nervous system in the mouse. *Int. J. Dev. Neurosci.* **25**, 455–463 (2007).

240. Rauch, F., Prud'homme, J., Arabian, A., Dedhar, S. & St-Arnaud, R. Heart, Brain, and Body Wall Defects in Mice Lacking Calreticulin. *Exp. Cell Res.* **256**, 105–111 (2000).

241. Shu, Q., Li, W., Li, H. & Sun, G. Vasostatin Inhibits VEGF-Induced Endothelial Cell Proliferation, Tube Formation and Induces Cell Apoptosis under Oxygen Deprivation. *Int. J. Mol. Sci.* **15**, 6019–6030 (2014).

242. Shibuya, M. Vascular Endothelial Growth Factor (VEGF) and Its Receptor (VEGFR) Signaling in Angiogenesis: A Crucial Target for Anti- and Pro-Angiogenic Therapies. *Genes Cancer* **2**, 1097–1105 (2011).

243. Pike, S. E. *et al.* Vasostatin, a calreticulin fragment, inhibits angiogenesis and suppresses tumor growth. *J. Exp. Med.* **188**, 2349–2356 (1998).

244. Yao, L., Pike, S. E. & Tosato, G. Laminin binding to the calreticulin fragment vasostatin regulates endothelial cell function. *J. Leukoc. Biol.* **71**, 47–53 (2002).

245. Xiao, F. *et al.* A gene therapy for cancer based on the angiogenesis inhibitor, vasostatin. *Gene Ther.* **9**, 1207–1213 (2002).

246. Jazowiecka-Rakus, J., Jarosz, M. & Szala, S. Combination of vasostatin gene

therapy with cyclophosphamide inhibits growth of B16(F10) melanoma tumours. *Acta Biochim. Pol.* **53**, 199–202 (2006).

247. Ma, L. *et al.* Complete eradication of hepatocellular carcinomas by combined vasostatin gene therapy and B7H3-mediated immunotherapy. *J. Hepatol.* **46**, 98–106 (2007).

248. Cai, K. X. *et al.* Suppression of Lung Tumor Growth and Metastasis in Mice by Adeno-Associated Virus-Mediated Expression of Vasostatin. *Clin. Cancer Res.* **14**, 939–949 (2008).

249. Liu, M., Imam, H., Öberg, K. & Zhou, Y. Gene Transfer of Vasostatin, a Calreticulin Fragment, into Neuroendocrine Tumor Cells Results in Enhanced Malignant Behavior. *Neuroendocrinology* **82**, 1–10 (2005).

250. Vannucchi, A. M. *et al.* Calreticulin mutation-specific immunostaining in myeloproliferative neoplasms: pathogenetic insight and diagnostic value. *Leukemia* **28**, 1811–1818 (2014).

251. Clark, R. A. *et al.* Regulation of calreticulin expression during induction of differentiation in human myeloid cells. Evidence for remodeling of the endoplasmic reticulum. *J. Biol. Chem.* **277**, 32369–32378 (2002).

252. Fadel, M. P. *et al.* Calreticulin Affects β-Catenin-associated Pathways. *J. Biol. Chem.* **276**, 27083–27089 (2001).

253. Opas, M. Calreticulin modulates cell adhesiveness via regulation of vinculin expression. *J. Cell Biol.* **135**, 1913–1923 (1996).

254. Fadel, M. P. *et al.* Calreticulin Affects Focal Contact-dependent but Not Close Contact-dependent Cell-substratum Adhesion. *J. Biol. Chem.* **274**, 15085–15094 (1999).

255. Coppolino, M., Leung-Hagesteijn, C., Dedhar, S. & Wilkins, J. Inducible Interaction of Integrin $\alpha_2\beta_1$ with Calreticulin: DEPENDENCE ON THE ACTIVATION STATE OF THE INTEGRIN. *J. Biol. Chem.* **270**, 23132–23138 (1995).

256. Coppolino, M. G. & Dedhar, S. Ligand-specific, transient interaction between integrins and calreticulin during cell adhesion to extracellular matrix proteins is dependent upon phosphorylation/dephosphorylation events. *Biochem. J.* **340 (Pt 1)**, 41–50 (1999).

257. Papp, S., Szabo, E., Kim, H., McCulloch, C. A. & Opas, M. Kinase-dependent adhesion to fibronectin: regulation by calreticulin. *Exp. Cell Res.* **314**, 1313–1326 (2008).

258. Villagomez, M. *et al.* Calreticulin and focal-contact-dependent adhesion. *Biochem. Cell Biol.* **87**, 545–556 (2009).

259. Luo, W. & Yu, Z. Calreticulin (CALR) mutation in myeloproliferative neoplasms (MPNs). *Stem Cell Investig.* **2**, 16 (2015).

260. Araki, M. & Komatsu, N. Novel molecular mechanism of cellular transformation by a mutant molecular chaperone in myeloproliferative neoplasms. *Cancer Sci.* **108**, 1907–1912 (2017).

261. Caramelo, J. J. & Parodi, A. J. Getting In and Out from Calnexin/Calreticulin Cycles. *J. Biol. Chem.* **283**, 10221–10225 (2008).

262. Mondet, J. *et al.* Endogenous megakaryocytic colonies underline association between megakaryocytes and calreticulin mutations in essential thrombocythemia. *Haematologica* **100**, e176–e178 (2015).

263. Marty, C. *et al.* Calreticulin mutants in mice induce an MPL-dependent thrombocytosis with frequent progression to myelofibrosis. *Blood* **127**, 1317–1324 (2016).

264. Araki, M. *et al.* Activation of the thrombopoietin receptor by mutant calreticulin in CALR-mutant myeloproliferative neoplasms. *Blood* **127**, 1307–1316 (2016).

265. Han, L. *et al.* Calreticulin-mutant proteins induce megakaryocytic signaling to transform hematopoietic cells and undergo accelerated degradation and Golgi-mediated secretion. *J. Hematol. Oncol.J Hematol Oncol* **9**, 45 (2016).

266. Chachoua, I. *et al.* Thrombopoietin receptor activation by myeloproliferative neoplasm associated calreticulin mutants. *Blood* **127**, 1325–1335 (2016).

267. Alexander, W. S. *et al.* Studies of the c‐Mpl Thrombopoietin Receptor

through Gene Disruption and Activation. *Stem Cells* **14**, 124–132 (1996).

268. Brooks, A. J. *et al.* Mechanism of Activation of Protein Kinase JAK2 by the Growth Hormone Receptor. *Science* **344**, 1249783–1249783 (2014).

269. Matthews, E. E. *et al.* Thrombopoietin receptor activation: transmembrane helix dimerization, rotation, and allosteric modulation. *FASEB J.* **25**, 2234–2244 (2011).

270. Staerk, J. *et al.* Orientation-specific signalling by thrombopoietin receptor dimers: Orientation-specific TpoR signalling. *EMBO J.* **30**, 4398–4413 (2011).

271. Imai, M., Araki, M. & Komatsu, N. Somatic mutations of calreticulin in myeloproliferative neoplasms. *Int. J. Hematol.* **105**, 743–747 (2017).

272. Pecquet, C. *et al.* Calreticulin mutants as oncogenic rogue chaperones for TpoR and traffic-defective pathogenic TpoR mutants. *Blood* **133**, 2669–2681 (2019).

273. Elf, S. *et al.* Defining the requirements for the pathogenic interaction between mutant calreticulin and MPL in MPN. *Blood* **131**, 782–786 (2018).

274. Takei, H. *et al.* Skewed megakaryopoiesis in human induced pluripotent stem cell-derived haematopoietic progenitor cells harbouring calreticulin mutations. *Br. J. Haematol.* **181**, 791–802 (2018).

275. Dedhar, S. *et al.* Inhibition of nuclear hormone receptor activity by calreticulin. *Nature* **367**, 480–483 (1994).

276. Holaska, J. M. *et al.* Calreticulin Is a Receptor for Nuclear Export. *J. Cell Biol.* **152**, 127–140 (2001).

277. Pronier, E. *et al.* Targeting the CALR interactome in myeloproliferative neoplasms. *JCI Insight* **3**, e122703 (2018).

278. Di Buduo, C. A. *et al.* Defective interaction of mutant calreticulin and SOCE in megakaryocytes from patients withmyeloproliferative neoplasms. *Blood* blood.2019001103 (2019) doi:10.1182/blood.2019001103.

279. Guglielmelli, P. *et al.* Ruxolitinib is an effective treatment for *CALR* -positive patients with myelofibrosis. *Br. J. Haematol.* **173**, 938–940 (2016).

280. Kollmann, K. *et al.* A novel signalling screen demonstrates that CALR mutations activate essential MAPK signalling and facilitate megakaryocyte differentiation. *Leukemia* **31**, 934–944 (2017).

281. Whalen, A. M., Galasinski, S. C., Shapiro, P. S., Nahreini, T. S. & Ahn, N. G. Megakaryocytic differentiation induced by constitutive activation of mitogen-activated protein kinase kinase. *Mol. Cell. Biol.* **17**, 1947–1958 (1997).

282. Herrera, R., Hubbell, S., Decker, S. & Petruzzelli, L. A Role for the MEK/MAPK Pathway in PMA-Induced Cell Cycle Arrest: Modulation of Megakaryocytic Differentiation of K562 Cells. *Exp. Cell Res.* **238**, 407–414 (1998).

283. Guerriero, R. *et al.* Inhibition of TPO-induced MEK or mTOR activity induces opposite effects on the ploidy of human differentiating megakaryocytes. *J. Cell Sci.* **119**, 744–752 (2006).

284. Chao, M. P. *et al.* Calreticulin Is the Dominant Pro-Phagocytic Signal on Multiple Human Cancers and Is Counterbalanced by CD47. *Sci. Transl. Med.* **2**, 63ra94-63ra94 (2010).

285. Shide, K. *et al.* Calreticulin mutant mice develop essential thrombocythemia that is ameliorated by the JAK inhibitor ruxolitinib. *Leukemia* **31**, 1136–1144 (2017).

286. Li, J. *et al.* Mutant calreticulin knockin mice develop thrombocytosis and myelofibrosis without a stem cell self-renewal advantage. *Blood* **131**, 649–661 (2018).

287. Balligand, T. *et al.* Knock-in of murine Calr del52 induces essential thrombocythemia with slow-rising dominance in mice and reveals key role of Calr exon 9 in cardiac development. *Leukemia* (2019) doi:10.1038/s41375-019-0538-1.

288. Lushchak, V. I. Free radicals, reactive oxygen species, oxidative stress and its classification. *Chem. Biol. Interact.* **224**, 164–175 (2014).

289. Skulachev, V. P. Mitochondria-Targeted Antioxidants as Promising Drugs for Treatment of Age-Related Brain Diseases. *J. Alzheimers Dis.* **28**, 283–289 (2012).

290. De Marchi, E., Baldassari, F., Bononi, A., Wieckowski, M. R. & Pinton, P. Oxidative Stress in Cardiovascular Diseases and Obesity: Role of p66Shc and Protein Kinase C. *Oxid. Med. Cell. Longev.* **2013**, 1–11 (2013).

291. Zheng, S. *et al.* Advanced Oxidation Protein Products Induce Inflammatory Response in Fibroblast-Like Synoviocytes through NADPH Oxidase -Dependent Activation of NF-κB. *Cell. Physiol. Biochem.* **32**, 972–985 (2013).

292. Sies, H. Oxidative stress: a concept in redox biology and medicine. *Redox Biol.* **4**, 180–183 (2015).

293. Mandal, S., Yadav, S. & Nema, R. k. Antioxidants: A Review. **Journal of Chemical and Pharmaceutical Research**, 102–104 (2009).

294. Lardone, P. J., Sanchez N., A.-S., J.M., G. & A., C.-V. Melatonin and Glucose Metabolism: Clinical Relevance. *Curr. Pharm. Des.* **20**, 4841–4853 (2014).

295. Lushchak, V. I. Glutathione Homeostasis and Functions: Potential Targets for Medical Interventions. *J. Amino Acids* **2012**, 1–26 (2012).

296. Frand, A. R. & Kaiser, C. A. Two Pairs of Conserved Cysteines Are Required for the Oxidative Activity of Ero1p in Protein Disulfide Bond Formation in the Endoplasmic Reticulum. *Mol. Biol. Cell* **11**, 2833–2843 (2000).

297. Nakamura, H., Nakamura, K. & Yodoi, J. Redox regulation of cellular activation. *Annu. Rev. Immunol.* **15**, 351–369 (1997).

298. Circu, M. L. & Aw, T. Y. Reactive oxygen species, cellular redox systems, and apoptosis. *Free Radic. Biol. Med.* **48**, 749–762 (2010).

299. McCord, J. M. & Fridovich, I. Superoxide dismutase. An enzymic function for erythrocuprein (hemocuprein). *J. Biol. Chem.* **244**, 6049–6055 (1969).

300. Commoner, B., Townsend, J. & Pake, G. E. Free Radicals in Biological Materials. *Nature* **174**, 689–691 (1954).

301. Gerschman, R., Gilbert, D. L., Nye, S. W., Dwyer, P. & Fenn, W. O. Oxygen Poisoning and X-irradiation: A Mechanism in Common. *Science* **119**, 623–626 (1954).

302. Katerji, M., Filippova, M. & Duerksen-Hughes, P. Approaches and Methods to Measure Oxidative Stress in Clinical Samples: Research Applications in the Cancer Field. *Oxid. Med. Cell. Longev.* **2019**, 1–29 (2019).

303. Ubezio, P. & Civoli, F. Flow cytometric detection of hydrogen peroxide production induced by doxorubicin in cancer cells. *Free Radic. Biol. Med.* **16**, 509–516 (1994).

304. Benov, L., Sztejnberg, L. & Fridovich, I. Critical evaluation of the use of hydroethidine as a measure of superoxide anion radical. *Free Radic. Biol. Med.* **25**, 826–831 (1998).

305. Peshavariya, H. M., Dusting, G. J. & Selemidis, S. Analysis of dihydroethidium fluorescence for the detection of intracellular and extracellular superoxide produced by NADPH oxidase. *Free Radic. Res.* **41**, 699–712 (2007).

306. Pryor, W. A. Oxy-Radicals and Related Species: Their Formation, Lifetimes, and Reactions. *Annu. Rev. Physiol.* **48**, 657–667 (1986).

307. Chiou, C.-C. *et al.* Urinary 8-hydroxydeoxyguanosine and its analogs as DNA marker of oxidative stress: development of an ELISA and measurement in both bladder and prostate cancers. *Clin. Chim. Acta* **334**, 87–94 (2003).

308. Fernandez-Capetillo, O., Lee, A., Nussenzweig, M. & Nussenzweig, A. H2AX: the histone guardian of the genome. *DNA Repair* **3**, 959–967 (2004).

309. Rogakou, E. P., Pilch, D. R., Orr, A. H., Ivanova, V. S. & Bonner, W. M. DNA Double-stranded Breaks Induce Histone H2AX Phosphorylation on Serine 139. *J. Biol. Chem.* **273**, 5858–5868 (1998).

310. Bassing, C. H. *et al.* Increased ionizing radiation sensitivity and genomic instability in

the absence of histone H2AX. *Proc. Natl. Acad. Sci.* **99**, 8173–8178 (2002).

311. Halliwell, B. & Gutteridge, J. M. C. Oxygen free radicals and iron in relation to biology and medicine: Some problems and concepts. *Arch. Biochem. Biophys.* **246**, 501–514 (1986).

312. Zelko, I. N., Mariani, T. J. & Folz, R. J. Superoxide dismutase multigene family: a comparison of the CuZn-SOD (SOD1), Mn-SOD (SOD2), and EC-SOD (SOD3) gene structures, evolution, and expression. *Free Radic. Biol. Med.* **33**, 337–349 (2002).

313. Peskin, A. V. & Winterbourn, C. C. Assay of superoxide dismutase activity in a plate assay using WST-1. *Free Radic. Biol. Med.* **103**, 188–191 (2017).

314. Dröge, W. Free Radicals in the Physiological Control of Cell Function. *Physiol. Rev.* **82**, 47–95 (2002).

315. Valko, M. *et al.* Free radicals and antioxidants in normal physiological functions and human disease. *Int. J. Biochem. Cell Biol.* **39**, 44–84 (2007).

316. Sosa, V. *et al.* Oxidative stress and cancer: An overview. *Ageing Res. Rev.* **12**, 376–390 (2013).

317. Gupta, S. C. *et al.* Upsides and Downsides of Reactive Oxygen Species for Cancer: The Roles of Reactive Oxygen Species in Tumorigenesis, Prevention, and Therapy. *Antioxid. Redox Signal.* **16**, 1295–1322 (2012).

318. Waris, G. & Ahsan, H. Reactive oxygen species: role in the development of cancer and various chronic conditions. *J. Carcinog.* **5**, 14 (2006).

319. Hurt, E. M., Thomas, S. B., Peng, B. & Farrar, W. L. Integrated molecular profiling of SOD2 expression in multiple myeloma. *Blood* **109**, 3953–3962 (2007).

320. Vener, C. *et al.* Oxidative stress is increased in primary and post−polycythemia vera myelofibrosis. *Exp. Hematol.* **38**, 1058–1065 (2010).

321. Gorrini, C., Harris, I. S. & Mak, T. W. Modulation of oxidative stress as an anticancer strategy. *Nat. Rev. Drug Discov.* **12**, 931–947 (2013).

322. Bjørn, M. E. & Hasselbalch, H. C. The Role of Reactive Oxygen Species in Myelofibrosis and Related Neoplasms. *Mediators Inflamm.* **2015**, 1–11 (2015).

323. Nakatake, M. *et al.* JAK2V617F negatively regulates p53 stabilization by enhancing MDM2 via La expression in myeloproliferative neoplasms. *Oncogene* **31**, 1323–1333 (2012).

324. Hurtado-Nedelec, M. *et al.* Increased reactive oxygen species production and p47phox phosphorylation in neutrophils from myeloproliferative disorders patients with JAK2 (V617F) mutation. *Haematologica* **98**, 1517–1524 (2013).

325. Walz, C. *et al.* Activated Jak2 with the V617F Point Mutation Promotes G_1/S Phase Transition. *J. Biol. Chem.* **281**, 18177–18183 (2006).

326. Sallmyr, A. *et al.* Internal tandem duplication of FLT3 (FLT3/ITD) induces increased ROS production, DNA damage, and misrepair: implications for poor prognosis in AML. *Blood* **111**, 3173–3182 (2008).

327. Plo, I. *et al.* JAK2 stimulates homologous recombination and genetic instability: potential implication in the heterogeneity of myeloproliferative disorders. *Blood* **112**, 1402–1412 (2008).

328. Tefferi, A. & Vainchenker, W. Myeloproliferative Neoplasms: Molecular Pathophysiology, Essential Clinical Understanding, and Treatment Strategies. *J. Clin. Oncol.* **29**, 573–582 (2011).

329. Hasselbalch, H. C. *et al.* Whole Blood Transcriptional Profiling Reveals Deregulation of Oxidative and Antioxidative Defence Genes in Myelofibrosis and Related Neoplasms. Potential Implications of Downregulation of Nrf2 for Genomic Instability and Disease Progression. *PLoS ONE* **9**, e112786 (2014).

330. Andréasson, B., Swolin, B. & Kutti, J. Increase of CD34 positive cells in polycythaemia vera. *Eur. J. Haematol.* **59**, 171–176 (2009).

331. Wu, Y., Davies, K. E. & Oliver, P. L. The antioxidant protein Oxr1 influences aspects of mitochondrial morphology. *Free Radic. Biol. Med.* **95**, 255–267 (2016).

332. Yang, M. *et al.* Human OXR1 maintains mitochondrial DNA integrity and counteracts hydrogen peroxide-induced oxidative stress by regulating antioxidant pathways involving p21. *Free Radic. Biol. Med.* **77**, 41–48 (2014).

333. Yang, M. *et al.* Transcriptome analysis of human OXR1 depleted cells reveals its role in regulating the p53 signaling pathway. *Sci. Rep.* **5**, 17409 (2015).

334. Jiang, X. & Wang, X. Cytochrome ***C*** - Mediated Apoptosis. *Annu. Rev. Biochem.* **73**, 87–106 (2004).

335. Xu, C. Endoplasmic reticulum stress: cell life and death decisions. *J. Clin. Invest.* **115**, 2656–2664 (2005).

336. Nagelkerke, A., Bussink, J., Sweep, F. C. G. J. & Span, P. N. The unfolded protein response as a target for cancer therapy. *Biochim. Biophys. Acta BBA - Rev. Cancer* **1846**, 277–284 (2014).

337. Oakes, S. A. Endoplasmic reticulum proteostasis: a key checkpoint in cancer. *Am. J. Physiol.-Cell Physiol.* **312**, C93–C102 (2017).

338. Wang, M., Law, M. E., Castellano, R. K. & Law, B. K. The unfolded protein response as a target for anticancer therapeutics. *Crit. Rev. Oncol. Hematol.* **127**, 66–79 (2018).

339. Ma, Y. & Hendershot, L. M. ER chaperone functions during normal and stress conditions. *J. Chem. Neuroanat.* **28**, 51–65 (2004).

340. Ron, D. & Walter, P. Signal integration in the endoplasmic reticulum unfolded protein response. *Nat. Rev. Mol. Cell Biol.* **8**, 519–529 (2007).

341. Pincus, D. *et al.* BiP Binding to the ER-Stress Sensor Ire1 Tunes the Homeostatic Behavior of the Unfolded Protein Response. *PLoS Biol.* **8**, e1000415 (2010).

342. Osorio, F. *et al.* The unfolded-protein-response sensor IRE-1α regulates the function of CD8α+ dendritic cells. *Nat. Immunol.* **15**, 248–257 (2014).

343. Clarke, H. J., Chambers, J. E., Liniker, E. & Marciniak, S. J. Endoplasmic Reticulum Stress in Malignancy. *Cancer Cell* **25**, 563–573 (2014).

344. Yoshida, H., Matsui, T., Yamamoto, A., Okada, T. & Mori, K. XBP1 mRNA Is Induced by ATF6 and Spliced by IRE1 in Response to ER Stress to Produce a Highly Active Transcription Factor. *Cell* **107**, 881–891 (2001).

345. Nishitoh, H. ASK1 is essential for endoplasmic reticulum stress-induced neuronal cell death triggered by expanded polyglutamine repeats. *Genes Dev.* **16**, 1345–1355 (2002).

346. Urano, F. Coupling of Stress in the ER to Activation of JNK Protein Kinases by Transmembrane Protein Kinase IRE1. *Science* **287**, 664–666 (2000).

347. Tam, A. B., Koong, A. C. & Niwa, M. Ire1 Has Distinct Catalytic Mechanisms for XBP1/HAC1 Splicing and RIDD. *Cell Rep.* **9**, 850–858 (2014).

348. Shi, Y. *et al.* Identification and characterization of pancreatic eukaryotic initiation factor 2 alpha-subunit kinase, PEK, involved in translational control. *Mol. Cell. Biol.* **18**, 7499–7509 (1998).

349. Brewer, J. W. & Diehl, J. A. PERK mediates cell-cycle exit during the mammalian unfolded protein response. *Proc. Natl. Acad. Sci.* **97**, 12625–12630 (2000).

350. Wang, M. & Kaufman, R. J. Protein misfolding in the endoplasmic reticulum as a conduit to human disease. *Nature* **529**, 326–335 (2016).

351. Zong, Z.-H. *et al.* Implication of Nrf2 and ATF4 in differential induction of CHOP by proteasome inhibition in thyroid cancer cells. *Biochim. Biophys. Acta BBA - Mol. Cell Res.* **1823**, 1395–1404 (2012).

352. Palam, L. R., Baird, T. D. & Wek, R. C. Phosphorylation of eIF2 Facilitates Ribosomal Bypass of an Inhibitory Upstream ORF to Enhance *CHOP* Translation. *J. Biol. Chem.* **286**, 10939–10949 (2011).

353. Ye, J. *et al.* ER Stress Induces Cleavage of Membrane-Bound ATF6 by the Same Proteases that Process SREBPs. *Mol. Cell* **6**, 1355–1364 (2000).

354. Ghosh, R. *et al.* Allosteric Inhibition of the IRE1α RNase Preserves Cell Viability and

Function during Endoplasmic Reticulum Stress. *Cell* **158**, 534–548 (2014).

355. Yamamoto, K. *et al.* Transcriptional Induction of Mammalian ER Quality Control Proteins Is Mediated by Single or Combined Action of ATF6α and XBP1. *Dev. Cell* **13**, 365–376 (2007).

356. Hirsch, I., Weiwad, M., Prell, E. & Ferrari, D. M. ERp29 deficiency affects sensitivity to apoptosis via impairment of the ATF6–CHOP pathway of stress response. *Apoptosis* **19**, 801–815 (2014).

357. Wouters, B. G. & Koritzinsky, M. Hypoxia signalling through mTOR and the unfolded protein response in cancer. *Nat. Rev. Cancer* **8**, 851–864 (2008).

358. Nami, B., Donmez, H. & Kocak, N. Tunicamycin-induced endoplasmic reticulum stress reduces in vitro subpopulation and invasion of CD44+/CD24- phenotype breast cancer stem cells. *Exp. Toxicol. Pathol.* **68**, 419–426 (2016).

359. Zhang, Y. *et al.* Tunicamycin-induced ER stress regulates chemokine CCL5 expression and secretion via STAT3 followed by decreased transmigration of MCF-7 breast cancer cells. *Oncol. Rep.* **32**, 2769–2776 (2014).

360. Rogers, T. B., Inesi, G., Wade, R. & Lederer, W. J. Use of thapsigargin to study Ca2+ homeostasis in cardiac cells. *Biosci. Rep.* **15**, 341–349 (1995).

361. Ferreira, R. B. *et al.* Disulfide bond disrupting agents activate the unfolded protein response in EGFR- and HER2-positive breast tumor cells. *Oncotarget* **8**, (2017).

362. Alliegro, M. C. Effects of Dithiothreitol on Protein Activity Unrelated to Thiol–Disulfide Exchange: For Consideration in the Analysis of Protein Function with Cleland's Reagent. *Anal. Biochem.* **282**, 102–106 (2000).

363. Blais, J. D. *et al.* Perk-Dependent Translational Regulation Promotes Tumor Cell Adaptation and Angiogenesis in Response to Hypoxic Stress. *Mol. Cell. Biol.* **26**, 9517–9532 (2006).

364. Koritzinsky, M. *et al.* Gene expression during acute and prolonged hypoxia is regulated by distinct mechanisms of translational control. *EMBO J.* **25**, 1114–1125 (2006).

365. Köditz, J. *et al.* Oxygen-dependent ATF-4 stability is mediated by the PHD3 oxygen sensor. *Blood* **110**, 3610–3617 (2007).

366. Horne, S. D., Chowdhury, S. K. & Heng, H. H. Q. Stress, genomic adaptation, and the evolutionary trade-off. *Front. Genet.* **5**, (2014).

367. Moenner, M., Pluquet, O., Bouchecareilh, M. & Chevet, E. Integrated Endoplasmic Reticulum Stress Responses in Cancer: Figure 1. *Cancer Res.* **67**, 10631–10634 (2007).

368. Ghosh, R. *et al.* Transcriptional Regulation of VEGF-A by the Unfolded Protein Response Pathway. *PLoS ONE* **5**, e9575 (2010).

369. Hu, P., Han, Z., Couvillon, A. D., Kaufman, R. J. & Exton, J. H. Autocrine Tumor Necrosis Factor Alpha Links Endoplasmic Reticulum Stress to the Membrane Death Receptor Pathway through IRE1 -Mediated NF- B Activation and Down-Regulation of TRAF2 Expression. *Mol. Cell. Biol.* **26**, 3071–3084 (2006).

370. Vacchelli, E. *et al.* Trial Watch: Chemotherapy with immunogenic cell death inducers. *OncoImmunology* **3**, e27878 (2014).

371. Greenman, C. *et al.* Patterns of somatic mutation in human cancer genomes. *Nature* **446**, 153–158 (2007).

372. Chen, L. *et al.* IRE1α-XBP1 signaling pathway, a potential therapeutic target in multiple myeloma. *Leuk. Res.* **49**, 7–12 (2016).

373. Carrasco, D. R. *et al.* The Differentiation and Stress Response Factor XBP-1 Drives Multiple Myeloma Pathogenesis. *Cancer Cell* **11**, 349–360 (2007).

374. van Galen, P. *et al.* The unfolded protein response governs integrity of the haematopoietic stem-cell pool during stress. *Nature* **510**, 268–272 (2014).

375. Tang, C.-H. A. *et al.* Inhibition of ER stress–associated IRE-1/XBP-1 pathway reduces leukemic cell survival. *J. Clin. Invest.*

124, 2585–2598 (2014).

376. Rieger, M. A. & Schroeder, T. Hematopoiesis. *Cold Spring Harb. Perspect. Biol.* **4**, a008250–a008250 (2012).

377. Osawa, M., Hanada, K. -i., Hamada, H. & Nakauchi, H. Long-Term Lymphohematopoietic Reconstitution by a Single CD34-Low/Negative Hematopoietic Stem Cell. *Science* **273**, 242–245 (1996).

378. Wognum, A. W. & Szilvassy, S. J. DOCUMENT #29068 VERSION 6.0.0. (2015).

379. Kondo, M., Weissman, I. L. & Akashi, K. Identification of Clonogenic Common Lymphoid Progenitors in Mouse Bone Marrow. *Cell* **91**, 661–672 (1997).

380. Doulatov, S., Notta, F., Laurenti, E. & Dick, J. E. Hematopoiesis: A Human Perspective. *Cell Stem Cell* **10**, 120–136 (2012).

381. Wen, Q., Goldenson, B. & Crispino, J. D. Normal and malignant megakaryopoiesis. *Expert Rev. Mol. Med.* **13**, e32 (2011).

382. Mukai, H. Y. *et al.* Transgene Insertion in Proximity to thec-myb Gene Disrupts Erythroid-Megakaryocytic Lineage Bifurcation. *Mol. Cell. Biol.* **26**, 7953–7965 (2006).

383. Woolthuis, C. M. & Park, C. Y. Hematopoietic stem/progenitor cell commitment to the megakaryocyte lineage. *Blood* **127**, 1242–1248 (2016).

384. Dzierzak, E. & Philipsen, S. Erythropoiesis: Development and Differentiation. *Cold Spring Harb. Perspect. Med.* **3**, a011601–a011601 (2013).

385. Zhang, L., Sankaran, V. G. & Lodish, H. F. MicroRNAs in erythroid and megakaryocytic differentiation and megakaryocyte–erythroid progenitor lineage commitment. *Leukemia* **26**, 2310–2316 (2012).

386. Love, P. E., Warzecha, C. & Li, L. Ldb1 complexes: the new master regulators of erythroid gene transcription. *Trends Genet. TIG* **30**, 1–9 (2014).

387. Papetti, M., Wontakal, S. N., Stopka, T. & Skoultchi, A. I. GATA-1 directly regulates p21 gene expression during erythroid differentiation. *Cell Cycle* **9**, 1972–1980 (2010).

388. Olweus, J., Thompson, P. & Lund-Johansen, F. Granulocytic and monocytic differentiation of CD34hi cells is associated with distinct changes in the expression of the PU.1-regulated molecules, CD64 and macrophage colony-stimulating factor receptor. *Blood* **15**, (1996).

389. Friedman, A. D. *et al.* Regulation of granulocyte and monocyte differentiation by CCAAT/enhancer binding protein α. *Blood Cells. Mol. Dis.* **31**, 338–341 (2003).

390. Kummalue, T. & Friedman, A. D. Cross-talk between regulators of myeloid development: C/EBPα binds and activates the promoter of the PU.1 gene. *J. Leukoc. Biol.* **74**, 464–470 (2003).

391. Laiosa, C. V., Stadtfeld, M. & Graf, T. DETERMINANTS OF LYMPHOID-MYELOID LINEAGE DIVERSIFICATION. *Annu. Rev. Immunol.* **24**, 705–738 (2006).

392. Laiosa, C. V., Stadtfeld, M., Xie, H., de Andres-Aguayo, L. & Graf, T. Reprogramming of Committed T Cell Progenitors to Macrophages and Dendritic Cells by C/EBPα and PU.1 Transcription Factors. *Immunity* **25**, 731–744 (2006).

393. DeKoter, R. P. Regulation of B Lymphocyte and Macrophage Development by Graded Expression of PU.1. *Science* **288**, 1439–1441 (2000).

394. Ortmann, C. A. *et al.* Effect of Mutation Order on Myeloproliferative Neoplasms. *N. Engl. J. Med.* **372**, 601–612 (2015).

395. Grande, A. *et al.* Transcriptional targeting of retroviral vectors to the erythroblastic progeny of transduced hematopoietic stem cells. *Blood* **93**, 3276–3285 (1999).

396. Gajski, G. *et al.* Melittin induced cytogenetic damage, oxidative stress and changes in gene expression in human peripheral blood lymphocytes. *Toxicon* **110**, 56–67 (2016).

397. Zhou, L. *et al.* Miltirone exhibits antileukemic activity by ROS-mediated

endoplasmic reticulum stress and mitochondrial dysfunction pathways. *Sci. Rep.* **6**, 20585 (2016).

398. Yahata, T. *et al.* Accumulation of oxidative DNA damage restricts the self-renewal capacity of human hematopoietic stem cells. *Blood* **118**, 2941–2950 (2011).

399. Salati, S. *et al.* Calreticulin Affects Hematopoietic Stem/Progenitor Cell Fate by Impacting Erythroid and Megakaryocytic Differentiation. *Stem Cells Dev.* **27**, 225–236 (2018).

400. Salati, S. *et al.* Calreticulin Ins5 and Del52 mutations impair unfolded protein and oxidative stress responses in K562 cells expressing CALR mutants. *Sci. Rep.* **9**, 10558 (2019).

401. Lavi, N. Calreticulin Mutations in Myeloproliferative Neoplasms. *Rambam Maimonides Med. J.* **5**, e0035 (2014).

402. Martin, S., Wright, C. M. & Scott, L. M. Progenitor genotyping reveals a complex clonal architecture in a subset of *CALR*-mutated myeloproliferative neoplasms. *Br. J. Haematol.* **177**, 55–66 (2017).

403. Tefferi, A. *et al.* CALR vs JAK2 vs MPL-mutated or triple-negative myelofibrosis: clinical, cytogenetic and molecular comparisons. *Leukemia* **28**, 1472–1477 (2014).

404. Tefferi, A. *et al.* Calreticulin mutations and long-term survival in essential thrombocythemia. *Leukemia* **28**, 2300–2303 (2014).

405. Boren, E. & Gershwin, M. E. Inflamm-aging: autoimmunity, and the immune-risk phenotype. *Autoimmun. Rev.* **3**, 401–406 (2004).

406. Coussens, L. M. & Werb, Z. Inflammation and cancer. *Nature* **420**, 860–867 (2002).

407. Guglielmelli, P. *et al.* Ruxolitinib is an effective treatment for *CALR* -positive patients with myelofibrosis. *Br. J. Haematol.* **173**, 938–940 (2016).

408. Pronier, E. *et al.* Targeting the CALR interactome in myeloproliferative neoplasms. *JCI Insight* **3**, e122703 (2018).

409. Rutkowski, D. T. & Kaufman, R. J. A trip to the ER: coping with stress. *Trends Cell Biol.* **14**, 20–28 (2004).

410. Nam, A. S. *et al.* Somatic mutations and cell identity linked by Genotyping of Transcriptomes. *Nature* **571**, 355–360 (2019).

411. Lau, W. W. Y., Hannah, R., Green, A. R. & Göttgens, B. The JAK-STAT signaling pathway is differentially activated in CALR-positive compared with JAK2V617F-positive ET patients. *Blood* **125**, 1679–1681 (2015).

412. Tan, B. L., Norhaizan, M. E., Liew, W.-P.-P. & Sulaiman Rahman, H. Antioxidant and Oxidative Stress: A Mutual Interplay in Age-Related Diseases. *Front. Pharmacol.* **9**, 1162 (2018).